UNIVERSITY OF ADELAIDE

DEPARTMENT OF PHYSICS AND MATHEMATICAL PHYSICS

The Spin and Flavour Structure of the Nucleon[‡]

Fernando Monti Steffens

B. Phys and M. Sc.

Adelaide

June 1996

[‡]This work was supported by the Australian Research Council and by CAPES.

Contents

ABSTRACT

The objective of this thesis is to study the spin and flavour structure of the nucleon. To this end, we dedicate most of the work to the interpretation and understanding of a few seminal experiments in the area. In the flavour sector, we study possible charge symmetry breaking effects in a recent experiment that claims to have measured the ratio $\overline{d}/\overline{u}$ in the proton and find that their result correponds only to a limit where isospin between the proton and neutron is exact. We then study what possible effects antisymmetry between the quarks inside the proton may have in the flavour distribution of the sea quarks. In the spin sector, we reinforce the idea that the current experiments are unable to determine the total quark helicity in the proton. We then make a careful study of how to extract the quark helicity from present experiments once the amount of polarized glue is given. In particular, we find that the charm quark cannot be disregarded in such an analysis. Finally, we study the x dependence of the polarized and unpolarized quark distributions in leading and next-to-leading order QCD evolution.

This work contains no material which has been accepted for the award of any other degree or diploma in any other university or other tertiary institution and, to the best of my knowledge and belief, contains no material previously published or written by another person, except where due reference has been made in the text.

I give consent to this copy of my thesis, when deposited in the University Library, being available for loan and photocopying.

ACKNOWLEDGEMENTS

The guidance, support and friendship that I received from my supervisor, Tony Thomas, over the three and a half years since the day I arrived in Adelaide were the determining factor towards the completion of my thesis. I deeply acknowledge him for his assistance and the very often enlightening comments on my work. My understanding of physics had a dramatic improvement during my stay in Adelaide and Tony's enthusiasm and practical views of the current problems in the area were the critical factors in this change. They are also the factors that will certainly guide my work in the future. I am also in debit with his patience for my problems in expressing myself in the correct way in English. His support for travel to attend meetings overseas is also greatly acknowledged.

I profited from many discussions with many collegues and visitors that passed through Adelaide in the last few years. I would like to especially thank Wally Melnitchouk for the countless discussions we had over the most possible diverse topics. His influence is also felt over this thesis. Ken Kusaka, Jim McCarthy, Gunther Piller and Kazuo Tsushima are also specially acknowledged. Their doors were always open to any physics question I would take to them. Thanks for many helpful discussions in theoretical physics also goes to: Steven Bass, Shane Braendler, Rod Crewther, Sacha Dorokhov, Tetsuo Hatsuda, Harald Holtmann, Gottfried Holzwarth, Guo Liu, Enrico Predazzi, Andreas Schreiber and Tony Signal.

During my Ph. D. I had the opportunity to visit a few institutions and I would like to thank G.Krein (IFT), M. Robilotta (USP), J. Speth (Jülich) and W. Weise (Munich) for their hospitality.

I also thank to Eliane Veit and Victoria Herscovitz for their effort in making my time in Adelaide possible. Without their help I very probably would not be able to come here.

Finally, on the personal side, I was fortunate enough to make a few friends during my years in Adelaide. In particular, Philippe, Anja, Markus, George, Loreta, Nicole, Ellen, Richard, Neil, Angela, Dominique, Armin, Marcelo, Roberto, Salgado and my band will be always remembered for their continuous support and friendship. The long talks with E. Heath are deeply appreciated. And Carla with whom I shared many good moments. And for being always there (on the phone) for me.

Chapter 1

Introduction

Modern science in general, and physics in particular, has been built upon (and profited from) reductionism. The urge to explain the whole in terms of its components has, over the years, pushed our knowledge to its limit and provided a unified view of nature. The classification of related phenomena in terms of an underlying structure has simplified and empowered our description of the natural world. It has been so, for instance, with the discovery of the structure of DNA in biology. Physics itself has led this race, not without ruptures, and it is, perhaps, the foremost example of the ideology of reductionism. However, the use of fundamental constituents may provide a solid base for a given discipline but it is unlikely to solve all the problems related to it. In this sense, the DNA structure in biology is unlike to say much about the dynamics of populations as the knowledge of the fundamental laws of classical dynamics in physics are not enough to foresee the weather. For these reasons, the search for basic laws, breaking matter to its ultimate constituent parts, in order to describe the whole, have been often criticized. In any case, it is important bear in mind the observation that knowledge of the basic structure does not necessarily imply that problems

problems in a less fundamental level will be readily solved.

Quarks and gluons are a mark in the reductionist philosophy. Before them, physicists had broken matter into atoms, just to break it again when the electron was discovered. Then it was found that the atom could be split into electrons and nuclei. The nuclei, in turn, could then be resolved in terms of protons and neutrons. It was, by the time. a natural consequence of the idea that everything that possesses some structure, and by structure we mean that the electrical charge of the object in question has a spatial distribution, could be broken up. Not so for the proton and the neutron as the many experiments made, then and now, indicate that, irrespective of the energy one gives to them , it is not possible to break them into fundamental constituents relative to that same energy. The quarks and gluons, which are believed to be the fundamental constituents of protons, neutrons and many other particles, could not (and still cannot) be made free. Hence the mark in the reductionist thinking; for the first time in the history of modern physics, matter with a given structure could not be resolved into more fundamental parts. Moreover, just as in many other examples in science, our acknowledgement of the existence of quarks and gluons and a now regarded fundamental theory for them [1, 2, 3, 4], does not mean that we can fully derive some very basic properties of the proton from them. The quark picture has given enormous insights in our understanding of the natural world and, by now, they are incorporated in a general scheme for the basic laws of physics called Standard Model. But where did the idea of quarks and gluons come from? How do we know that the proton and neutron have this particular structure that cannot itself be isolated? The answer to these questions goes back to the 60's.

The vast number of particles related to nuclear phenomena, discovered in the postwar years, led many to try to organize them in terms of symmetries. Many schemes were proposed, ranging from the Sakata model, where in its SU(2) version, the proton and neutron were believed to be the fundamental particles, to the SU(3) scheme of Gell-Mann [5] and

Zweig [6] where all the particles experiencing nuclear forces were classified according to special combinations of 3 fictitious particles named quarks. Until the first experiment done at SLAC in 1969 [7], when the proton was probed by electrons in its deep structure, the quarks were no more than a useful but still fictitious way to classify particles. The experimental results of SLAC allowed a interpretation, due to Feynman [8, 9], Bjorken and Paschos [10], where the scattering was actually taking place between the electron and point like objects inside the proton. These point like objects were named partons and their interpretation in terms of quarks was a natural extension. Among problems remaining in this relation, was that there was only 3 quarks in the Gell-Mann Zweig model but the number of partons, in principle, could be infinity. Moreover, there appeared to be neutral partons. This problem was solved through the discovery of Quantum Chromo Dynamics (QCD) [1, 2, 3, 4], the field theory for quarks and gluons.

Originally, the introduction of the concept of quarks generated successful insights, but it also presented some limitations that came out to be a bonus to the whole scheme. Remarkably, there was one particle in the scheme of quark classification that defied the Pauli Principle. This particle was the Δ^{++} and the quark model scheme predicted for it a composition uuu, where u is the up quark, with all the spins pointing to the same direction. In order to circumvent this problem (the quarks were believed to be fermions), a new internal quantum number was introduced (in addition to spin and flavour u, d and s) called colour [11]. The symmetry group was the same as that of Gell-Mann and Zweig but the symmetry was now based in colour rather then quark flavour.

With these ingredients, QCD was built in analogy with Quantum Electro-Dynamics (QED) with the colour number being carried by compensating gauge fields, generated through the imposition of local gauge invariance to the quark fields, called the gluon field. The gluons are responsible for the interactions among coloured charged quarks as the photons are

responsible for the interactions between electrically charged particles. The novelty of QCD is that the gluons, as opposed to photons, can interact with themselves. Moreover, QCD has, as will be seen in chapter 2, the property of asymptotic freedom [12, 13, 14] which means that the quarks behave as free particles when seen from very short distances. On the other hand, the equations that give asymptotic freedom also say that the interaction between the quarks becomes stronger as the distance between them grows, although we do not know how strong it becomes because after a certain point, the equations can not be trusted anymore. In any case, the strength of the interactions between quarks grows with the distance between them. Quarks, no matter how hard the interaction between the electron (or muon or any other lepton) and proton is, have never been isolated. This property is called confinement and it is believed to exist although up to now no one has proven it. In this sense, the study of the proton structure is the last in a long reductionist tradition. If confinement, as it is believed now, is a rigid reality, then we cannot go further in breaking matter. Thus, the proton system is unique. To comprehend its structure, when we cannot separate it, is a formidable task. It is the objective of this thesis to add to the world wide discussion on how the proton properties are shared among its constituents. In particular, we are interested in how the flavour of the sea quarks is decomposed and how the proton spin is shared among its parts.

In chapter 2 we review the basic tools necessary to study the proton structure in terms of its constituents. We describe the experiments performed at SLAC, Deep Inelastic Scattering (DIS), and the parton interpretation of their results. The notion of the structure function is introduced. We then develop the concept of the Operator Product Expansion (OPE) [15, 16, 17] which enables us to separate in a elegant way the measured proton cross sections into a region where asymptotic freedom is valid (perturbative QCD) and a region where it is not (non-perturbative QCD). The renormalization group equations, which are used to study

how the structure functions vary with the scale in the perturbative regime, and its powerful consequences are then studied.

As a first application of the parton model language, we analyse in chapter 3 the present situation regarding the flavour of the nucleon sea. Basically, two main experiments, the New Muon Collaboration (NMC) [18] and the NA51 [19] experiments, have provided vital information to this area. We point out that although they together lead to the conclusion that $\overline{d} > \overline{u}$, the size of this asymmetry can not be determined by them alone because of possible charge symmetry breaking effects. The mechanisms that can lead to such asymmetry, viz. gluon decay into a $q\overline{q}$ pair and pion emmision, and their relations to the Pauli Exclusion Principle, are addressed. Pertinent conclusions related to antisymmetrization effects between sea and valence quarks are then drawn.

An other huge problem has challenged physicists in the last few years since the European Muon Collaboration (EMC) [20] released measurements of the proton spin structure function in a region previously unexplored. Their conclusion was astonishing: the quarks carry little or no spin. In chapter 4 we briefly review the problem and the experimental situation in the area. We then analyse in section 4.2 the proton spin decomposition in the light of gauge invariance and renormalization scheme dependence. We also discuss why the EMC experiment and others do not measure the spin content of the proton carried by quarks but only its singlet axial charge [21, 22]. Both quantities are related only if special assumptions related to choice of gauge and renormalization scheme are made. We exemplify this discussion with an explicit calculation of the spin structure function using a scheme where the spin carried by quarks can be related to the singlet axial charge if gluons are included. Mass effects are incorporated in the calculation and we show why it would be wrong to exclude charm from the present calculations. To give a focus to the discussion on mass effects, we calculated their impact on the amount of polarized gluon needed to fit the experimental

data and its x dependence. To complete the discussion on this subject, we also show how a simple change of renormalization scheme can led to different interpretations of the singlet axial charge, keeping intact the spin structure function.

Chapter 5 is dedicated to study different factors that can influence the x dependence of the quark distributions and of the structure functions. We pay particular attention to the spin structure function. In the case, we study the effect of next-to-leading order (NLO) QCD evolution and the effect of a meson cloud on the quark distributions of the proton. We also make some observations regarding the ambiguity in the definition of parton distributions when we depart from leading order calculations as well as in the calculation of the moments of the structure functions.

Finally, we use chapter 6 to make a summary of what was achieved, as well as possible directions for future work in the subject.

Chapter 2

DIS, OPE and the Parton Model

2.1 Deep Inelastic Scattering

We will be interested in the following process:

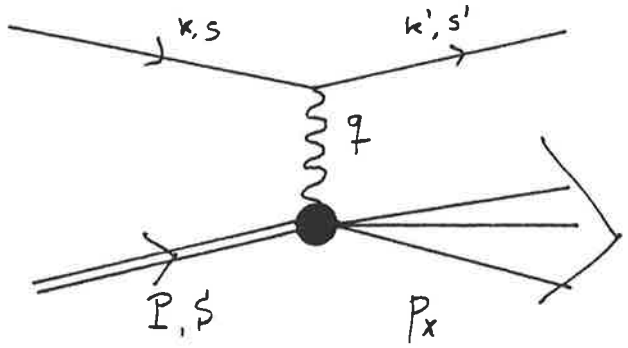

Figure 2.1: Inclusive scattering of a lepton of momentum k on a nucleon of momentum p. The measured scattered lepton has momentum k' and the unobserved hadron final state has momentum p_X. The interaction is through one photon exchange.

The differential cross section in the LAB frame for the lepton be scattered into a solid

angle $d\Omega$ and have a final energy in the range dE' is [23]:

$$\frac{d^2\sigma}{d\Omega dE'} = \frac{\alpha^2}{q^4}\frac{E'}{E}L_{\mu\nu}W^{\mu\nu}, \tag{2.1}$$

with

$$L_{\mu\nu} = \sum_{s'} \overline{u}(k,s)\gamma_\mu u(k',s')\overline{u}(k',s')\gamma_\nu u(k,s) \tag{2.2}$$

the leptonic tensor,

$$W_{\mu\nu} = \frac{1}{2\pi}\sum_X < P,S|j_\mu(0)|X >< X|j_\nu(0)|P,S > (2\pi)^4\delta^4(p_X - P - q) \tag{2.3}$$

the hadronic tensor, $\alpha = e^2/4\pi$, j_μ the electromagnetic current and s and S the spin vectors. As we are in the lab frame, the explicit form of the four vectors is:

$$P = (M,\vec{0}),\ \ k = (E,\vec{k}),\ \ k' = (E',\ \ \vec{k}'),\ \ q = k - k'. \tag{2.4}$$

The spin vectors s is subject to the following constraints [23]: $s.k = 0$ and $s.s = -1$. From these two expressions, following Bjorken [23], we get:

$$s^0 = \frac{\vec{s}\cdot\vec{k}}{E} = \vec{s}\cdot\vec{\beta};\ \ |\vec{s}| = \frac{1}{\sqrt{1-(\hat{s}\cdot\vec{\beta})^2}} \tag{2.5}$$

Now, if we notice that $(\hat{s}\cdot\vec{\beta})^2 = (s^0)^2/|\vec{s}|^2$, we deduce:

$$\hat{s}\cdot\vec{\beta} = \pm\beta;\ \ s^0 = \pm\beta|\vec{s}|, \tag{2.6}$$

where the "+" indicates that the spin of the lepton is parallel to its momentum (right handed lepton) and the "-" indicates that the spin of the lepton is anti-parallel to its momentum (left handed lepton). In this thesis we will not explore lepton transverse polarizations and

hence the cases of longitudinal polarization quoted above will suffice for our discussions. We can relate the longitudinal polarization vector directly to the lepton momentum by noting that $s^0 = \vec{s}\cdot\vec{s}/|\vec{s}|$. Comparing with Eq. (2.6), we have:

$$\vec{s} = \pm\frac{\vec{k}}{m\beta}, \tag{2.7}$$

where m is the lepton mass. By construction, it is possible to write:

$$s^\mu = \pm\frac{k^\mu}{m\beta} \mp \frac{\sqrt{1-\beta^2}}{\beta}g^{\mu 0}. \tag{2.8}$$

In the relativistic limit (or for $m \to 0$), $m/E \to 0 \Rightarrow \beta = 1$ and then

$$s^\mu = \pm\frac{k^\mu}{m} \tag{2.9}$$

for relativistic particles.

The leptonic tensor is rewritten as:

$$L_{\mu\nu} = \sum_{s'} \overline{u}_\alpha(k,s)(\gamma_\mu)_{\alpha\beta}u_\beta(k',s')\overline{u}_a(k',s')(\gamma_\nu)_{ab}u_b(k,s). \tag{2.10}$$

With the help of the projectors $\sum_{s'} u_\beta(k',s')\overline{u}_a(k',s') = (\not{k}' + m)_{\beta a}$ and $u_b(k,s)\overline{u}_\alpha(k,s) = (\not{k} + m)_{b\gamma}[(1+\gamma_5\not{s})/2]_{\gamma\alpha}$, we get:

$$\begin{aligned} L_{\mu\nu} &= \frac{1}{2}Tr\{(\not{k}+m)(1+\gamma_5\not{s})\gamma_\mu(\not{k}'+m)\gamma_\nu\} \\ &= 2(k_\mu k'_\nu + k_\nu k'_\mu + \frac{q^2}{2}g^{\mu\nu}) \pm 2i\epsilon_{\mu\nu\rho\sigma}k^\rho q^\sigma \\ &= L^{(s)}_{\mu\nu} \pm L^{\mu\nu(a)}, \end{aligned} \tag{2.11}$$

where we used: $q^2 = 2m^2 - 2k\cdot k' \sim -2k\cdot k'$, $ms^\mu = \pm k^\mu$ and $\epsilon^{0123} = 1$. The symmetric part of the leptonic tensor, $L^{(s)}_{\mu\nu}$, was derived from the spin averaged projectors thus corresponding

to unpolarized leptons. Conversely, the antisymmetric part, $L^{(a)}_{\mu\nu}$, corresponds to polarized particles with the "+" ("-") sign denoting the case that the spin is parallel (antiparallel) to the direction of motion.

Like the leptonic tensor, the hadronic tensor can also be decomposed into symmetric and antisymmetric parts:

$$W_{\mu\nu} = W^{(s)}_{\mu\nu} + W^{(a)}_{\mu\nu}. \tag{2.12}$$

As the contraction of a symmetric tensor with an antisymmetric one is zero, the symmetric part of the hadronic tensor corresponds to the spin averaged case, which is the case we study first. To this end, the hadronic tensor will be parametrized in terms of structure functions (which just express our ignorance on the photon nucleon vertex). As in our specific case of inelastic scattering there are two independent scalar variables that we choose to be the momentum transfer $Q^2 = -q^2 = -(k-k')$ and the energy transfer $\nu = p.q/M$, the structure functions will depend on these variables. Moreover, to preserve Lorentz invariance, $W^{(s)}_{\mu\nu}$ must be build upon the available four vectors, e.g, P, q and $g_{\mu\nu}$. Its general form is then:

$$W^{(s)}_{\mu\nu} = A(Q^2,\nu)g_{\mu\nu} + \frac{B(Q^2,\nu)}{M^2}q_\mu q_\nu + \frac{C(Q^2,\nu)}{M^2}(q_\mu P_\nu + q_\nu P_\mu) + \frac{D(Q^2,\nu)}{M^2}P_\mu P_\nu. \tag{2.13}$$

In principle, we could also have a term of the form $\epsilon_{\mu\nu\alpha\beta}P^\alpha q^\beta E$ [1]. But the antisymmetric tensor ϵ is an axial quantity in the sense that it behaves in the same way as γ^5 under parity transformations. As the electromagnetic interaction conserves parity, this extra term is not included. For neutrino nucleon scattering, mediated through the electroweak interaction, such a term should be present. A further constraint is imposed by the conservation of the

[1] This term is of course antisymmetric and we mention it here in the sense that it would enter in the general definition of the spin averaged tensor.

electromagnetic current: $\partial_\mu j^\mu = 0 = q_\mu < j^\mu >$. It implies that $q_\mu W^{\mu\nu} = W^{\mu\nu} q_\nu = 0$. Notice that in (2.13), terms that would violate current conservation, like the ones containing $q_\mu q_\nu$, were also disregarded from the start. Current conservation implies in two equations for the functions $A...D$. The structure functions B and C are eliminated in favour of A and D and if we call $W_1 = -A$ and $W_2 = D$, we have the standard form for the spin averaged hadronic tensor:

$$W^{(s)}_{\mu\nu} = \left[-g_{\mu\nu} + \frac{q_\mu q_\nu}{q^2}\right] W_1(Q^2,\nu) + \left[\left(P_\mu - \frac{P.q}{q^2}q_\mu\right)\left(P_\nu - \frac{P.q}{q^2}q_\nu\right)\right]\frac{W_2(Q^2,\nu)}{M^2}. \quad (2.14)$$

A similar analysis can be made for the antisymmetric part of $W_{\mu\nu}$. Its general form is:

$$W^{(a)}_{\mu\nu} = i\epsilon_{\mu\nu\alpha\beta}[A(Q^2,\nu)q^\alpha S^\beta + B(Q^2,\nu)q^\alpha P^\beta + C(Q^2,\nu)P^\alpha S^\beta]. \quad (2.15)$$

Because of the antisymmetric property of $\epsilon_{\mu\nu\alpha\beta}$ and current conservation, it follows that $C = 0$. Moreover, the coefficient B has to be an axial. The convention usually used in the literature is $A = MG_1 + (P\cdot q)G_2/M$ and $B = -(S\cdot q)G_2/M$. We then have:

$$W^{(a)}_{\mu\nu} = i\epsilon_{\mu\nu\alpha\beta}q^\alpha\left[MS^\beta G_1(Q^2,\nu) + ((P\cdot q)S^\beta - (S\cdot q)P^\beta)\frac{G_2(Q^2,\nu)}{M}\right]. \quad (2.16)$$

We are now ready to compute the cross section, Eq. (2.1). The contraction of the symmetric parts of $L_{\mu\nu}$ and $W_{\mu\nu}$ is:

$$L^{(s)}_{\mu\nu}W^{\mu\nu(s)} = 4EE'(2sin^2\frac{\theta}{2}\,W_1(Q^2,\nu) + cos^2\frac{\theta}{2}\,W_2(Q^2,\nu)), \quad (2.17)$$

where the relativistic limit, $E \sim |\vec{k}|$, was used.

To perform the contraction of the antisymmetric parts, we will need help of the geometrical configuration of Fig. (?). The nucleon at rest will be allowed to have an arbitrary

polarization in the sense that its spin is along an arbitrary direction $\hat{S}$. The angle between this arbitrary direction $\hat{S}$ and the incident lepton with momentum $\vec{k}$ will be α. The lepton scattering angle is θ and the angle between the scattered lepton and the vector $\hat{S}$ is Θ. Finally, the angle between the planes $\vec{k}$, $\vec{k}'$ and $\vec{k}$, $\hat{S}$ is ϕ. We then easily see that:

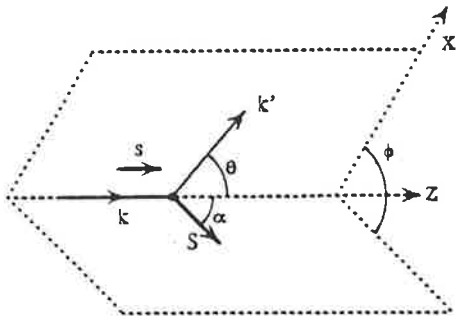

Figure 2.2: Geometrical configuration of the lepton nucleon scattring.

$$L^{(a)}_{\mu\nu}W^{\mu\nu(a)} = -2MQ^2[(Ecos\alpha + E^{'}cos\Theta)G_1(Q^2,\nu) + 2(-EE^{'}cos\alpha + EE^{'}cos\Theta)\frac{G_2(Q^2,\nu)}{M}]. \tag{2.18}$$

Using the trigonometric property $cos\Theta = sin\theta sin\alpha cos\phi + cos\theta cos\alpha$ we write the final expression for the cross section:

$$\begin{aligned}\frac{d^2\sigma}{d\Omega dE'} &= \frac{4\alpha^2}{Q^4}E'^2\left\{2sin^2\frac{\theta}{2}\,W_1(Q^2,\nu) + cos^2\frac{\theta}{2}\,W_2(Q^2,\nu)\right\} \\ &\pm (-1)\frac{2\alpha^2}{Q^2}\frac{E'}{E}\left\{cos\alpha[(E+E^{'}cos\theta)MG_1(Q^2,\nu) - Q^2G_2(Q^2,\nu)]\right. \\ &\left. +sin\theta sin\alpha cos\phi E^{'}[MG_1(Q^2,\nu) + 2EG_2(Q^2,\nu)]\right\}. \end{aligned} \tag{2.19}$$

From this equation we can calculate the cross section for the scattering of a longitudinally polarized lepton from a nucleon polarized in any direction.

Later in this chapter we will be dealing with the parton model. It will also be seen that it is convenient to express the hadronic tensor in terms of the forward virtual Compton scattering (i.e. forward scattering of virtual photons on nucleons). In such a case, we can reexpress the structure functions in terms of virtual photon nucleon cross sections. In fact, the reason why there are four independent structure functions is because there is four independent ways for the the helicities of the virtual photon and of the nucleon to combine [24, 25]. Of course, the virtual photon cross section is not uniquely defined. But following general convention [24, 9, 26, 27], we take the virtual cross section to have the same form as that for a real photon on an unpolarized target [9, 28]:

$$\sigma_\lambda(\gamma^v p \to X) = \frac{4\pi\alpha}{K}\varepsilon^*_\mu(\lambda)\varepsilon_\nu(\lambda)W^{\mu\nu}, \tag{2.20}$$

where λ is the photon polarization and K is the flux of virtual photons. The flux is also a matter of convention. Here, the Hand convention [29], $K = \nu - Q^2/2M$, will be used where K is interpreted as the energy that produces a hadron with the same mass as the hadron created by a real photon of energy ν. The virtual photons are massive particles with spin 1. If the photon is moving along the z direction, the polarization vectors are [26, 30] $\varepsilon_\mu(\pm 1) = \mp(0, 1, \pm i, 0)/\sqrt{2}$ for transverse polarization and $\varepsilon_\mu(0) = (\sqrt{\nu^2 + Q^2}, 0, 0, \nu)/\sqrt{Q^2}$ for longitudinal polarization. For a polarized target, the spin (of photon + nucleon) projection along the photon momentum can be 1/2 or 3/2. There is also a third combination coming from the interference between the longitudinal (S) and the transverse (T) photon. For the unpolarized scattering one has the separate contributions from the transverse and longitudinal photons. From Eq. (2.20) one has [24, 31]:

$$\begin{aligned}
\sigma_{1/2} &= \sigma_T + \frac{4\pi^2\alpha}{K}(M\nu G_1 - Q^2 G_2), \\
\sigma_{3/2} &= \sigma_T - \frac{4\pi^2\alpha}{K}(M\nu G_1 - Q^2 G_2), \\
\sigma_{TS} &= \frac{4\pi^2\alpha\sqrt{Q^2}}{K}(MG_1 + \nu G_2), \\
\sigma_T &= \frac{4\pi^2\alpha}{K}W_1 = \frac{1}{2}(\sigma_{1/2} + \sigma_{3/2}), \\
\sigma_S &= \frac{4\pi^2\alpha}{K}W_2\left(\frac{Q^2+\nu^2}{Q^2}\right) - \sigma_T.
\end{aligned} \tag{2.21}$$

We then can use the virtual polarized cross sections to define virtual asymmetries:

$$\begin{aligned}
A_1 = \frac{\sigma_{1/2} - \sigma_{3/2}}{2\sigma_T} = \frac{M\nu G_1 - Q^2 G_2}{W_1}, \\
A_2 = \frac{\sigma_{TS}}{\sigma_T} = \sqrt{Q^2}\frac{MG_1 + \nu G_2}{W_1}.
\end{aligned} \tag{2.22}$$

One of the advantages of using these asymmetries is that the kinematical factors can be factored in a clean way in the measured longitudinal asymmetry A:

$$A = \frac{\frac{d\sigma^{\rightleftarrows}}{d\Omega dE'} - \frac{d\sigma^{\rightrightarrows}}{d\Omega dE'}}{\frac{d\sigma^{\rightleftarrows}}{d\Omega dE'} + \frac{d\sigma^{\rightrightarrows}}{d\Omega dE'}} = \frac{Q^2}{2EE'}\frac{(E + E'cos\theta)MG_1 - Q^2 G_2}{2sin^2\frac{\theta}{2}W_1 + cos^2\frac{\theta}{2}W_2} = D(A_1 + \eta A_2), \tag{2.23}$$

with

$$\begin{aligned}
D &= \frac{1 - (E'/E)\varepsilon}{1 + \varepsilon R}, \quad \eta = \frac{\varepsilon\sqrt{Q^2}}{E - E'\varepsilon}, \\
\epsilon &= \left(1 + 2(1 + \nu^2/Q^2)tan^2\frac{\theta}{2}\right)^{-1}, \\
R &= \frac{\sigma_S}{\sigma_T} = \frac{W_2}{W_1}\frac{Q^2+\nu^2}{Q^2} - 1.
\end{aligned} \tag{2.24}$$

The notation for the arrows in (2.23) is as follows: "$\rightarrow$" means that the spin of the lepton is in the same direction of its momentum (the "+" sign in the cross section (2.19)) while for "$\Rightarrow$", $\alpha = 0$ and for "$\Leftarrow$", $\alpha = \pi$.

It is also possible to define an asymmetry for the case where the spin of the nucleon is perpendicular to the momentum of the incident particle. It means that in Eq. (2.19), α is $\pi/2$ ($\Uparrow$) or $3\pi/2$ ($\Downarrow$) and the asymmetry is:

$$A_T = \frac{\frac{d\sigma^{\rightarrow\Downarrow}}{d\Omega dE'} - \frac{d\sigma^{\rightarrow\Uparrow}}{d\Omega dE'}}{\frac{d\sigma^{\rightarrow\Downarrow}}{d\Omega dE'} + \frac{d\sigma^{\rightarrow\Uparrow}}{d\Omega dE'}} = \frac{Q^2}{2E}\frac{sin\theta(MG_1 + 2EG_2)}{2sin^2\frac{\theta}{2}W_1 + cos^2\frac{\theta}{2}W_2}cos\phi = d(A_2 - \zeta A_1)cos\phi, \tag{2.25}$$

with

$$d = D\sqrt{\frac{2\varepsilon}{1+\varepsilon}}, \quad \zeta = \frac{\eta(1+\varepsilon)}{2\varepsilon}. \tag{2.26}$$

In principle, the transverse asymmetry depends on the azimuthal angle, ϕ. This problem can be fixed by measuring only the upward scattered particles so that $\phi = 0$. Another possibility, as used in the recent measurement of A_T by the SMC group [32], is to define an asymmetry averaged in $cos\phi$.

We now have two equations relating the unknown G_1 and G_2. The two asymmetries can be measured and hence one can fix the virtual asymmetries A_1 and A_2. From (2.22) and (2.24), the following expressions for the polarized structure functions can be written:

$$\begin{aligned} G_1 &= \frac{W_2\nu}{MQ^2(1+R)}(A_1 + \gamma A_2), \\ G_2 &= -\frac{W_2}{Q^2(1+R)}\left(A_1 - \frac{A_2}{\gamma}\right), \end{aligned} \tag{2.27}$$

where $\gamma = \sqrt{Q^2}/\nu$, is, generally, a small number. Moreover, it has been known [33] for a long time that $|A_2| < \sqrt{R}$, with $\sqrt{R}$ already a small number itself [34]. This fact has been used

[20] to disregard the contribution from A_2 in (2.27) and determine G_1. We will return to this point later in this chapter and extensively study throughout this thesis the experimental determination of G_1 and its theoretical interpretations and consequences. Finally, we point out that if A_2 is zero (no interference between longitudinal and transverse photons), then $G_2 = -MG_1/\nu$.

From the equations just displayed we see that to determine polarized structure functions we need to know the unpolarized ones. As this is already an extremely important subject by itself, we briefly outline how to extract the unpolarized structure functions W_2 and R from experiments. If we look at the unpolarized part of the differential cross section (2.19), we see that choosing different scattering angles θ we can select the different structure functions W_2 and R (according to R given in Eq. (2.24)). As we want both structure functions at the same ν and Q^2, incident beams of different energies have to be used (for instance, $cos\theta = (E^2 - E\nu - Q^2/2)/(E^2 - E\nu)$ if the lepton mass is disregarded). This procedure has been extensively used by experimentalists and by now the unpolarized structure functions for the nucleon are fairly well determined [35].

We now proceed to show that the data on these inclusive structure functions can be qualitatively, and to a large extent also quantitatively, understood in terms of the parton model.

2.2 The Parton Model

The first measurements of inclusive cross sections were performed at the SLAC in Stanford in the end of the 1960's and the results were published in 1969 [7]. The experiment measured the inclusive electron-proton cross sections for various values of the final state mass, $p_X^2 = W^2 = M^2 + 2M\nu + Q^2$ and momentum transfer Q^2. We look again to the inclusive unpolarized

cross section, now in terms of the Mott cross section:

$$\frac{d^2\sigma}{d\Omega dE'} = \left(\frac{d\sigma}{d\Omega}\right)_M W_2(Q^2,\nu)\left(1+2\frac{Q^2+\nu^2}{(1+R)Q^2}tan^2\frac{\theta}{2}\right), \tag{2.28}$$

with $(d\sigma/d\Omega)_M = \alpha^2 cos^2(\theta/2)/4E^2 sin^4(\theta/2)$. Their results show that when the mass of the final state gets away from the elastic scattering ($W^2 = M^2$) region, $W_2(Q^2,\nu)(1 + 2\frac{Q^2+\nu^2}{(1+R)Q^2}tan^2\frac{\theta}{2})$ becomes almost Q^2 independent, in contrast with the strong Q^2 dependence of the elastic electron-proton scattering. On the other hand, Bjorken [36] had proposed a short time before this experiment, based on current algebra, that for very large ν and Q^2 but ν/Q^2 fixed, the structure functions $W_{1,2}(Q^2,\nu)$ should behave as a function of a single variable:

$$\begin{aligned} MW_1(Q^2,\nu) &\to F_1(x) \\ \nu W_2(Q^2,\nu) &\to F_2(x) \end{aligned} \tag{2.29}$$

where $x = Q^2/2M\nu$ is the Bjorken x and the above property of the structure functions is known as scaling. The SLAC-MIT group [7] extracted $\nu W_2(Q^2,\nu)$ from the cross section Eq. (2.28) for the two extreme cases of $R = 0$ and $R = \infty$. What they concluded was that for $R = 0$, there is indeed the scaling for the structure function as predicted by Bjorken but that the same does not occur for $R = \infty$. Why is it that $R \sim 0$ is so special? If we look back to the definition of R, Eq. (2.24), we see that $R = 0$ means $\sigma_s = 0$. In other words, the photon is coupling to a particle with spin 1/2. The general argument [24, 27] to see this is to consider the photon being collinear to the incident particle (both the photon and the incident particle are in the same line but in opposite directions). If helicity is to be conserved, then the photon has to have angular momentum ± 1 in its direction of motion.

Hence the cross section for a scalar photon should be zero. This result can also be derived if we consider that the photon is making elastic scattering with point charged particles with spin 1/2 - the partons as introduced by Feynman [8, 9]. Thus it seems that the scaling as observed at SLAC finds an explanation if one consider that the nucleon is composed of a set of point like particles that interact elastically with the incident leptons.

The elastic cross sections for two spin-1/2, point-like charged particles is given by equation (2.1) just if we notice that the hadronic tensor is replaced by [2]:

$$W_{\mu\nu} = \frac{1}{m_i}(p_\mu p'_\nu + p_\nu p'_\mu + \frac{q^2}{2} g^{\mu\nu})\delta(Q^2 - 2p \cdot q). \tag{2.30}$$

where p is the parton four momentum and the delta function reflects the fact that we are now dealing with elastic scattering and we have only one variable in the problem, in contrast with the two variables of the inclusive scattering. In this parton picture. the Bjorken prediction that the structure functions depend of only one variable comes out quite naturally. The cross section is then:

$$\frac{d^2\sigma^i}{d\Omega dE'} = \frac{4\alpha^2}{Q^4} E'^2 \left\{ e_i^2 \frac{Q^2}{2m_i^2} sin^2\frac{\theta}{2} + e_i^2 cos^2\frac{\theta}{2} \right\} \delta(\nu - \frac{Q^2}{2m_i}) \tag{2.31}$$

where the scattered parton is allowed to have just a fraction e_i of the electron charge e. The total cross section is then assumed to be the sum of the individual i partonic cross sections $d^2\sigma^i/d\Omega dE'$. Comparing Eq. (2.31) with Eq. (2.19) and using $m_i = xM$, it is seem that the contribution of each parton to the structure function is:

[2] In writing Eq. (2.1) we shift a factor $2m_i$, where m_i is the mass of the i parton, in the denominator of the hadronic tensor as this is the convention we are using, as seen from Eq. (2.1)

$$
\begin{aligned}
W_1^i &= e_i^2 \frac{Q^2}{4x^2M^2}\delta(\nu - \frac{Q^2}{2xM}) \\
W_2^i &= e_i^2 \delta(\nu - \frac{Q^2}{2xM})
\end{aligned}
\tag{2.32}
$$

As said before, the total contribution is given by the sum over all i partons. It is also necessary to integrate over all x and the integral must be weighted by some probabilities $f_i(x)$ for the i parton to be found with a certain fraction x of the nucleon mass (and hence momentum):

$$
\begin{aligned}
W_2(\nu, Q^2) &= \sum_i \int_0^1 dx' f_i(x') e_i^2 \delta\left(\nu - \frac{Q^2}{2x'M}\right) = \sum_i e_i^2 \frac{x}{\nu} f_i(x) = \frac{1}{\nu} F_2(x), \\
W_1(\nu, Q^2) &= \sum_i \int_0^1 dx' f_i(x') e_i^2 \frac{Q^2}{4x'^2M^2}\delta\left(\nu - \frac{Q^2}{2x'M}\right) = \sum_i e_i^2 \frac{f_i(x)}{2M} = \frac{1}{M} F_1(x)
\end{aligned}
\tag{2.33}
$$

From the above relation one gets the so called Callan-Gross [37] relation:

$$
F_2(x) = 2xF_1(x). \tag{2.34}
$$

This implies $R = 4M^2x^2/Q^2$, which goes to zero in the Bjorken limit.

The whole reasoning exposed in developing the idea that the approximate scaling observed in deep inelastic experiments can be explained in terms of elastic scattering off point like particles or partons, is due to Feynman [8, 9] and developed by Bjorken and Paschos [10]. More detailed derivations of the model can be found in the original Bjorken article [10], in Feynman's book [9] or in the many text books on the subject [24, 26, 27].

In principle, the same kind of reasoning could be applied to the spin dependent part and one could derive parton model expressions for G_1 and G_2 through elastic scattering between

two point like, polarized particles. In this case, the antisymmetric part of the hadronic tensor would be replaced by a partonic tensor:

$$W_{\mu\nu}^{(a)} = i\varepsilon_{\mu\nu\alpha\beta}S^{\alpha}q^{\beta}\delta(Q^2 - 2p.q). \tag{2.35}$$

If we compare this expression with the antisymmetric tensor, Eq. (2.16), we immediately see that:

$$\begin{aligned} G_1^i(\nu, Q^2) &= \frac{e_i^2}{2M^2\nu}\delta(x - \frac{Q^2}{2M\nu}) \\ G_2^i(\nu, Q^2) &= 0. \end{aligned} \tag{2.36}$$

This means that in the simple parton model there is, in fact, only one polarized structure function. This result comes from the fact that the parton is treated as a free particle, as can be seen from Eq. (2.35). As emphasized in some works [38, 39], the partons must be interacting or virtual in order to render a nonzero value to G_2. Later, when we study the problem through the operator product expansion (OPE) technique, we will see that G_2, in principle, is not zero.

BJorken also predicted scaling for the polarized structure functions and, according to Eqs. (2.22,2.34,2.36), we write:

$$\begin{aligned} M^2\nu G_1(\nu, Q^2) &\to g_1(x) = \frac{1}{2}\sum_i e_i^2 \Delta f_i(x) \\ M\nu^2 G_2(\nu, Q^2) &\to g_2(x), \end{aligned} \tag{2.37}$$

where Δf_i is the probability to find the i parton with its spin along the nucleon spin and, as discussed, there is no such interpretation for $g_2(x)$ in the simple parton model.

2.2.1 The Covariant Parton Model

The derivation in the last section of some properties of the parton model may look a little crude to some readers. There are other ways to get the same results but whatever means one uses, always the implicit impulse approximation assumed by us has to be valid. In general, this means that:
- The parton is essentially free during the interaction what implies that the time of interaction between the external current and the target is much smaller than the lifetime of any possible virtual state, and
- the energy transfered is large enough so that the parton binding energy, if any, is neglected. Hence the parton behaves as a free particle.

The assumption of scaling as proposed by Bjorken requires that the energy transfer tends to infinity. Thus, the second requirement is naturally satisfied. To show that the first requirement is true one usually turns to the infinite momentum frame [8, 9, 24, 26, 36], where can be shown that the requirement is met provided that the energy transfer is large enough. However, it is not necessary to work in the infinite momentum frame. As emphasized by Jaffe [40], the physics is independent of frame and a formulation of the parton model in the nucleon rest frame is more natural and simple. Indeed, Jaffe presented a very formal and nice formulation of the model in that frame that we will follow more closely in chapter 4 when we give some details of calculations of parton distributions as developed by Signal and Thomas [41, 42].

We then would like to look for a more general calculation of parton distributions. To this end, we present some simple calculations in a covariant frame according to the works of Landshoff and Polkinghorne [43] and Jackson et al. [44]. The parton elastic scattering that we discussed before is given basically by the handbag diagram:

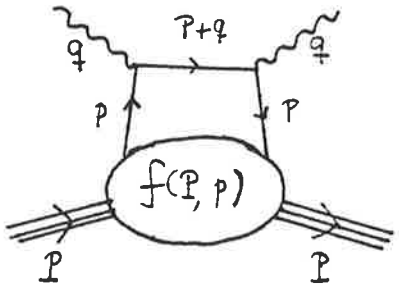

Figure 2.3: The handbag diagram.

A general function $f(P,p)$ is introduced to express the strong interactions in the parton-nucleon vertex. It is a Lorentz scalar and in principle [43] it depends only on the scalar $P.p$. The unpolarized part of the hadronic tensor is then given by:

$$W_{\mu\nu}(P,q) = \sum_{i,s} \int d^4p_i f_s^i(P.p_i) w_{\mu\nu}^i(p_i,q) \delta((p_i^2 - m_i^2) \delta((p_i+q)^2 - m_i^2), \tag{2.38}$$

where m_i is the parton mass and $w_{\mu\nu}^i(p_i,q)$ the parton-photon interaction term and it is given, as seen before, by:

$$w_{\mu\nu}^i(p,q) = \frac{1}{m_i}[p_{i\mu}p'_{i\nu} + p_{i\nu}p'_{i\mu} + g_{\mu\nu}\frac{q^2}{2}]. \tag{2.39}$$

We then notice that $\int d^4p_i = \int dp_{i+}dp_{i-}d^2p_{i\perp} = \pi \int dx dp_i^2 dp_{i\perp}^2/2x$ due to the fact that in light coordinates, $p_{i+} = xP_{i+}$ and the scalar product in light coordinates, $p_i^2 = 2p_{i+}p_{i-} - p_{i\perp}^2$ was used. If we notice that $\int dp_i^2 \delta(p_i^2 - m_i^2) = 1$ and that $x_i = p_i.q/P.q$ as the momentum fraction of the i quark, then:

$$W_{\mu\nu}(P,q) = \frac{\pi}{4}\sum_i \frac{e_i^2}{m_i}\int \frac{dx}{x} dp_{i\perp}^2 [p_{i\mu}p'_{i\nu} + p_{i\nu}p'_{i\mu} + g_{\mu\nu}\frac{q^2}{2}](f_+^i(P.p_i) + f_-^i(P.p_i))\frac{1}{P\cdot q}\delta(x - x_i)$$
$$= \frac{1}{4}\sum_i x\frac{e_i^2}{m_i^2\nu}[p_{i\mu}p'_{i\nu} + p_{i\nu}p'_{i\mu} + g_{\mu\nu}\frac{q^2}{2}]q_i(x), \tag{2.40}$$

where the parton distribution $q(x)$, defined as the integral over the parton transverse momentum of the vertex functions f, is:

$$q_i(x) = \pi\int dp_\perp^2 (f_+^i(P.p) + f_-^i(P.p)). \tag{2.41}$$

It is then straightforward to get the structure functions in terms of the defined parton distributions. One may do it as we did it before, contracting $W_{\mu\nu}$ with the leptonic tensor and comparing with the cross section (2.19). Eq. (2.34) then follows.

For the antisymmetric part the procedure is similar and for details we refer the reader to the original work of Jackson, Ross and Roberts [44]. The important feature is that in a covariant calculation of the parton model, if we denote $g_2(x)$ of this calculation by $g_2^{ww}(x)$, one gets:

$$g_2^{ww}(x) = \int_x^1 \frac{dy}{y} g_1(y) - g_1(x). \tag{2.42}$$

It is then easy to get the Wandura-Wilczek [45] set of sum rules:

$$\int_0^1 dx x^{n-1}\left(\frac{n-1}{n}g_1(x) + g_2^{ww}(x)\right) = 0, \tag{2.43}$$

which were, originally, derived in the context of the OPE.

The just mentioned result disagrees with the naive expectation for $g_2(x)$ (=0) of last section. In the context of the operator product expansion, there is an extra contribution

to g_2 from the quark mass term [46]. In this case, g_2 is given by $g_2 = g_2^{ww} + \overline{g}_2$, where $\overline{g}_2$ is an extra contribution from the mass of the quark and quark-gluon interactions. In this context, it seems that in the naive approach of last section, g_2 is somehow contaminated by this extra contribution. In general terms, these conflicting results for g_2 go to the heart of the parton model formulation - the impulse approximation. Jaffe and Ji [38] argued that the problem with g_2 is directly related to the lack of off-shell partons in the naive parton model and Anselmino et al. [47] make a very simple extension of the present presentation where, when deriving Eq. (2.35), they allow p'^2 be on mass shell (free parton) but p^2 is the mass of some bound state. They argue that for longitudinal polarization the fact that the two masses are not the same is not relevant but for transverse polarization, the one that matters for g_2, this mass difference has an effect. Moreover, gauge invariance is broken. It seems to us that this arises from the fact the partonic interpretation of g_2 is not defined and any attempt to construct such a thing will lead to contradiction.

2.2.2 Partons as Quarks and Sum Rules

It seems a natural step to identify the partons with the quarks introduced by Gell-Mann [5] and Zweig [6] in 1964. In this case, the probability to find the i parton is interpreted as the probability to find a quark of a given flavour with a certain fraction of the nucleon momentum or helicity. From Eqs. (2.33) and (2.37) one then would have the following relations for the proton:

$$\begin{aligned} F_2^p(x) &= x\left[\frac{4}{9}(u(x)+\overline{u}(x)) + \frac{1}{9}(d(x)+\overline{d}(x)) + \frac{1}{9}(s(x)+\overline{s}(x)) + ...\right] \\ g_1^p(x) &= \frac{1}{2}\left[\frac{4}{9}(\delta u(x)+\delta\overline{u}(x)) + \frac{1}{9}(\delta d(x)+\delta\overline{d}(x)) + \frac{1}{9}(\delta s(x)+\delta\overline{s}(x)) + ...\right] \end{aligned} \quad (2.44)$$

where the notation used is quite obvious: $q(x)$ is the quark distribution and $\overline{q}(x)$ is the antiquark distribution. We can go further and break the distributions into distributions where the spin is aligned or antialigned with the proton: $q(x) = q^{\uparrow}(x) + q^{\downarrow}(x)$ and $\delta q(x) = q^{\uparrow}(x) - q^{\downarrow}(x)$. The parton model structure functions for the neutron can be determined by isospin symmetry: $u^p(x) = d^n(x)$, $d^p(x) = u^n(x)$, $\overline{u}^p(x) = \overline{d}^n(x)$, $\overline{d}^p(x) = \overline{u}^n(x)$ and the same for the polarized distributions.

The quark model is based on the assumption that nucleons are made of 3 quarks, mesons of 2 quarks, etc. In this sense, one usually defines the concept of valence (v) and sea (s) quarks with $q(x) = q_v(x) + q_s(x)$ and :

$$\begin{aligned} \int_0^1 dx u_v^p(x) &= \int_0^1 dx (u^p(x) - \overline{u}^p(x)) = 2, \\ \int_0^1 dx d_v^p(x) &= \int_0^1 dx (d^p(x) - \overline{d}^p(x)) = 1, \end{aligned} \tag{2.45}$$

which ensure that the proton is made of one d and two u quarks. It was also assumed that in the nucleon $q_s(x) = \overline{q}(x)$. This assumption is general and in particular it implies that the nucleon has no net strangeness:

$$\int_0^1 dx [s(x) - \overline{s}(x)] = 0. \tag{2.46}$$

Various others sum rules can be constructed for the structure functions. Here, we mention the most important ones:

- *The Bjorken sum rule*

This sum rule was derived in 1966 by Bjorken [48] using the algebra of currents. The parton model reproduces the results of Bjorken, showing the flexibility and power of the model:

$$\int_0^1 dx(g_1^p(x) - g_1^n(x)) = \frac{1}{6}(\delta u + \delta\overline{u} - \delta d - \delta\overline{d}) = \frac{1}{6}g_a. \tag{2.47}$$

The interesting aspect of this equation is that g_a is the neutron axial coupling constant while g_1 reflects the strong forces inside the nucleon. Thus, this sum rule relates weak and strong interactions and its verification is considered to be fundamental to the understanding of our view of nature (see, for instance, Feynman's book [9]). Its study has been subject to very intense experimental [49, 50, 51, 52, 53, 54] as well as theoretical [55, 56, 57, 58, 59, 60, 61] activity. We will return later to the study of this important subject.

- *The Gottfried sum rule*

This sum rule was derived by Gottfried [62] in 1967 using Gell-Mann's current algebra. It is an another major success of the parton model to obtain the same result:

$$\int_0^1 \frac{dx}{x}(F_2^p(x) - F_2^n(x)) = \frac{1}{3}, \tag{2.48}$$

where it was assumed that charge symmetry between proton and neutron holds and, most important, that the light sea in the nucleon is symmetric, e.g, $u_s(x) = d_s(x)$. In the next chapter we will study this assumption in some detail and see that there is experimental evidence [18, 19] against a symmetric sea. Thus, we are already getting a bonus from the partonic interpretation of inclusive reactions: it allows us to decompose the nucleon structure in great detail.

- *The Ellis-Jaffe sum rule*

In principle, as seen in Eq. (2.44), to know the value of g_1 one would need to know the value of the individual contributions from the various quark flavours present in the nucleon. Or in reverse, the measurement of g_1 alone would not allow us to know exactly the spin decomposition in terms of the individual quarks. Also, polarized scattering involving

deuterons or ^{3}He (to extract the neutron structure function and then to eliminate an extra variable) is a delicate experiment made available only recently. Ellis and Jaffe [63] proposed, back in 1974, a sum rule for polarized protons and neutrons separately. The main assumption made was that the sea quarks in the proton or neutron are not polarized. This means that:

$$\int_0^1 dx g_1^p(x) = \frac{1}{12}(\Delta u_v(x) - \Delta d_v(x)) + \frac{5}{36}(\Delta u_v(x) + \Delta d_v(x)) = \frac{1}{12} g_a + \frac{5}{36}\Delta q_8, \qquad (2.49)$$

with a similar expression for the neutron. The charge Δq_8 can be extracted from experiments on hyperon β-decay and then a quark model prediction for g_1 can be made. Again in reverse, the structure function can be measured and, together with the well established value for g_a, the value for the total spin of the quarks in the direction of the proton spin can be determined. This has been done [20, 52, 64] and the measured g_1 was found to be much smaller than predicted by Eq. (2.49). This result is known as the proton spin problem and it will be extensively studied throughout this thesis.

- *The Gross and Llewellyn Smith sum rule*

Up to now we dealt only with electromagnetic structure functions. Of course, we could also have treated the case where the incident lepton and the target interact via weak interactions. In this case, as discussed after Eq. (2.13), we would have an extra structure function, called F_3. Its derivation follows exactly the same route as presented before but now the exchanged particle is a charged W (charged current) or a neutral Z (neutral current). Details are provided, for instance, in the references [26, 65]. For charged currents, it is found that:

$$x F_3^{\overset{(-)}{\nu} p}(x) = xV(x) \pm x\Delta(x) \qquad (2.50)$$

where $V(x)$ stands for the valence quark distribution and $\Delta(x) = [\overline{c}(x) - \overline{s}(x)] + [c(x) - s(x)]$, if up to two quark generations are included. With this in mind, it is found that [66]:

$$\int_0^1 dx(F_3^{\bar{\nu}p}(x) + F_3^{\nu p}) = 6 \tag{2.51}$$

where the sum rules (2.45) were used. The above equation is known as the Gross and Llewellyn Smith [66] sum rule and its verification is a test of the assumption that the proton (or neutron) is built of 3 valence quarks. It has been tested [67, 68, 69, 70, 71, 72] and within QCD corrections, that we will be introduced soon, it appears to be verified [72].

- *Momentum sum rule*

If we multiply each quark distribution by x, the fraction of momentum that each flavour carries, we finish with the total momentum carried by quarks. If there are only quarks in the nucleon, then this sum necessarily should add to one:

$$\int_0^1 dx x[u(x) + \overline{u}(x) + d(x) + \overline{d}(x) + s(x) + \overline{s}(x) + ...] = 1. \tag{2.52}$$

It is easy to test this assumption if we remember the definition of the F_2 structure function, Eq. (2.44). If we consider up to three flavours, this leads us to [24]:

$$\int_0^1 dx x(u(x) + \overline{u}(x) + d(x) + \overline{d}(x) + s(x) + \overline{s}(x)) = \frac{9(1+\delta)}{5+2\delta} \int_0^1 dx(F_2^p(x) + F_2^n(x)), \tag{2.53}$$

where $\delta = \int_0^1 dx x[s(x)+\overline{s}(x)] / \int_0^1 dx x[u(x)+\overline{u}(x)+d(x)+\overline{d}(x)]$, is the fraction of momentum carried by strange quarks compared to nonstrange quarks. It happens that the measured F_2 structure function does not saturate Eq. (2.53) to one unless δ is unreasonably large [9]. Something is then missing. All the partons that are charged were already included in the derivation of F_2 meaning that the missing constituints are neutral and they are identified with gluons.

Many of the sum rules just mentioned will receive corrections when we depart from the simple quark model and take into account the fact that the partons/quarks are not free but

interacting. However, the main point is that the parton/quark model picture is intuitively simple and provides a good approximation to the observed quantities. The corrections to be added by QCD are fine but important tuning that both corroborate the model and help establish QCD as the theory of nucleon structure.

2.3 The Operator Product Expansion

We saw at the beginning of this chapter that the hadronic tensor is given by

$$\begin{aligned} W_{\mu\nu} &= \frac{1}{2\pi}\sum_{X,S}\frac{1}{2} < P,S|j_\mu(0)|X >< X|j_\nu(0)|P,S > (2\pi)^4\delta^4(p_X - P - q) \\ &= \frac{1}{2\pi}\sum_{X,S}\int d^4z e^{i(p_X - P - q).z}\frac{1}{2} < P,S|e^{-i\hat{P}.z}j_\mu(z)e^{i\hat{P}.z}|X >< X|j_\nu(0)|P,S > \\ &= \frac{1}{2\pi}\int d^4z e^{iq.z}\frac{1}{2}\sum_S < P,S|[j_\mu(z), j_\nu(0)]|P,S >, \end{aligned} \tag{2.54}$$

because $\int d^4z e^{iq.z} < P|j_\mu(0)j_\nu(x)|P >= \sum_X < P|j_\mu(0)|X >< X|j_\nu(0)|P > (2\pi)^4\delta^4(q - P + p_X) = 0$ ($p_X = P - q$, because the final state would have a smaller mass than the initial state).

The interesting aspect of representing the hadronic tensor through the commutator of currents is that we can easily see which region dominates the physics of deep inelastic scattering. First, by causality, we have that $[j_\mu(z), j_\nu(0)] = 0$ for $z^2 < 0$. On the other hand, the Riemann-Lebesgue lemma [73] says that if a function $f(q)$ is an ordinary function, absolutely integrable, and $g(x)$ is its Fourier transform, then $g(z) \to 0$ as $|z| \to \infty$. This means that the main contribution in $W_{\mu\nu}$ comes from the region where $q.z$ is finite. To see where exactly this contribution is, consider the lepton nucleon scattering in the target rest frame where the photon momentum transfer is $q = (\nu, 0, 0, -\sqrt{\nu^2 + Q^2})$. In this case, if we

take the Bjorken limit, the light cone coordinates are $q^+ = \frac{1}{\sqrt{2}}(q^0 + q^3) \sim -Mx/\sqrt{2}$ and $q^- = \frac{1}{\sqrt{2}}(q^0 - q^3) \sim \sqrt{2}\nu$. We then have that $q.z = q^+z^- + q^-z^+$ is finite if and only if $z^- \sim 1/x$ and $z^+ \sim 1/\nu$. As $z^2 = 2z^+z^- - z_\perp^2 \geq 0$ by causality, $z_\perp^2 \sim 0$ in the Bjorken limit as z^+z^- itself goes to zero in that limit. Hence, $z^2 \sim 0$. In this sense, $W_{\mu\nu}$ and deep inelastic scattering is said to be light-cone dominated.

The problem with light-cone dominance is that the commutator of currents is not well defined in that region [4, 74] as can be seen from the following. If the commutator of currents is explicitly evaluated with, say, $j_\mu = \overline{\psi}(x)\gamma_\mu\psi(x)$, we have:

$$[j_\mu(z), j_\nu(0)] \propto S(z) \tag{2.55}$$

where $S(z) = (i\not{\partial} + m)\Delta(z)$. For $z^2 \sim 0$, it is found that [28, 23, 4, 74, 75]:

$$\Delta(z) = \frac{1}{4\pi^2}\frac{1}{z^2 - i\epsilon} + \textit{less singular terms.} \tag{2.56}$$

Thus the commutator is in fact divergent on the light cone. In general, the product of any two fields at the same space time point (called a composite operator) is divergent [4]. The general procedure to deal with these singularities is due to Wilson [15] and it is what is meant by the Operator Product Expansion (OPE).

To systematically study the product of currents in DIS we will employ the forward scattering virtual Compton amplitude $T_{\mu\nu}$:

$$T_{\mu\nu} = i\int d^4z e^{iq.z} < P|T[j_\mu(z)j_\nu(0)]|P > \tag{2.57}$$

where a simplified notation, $< P|...|P >= \frac{1}{2}\sum_S < P, S|...|P, S >$, was introduced. There is no real reason to work with this virtual amplitude and we do it just to follow the majority of

authors. Also, due to some properties of $T_{\mu\nu}$ it is often convenient to perform integrations. The main properties of $T_{\mu\nu}$ are [40, 76]:

- It has the crossing symmetry property: $T_{\mu\nu}(q^2,\nu) = T_{\nu\mu}(q^2,-\nu)$.
- It is an analytic function: $T_{\mu\nu}(q^2,\nu^*) = T^*_{\mu\nu}(q^2,\nu)$. As a matter of fact, it is analytic only in the points where the states described by T are physical [40]. This means that the region $w = 2M\nu/Q^2 \geq 1$ (and $w \leq 1$ as seen from crossing symmetry) are not analytic.

The relation between $W_{\mu\nu}$ and $T_{\mu\nu}$ is given by:

$$W_{\mu\nu} = \frac{1}{2i}[T_{\mu\nu}(q_0 + i\epsilon) - T_{\mu\nu}(q_0 - i\epsilon)] = \frac{1}{\pi} Abs T_{\mu\nu}. \tag{2.58}$$

There is also a very useful integral relating $T_{\mu\nu}$ and $W_{\mu\nu}$. By the Cauchy theorem, the integral over a closed path of an analytic function is zero. In the case of $T_{\mu\nu}$ we noticed before that this function has poles at $w = \pm 1$ and branch cuts for $w \geq 1$ and $w \leq -1$. If we then integrate $T_{\mu\nu}$ over the path show in figure 2.4, four integrals have to be done: $\int_c \frac{1}{w^m} T_{\mu\nu} dw = \int_{1,up}^{\infty} \frac{1}{w^m} T_{\mu\nu} dw + \int_{-\infty,up}^{-1} \frac{1}{w^m} T_{\mu\nu} dw + \int_{-1,down}^{-\infty} \frac{1}{w^m} T_{\mu\nu} dw + \int_{\infty,down}^{1} \frac{1}{w^m} T_{\mu\nu} dw$. For m even, using crossing symmetry, we see that the real part of $T_{\mu\nu}$ from the up and down planes cancels and the imaginary part sums up. We then get:

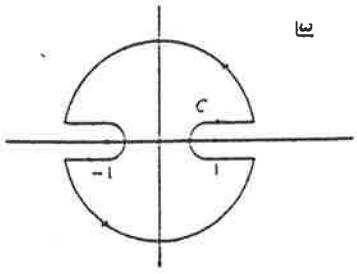

Figure 2.4: Path of integration in the complex ν plane.

$$\frac{1}{2\pi i}\int_c \frac{1}{w^m} T_{\mu\nu} dw = \frac{2}{\pi}\int_1^\infty \frac{1}{w^m} AbsT_{\mu\nu} dw = 2\int_0^1 dx x^{m-2} W_{\mu\nu}. \tag{2.59}$$

Another useful integral is:

$$\frac{1}{2\pi i}\int_c dw w^{n-m} = \delta_{n,m-1} \tag{2.60}$$

The OPE, as first developed by Wilson [15], employed the expansion for short distances only. The idea behind this is that the product of any two operators can be expanded in a series of well defined local operators, O, multiplied by some singular c-numbers, C, known as the Wilson coefficients, organized in order of singularity (the first term in the expansion is the most singular and so on):

$$T[j_\mu(z_1) j_\nu(z_2)] \longrightarrow \sum_i C_i(0) O_i(z), \tag{2.61}$$

as z_1, $z_2 \to z$. This expansion was proven by Zimmermann [17, 77] in the context of perturbation theory. In the specific case of DIS, we need an expansion for the light cone and not for short distances. The generalization to the light cone expansion can be found in the works of Brandt and Preparata [16] as well as Zimmermann [77]:

$$T[j_\mu(z) j_\nu(0)] \longrightarrow \sum_{n=0}^{\infty} i^{n-1} C_i^n(z^2 - i\epsilon) z^{\mu_1} z^{\mu_2} ... z^{\mu_n} O^{i,n}_{\mu_1\mu_2...\mu_n}(0), as \;\; z^2 \to 0 \tag{2.62}$$

and where we promoted a small change of notation in comparison with (2.61) for reasons of convenience. The index i labels the various different operators that can have the same quantum numbers as the product of currents for each n in the expansion. The contrast with the short distance expansion is that the light cone expansion involves a sum that goes to infinity [16]. The various operators with the same quantum numbers as the product of

currents can be organized in what is called the " twist" of an operator. To see that, consider the mass dimension of the Wilson coefficients. If d_J is the mass dimension of the current j, d_o the mass dimension of the operator O and n the mass dimension of the product $z^{\mu_1}z^{\mu_2}...z^{\mu_n}$, then the mass dimension of the coefficients C has to be:

$$[C^n] = 2d_j + n - d_o = 2d_j - \tau, \tag{2.63}$$

where $\tau = d_o - n$ is defined as the twist of a given operator O. The smaller the twist of an operator, the more singular the coefficient is. It is easy to see that the smallest possible twist for a composite operator is 2. One of the simplest gauge invariant operator for O that we can think of is $\overline{\psi}\gamma_\mu\psi$, that has twist 2 (according to (2.62), $n = 1$ and $d_\psi = 3/2$). We can add derivatives to this simplest operator and still preserve its twist. The general twist 2 operator involving fermions would then be [12]:

$$O^n_{\mu_1\mu_2...\mu_n} = i^{n-1}S\overline{\psi}\gamma_{\mu_1}D_{\mu_2}...D_{\mu_n}\psi, \tag{2.64}$$

where D_μ is the covariant derivative and S is a permutation over the Lorentz indices and the factors i were introduced for convenience when deriving Feynman rules for vertices involving the composite operators. In QCD, ψ are the quark fields and we see from the last expression that there is no distinction over quark flavors. Such operators are called singlets. In contrast, we can also have twist 2 operators that are not invariant under flavor transformations. These are called nonsinglet [12]:

$$O^{j,n}_{\mu_1...\mu_n} = i^{n-1}S\overline{\psi}\gamma_{\mu_1}D_{\mu_2}...D_{\mu_n}\frac{\lambda^j}{2}\psi, \tag{2.65}$$

where the λ^j are the Gell-Mann matrices. Similarly, a twist 2 gluon operator can be constructed:

$$O^G_{\mu\nu} = \frac{1}{2} S G_{\mu\alpha} G^{\alpha}_{\nu}, \tag{2.66}$$

and its generalization [12]:

$$O^G_{\mu_1 \ldots \mu_n} = \frac{i^{n-2}}{2} S G_{\mu_1 \alpha} D_{\mu_2} \ldots D_{\mu_{n-1}} G^{\alpha}_{\mu_n}. \tag{2.67}$$

We now work with the specific example of the product of two electromagnetic currents. The most general form for this product, in coordinate space, is given by [78]:

$$\begin{aligned} T[j_\mu(z) j_\nu(0)] \;=\; & -(g_{\mu\nu}\Box - \partial_\mu \partial\nu) O_L + \\ & (g_{\mu\lambda}\partial_\rho \partial_\nu + g_{\rho\nu}\partial_\mu \partial_\lambda - g_{\mu\lambda} g_{\rho\nu}\Box - g_{\mu\nu}\partial_\rho \partial_\lambda) O_2^{\lambda\rho} \\ & -i\varepsilon_{\mu\nu\lambda\rho}\partial^\lambda R_1^\rho - i(\partial_\nu \varepsilon_{\mu\sigma\lambda\rho}\partial^\sigma - \partial_\mu \varepsilon_{\nu\lambda\rho\sigma}\partial^\sigma - \Box \varepsilon_{\mu\nu\lambda\rho}) R_2^{\lambda\rho} \end{aligned} \tag{2.68}$$

Similarly to the unpolarized operators O, polarized operators R were introduced. As before, we have the twist 2 tower of operators [78, 79, 31]:

$$\begin{aligned} R^{1,n}_{\mu\mu_1 \ldots \mu_{n-1}} &= i^{n-1} S \overline{\psi} \gamma_5 \gamma_\mu D_{\mu_1} \ldots D_{\mu_{n-1}} \psi, \\ R^{1,j,n}_{\mu\mu_1 \ldots \mu_{n-1}} &= i^{n-1} S \overline{\psi} \gamma_5 \gamma_\mu D_{\mu_1} \ldots D_{\mu_{n-1}} \frac{\lambda^j}{2} \psi, \\ R^{1,G}_{\mu\mu_1 \ldots \mu_{n-1}} &= \frac{i^{n-1}}{2} S \varepsilon_{\mu\nu\alpha\beta} G^{\alpha\beta} D_{\mu_1} \ldots D_{\mu_{n-2}} G^{\nu}_{\mu_{n-1}}. \end{aligned} \tag{2.69}$$

For R_2, the leading operators are twist 3 [78, 79, 31]:

$$\begin{aligned} R^{2,n,F}_{\mu\mu_1 \ldots \mu_{n-1}} &= \frac{i^{n-1}}{n} [(n-1) \overline{\psi} \gamma_5 \gamma_\mu D_{\{\mu_1} \ldots D_{\mu_{n-1}\}} \psi - \sum_{l=1}^{n-1} \overline{\psi} \gamma_5 \gamma_{\mu_l} D_{\{\mu} D_{\mu_1} \ldots D_{\mu_{l-1}} D_{\mu_{l+1}} \ldots D_{\mu_{n-1}\}} \psi], \\ R^{2,n,m}_{\mu\mu_1 \ldots \mu_{n-1}} &= i^{n-2} m \overline{\psi} \gamma_5 \gamma_\mu D_{\{\mu_1} \ldots D_{\mu_{n-2}} \gamma_{\mu_{n-1}\}} \psi, \\ R^{2,n,j}_{\mu\mu_1 \ldots \mu_{n-1}} &= \frac{1}{2n} (V_j - V_{n-1-j} + U_j + U_{n-1-j}), \end{aligned} \tag{2.70}$$

where

$$\begin{aligned} V_j &= i^n g\overline{\psi}\gamma_5 D_{\mu_1}...G_{\mu\mu_j}...D_{\mu_{n-2}}\gamma_{\mu_{n-1}}\psi \\ U_j &= i^{n-3} g\overline{\psi}\gamma_5 D_{\mu_1}...\tilde{G}_{\mu\mu_j}...D_{\mu_{n-2}}\gamma_{\mu_{n-1}}\psi, \end{aligned} \tag{2.71}$$

and $\{\}$ denotes symmetrization over the Lorentz indexes.

We first restrict ourselves to the unpolarized sector, involving the O operators. The operator product expansion applied to them yields:

$$\begin{aligned} O_L(z,0) &= \sum_{n,i} i^{n-1} C_L^{n,i}(z^2 - i\epsilon) O^{i,L}_{\mu_1...\mu_n} z_{\mu_1}...z_{\mu_n} \\ O_2(z,0) &= \sum_{n,i} i^{n-1} C_2^{n,i}(z^2 - i\epsilon) O^{i,2}_{\mu_1...\mu_n} z_{\mu_1}...z_{\mu_n}. \end{aligned} \tag{2.72}$$

When inserting Eqs. (2.68) and (2.72) in the expression for $T_{\mu\nu}$ and then perform the Fourier transform, it will be extremely convenient to express the z_{μ_j} in terms of derivatives. We then make the following replacement:

$$z_{\mu_1}...z_{\mu_n} \to (-i)^n \frac{\partial}{\partial q^{\mu_1}}...\frac{\partial}{\partial q^{\mu_n}} = (-2i)^n q_{\mu_1}...q_{\mu_n}\left(\frac{\partial}{\partial q^2}\right)^n \tag{2.73}$$

The unpolarized part of $T_{\mu\nu}$ is then written as:

$$\begin{aligned} T_{\mu\nu} &= \int d^4z \sum_{n,i} \Big\{ (...) C_L^{n,i}(z^2 - i\epsilon) < P|O^{i,L}_{\mu_1...\mu_n}|P > (-2)^n q_{\mu_1}...q_{\mu_n}\left(\frac{\partial}{\partial q^2}\right)^n \\ &+ (...)^{\lambda\rho} C_2^{n,i}(z^2 - i\epsilon) < P|O^{i,2}_{\lambda\rho\mu_1...\mu_n}|P > (-2)^n q_{\mu_1}...q_{\mu_n}\left(\frac{\partial}{\partial q^2}\right)^n \Big\} e^{iq.z}. \end{aligned} \tag{2.74}$$

The matrix elements of the O operators have, necessarily, to be a function of the momenta P. Their general form is [76]:

$$
\begin{aligned}
< P|O^{i,L}_{\mu_1 \ldots \mu_n}|P > &= A^{i,L}_n P_{\mu_1} \ldots P_{\mu_n} \\
< P|O^{i,2}_{\lambda\rho\mu_1 \ldots \mu_n}|P > &= A^{i,2}_{n+2} P_{\mu_1} \ldots P_{\mu_n} P_\lambda P_\rho .
\end{aligned} \tag{2.75}
$$

Of course, both matrix elements also contain a sum of terms of the kind $P^2 g_{\mu_1\mu_2} P_{\mu_3} \ldots P_{\mu_n}$ and others with two or more metric tensors. But in the Bjorken limit these terms vanish in comparison with the the dominant term shown in expressions (2.75). $T_{\mu\nu}$ is then written as:

$$
\begin{aligned}
T_{\mu\nu} &= \sum_{n,i} \left\{ (q_\mu q\nu - q^2 g_{\mu\nu})(-2P.q)^n A^{i,L}_n \left(\frac{\partial}{\partial q^2}\right)^n \int d^4 z C^{n,i}_L (z^2 - i\epsilon) e^{iq.z} \right. \\
&+ \left. (P.q P_\mu q_\nu + P.q q_\mu P_\nu - q^2 P_\mu P_\nu - g_{\mu\nu}(P.q)^2)(-2P.q)^n A^{i,2}_{n+2} \left(\frac{\partial}{\partial q^2}\right)^n \int d^4 z C^{n,i}_2 (z^2 - i\epsilon) e^{iq.z} \right\} \\
&= \sum_{n,i} \left\{ -e_{\mu\nu} w^n (q^2)^{n+1} A^{i,L}_n \left(\frac{\partial}{\partial q^2}\right)^n \int d^4 z C^{n,i}_L (z^2 - i\epsilon) e^{iq.z} \right. \\
&+ \left. d_{\mu\nu} w^{n+2} \frac{(q^2)^{n+2}}{4} A^{i,2}_{n+2} \left(\frac{\partial}{\partial q^2}\right)^n \int d^4 z C^{n,i}_2 (z^2 - i\epsilon) e^{iq.z} \right\},
\end{aligned} \tag{2.76}
$$

where

$$
\begin{aligned}
e_{\mu\nu} &= -\frac{q_\mu q_\nu}{q^2} + g_{\mu\nu} \\
d_{\mu\nu} &= (P_\mu q_\nu + P_\nu q_\mu)\frac{1}{P.q} - \frac{q^2}{(P.q)^2} P_\mu P_\nu - g_{\mu\nu}.
\end{aligned} \tag{2.77}
$$

We now notice that in the case of free fields, the coefficients C are well known [76, 74]:

$$
\begin{aligned}
C^{free}_2(z^2 - i\epsilon) &\propto \frac{1}{(z^2 - i\epsilon)} \Rightarrow \int d^4 z e^{-iq.z} \frac{1}{(z^2 - i\epsilon)} \propto \frac{1}{(q^2 + i\epsilon)} \\
C^{free}_L(z^2 - i\epsilon) &\propto \frac{1}{(z^2 - i\epsilon)^2} \Rightarrow \int d^4 z e^{-iq.z} \frac{1}{(z^2 - i\epsilon)^2} \propto -log(q^2 + i\epsilon).
\end{aligned} \tag{2.78}
$$

Based on this, we define the following Fourier transform for the general Wilson coefficients:

$$\begin{aligned} C_2^{n+2,i}(q^2) &= \frac{(q^2)^{n+2}}{8}\left(\frac{\partial}{\partial q^2}\right)^n \int d^4z C_2^{n,i}(z^2 - i\epsilon)e^{iq.z} \\ C_L^{n,i}(q^2) &= -\frac{(q^2)^{n+1}}{2}\left(\frac{\partial}{\partial q^2}\right)^n \int d^4z C_L^{n,i}(z^2 - i\epsilon)e^{iq.z}. \end{aligned} \tag{2.79}$$

So:

$$T_{\mu\nu} = 2\sum_{n,i}\left\{e_{\mu\nu}w^n A_n^{i,L}C_n^{i,L}(q^2) + d_{\mu\nu}w^{n+2}A_{n+2}^{i,2}C_{n+2}^{1,2}(q^2)\right\}, \tag{2.80}$$

where n is even by crossing symmetry.

On the other hand, the hadronic tensor is rewritten with the help of Eqs. (2.14), (2.29) and (2.77) as:

$$\begin{aligned} W_{\mu\nu} &= \frac{1}{x}e_{\mu\nu}[F_2 - 2xF_1] + \frac{1}{x}d_{\mu\nu}F_2 \\ &= \frac{1}{x}e_{\mu\nu}F_L + \frac{1}{x}d_{\mu\nu}F_2, \end{aligned} \tag{2.81}$$

where the longitudinal structure function, F_L, was defined. Also notice that we took out the factor $2M$ from the denominator of the hadronic tensor, thus changing our convention in order to agree with the definition of $T_{\mu\nu}$.

It is now easy to find an expression for the integrals of the structure functions F in terms of the Wilson coefficients if we use Eqs. (2.59) and (2.60)[3]:

[3]With a slight modification in the power m

$$\begin{aligned}\int_0^1 dx x^{n-2} F_L(x,Q^2) &= \sum_i A_n^{i,L} C_n^{i,L}(Q^2), \quad n=0,2,4,...\\ \int_0^1 dx x^{n-2} F_2(x,Q^2) &= \sum_i A_n^{i,2} C_n^{i,2}(Q^2). \quad n=0,2,4,...\end{aligned} \tag{2.82}$$

For the antisymmetric part of the expansion of the product of currents, Eq. (2.68), a similar treatment can be performed. The operators R_1 and R_2 are expanded in the same way as the unpolarized operators, Eq. (2.72), and are proportional to the Wilson coefficients which in this case we denote by E. Following the same steps as before, one gets [78, 79]:

$$\begin{aligned}\int_0^1 dx x^n g_1(x,Q^2) &= \sum_i A_n^{i,1} E_n^{i,1}(Q^2), \quad n=0,2,4,...\\ \int_0^1 dx x^n g_2(x,Q^2) &= \sum_i \frac{n}{n+1}(A_n^{i,2} E_n^{i,2}(Q^2) - A_n^{i,1} E_n^{i,1}(Q^2)), \quad n=2,4,...\end{aligned} \tag{2.83}$$

In particular, if no twist 3 were present, $E^{i,2} = 0$ and one would recover Eq. (2.43), the Wandura-Wilzeck set of sum rules [45]. If we call, as we did before, the twist 2 piece of g_2 of g_2^{ww}, we would get the Burkhardt-Cottingham (BC) sum rule [80] ($\int_0^1 g_2(x)dx = 0$) for the twist 2 piece: $\int_0^1 g_2^{ww}(x)dx = 0$. As the full g_2 is $g_2^{ww} + \overline{g}_2$, where $\overline{g}_2$ is the twist three contribution, we would have that $\int_0^1 dx \overline{g}_2(x) = 0$ itself - a conclusion only supported by completely inconclusive experiments on the transverse asymmetry [32, 81], where the integral of $\overline{g}_2(x)$ is compatible with zero and also with the integral of g_2^{ww} itself. This matter is the object of much discussion in the literature [46, 38, 39, 47]. There is no clear agreement about the validity of the BC sum rule in the OPE because, while the moment of g_2 in Eq. (2.83) is not defined for $n = 0$, in the partonic language of Altarelli and Parisi [82], where the x dependence of the structure functions are calculated, it seems that the BC sum rule

is valid at least up to two loops in perturbative QCD [39, 83]. If the two approaches are to be equivalent, then the BC sum rule should also be valid in the OPE approach. This is one of the examples of the advantages and disadvantages of the OPE approach compared with other approaches to perturbative QCD, like the parton model of Altarelli-Parisi which we will see in some detail in the chapters ahead.

Recently, Roberts and Ross [84] proposed a solution to the disagreement between the naive parton model, the covariant parton model and the OPE results for g_2. As we saw before, in the naive parton model one calculates the partonic tensor and, by comparison to the general form of the hadronic tensor, one gets $g_2(x) = 0$. Moreover, in this case the partons have to have a mass as we cannot use the relativistic approximation $s^\mu = p^\mu/m$ because in this case the coefficient of g_2 in the hadronic tensor would vanish. On the other hand, an analysis [84] of the twist 3 piece of the OPE in a valence approximation (no gluons) shows that the remaining twist 3 piece (due to the mass of the partons) and the twist 2 piece exactly cancel - thus rendering the naive quark model result. This is a rich topic and we will explore it somewhat more when we go deeper in the study of the longitudinal structure function, g_1. On the other hand, when calculating g_2 in a covariant parton model, the relativistic approximation for the partons can be used resulting in the vanishing of all twist 3 contributions. Hence, only the twist 2 survives and the well known Wandura-Wilzeck [45] results follow.

2.4 The Renormalization Group

In the last section it was implicitly assumed that all quantities involved are already the renormalized ones. In this case, some useful information can be obtained about, for instance, the Wilson coefficients if one employs the analysis of the renormalization group [85, 86, 87,

88].

In general terms, quantum field theories, like QCD, are constructed upon two main pillars: gauge invariance and renormalizability. The point is that any renormalization introduces an extra, artificial, mass scale in the theory. This can be seen from the following. The need for renormalization comes from the fact that when calculating quantities of physical interest, the integrals over momentum space diverge. There are many ways to regularize (isolate the divergent piece) like the Pauli-Villars [89] or minimal subtraction [90] methods and subsequently subtract this divergent piece using, for instance, on-shell or minimal subtraction renormalization schemes. But, invariably, all different ways of regularization induce a mass scale dependence that reflects where exactly the subtraction of the divergence will be done. In this sense, the renormalized quantities depend in principle on the renormalization point μ. The same, by construction, does not happen with the unrenormalized quantities. In addition, as the introduced renormalization point is arbitrary, no observable is allowed to depend on it.

The mentioned divergences appear when we use perturbation theory. This means that if we go to higher orders in perturbation theory, more integrals and hence more subtractions will have to be done. Renormalization is achieved if we can make a redefinition of a finite number of quantities like the fields, currents, coupling constants, Green functions etc and this redefinition is enough to make the integrals finite up to any order. One way to do it is to make use of renormalization constants Z:

$$J = Z_3^{1/2} J^0, \quad \psi = Z_2^{1/2} \psi^0, \quad g = Z_g^{-1} g^0, \quad etc \tag{2.84}$$

where 0 labels the unrenormalized quantities, J is a current, ψ is a fermion field and g a coupling constant. It is worth noticing that the renormalization constants are infinite

numbers! They are dropped in the end when the subtraction is made but still we have an intermediate stage of the calculation where we are summing and subtracting infinities.

The Wilson coefficients introduced before are a function of the mass scale introduced by renormalization as are the set of operators O. We can take advantage of this fact and study the dependence of these quantities on the scale. This is a fortunate situation because as a result, it means that if we know these renormalized quantities at some scale, then we can predict their behaviour at any other scale (provided perturbation theory is valid in the region in question). To this end, we remember that the unrenormalized quantities are independent of μ. We also remember that, according to the operator product expansion, the product of currents has always a form like follows [65]:

$$< |JJ| >= \sum_n C_n < |O^n| >, \tag{2.85}$$

where C_n refers to any Wilson coefficient (not only the unpolarized ones of last section) but we are restricting here to the case where there is no mixing of the operators O^n under renormalization. As seen before, we classified the operators, as nonsinglet and singlet. For the singlet case we had two kinds of operators - the quark singlet (2.64) and the gluon (2.67). As they have the same quantum numbers, there is no way to distinguish them when renormalizing [91]. Thus, they are not multiplicatively renormalizable and mix under renormalization. The nonsinglet operator is unique and hence does not mix with any other. We then have:

$$\begin{aligned} \frac{d}{d\mu}[_0< |J^0J^0| >_0] &= \frac{d}{d\mu}[Z_2^{-1}Z_3^{-1} < |JJ| >] = 0 \\ \Rightarrow \quad & [\mu\frac{\partial}{\partial\mu} + \beta(g)\frac{\partial}{\partial g} - 2\gamma_\psi - 2\gamma_j] < |JJ| >= 0, \end{aligned} \tag{2.86}$$

where

$$\begin{aligned} \gamma_\psi &= \frac{1}{2}\mu\frac{\partial ln Z_2}{\partial \mu}, \\ \gamma_j &= \frac{1}{2}\mu\frac{\partial ln Z_3}{\partial \mu}, \end{aligned} \tag{2.87}$$

are defined as the anomalous dimensions of the fermion and of the current, respectively, and

$$\beta(g) = \mu\frac{\partial g}{\partial \mu}, \tag{2.88}$$

is defined as the beta function.

We follow the same procedure for the operator O^n:

$$\begin{aligned} \frac{d}{d\mu}[_0< |O^{n,0}| >_0] &= \frac{d}{d\mu}[Z_2^{-1} Z_o^n < |O^n| >] = 0 \\ \Rightarrow \quad & [\mu\frac{\partial}{\partial \mu} + \beta(g)\frac{\partial}{\partial g} - 2\gamma_\psi + \gamma_o^n] < |O^n| >= 0, \end{aligned} \tag{2.89}$$

where we introduced the renormalization constant of the nonsinglet operator O, $O^{n,0} = Z_o^n O^n$, and $\gamma_o^n = \mu\frac{\partial ln Z_o^n}{\partial \mu}$ is its anomalous dimension. If we now use Eqs. (2.85) and (2.89) in Eq. (2.86), and notice that $< |O^n| >\neq 0$, we have for each n that:

$$[\mu\frac{\partial}{\partial \mu} + \beta(g)\frac{\partial}{\partial g} - \gamma_o^n]C^n(Q^2, \mu^2, g^2) = 0, \tag{2.90}$$

where we used the fact that for conserved currents (like the EM current of our case), $Z_3 = 1$ and thus its anomalous dimension is zero [91]. We point out that some calculations in two loops and higher involving axial currents, generate an extra contribution to the current giving rise to what is known as the axial anomaly [92]. In this case, as shown by Kodaira [93], the

anomalous dimension is not zero. We will come back to this important issue later when studying in detail the spin content of the nucleon.

Eq. (2.90) has a very simple solution if we notice the following. Let $t = \frac{1}{2} ln(Q^2/\mu^2)$ and $\overline{g}(\mu^2) = \overline{g}(t = 0) = g$, such that:

$$\frac{d}{dt}\overline{g}(t) = \beta(\overline{g}) \Rightarrow t = \int_{\overline{g}(\mu^2)}^{\overline{g}(Q^2)} \frac{dg}{\beta(g)}. \tag{2.91}$$

If we change g to $\overline{g}(t)$ in Eq. (2.90) we then get:

$$\begin{aligned} C_n(Q^2, \mu^2, g^2) &= C_n(1, \overline{g}^2) exp\left[- \int_0^t dt' \gamma_o^n(\overline{g}(t', g)) \right] \\ &= C_n(1, \overline{g}^2) exp\left[- \int_{\overline{g}(\mu^2)}^{\overline{g}(Q^2)} dg' \frac{\gamma_o^n(g')}{\beta(g')} \right]. \end{aligned} \tag{2.92}$$

The study of the solutions of the renormalization group equations in QCD by Gross and Wilczek [12] and Georgi and Politzer [13, 14] opened up the possibility of extensive use of perturbation theory in that theory. This can be seen in the following way. In a minimal subtraction scheme, we have [90] $g \rightarrow g\mu^\epsilon$ and $g_0 \rightarrow g_0 \mu_0^\epsilon$, where the couplings now are nondimensional and ϵ is the dimension shift. With the help of Eqs. (2.84) and (2.88), we then get $\beta = -\epsilon g - \mu \frac{dlnZ_g}{d\mu} g$. The authors of refs. [12, 13, 14] calculated Z_g and their results lead to:

$$\beta(g) = -\frac{33 - 2N_f}{3} \frac{g^3}{(4\pi)^2} + O(g^5) \equiv -\beta_0 \frac{g^3}{(4\pi)^2} + O(g^5), \tag{2.93}$$

where N_f is the number of flavors. The use of this solution in Eq. (2.91) provides the following equation for the running coupling constant $\overline{g}$:

$$\overline{g}^2(Q^2) = \frac{\overline{g}^2(\mu^2)}{1 + \beta_0 \frac{\overline{g}^2(\mu^2)}{(4\pi)^2} ln(Q^2/\mu^2)}. \tag{2.94}$$

This expression is usually rewritten as:

$$\alpha_s(Q^2) = \frac{4\pi}{\beta_0 ln(Q^2/\Lambda^2)}, \tag{2.95}$$

where $\alpha_s = \overline{g}^2/4\pi$ and $\Lambda^2 = \mu^2 exp[-(4\pi/\beta_0\alpha_s(\mu^2)]$ is a free parameter in QCD, known as the scale parameter. From this solution, QCD is said to be asymptotically free because the coupling goes to zero as $Q^2 \to \infty$. This is a very important result and it is due to properties of the beta function. One can verify that asymptotic freedom holds as long as $\beta_0 > 0$, which can be achieved as long as $N_f < 16$ and even in the absence of quarks. In the other hand, any theory that has $\beta_0 < 0$ does not have asymptotic freedom, as is the case for quantum electrodynamics [94]. A nice treatment of the subject can be found in Muta's book [4].

We now turn to the case of singlet operators. In this case, we have to worry about mixing in the renormalization of the operators involved [65, 91]. If we denote the two set of singlet operators (quark singlet and gluon) by a column matrix, then the renormalization constant is a 2×2 matrix [65]:

$$O_i^n = \sum \left(\frac{1}{Z^n}\right)_{ab} O_b^{n,0}, \;\; i,j = \psi, \; gluon. \tag{2.96}$$

To get an equation for the singlet Wilson coefficients we follow the same steps as for the nonsinglet case just noticing that we are now dealing with matrices and that $< j|JJ|j >= \sum_{n,i} C_n^i O_{i,j}^n$. We then get:

$$[\mu\frac{\partial}{\partial\mu} + \beta(g)\frac{\partial}{\partial g}]C_n^i(Q^2/\mu^2, g^2) = \sum_j \gamma_n^{ji} C_n^j(Q^2/\mu^2, g^2) \tag{2.97}$$

Similar to the nonsinglet case, the solution of (2.97) is:

$$C_n^i(Q^2/\mu^2, g^2) = \sum_j C_n^j(1, \overline{g}^2) \left\{ Texp \left[- \int_0^t dt' \gamma_o^n(\overline{g}(t', g)) \right] \right\}^{ij}, \tag{2.98}$$

where the T product is $Texp \int dt F(t) = 1 + \int dt F(t) + \int dt \int dt' F(t)F(t') + ...$ because , in general, $[F(t), F(t')] \neq 0$.

It is worthwhile to stress that the Wilson coefficients are fully calculable in perturbation theory [76, 12, 13, 14, 79, 95, 65] and are, of course, dependent on the particular structure function studied but independent of target while the constants A_n, defined in (2.75), depend on the specific target. Moreover, as the operators are renormalized they will depend on the renormalization scale μ^2. As a consequence, $A_n = A_n(\mu^2)$.

With the solutions for the Wilson coefficients as given by the renormalization group we complete our study of basic tools of deep inelastic scattering. We started from the cross section for scattering between a lepton and a nucleon in terms of unknown structure functions and ended up with some integrals of these structure functions, Eqs. (2.82) and (2.83), in terms of, again, some unknown constants A_n. It may seem that we did not achieve much as we started and ended with unknown quantities. The difference is that we saw various ways to constrain such quantities through, for instance, the parton model. Take the case of the Ellis and Jaffe sum rule [63], Eq. (2.49), where the integral of g_1 is proportional to the helicity carried by quarks. The solutions of the renormalization group equations, Eqs. (2.92) and (2.98), tell us that if we know this helicity partition at some scale, we know it at any other scale. This is real progress. The same is true for any other structure function. For example, we learned that specific measurements can tell us about the valence quark structure of the nucleon or about the sea flavour - another real gain. Of course, we would like to calculate the constants A_n in QCD. This looks, at present, impossible as the hadron wave functions are not known. The maximum that can be done is model such

wave functions and hence calculate the A_n. Again, the integrals for the structure functions are vital because if experiments are performed at some scale, these wave functions can be constrained at the scale μ^2, in a procedure that could be more effective if μ^2 were not, itself, a (quasi) free parameter. We can conclude this chapter with the idea in mind that deep inelastic experiments in conjunction with the parton/quark model interpretation of such experiments plus the OPE and renormalization group analysis, allow us to track down the nucleon structure in great detail. This subject is the main interest of the present work.

Chapter 3

The Quark Sea in the Nucleon

3.1 Introduction

In this chapter we shall be concerned with the flavour structure of the unpolarized nucleon sea. We will center our discussion on the sea because the valence structure is relatively well established. For example, the Gross-Llewellyn Smith sum rule [66] seems to be well verified [72] and confirms the quark model assumption that the nucleon has three valence quarks. On the other hand, things do not look so settled when antiquarks, particularly antiquarks of different flavours, come into play. We will develop here a discussion involving $\overline{u}$ and $\overline{d}$ antiquarks. Specifically we will investigate the theoretical and experimental evidence for $\overline{u} \neq \overline{d}$.

Inspired by early, inconclusive data on the F_2 electromagnetic structure function of the proton and neutron, Field and Feynman [96] were the first to conjecture that $\overline{u} < \overline{d}$ in the nucleon. They invoked the Pauli principle by arguing that the presence of more valence u quarks than d quarks suppresses the creation of $u\overline{u}$ pairs in the sea. Later, Ito et al.

[97] measured continuum dimuon production and determined the sea quark distribution in the context of the Drell-Yan description of dilepton production. From an analysis of the logarithmic derivative of the measured cross section, they inferred that the Drell-Yan model, assuming symmetric sea, underestimated the measured slope. This fact was interpreted as indication of broken symmetry in the sea, with $\overline{u} < \overline{d}$. Somewhat later, Thomas [98], following Sullivan's suggestion [99] that the pion cloud can contribute to the nucleon structure function, realized that pion dressing of the nucleon naturally predicts an excess of $\overline{d}$ over $\overline{u}$. This is so because, for instance, the proton has a greater probability to emit a π^+ than a π^0 or a π^-. In fact, this observation was used [100] to interpret the Ito et al. results on dilepton production. Further theoretical evidence for asymmetry in the sea was found in the work of Signal and Thomas [42] on the calculation of quark distributions. The matrix elements of the quark distribution involve intermediate states where the photon scatters on a valence quark and also intermediate states where the photon oscillates into a $q\overline{q}$ pair and a quark or antiquark is inserted in the nucleon. Again, following the idea of Field and Feynman, it is easier to insert a d than a u quark into the proton.

Even with all this evidence, the nucleon continued to be seen as having a symmetric sea. There is a simple explanation for this. The whole set of data available could be described by parametrizations of parton distributions where it was assumed that $\overline{u}(x) = \overline{d}(x)$, with the price of a slightly odd behaviour of the valence quark distribution when $x \to 0$ [101]. Only with the advent of a precise measurement of the Gottfried sum rule [62] by the New Muon Collaboration (NMC) [18] in 1991 was it that the possibility $\overline{u}(x) \neq \overline{d}(x)$ began to be extensively studied. Basically, two mechanisms were raised to explain the NMC result. In one of them, it was argued that the Regge behaviour of the parton distributions starts at a lower x than assumed by the NMC [101, 102, 103]. The other possibility involves the violation of flavour symmetry in the nucleon sea [104, 105, 106, 107, 108, 109, 110, 111, 112]. To a

great extent, the physical mechanism behind the breaking of the symmetry was attributed to the pion dressing of the nucleon. Based on the Sullivan approach for the pionic contribution in DIS, corrections to the integrated value of F_2 were calculated [104, 105, 107, 110, 111] as well the x dependence of these corrections [106, 107, 111]. Some successful calculations on the sea asymmetry were also made in terms of chiral field theory [109, 113]. However, the most recent update of the mesonic corrections [114] seems to reinforce the idea that mesons alone are not able to give the entire sea quark distribution of the nucleon. In this work it is suggested that, even for small Q^2, fitting the flavour breaking of the sea (and this would mean using meson-nucleon vertices different from the ones that have traditionally been used in low energy physics) implies that the singlet sector of the quark distributions is poorly described for $x < 0.3$. The obvious conclusion to be drawn is that gluons are important not only for high but also for small Q^2. The problem is that it has been known since the work of Ross and Sachrajda [115] that perturbative QCD is unable to generate a sea that significantly distinguishes between $\overline{u}$ and $\overline{d}$. This means that there should be some nonperturbative glue in the nucleon in order to enhance the singlet distributions at small x. This discussion exemplifies very well how powerful deep inelastic experiments can be to give hints on the structure of the nucleon at low energy.

In view of the importance that pions and gluons may have in the understanding of the flavour structure of the nucleon, we will study them in more detail in this chapter. In particular, we will study the effects of the Pauli exclusion principle on the pair creation inside a nucleon composed of three valence quarks. We start in section 2.2 discussing the two main experiments that suggest that the nucleon sea is asymmetric. We also point out that in one of the experiments, the NA51 Drell-Yan experiment, the claim that the ratio $\overline{u}(x)/\overline{d}(x)$ is measured is correct only in the sense that the value quoted corresponds to the limit where isospin symmetry between the proton and neutron is exact for *all* x. We then go

to discuss the interplay between the Pauli principle and antisymmetrization effects when a $q\overline{q}$ pair is created inside the proton through gluon emission. In view of the results obtained, in section 2.4 we extend our discussion to the case where the pair is created through pion emission.

3.2 Two Experiments

The difference between the proton and the neutron electromagnetic structure functions, weighted by $1/x$ and integrated over Bjorken x gives:

$$S_G = \int_0^1 (F_2^p(x) - F_2^n(x))\frac{dx}{x} = \frac{1}{3} + \frac{2}{9}\int_0^1 (4\overline{u}^p(x) + \overline{d}^p(x) - 4\overline{u}^n(x) - \overline{d}^n(x))dx. \qquad (3.1)$$

The assumptions of exact SU(2) flavour symmetry in the sea, $\overline{u} = \overline{d}$, and charge symmetry between the proton and the neutron, $\overline{u}^p = \overline{d}^n, \overline{d}^p = \overline{u}^n$, reduces the RHS of Eq. (3.1) to 1/3. This result is known, as seen before in Eq. (2.48), as the Gottfried sum rule [62]. To test its validity is to check whether or not the sea is symmetric. To some extent, this test could also say something about the isospin symmetry between the proton and the neutron [116].

In order to test the Gottfried sum rule, the NMC [18] performed deep inelastic muon scattering on hydrogen and deuterium and measured the deuteron/proton cross-section ratio. To extract the proton and neutron structure functions, they used the simple relation $F_2^p(x) - F_2^n(x) = 2F_2^d(x)(1-F_2^n(x)/F_2^p(x))/(1+F_2^n(x)/F_2^p(x))$, with $F_2^n(x)/F_2^p(x) = 2F_2^d(x)/F_2^p(x) - 1$. A parametrization [18, 117] for $F_2^p(x)$ based on NMC, SLAC and BCDMS data was used. The NMC reported the following value for the Gottfried sum rule:

$$\begin{aligned} S_G(0.004 \leq x \leq 0.8) &= 0.221 \pm 0.008(stat) \pm 0.019(syst), \\ S_G &= 0.235 \pm 0.026, \end{aligned} \tag{3.2}$$

where the contribution for $x > 0.8$ was estimated using a smooth extrapolation of F_2^n/F_2^p and for the region $x < 0.004$ they assumed a Regge-like behavior (ax^b with $a = 0.2 \pm 0.03$ and $b = 0.59 \pm 0.06$). It is worth noticing that in the extraction of F_2^n/F_2^p, target mass corrections and nuclear effects were not included,nor where higher twist corrections included in the sum rule as a whole.

The experimental result from the NMC, interpreted together with $\overline{u}^p = \overline{d}^n$, $\overline{d}^p = \overline{u}^n$, yields:

$$\int_0^1 dx(\overline{u}(x) - \overline{d}(x)) = -0.1475 \pm 0.039. \tag{3.3}$$

In this scenario, the flavour symmetry is broken. Conversely, one can set the sea flavour to be symmetric [116] and put all the discrepancy from the experimentally measured sum rule into isospin breaking between the neutron and the proton, resulting in:

$$\int_0^1 dx(\overline{q}^p(x) - \overline{q}^n(x)) = -0.0885 \pm 0.0234 \tag{3.4}$$

A third possible way out is to set both the sea flavour and the isospin between the neutron and the proton to be exact symmetries and modify the small x behaviour of $F_2(x)$ such that the integral of $(F_2^p(x) - F_2^n(x))/x$ saturates the naive expectation 1/3. This proposal of large contributions from the unmeasured region $x \leq 0.004$ was made by Martin, Roberts and Stirling [102].

We thus have a few possibilities for the interpretation of the deviation of the measured S_G from its theoretical expectation. The NMC experiment is unable to discriminate among

the mechanisms responsible for the small value of S_G but from general knowledge of charge symmetry breaking we know that this effect should be of order of 1%. If this is true, we are left with the anomalous behaviour of F_2 at small x and the breaking of sea flavour symmetry. To discriminate between these two possibilities, Ellis and Stirling [103] proposed an experiment based on dilepton production in the Drell-Yan process. Basically, they argued that the $p-n$ cross section asymmetry defined as

$$A_{DY}(x) = \frac{\sigma^{pp}(x) - \sigma^{pn}(x)}{\sigma^{pp}(x) + \sigma^{pn}(x)}, \tag{3.5}$$

can tell whether the sea is symmetric or not, depending on wheter the asymmetry is positive or negative. This would be possible because $\sigma^{pN}(x) \propto \sum_i (q_i^p(x)\overline{q}_i^N(x) + \overline{q}_i^p(x)q_i^N(x))$ and then A_{DY} can be expressed as:

$$A_{DY}(x) = \frac{(4\lambda_v(x)-1)(\lambda_s(x)-1) + (\lambda_v(x)-1)(4\lambda_s(x)-1) + 2\overline{d}(x)(4\lambda_s(x)-1)(\lambda_s(x)-1)/d_v(x)}{(4\lambda_v(x)+1)(\lambda_s(x)+1) + (\lambda_v(x)+1)(4\lambda_s(x)+1) + 2\overline{d}(x)(4\lambda_s(x)+1)(\lambda_s(x)+1)/d_v(x)}, \tag{3.6}$$

with

$$\begin{aligned} \lambda_v(x) &= \frac{u_v(x)}{d_v(x)}, \\ \lambda_s(x) &= \frac{\overline{u}(x)}{\overline{d}(x)}. \end{aligned} \tag{3.7}$$

For completeness, we included sea-sea corrections in Eq. (3.6). It is then clear that if $\lambda_s = 1$, the asymmetry is always positive once λ_v is larger than unity. On the other hand the asymmetry can change sign for $\lambda_s \neq 1$. In particular if $\lambda_v = 2$, the asymmetry is negative for $\lambda_s < 0.72$ - where, for simplicity, the last term (the sea-sea term) was neglected. However, the important feature of the $p-n$ cross section asymmetry is that, given a value for λ_v, the

measured asymmetry determines whether or not there is any sort of isospin breaking. Ellis and Stirling concentrated on the breaking of the sea symmetry but, as it will be clear in expression (3.10), it could also indicate a broken isospin between the neutron and the proton at a given x.

The experiment proposed by Ellis and Stirling was carried out by the NA51 collaboration [19] which measured the Drell-Yan asymmetry A_{DY}. They quoted the following result:

$$A_{DY}(x = 0.18) = -0.09 \pm 0.02(stat) \pm (0.025) \tag{3.8}$$

from which they derived

$$\lambda_s(x = 0.18) = 0.51 \pm 0.04(stat) \pm 0.05(syst), \tag{3.9}$$

where sea-sea corrections were included but nuclear effects were left out. In this interpretation, the experiment indicates that there is a strongly asymmetric sea at $x = 0.18$. We are now going to show that in fact, the λ_s quoted in Eq. (3.9) is only a limit set within the framework of Eq. (3.6) which was based on the assumption $\overline{u}^p(x) = \overline{d}^n(x)$ and $\overline{d}^p(x) = \overline{u}^n(x)$. We could as well have set the sea to be flavour symmetric and derived the following expression for the Drell-Yan asymmetry:

$$\begin{aligned} A_{DY}(x) \;=\; & \Big\{3(\lambda_v(x) - 1) - (1 + 4\lambda_v(x))\overline{\delta}(x)/\overline{q}(x) + 3\delta(x)/d_v(x) \\ & -10\overline{\delta}(x)/d_v(x)\Big\} / \\ & \Big\{13\lambda_v(x) + 7 + (4\lambda_v(x) + 1)\overline{\delta}(x)/\overline{q}(x) - 3\delta(x)/d_v(x) + \\ & 10\overline{\delta}(x)/d_v(x) + 20\overline{q}(x)/d_v(x)\Big\}. \end{aligned} \tag{3.10}$$

Here, we used $\overline{u}(x) \equiv \overline{u}^p(x) = \overline{d}^n(x) - \overline{\delta}(x)$, $\overline{d}(x) \equiv \overline{d}^p(x) = \overline{u}^n - \overline{\delta}(x)$, $u_v(x) = u_v^p(x) =$

$d_v^n(x) - \delta(x)$ and $d_v(x) \equiv d_v^p(x) = u_v^n(x) + \delta(x)$. The function $\delta(x)$ does not need to be the same for u_v and for d_v but we use the same function to simplify the expressions as we illustrate the main idea. Also notice that different signs are used for the corrections in d_v^n and u_v^n as this seems to be suggested by theoretical evidence [118]. We have also considered the case where both signs coincide and the conclusions presented here are insensitive to such a choice. Of course, $\int_0^1 dx\delta(x) = 0$ to preserve the number of valence quarks. Using the experimental result for $A_{DY}(x)$, we can estimate the amount of charge symmetry breaking.

For that purpose, we will work with the MRS parametrization S_0' for $\overline{q}(x)$, $u_v(x)$ and $d_v(x)$. In this parametrization the sea is symmetric and, for $x = 0.18$, $Q^2 = (5.22\ GeV)^2 = x^2 s$ for $s = (29\ GeV)^2$ the square of the center of mass energy of the NA51 experiment, it gives $\overline{q}(x = 0.18) = 0.348$, $u_v(x = 0.18) = 3.13$ and $d_v(x = 0.18) = 1.486$. We then obtain:

$$\overline{\delta}(x = 0.18) = 0.2088 - 0.0933\delta(x = 0.18). \tag{3.11}$$

In calculating Eq. (3.11) we disregarded the sea-sea correction term $(20\overline{q}(x)/d_v(x))$ and took only the central value of the measured asymmetry. This is a good approximation as, using the same procedure when recalculating result (3.9), we get $\lambda_s(x = 0.18) \simeq 0.53$. Eq. (3.11) tells us that the interpretation of the Drell-Yan asymmetry purely in terms of charge symmetry violation is very unlikely because of the size of the breaking necessary to fit the data. Of course, the procedure is not entirely consistent because the S_0' parametrization was constructed with the assumption $\overline{\delta}(x) = \delta(x) = 0$. Thus, Eq. (3.11) should be seen as only a guide.

If we take for instance $\delta(x) = \overline{\delta}(x)$, we have $\overline{\delta}(x = 0.18) \simeq 0.19$, which means that the factor giving the breaking is about 55% of the antiquark distribution itself - clearly too large value. On the other hand, there is no reason at all to interpret the NA51 result solely

in terms of isospin breaking between the proton and the neutron. In the general case, the Drell-Yan asymmetry would be:

$$\begin{aligned} A_{DY}(x) \;=\; & \{(4\lambda_v(x)-1)(\lambda_s(x)-1)+(4\lambda_s(x)-1)(\lambda_v(x)-1) \\ & -(4\lambda_v(x)+1)\overline{\delta}(x)/\overline{d}(x)-(1-4\lambda_s(x))\delta(x)/d_v(x) \\ & -2(4\lambda_s(x)+1)-2(4\lambda_s(x)-1)(\lambda_s(x)-1)\overline{d}(x)/d_v(x)\Big\}\,/ \\ & \{(4\lambda_v(x)+1)(\lambda_s(x)+1)+(4\lambda_s(x)+1)(\lambda_v(x)+1) \\ & +(4\lambda_v(x)+1)\overline{\delta}(x)/\overline{d}(x)+(1-4\lambda_s(x))\delta(x)/d_v(x) \\ & +2(4\lambda_s(x)+1)+2(4\lambda_s(x)+1)(\lambda_s(x)+1)\overline{d}(x)/d_v(x)\Big\}. \end{aligned} \tag{3.12}$$

To write Eq. (3.12) we made the simplification that, even for broken sea flavour symmetry, the correction $\overline{\delta}(x)$ from charge symmetry breaking in the sea has the same form for the $\overline{u}$ and for the $\overline{d}$ quarks. Of course, this does not necessarily need to be the case.

Again, to extract any number from Eq. (3.12) we need to know the value of the sea and valence quark distributions at a given x. As we include isospin breaking terms, we have the problem that there is no standard quark distribution including these corrections. Moreover, the term involving $\overline{\delta}(x)$ is potentially important as it is multiplied by a large factor and divided by a small number (viz. $\overline{d}$). This is true whether the integral over x of $\overline{\delta}(x)$ (and $\delta(x)$) is zero or not. This means that to extract $\lambda_s(x)$ using the measured Drell-Yan asymmetry is at best ambiguous. To estimate the order of magnitude of $\delta(x)$ and of $\overline{\delta}(x)$, we will assume that the quark and antiquark distributions are described by the D'_0 and D'_- parametrizations. For the D'_0 set, the Gottfried sum rule is 0.26 and for the D'_- this value is 0.24, which means that for both sets, $\int_0^1 \overline{\delta}(x)dx \simeq 0$, but this does not mean that $\overline{\delta}(x) = 0$ at $x = 0.18$. Using the measured asymmetry and disregarding sea-sea corrections, one gets:

$$\begin{aligned} \overline{\delta}(x=0.18) &= 0.169 - 0.053\delta(x=0.18), \ \lambda_s \sim 0.88, \ D'_0 \\ \overline{\delta}(x=0.18) &= 0.125 - 0.045\delta(x=0.18). \ \lambda_s \sim 0.78, \ D'_- \end{aligned} \tag{3.13}$$

In fig. 3.1 we show the behaviour of $\overline{\delta}(x)$ as a function of $\delta(x)$ for the various parametrizations discussed. A few comments are appropriate. First, we see that $\overline{\delta}$ is not strongly dependent on δ and this dependence becomes weaker as λ_s decreases. Moreover, we see that for $\lambda_s = 0.78$, the charge symmetry breaking is of the order 30% $\sim$ 40% of the antiquark distribution. Although this value is high, it is at a specific value of x and we remember that $\lambda_s = 0.78$ is a correction of about 50% to the central value of $\lambda_s = 0.51$ quoted by the NA51 group. We could be less drastic and propose corrections of the order of 20%, bringing the measured central value to $\lambda_s = 0.6$, which is itself a huge correction, providing a sensitive test for any model trying to describe the flavour of the nucleon sea. As a consequence, if we make a linear extrapolation of $\overline{\delta}(x)$ with λ_s as suggested by Fig. 3.1, this correction of 20% would correspond to a value of $\overline{\delta}$ around 10% of the antiquark distribution itself. This could well be possible and, from this point of view, the λ_s quoted as being experimentally measured only sets a lower limit corresponding to $\overline{\delta}(x) = \delta(x) = 0$.

We can summarise this section by saying that, in principle, the discrepancy between theory and experiment found by the NMC [18] could come from flavour symmetry violation in the nucleon sea and charge symmetry breaking in either the the nucleon sea or valence distributions. However, because of the enormous value for $\overline{\delta}$ needed to fit the experiment with charge symmetry breaking alone, it is more likely that the NMC result implies some strong flavour symmetry breaking in the nucleon sea with a small $\overline{\delta}$ admixture.

Of course, there are many successful calculations based on pion physics [112, 114, 119] that give a clear indication of an excess of $\overline{d}$ over $\overline{u}$ in the nucleon. On the other hand,

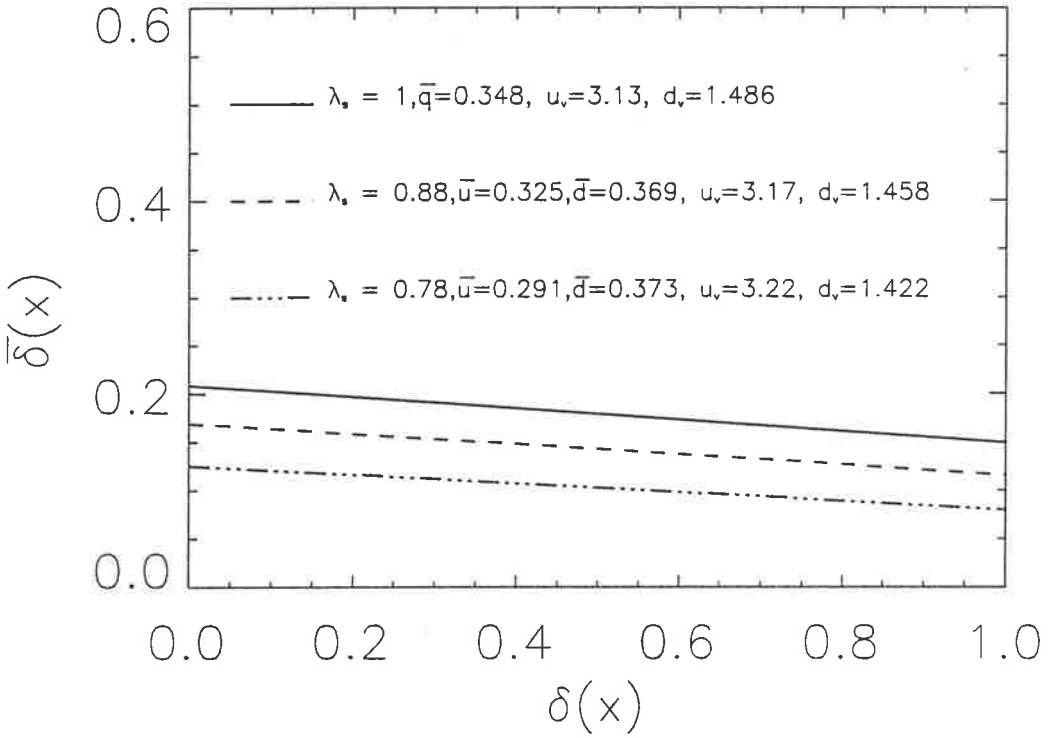

Figure 3.1: $\overline{\delta}(x)$ as a function of $\delta(x)$ for the various parametrizations discussed in the text.

the interpretation of the NMC experiment as a confirmation of broken sea symmetry, does not rule out the possibility that, at a particular x, charge symmetry breaking between the neutron and the proton may be at the same level as that of flavour symmetry breaking. Our analysis indicates that it is possible to have $\lambda_s(x)$ larger than the value quoted by the NA51 group at the cost of some charge symmetry breaking between the proton and the neutron at a particular x, even if the integrated value of this correction is zero or nearly zero. It is clearly an urgent matter to find experimental ways to separate these two contributions. For now, the important feature to note is that the NA51 result should be seen as a lower limit for $\lambda_s(x)$ and not as an anambiguous determination.

It remains to determine the physical mechanism behind the symmetry breaking in the sea. Throughout this chapter we mentioned many times the possible role of mesons. Although this is an extremely important subject, we are not going to make a detailed study of it here, as there are extensive investigation on this subject already in the literature [114, 112]. Rather, we will focus on the role of the Pauli principle and its interplay with antisymmetrization effects. This is a subject usually overlooked in the literature and we will dedicate the remainder of this chapter to it.

3.3 The Pauli Principle in the Proton Sea

The most natural idea to account for the observed discrepancy between theory and experiment is to invoke the Pauli principle. Field and Feynman [96] were the first ones to use this idea: if the proton is composed of two valence u quarks and one valence d quark then the creation of a quark - antiquark pair through gluon emission will tend to give more $d\overline{d}$ pairs than $u\overline{u}$ pairs. This is easy to understand because there are five empty states for the d quark and four for the u quark. Although this idea is attractive and essentially correct, there is one other effect to consider. We will see here, that we also have to consider graphs containing interference between the sea quarks generated in the gluon emission and the remaining quarks in the nucleon. This effect will, in fact, hide the excess of $\overline{d}$ over $\overline{u}$ due to the Pauli principle.

To illustrate our discussion, we begin by reviewing the pair creation through a gluon process following the calculations of Donoghue and Golowich [120]. The assumption made is that the bare proton is composed of two valence u quarks, one valence d quark and its colour, flavour and spin wave function is given by:

$$|p\rangle_0 = \frac{1}{18}\epsilon^{\alpha\beta\gamma}[b^\dagger(u,\uparrow,\alpha)b^\dagger(d,\downarrow,\beta) - b^\dagger(u,\downarrow,\alpha)b^\dagger(d,\uparrow,\beta)]b^\dagger(u,\uparrow,\gamma)|0\rangle. \tag{3.14}$$

The sea quarks are generated through a quark gluon interaction given by:

$$H_I(x) = g\overline{\psi}(x)\gamma^\mu\frac{\lambda^a}{2}\psi(x)A^a_\mu(x), \tag{3.15}$$

where g is the coupling constant, A^a are the gluon fields and ψ the quark field. We are not going to worry about the form of the spatial part of these operators but we will concentrate only on the colour, spin and flavour part of the proton dressed with a quark - antiquark pair:

$$|p\rangle = |p\rangle_0 + \frac{1}{E_0 - H_0}H_I\frac{1}{E_0 - H_0}H_I|p\rangle_0 + ..., \tag{3.16}$$

with H_0 the free Hamiltonian and we have omitted the term corresponding to the single gluon loop.

The vector coupling between quarks and gluons allows for vertices where the quark that emits the gluon either changes its spin or not. Another feature of the pair creation process is that since a particle has opposite intrinsic parity to an antiparticle, at least one quark (or the antiquark) or the two quarks and the antiquark have to be in a state of odd parity in order to conserve the parity of the proton. The proton wave function is then written as:

$$|p\rangle = |p\rangle_0 + C_s|\psi_s\rangle + C_v|\psi_v\rangle, \tag{3.17}$$

with $|\psi_v\rangle$ the wave function for the case where the quark that emits the gluon can change its spin and $|\psi_s\rangle$ the wave function for the case that the quark emitting the gluon does not change its spin. The factors C_s and C_v depend on the particular form for the spatial part of

the wave function, according to Eq. (3.16). We then have:

$$\begin{aligned}\langle p|p\rangle &= 1 + |C_s|^2\langle\psi_s|\psi_s\rangle + |C_v|^2\langle\psi_v|\psi_v\rangle \\ &+ C_s^* C_v\langle\psi_s|\psi_v\rangle + C_v^* C_s\langle\psi_v|\psi_s\rangle. \end{aligned} \tag{3.18}$$

The wave function involved in the vector coupling is calculated from Eqs. (3.15) and (3.16):

$$\begin{aligned}|\psi_v\rangle &= (-1)^{\tilde{n}-1/2} b^\dagger(s,n,\rho)\sigma^l_{n\tilde{n}}\lambda^a_{\rho\tilde{\rho}} d^\dagger(\overline{s},-\tilde{n},\tilde{\rho}) \\ &\quad b^\dagger(v,m,\delta)\sigma^l_{m\tilde{m}}\lambda^a_{\delta\tilde{\delta}} b(\tilde{v},\tilde{m},\tilde{\delta})|p\rangle_0 \\ &= \frac{(-1)^{\tilde{n}-1/2}}{\sqrt{18}}\sigma^l_{n\tilde{n}}\sigma^l_{m\tilde{m}}\lambda^a_{\rho\tilde{\rho}}\lambda^a_{\delta\tilde{\delta}} \\ &\quad \{\epsilon^{\alpha\beta\gamma}(\delta_{\tilde{v}u}\delta_{\tilde{\delta}\alpha}A^\dagger - \delta_{\tilde{v}d}\delta_{\tilde{\delta}\beta}B^\dagger + \delta_{\tilde{v}u}\delta_{\tilde{\delta}\gamma}C^\dagger)|0\rangle\}, \end{aligned} \tag{3.19}$$

where σ are the Pauli spin matrices, λ are the Gell-Mann flavour matrices and the spin and flavour indices are summed. We also have:

$$\begin{aligned} A^\dagger &= b^\dagger(s,n,\rho)d^\dagger(\overline{s},-\tilde{n},\tilde{\rho})[b^\dagger(v,m,\delta)b^\dagger(d,\downarrow,\beta)\delta_{\tilde{m}\uparrow} - b^\dagger(v,m,\delta)b^\dagger(d,\uparrow,\beta)\delta_{\tilde{m}\downarrow}]b^\dagger(u,\uparrow,\gamma) \\ B^\dagger &= b^\dagger(s,n,\rho)d^\dagger(\overline{s},-\tilde{n},\tilde{\rho})[b^\dagger(v,m,\delta)b^\dagger(u,\uparrow,\alpha)\delta_{\tilde{m}\downarrow} - b^\dagger(v,m,\delta)b^\dagger(u,\downarrow,\alpha)\delta_{\tilde{m}\uparrow}]b^\dagger(u.\uparrow,\gamma) \\ C^\dagger &= b^\dagger(s,n,\rho)d^\dagger(\overline{s},-\tilde{n},\tilde{\rho})b^\dagger(v,m,\delta)\delta_{\tilde{m}\uparrow}[b^\dagger(u,\uparrow,\alpha)b^\dagger(d,\downarrow,\beta) - b^\dagger(u,\downarrow,\alpha)b^\dagger(d,\uparrow,\beta)] \end{aligned} \tag{3.20}$$

For the scalar coupling the wave function is the same except that the Pauli spin matrices are omitted and $n = \tilde{n}$, $m = \tilde{m}$.

The calculation of the wave function overlap is very long and tedious. The results are displayed in table (3.1), where v refers to the state of the valence quark after the gluon emission, s corresponds to the state where the quark in the sea is created and g refers to the ground state. These calculations agree with the results of Donoghue and Golowich [120].

State	$\langle\psi_s\|\psi_s\rangle$	$\langle\psi_v\|\psi_v\rangle$	$\langle\psi_s\|\psi_v\rangle$
v=s=g	0	$4608 + 1792\delta_{su} - 1024\delta_{sd}$	0
v=g,s≠g	0	4608	0
v≠g, s=g	$1152 + 640\delta_{su} + 320\delta_{sd}$	$3456 + 1280\delta_{su} - 320\delta_{sd}$	$-320\delta_{su} - 640\delta_{sd}$
v=s≠g	$1152 + 128\delta_{su} + 64\delta_{sd}$	$3456 - 384\delta_{su} - 192\delta_{sd}$	$384\delta_{su} + 192\delta_{sd}$
v≠s, v≠g, s≠g	1152	3456	0

Table 3.1: Probabilities to find a quark in the sea for the various possible states of the sea quark and the valence quark that emits the gluon. These probabilities are based only on the spin-flavour-colour wave function.

The most striking result read from table (3.1) is that the probability to find the sea with a $u\overline{u}$ pair is bigger than the sea composed of a $d\overline{d}$ pair. This conclusion, in principle, contradicts the experimental result collected by the NMC [18] where the measured Gottfried sum rule is smaller than 1/3 - a result that implies $\overline{d} > \overline{u}$. How can we then understand that the intrinsic sea in the proton generated by gluons favours $u\overline{u}$ pairs over $d\overline{d}$ pairs? In principle, this result also contradicts the intuitive picture, as introduced by Field and Feynman [96], based on the Pauli principle: for each flavour there are 6 empty states (2 from spin and 3 from colour). As the bare proton has 2 u quarks and one d quark, there are four available states for insertion of u quarks and 5 available states for insertion of d quarks. Although this reasoning is correct, one also cannot forget that antisymmetrization between quarks is an additional complication. The same excess of u valence quarks that prevents $u\overline{u}$ pair creation in comparison with $d\overline{d}$ pair creation, also produces extra contributions because of antisymmetrization between the u quarks that does not exist for the d quarks.

To try to understand this effect, we consider the case where the quark that emits the gluon does not change its spin but goes to an excited state and the sea is created in the ground state or in a P state, according to parity conservation. This case was chosen because it is the simplest, as can be seen from table (3.1). In fig. 3.2 we show the graphs containing $u\overline{u}$ pairs and in fig. 3.3 the graphs containing $d\overline{d}$ pairs.

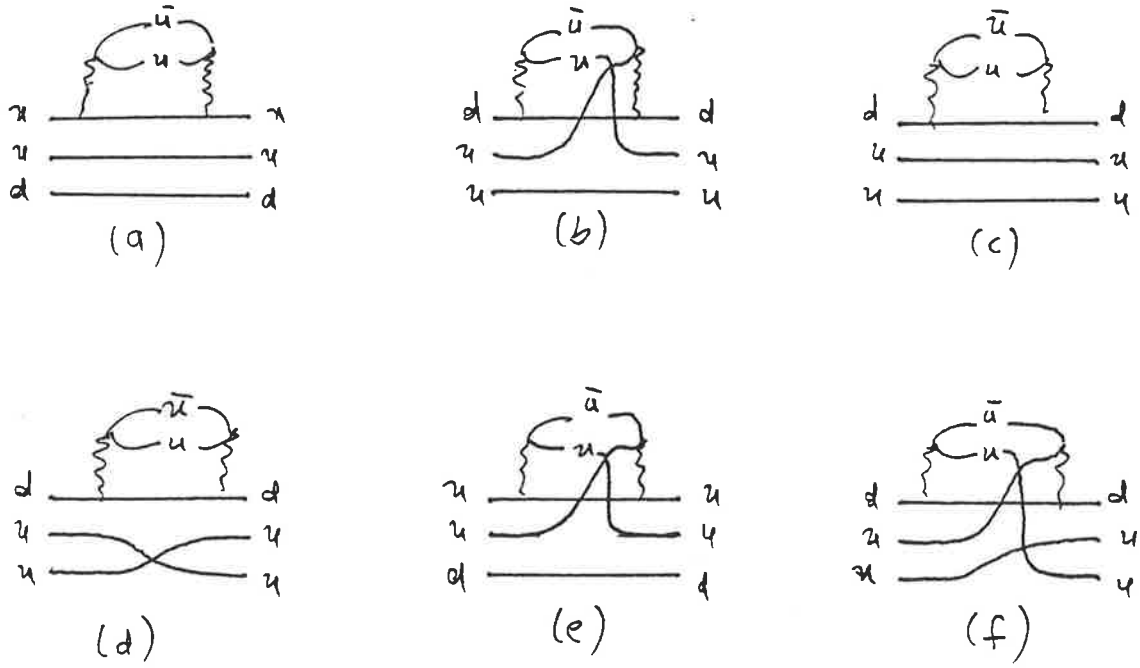

Figure 3.2: Graphs containing $u\overline{u}$ pairs.

The diagrams (a), (c) and (d) for $u\overline{u}$ are the analogues of the diagrams (a), (c) and (d) for $\overline{d}$. Their values are respectively the same because the created sea does not mix with the valence quarks and, for this reason, it is not possible to distinguish the sea flavour. Thus, in the case where the sea contracts with itself, the value of these graphs are the same for any flavour. Of course, the heavier the quark the smaller its contribution through these diagrams.

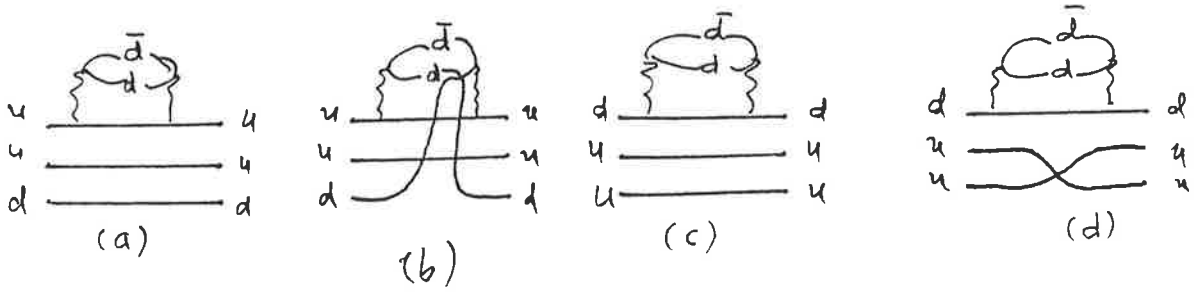

Figure 3.3: Graphs containing $d\overline{d}$ pairs.

But this is an effect related solely to mass and not to spin statistics. The computed value is $\langle\psi_s|\psi_s\rangle = 384$ for (a), $\langle\psi_s|\psi_s\rangle = 128$ for (c) and $\langle\psi_s|\psi_s\rangle = 64$ for (d). The diagram (b) for $\overline{u}$ is the analogue of diagram (b) for $\overline{d}$ and they only exist when $u\overline{u}$ and $d\overline{d}$ pairs are created. Their values are $\langle\psi_s|\psi_s\rangle = 4 \times 160/3$ for (b) of fig. 3.2 and $\langle\psi_s|\psi_s\rangle = 6 \times 160/3$ for (b) of fig. 3.3. Generally speaking, the set of diagrams just mentioned are the only ones comparable. From them, one easily see the Pauli principle in action and from it an excess of $\overline{d}$ over $\overline{u}$ as expected. However, we also have to include graphs (e) and (f) of fig. 3.2 for $\overline{u}$. They appear because there is an excess of u valence over d valence quarks. If the graphs (e) and (f) are included, as they should be, then the results change because these graphs give positive contributions: $\langle\psi_s|\psi_s\rangle = 320$ for (e) and $\langle\psi_s|\psi_s\rangle = 2 \times 160/3$ for (f). With these graphs included the probability to find a $\overline{u}$ antiquark in the proton is bigger than the probability to find a $\overline{d}$ in the same proton.

One could doubt this interpretation of the relation between the Pauli principle and antisymmetrization effects by counting only those graphs where a d quark emits a gluon. In this case, where a d quark emits a gluon, we would have 6 empty states for a d quark and only 4 empty states for the u quark (if the sea is created in the ground state). On the other

hand, from fig. 3.2 we see that graphs (b), (c) and (d) (also graph (f) if we include the one coming exclusively from the excess of u valence quarks) give a larger contribution than the corresponding graphs (c) and (d) of fig. 3.3. As the graphs (b), (c) and (d), in principle, are not related to the excess of u valence quarks, there is an apparent contradiction with the simple counting of states and the whole argument of the role of the interference graphs presented by us before. In reality, this contradiction is only apparent. To better understand what is happening, consider a proton made of only one u and one d quark. In this case, if a d quark emits a gluon, we would have in principle 6 empty states for the insertion of a d quark and 5 for the insertion of a u quark. The possible graphs would be the analogue of (b) and (c) from fig. 3.2 for a $u\overline{u}$ in the sea and the analogue of graph (c) from fig. 3.3 for a $d\overline{d}$ in the sea. Again, we would have more $u\overline{u}$ pairs than $d\overline{d}$ pairs and now it is clear why that happens: it happens because there is one free valence u quark that can be exchanged with the sea and there is no such free valence d quark to be exchanged (in the case of a $d\overline{d}$ sea). The opposite situation happens when the u quark emits the gluon such that the sum of all diagrams, gluon emission from u and d valence quarks, renders an equal probability for a $u\overline{u}$ and $d\overline{d}$ pair creation, as expected in a proton containing only one quark of each flavour. The lesson is that we cannot treat the gluon emission in the proton from different flavours separately, and expect the Pauli principle to work free of any other effects.

For the combined result, the probability to find a $\overline{u}$ is bigger than the probability to find a $\overline{d}$. One then can say that interference terms somehow shadow the naive expectation of the Pauli principle. This result is extremely important because it also says that if we have to antisymmetrize the sea quarks with valence quarks in the case where the sea quarks are generated through pions, then the whole set of conclusions about the importance of the pions to the Gottfried sum rule might need to be revised. In the next section we are going to investigate whether this is the case.

3.4 Antisymmetrization of the Quarks of the Pion

In this section we are going to study whether or not it is relevant to consider the quark structure of the pion. As discussed before, if the quark structure of the pion is taken into account, it will be necessary to antisymmetrize the five quark state. Similar to the gluon case, it might happen that the $\overline{u}$ antiquark can be favoured over the $\overline{d}$ antiquark. If this turns out to be true, the asymmetry in favour of $\overline{d}$ (from the processes $u \rightarrow d\pi^+$) over $\overline{u}$ (from $d \rightarrow u\pi^-$) may be at risk.

The relevant diagram to study antisymmetrization in the pion cloud is the one shown in fig. 3.4, involving two loops. However, we will be mainly interested in the relative importance of the two loops to the one loop. To this end we also need to compute the diagram (a) of fig. 3.4, which we do as a warm-up exercise. The calculations are going to be done at the quark level ($q \rightarrow \pi q$), which means that we need an interaction Hamiltonian between quarks and pions. To fix the calculation in a specific scheme, we are going to use the interaction between quarks and pions as given by the Cloudy Bag Model [121, 122]:

Figure 3.4: The one and two loop graph in pion emmision.

$$H_I = \frac{i}{2f}\int d^3x\overline{\psi}(x)\gamma_5\tau^i\psi(x)\phi^i\delta(r-R), \tag{3.21}$$

with R the bag radius and

$$\begin{aligned}
\vec{\phi}(\vec{x}) &= \frac{1}{(2\pi)^{2/3}}\int\frac{d\vec{k}}{(2\omega_k)^{1/2}}(\vec{a}_{\vec{k}}e^{i\vec{k}\cdot\vec{x}}+\vec{a}^{\dagger}_{\vec{k}}e^{-i\vec{k}\cdot\vec{x}}),\\
\psi^s(\vec{x}) &= \frac{N}{(4\pi)^{1/2}}\sum\left\{\begin{pmatrix} ij_0(\omega r/R)\\ -j_1(\omega r/R)\vec{\sigma}\cdot\hat{r}\end{pmatrix}\chi_m b(f,m,\alpha)+\begin{pmatrix}-ij_1(\omega r/R)\vec{\sigma}\cdot\hat{r}\\ j_0(\omega r/R)\end{pmatrix}\chi_m d^{\dagger}(f,m,\alpha)\right\}\\
\psi^p(\vec{x}) &= \frac{N}{(4\pi)^{1/2}}\sum\left\{\begin{pmatrix} ij_1(\omega r/R)\vec{\sigma}\cdot\hat{r}\\ j_0(\omega r/R)\end{pmatrix}\chi_m b(f,m,\alpha)+\begin{pmatrix}ij_0(\omega r/R)\\ j_1(\omega r/R)\vec{\sigma}\cdot\hat{r}\end{pmatrix}\chi_m d^{\dagger}(f,m,\alpha)\right\}
\end{aligned} \tag{3.22}$$

Here $N^2 = \omega^3/(2R^3(\omega-1)sin^2\omega)$, ω is the frequency associated with a given principal quantum number and orbital angular momentum and j_0 and j_1 are Bessel functions subject to the condition $j_0 = j_1$ at the bag surface, $r = R$. We wrote the explicit forms for the s and p waves for a quark inside a cavity because they are going to be used later on.

Three vertices are relevant to our diagrams: $q \to \pi q$, $\pi \to q\overline{q}$ and $0 \to \pi q\overline{q}$. As in the gluon case, there are some restrictions due to the conservation of parity, that can be helpful. As is well known, for fermions a particle has opposite intrinsic parity to the antiparticle. By convention, a particle has parity $+1$ and a antiparticle parity -1. Also, the parity of one particle relative to a set of others particles is given by $(-1)^l$, with l the orbital angular momentum of the particle in question. If $\overline{q}$ has parity -1 then one of the quarks (or the same antiquark) has to be in a state $l = 1$, or a p-wave, so that the proton parity is conserved. In general, the system must always be in a state of odd parity.

We now write down the explicit form for the interaction Hamiltonian for both vertices. It happens that their form, besides the creation operator for a quark or for a antiquark, is the same for both processes $q \to \pi q$ and $0 \to \pi q\overline{q}$:

$$H_I^{q^{\tilde{f}}\to\pi q^f} = H_I^{0\to\pi q^f\bar{q}^{\tilde{f}}} = \frac{i}{2f(2\pi)^{3/2}}\left(\frac{\omega^a\omega^b}{(\omega^a-1)(\omega^b-1)}\right)$$
$$\int \frac{d^3k}{(2\omega_k)^{1/2}}\chi_m^\dagger\vec{\sigma}\cdot\vec{k}\chi_{\tilde{m}}\frac{j_1(kR)}{kR}b^\dagger(f,m,\alpha)\tau^i_{f\tilde{f}}\begin{matrix}b(\tilde{f},\tilde{m},\tilde{\alpha})\\ d^\dagger(\tilde{f},\tilde{m},\tilde{\alpha})\end{matrix}a^{\dagger i}_{\vec{k}}. \qquad (3.23)$$

For the case $\pi \to q\bar{q}$ the interaction is just slightly different:

$$H_I^{\pi\to q^f\bar{q}^{\tilde{f}}} = \frac{-i}{2f(2\pi)^{3/2}}\left(\frac{\omega^a\omega^b}{(\omega^a-1)(\omega^b-1)}\right)$$
$$\int \frac{d^3k}{(2\omega_k)^{1/2}}\chi_m^\dagger\vec{\sigma}\cdot\vec{k}\chi_{\tilde{m}}\frac{j_1(kR)}{kR}b^\dagger(f,m,\alpha)\tau^i_{f\tilde{f}}d^\dagger(\tilde{f},\tilde{m},\tilde{\alpha})a^i_{\vec{k}}. \qquad (3.24)$$

In expressions (3.23) and (3.24) the indices a and b refers to the spatial wavefunctions of the quarks or/and antiquarks involved in a specific reaction.

Once we have the interaction Hamiltonian, it is easy to calculate the quantities we are interested in. As announced, we first calculate the probability to find a pion in the nucleon. To be specific, we set in Eq. (3.23) $\omega = \omega^a = \omega^b$, which means that the quark remains in the ground state after it emits the pion. In this case we get:

$$\frac{1}{E_0-H_0}H_I|p\rangle_0 = \frac{-i}{2f(2\pi)^{3/2}}\frac{\omega}{(\omega-1)}\int\frac{d^3k}{(2\omega_k)^{1/2}}\frac{1}{-\omega_k}\chi_m^\dagger\vec{\sigma}\cdot\vec{k}\chi_{\tilde{m}}\frac{j_1(kR)}{kR}$$
$$b^\dagger(v,m,\alpha)\tau^i_{v\tilde{v}}b(\tilde{v},\tilde{m},\tilde{\alpha})a^{\dagger i}_{\vec{k}}|p\rangle_0, \qquad (3.25)$$

where we used $(E_0-H_0)(H_I|p\rangle_0) = (E_0-(E_0+\omega_k))(H_I|p\rangle_0)$. The probability to find a pion is then given by:

$$
\begin{aligned}
P_\pi &= \left({}_0\langle p|H_I\frac{1}{E_0-H_0}\right)\left(\frac{1}{E_0-H_0}H_I|p\rangle_0\right) \\
&= \frac{\pi}{6f^2(2\pi)^3}\frac{\omega^2}{(\omega-1)^2}\int_0^\infty \frac{k^4dk}{\omega_k^3}\frac{j_1^2(kR)}{(kR)^2} \\
&\quad \times{}_0\langle p|b^\dagger(\vec{v}',\vec{m}'\vec{\delta}')\tau^i_{\vec{v}'v'}\sigma^j_{\vec{m}'m'}b(v',m',\delta')b^\dagger(v,m,\delta)\tau^i_{v\vec{v}}\sigma^j_{m\vec{m}}b(\vec{v},\vec{m},\vec{\delta})|p\rangle_0. \qquad (3.26)
\end{aligned}
$$

After some calculation, the expectation value between bare proton states is found to be 57. In terms of the pion components, this result reads $57 = 22\delta_{\pi^+} + 19\delta_{\pi^0} + 16\delta_{\pi^-}$. This means that, as expected, the probability to find a $\overline{d}$ in the nucleon is bigger than to find a $\overline{u}$. Using the identity $\omega/(f(\omega-1)) = \sqrt{4\pi}18f_{\pi NN}/5m_\pi$, where m_π is the physical pion mass and $f_{\pi NN}$ the pion nucleon nucleon coupling constant, expression (3.26) is rewritten as:

$$
P_\pi = \frac{57}{25}\left(\frac{f_{\pi NN}}{m_\pi}\right)^2\frac{3}{\pi}\int_0^\infty\frac{k^4dk}{\omega_k^3}\left(\frac{3j_1(kR)}{(kR)}\right)^2. \qquad (3.27)
$$

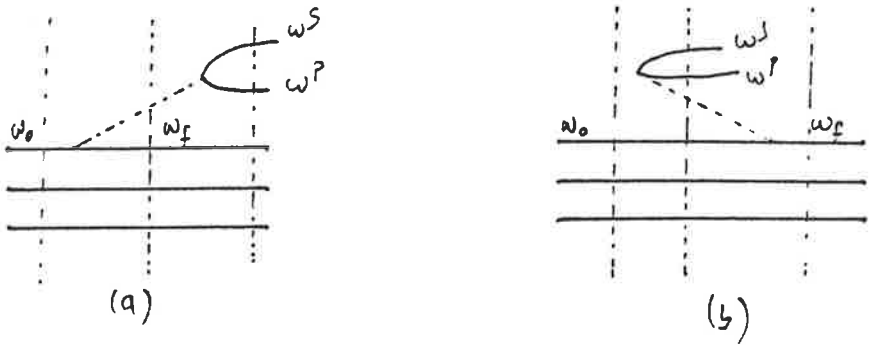

Figure 3.5: The two loop graph in time order.

The next step is the evaluation of the two-loop graph. Its calculation its a straightforward application of Eqs. (3.16), (3.23) and (3.24). We start with graph (a) of fig. 3.5. The process is the pion creation and subsequent decay into a $q\overline{q}$ pair:

$$\frac{1}{E_0-H_0}H_I^{\pi\to q\bar{q}}\frac{1}{E_0-H_0}H_I^{q\to\pi q}|p\rangle_0 = \frac{1}{(2f)^2(2\pi)^3}\sqrt{\frac{\omega_f\omega_o\omega^s\omega^p}{(\omega_f-1)(\omega_o-1)(\omega^s-1)(\omega^p-1)}}$$
$$\int d^3k'\int d^3k\frac{1}{(2\omega_{k'}2\omega_k)^{1/2}}\frac{R}{\omega_o-\omega_f-R\omega_k}\frac{R}{\omega_o-\omega_f-\omega^s-\omega^p}\times$$
$$\chi_n^\dagger\vec{\sigma}\cdot\vec{k}'\chi_{\tilde{n}}\frac{j_1(k'R)}{k'R}b^\dagger(s,n,\rho)\tau^j_{s\tilde{s}}d^\dagger(\tilde{s},\tilde{n},\rho)a^j_{\vec{k}'}\times$$
$$\chi_m^\dagger\vec{\sigma}\cdot\vec{k}\chi_{\tilde{m}}\frac{j_1(kR)}{kR}b^\dagger(v,m,\delta)\tau^i_{v\tilde{v}}b(\tilde{v},\tilde{m},\delta)a^{\dagger i}_{\vec{k}}|p\rangle_0. \quad (3.28)$$

The energies of the intermediate states are clearly indicated on the figure. The notation is the following: ω_0 and ω_f are, respectively, the quark frequencies before and after the pion emision or absorption, ω^s and ω^p are, respectively, the frequencies of the s wave quark and of the p wave antiquark.

Similarly to case (a), we calculate the contribution from graph (b), where a pion and a $q\bar{q}$ pair is created and the pion is subsequently absorbed by a quark:

$$\frac{1}{E_0-H_0}H_I^{q\pi\to q}\frac{1}{E_0-H_0}H_I^{0\to\pi q\bar{q}}|p\rangle_0 = \frac{1}{(2f)^2(2\pi)^3}\sqrt{\frac{\omega_f\omega_o\omega^s\omega^p}{(\omega_f-1)(\omega_o-1)(\omega^s-1)(\omega^p-1)}}$$
$$\int d^3k'\int d^3k\frac{1}{(2\omega_{k'}2\omega_k)^{1/2}}\frac{R}{\omega_o-\omega_f-\omega^s-\omega^p}\frac{R}{-\omega^s-\omega^p-R\omega_k}$$
$$\chi_n^\dagger\vec{\sigma}\cdot\vec{k}'\chi_{\tilde{n}}\frac{j_1(k'R)}{k'R}b^\dagger(v,n,\delta)\tau^i_{v\tilde{v}}b(\tilde{v},\tilde{n},\delta)a^i_{\vec{k}'}\times$$
$$\chi_m^\dagger\vec{\sigma}\cdot\vec{k}\chi_{\tilde{m}}\frac{j_1(kR)}{kR}b^\dagger(s,m,\rho)\tau^j_{s\tilde{s}}d^\dagger(\tilde{s},\tilde{m},\rho)a^{\dagger j}_{\vec{k}}|p\rangle_0. \quad (3.2$$

The total amplitude for the two loop process is then given by the sum of graphs (a) and (b). To better deal with this sum, we rewrite the product of operators in Eq. (3.29) as:

$$
\begin{aligned}
&b^\dagger(v,n,\delta)\tau^i_{v\tilde{v}}b(\tilde{v},\tilde{n},\delta)a^i_{\vec{k}'}b^\dagger(s,m,\rho)\tau^j_{s\tilde{s}}d^\dagger(\tilde{s},\tilde{m},\rho)a^{\dagger j}_{\vec{k}}|p\rangle_0 \\
&= b^\dagger(s,n,\rho)\tau^j_{s\tilde{s}}d^\dagger(\tilde{s},\tilde{n},\rho)b^\dagger(v,m,\delta)\tau^i_{v\tilde{v}}b(\tilde{v},\tilde{m},\delta)a^i_{\vec{k}'}a^{\dagger j}_{\vec{k}}|p\rangle_0 \\
&+\delta_{\tilde{v}s}\delta_{\tilde{n}m}\delta_{\delta\rho}b^\dagger(v,n,\delta)\tau^i_{v\tilde{v}}\tau^j_{s\tilde{s}}d^\dagger(\tilde{s},\tilde{m},\rho)a^i_{\vec{k}'}a^{\dagger j}_{\vec{k}})|p\rangle_0. \qquad (3.30)
\end{aligned}
$$

We then use $a^i_{\vec{k}'}a^{\dagger j}_{\vec{k}}|0\rangle = \delta^{ij}\delta(\vec{k}'-\vec{k})|0\rangle$ and write the sum of the graphs (a) and (b) as:

$$
\begin{aligned}
&\frac{1}{E_0-H_0}H_I^{\pi\to q\bar{q}}\frac{1}{E_0-H_0}H_I^{q\to\pi q}|p\rangle_0+\frac{1}{E_0-H_0}H_I^{q\pi\to q}\frac{1}{E_0-H_0}H_I^{0\to\pi q\bar{q}}|p\rangle_0 \\
&=\frac{1}{(2f)^2(2\pi)^3}\sqrt{\frac{\omega_f\omega_o\omega^s\omega^p}{(\omega_f-1)(\omega_o-1)(\omega^s-1)(\omega^p-1)}}\times \\
&\int d^3k\frac{(\vec{\sigma}\cdot\vec{k})_{n\tilde{n}}(\vec{\sigma}\cdot\vec{k})_{m\tilde{m}}}{2\omega_k}\frac{j_1^2(kR)}{(kR)^2}\frac{R^2}{\omega_o-\omega_f-\omega^s-\omega^p}\times \\
&\left\{\left(\frac{1}{\omega_o-\omega_f-R\omega_k}+\frac{1}{-\omega^s-\omega^p-R\omega_k}\right)b^\dagger(s,n,\rho)\tau^i_{s\tilde{s}}d^\dagger(\tilde{s},\tilde{n},\rho)b^\dagger(v,m,\delta)\tau^i_{v\tilde{v}}b(\tilde{v},\tilde{m},\delta)\right. \\
&\left.+\frac{1}{-\omega^s-\omega^p-R\omega_k}\delta_{\tilde{v}s}\delta_{\tilde{n}m}\delta_{\delta\rho}b^\dagger(v,n,\delta)\tau^i_{v\tilde{v}}\tau^i_{s\tilde{s}}d^\dagger(\tilde{s},\tilde{m},\rho)\right\}|p\rangle_0 \qquad (3.31)
\end{aligned}
$$

We are now ready to compute the probability $P_{\pi q\bar{q}}$ to find a $q\bar{q}$ in the nucleon. It is given by the square of the amplitude (3.31):

$$
\begin{aligned}
P_{\pi q\bar{q}} \;=\; & \left(\frac{1}{(2f)^2(2\pi)^3}\right)^2 \frac{\omega_f\omega_o\omega^s\omega^p}{(\omega_f-1)(\omega_o-1)(\omega^s-1)(\omega^p-1)}\left(\frac{4\pi}{3}\right)^2 \\
& \int_o^\infty \frac{k^4dk}{2\omega_k}\frac{j_1^2(kR)}{(kR)^2}\int_o^\infty \frac{k'^4dk'}{2\omega_{k'}}\frac{j_1^2(k'R)}{(k'R)^2}\left(\frac{R^2}{\omega_o-\omega_f-\omega^s-\omega^p}\right)^2\times \\
& \left\{\left(\frac{1}{\omega_o-\omega_f-R\omega_k}+\frac{1}{-\omega^s-\omega^p-R\omega_k}\right)\left(\frac{1}{\omega_o-\omega_f-R\omega_{k'}}+\frac{1}{-\omega^s-\omega^p-R\omega_{k'}}\right)\times\right. \\
& {}_o\langle p|b^\dagger(\tilde{v}',\tilde{m}',\delta')\tau^i_{\tilde{v}'v'}\sigma^j_{\tilde{m}'m'}b(v',m',\delta')d(\tilde{s}',\tilde{n}',\rho')\tau^i_{\tilde{s}'s'}\sigma^j_{\tilde{n}'n'}b(v',m',\delta') \\
& \qquad b^\dagger(s,n,\rho)\tau^k_{s\tilde{s}}\sigma^l_{n\tilde{n}}d^\dagger(\tilde{s},\tilde{n},\rho)b^\dagger(v,m,\delta)\tau^k_{v\tilde{v}}\sigma^l_{m\tilde{m}}b(\tilde{v},\tilde{m},\delta)|p\rangle_o \\
& +\frac{1}{-\omega^s-\omega^p-R\omega_k}\frac{1}{-\omega^s-\omega^p-R\omega_{k'}}\times \\
& \left.{}_o\langle p|d(\tilde{s}',\tilde{m}',\rho')\tau^i_{\tilde{s}'s'}\tau^i_{s'v'}\sigma^j_{\tilde{m}'m'}\sigma^j_{m'n'}b(v',n',\rho')b^\dagger(v,n,\rho)\tau^k_{vs}\tau^k_{s\tilde{s}}\sigma^l_{nm}\sigma^l_{m\tilde{m}}d^\dagger(\tilde{s},\tilde{m},\rho)|p\rangle_o\right\}
\end{aligned}
\tag{3.32}
$$

The last quantities to be calculated are the expectation values between the bare proton states. It is a very long but straightforward calculation. We calculated only the case where the quark that emits or absorbs the pion remains in the same orbital state. The results are:

$$
\begin{aligned}
& {}_o\langle p|b^\dagger(\tilde{v}',\tilde{m}',\delta')\tau^i_{\tilde{v}'v'}\sigma^j_{\tilde{m}'m'}b(v',m',\delta')d(\tilde{s}',\tilde{n}',\rho')\tau^i_{\tilde{s}'s'}\sigma^j_{\tilde{n}'n'}b(v',m',\rho') \\
& \qquad b^\dagger(s,n,\rho)\tau^k_{s\tilde{s}}\sigma^l_{n\tilde{n}}d^\dagger(\tilde{s},\tilde{n},\rho)b^\dagger(v,m,\delta)\tau^k_{v\tilde{v}}\sigma^l_{m\tilde{m}}b(\tilde{v},\tilde{m},\delta)|p\rangle_o = \\
& = 684-110\delta_{\tilde{s}\bar{u}}-181\delta_{\tilde{s}\bar{d}} \\
& {}_o\langle p|d(\tilde{s}',\tilde{m}',\rho')\tau^i_{\tilde{s}'s'}\tau^i_{s'v'}\sigma^j_{\tilde{m}'m'}\sigma^j_{m'n'}b(v',n',\rho')b^\dagger(v,n,\rho)\tau^k_{vs}\tau^k_{s\tilde{s}}\sigma^l_{nm}\sigma^l_{m\tilde{m}}d^\dagger(\tilde{s},\tilde{m},\rho)|p\rangle_o \\
& = 972-54\delta_{\tilde{s}\bar{u}}-81\delta_{\bar{s}\bar{d}}
\end{aligned}
\tag{3.33}
$$

The results contained in expressions (3.33) are quite surprising. They say that if the quark structure of the pion is important and if the quarks from the pion are allowed to anti-symmetrize with the quarks from the parent proton, then the probability for the antiquark

Integral	$R = 0.6\ fm$	$R = 0.8\ fm$	$R = 1\ fm$
I_1	1.6848	1.24065	0.980306
I_2	0.1946	0.1734430	0.157762
I_3	4.92548	2.65299	1.63279
$P_{\pi q\bar{q}}/P_\pi$	0.0217	0.0124	0.0081

Table 3.2: The two to one loop ratio for various bag radii.

in the pion to be a $\overline{u}$ is bigger than $\overline{d}$. The above result is also independent of particularities of a given model, in the sense that expressions (3.33) are a direct consequence of the bare proton wave function, Eq. (3.14). They are also a consequence of assuming a pion quark interaction.

To better realize how important are these second order effects, we will calculate the ratio of probabilities $P_{\pi q\bar{q}}/P_\pi$. To this end we need to perform the integrals over k and k' in Eqs. (3.27) and (3.32). These integrals are dependent on the particular value of the bag radius and here we will display the results for $R = 0.6,\ 0.8$ and $1\ fm$. We set $\omega_0 = \omega_f$ and define the following integrals:

$$
\begin{aligned}
I_1 &= \frac{1}{2}\int_0^\infty \frac{dx}{m_\pi^2 R^2 + x^2}\frac{\omega^s + \omega^p + 2(m_\pi^2 R^2 + x^2)^{1/2}}{\omega^s + \omega^p + (m_\pi^2 R^2 + x^2)^{1/2}}\left(\frac{sin^2 x}{x^2} + cos^2 x - \frac{sinxcosx}{x}\right), \\
I_2 &= \frac{1}{2}\int_0^\infty \frac{dx}{(m_\pi^2 R^2 + x^2)^{1/2}}\frac{1}{\omega^s + \omega^p + (m_\pi^2 R^2 + x^2)^{1/2}}\left(\frac{sin^2 x}{x^2} + cos^2 x - \frac{sinxcosx}{x}\right), \\
I_3 &= \int_0^\infty \frac{dx}{(m_\pi^2 R^2 + x^2)^{3/2}}\left(\frac{sin^2 x}{x^2} + cos^2 x - \frac{sinxcosx}{x}\right),
\end{aligned}
\tag{3.34}
$$

where we use $x = kR$. The numerical value of these integrals are displayed in table (3.2).

With these definitions we rewrite expression (3.32) as:

$$P_{\pi q\bar{q}} = \left(\frac{1}{(2Rf)^2(2\pi)^3}\right)^2 \frac{\omega_o^2}{(\omega_o-1)^2}\frac{\omega^s\omega^p}{(\omega^s-1)(\omega^p-1)}\left(\frac{4\pi}{3}\right)^2\left(\frac{1}{\omega^s+\omega^p}\right)^2 \left\{I_1^2\,(684-110\delta_{\bar{s}\bar{u}}-181\delta_{\bar{s}\bar{d}})+I_2^2\,(972-54\delta_{\bar{s}\bar{u}}-81\delta_{\bar{s}\bar{d}})\right\} \tag{3.35}$$

The ratio $P_{\pi q\bar{q}}/P_\pi$ is then easily expressed:

$$\frac{P_{\pi q\bar{q}}}{P_\pi} = \frac{1}{(2Rf)^2(2\pi)^3}\frac{\omega^s\omega^p}{(\omega^s-1)(\omega^p-1)}\frac{4\pi}{3}\left(\frac{1}{\omega^s+\omega^p}\right)^2 \left\{\frac{I_1^2}{I_3}\frac{(684-110\delta_{\bar{s}\bar{u}}-181\delta_{\bar{s}\bar{d}})}{57}+\frac{I_2^2}{I_3}\frac{(972-54\delta_{\bar{s}\bar{u}}-81\delta_{\bar{s}\bar{d}})}{57}\right\} \tag{3.36}$$

The value of this ratio for different sizes of the bag is also displayed in table (3.2) where we used $m_\pi = 140\ MeV$ for the pion mass and $f = 93\ MeV$ for the pion decay constant. There is a strong dependence of the calculated ratio on the bag size but even for the worst scenario, the case of a small bag, the size of the two-loop contribution is just around 2% of the one loop.

It appears to be safe to neglect possible antisymmetrization effects between pion quarks and the nucleon valence quarks. Of course, when writing the nucleon wave function one would have to add the contributions from all possible states:

$$|N>= Z^{1/2}[|N>_0+|N\pi>_0+\sum_{q\ states}|N\pi q\bar{q}>_0+...] \tag{3.37}$$

where the sum of all quark states (1s, 2s, etc...) was particularly emphasized. If the quark that emits the pion remains in the ground state the only contribution from antisymmetry

is the one in table (3.2). As we have to sum over all other possible states for this quark, it turns out that the antisymmetry effects are further diluted. However, we will also have some other contributions even in this case, because if the quark in the pion is in the ground state it can antisymmetrize with the two spectator valence quarks. Also, if the quark in the pion is in an excited state, it can combine with a particular excited state of the valence quark that emitted the pion in the first place, as in the gluon example. We did not make these calculations because of their level of complexity. Our goal was to examine the behaviour of the dominant contribution, displayed in table (3.2), and our results indicate that this number is itself already small. Of course, as the sum over quark states is infinite in Eq. (3.37), we can not rule out that eventually the antisymmetry graphs will be very important. We believe that this is improbable as, for instance, the contributions from graphs with no antisymmetry would grow possibly in the same proportion, keeping the dilution for any number of quark states that are summed over. As said before, it would be a long calculation to verify that due to the level of complexity in the renormalization. In Eq. (3.37) we displayed explicitly the mass renormalization constant Z. For instance, the expression for Z in one loop is[1]: $Z = 1/(1+_0 < N\pi|N\pi >_0) = 1-_0 < N\pi|N\pi >_0$. In addition to Z, in two loops we would also have to calculate the renormalization constant for the coupling constant in which case the calculations would be tremendously long [123]. This would, again, miss the point of the present calculation which was simply to check whether the antisymmetrization effects in pion emission could be safely disregarded.

[1]The expansion of Z has to be truncated at first order if we are in one loop, at second order if we are in two loops, etc. It would be a mistake to use the full Z to any order as this would introduce random corrections in the coupling constant once it appears in the denominator of Z.

Chapter 4

The Nucleon Spin

4.1 The Spin Problem

Much of the interest in the quark spin content of the nucleon was revived several years ago by the EMC experiment [20] where the proton spin structure function was measured in a region of small x previously unexplored. Their measurement, together with small and large x extrapolations, says that:

$$\Gamma_1^p = \int_0^1 g_1^p(x) = \int_0^1 dx \frac{A_1^p(x,Q^2)F_2^p(x,Q^2)}{2x[1+R(x,Q^2)]} = 0.126 \pm 0.01 \pm 0.015, \tag{4.1}$$

at the average $Q^2 = 10\ GeV^2$. On the other hand, from the parton model expression for g_1^p, Eq. (2.44), one can write:

$$g_1^p(x) = \frac{1}{12}\Delta q_3(x) + \frac{1}{36}\Delta q_8(x) + \frac{1}{9}\Delta\Sigma(x), \tag{4.2}$$

where $\Delta q_3 = g_a = \delta u(x) + \delta\overline{u}(x) - \delta d(x) - \delta\overline{d}(x)$, $\Delta q_8 = g_a^8 = \delta u(x) + \delta\overline{u}(x) + \delta d(x) + \delta\overline{d}(x) - 2\delta s(x) - 2\delta\overline{s}(x)$. The charges g_a and g_a^8 can be related to the factors F and D determined

from n and Σ beta decay [124]:

$$g_a = F + D, \quad g_a^8 = 3F - D, \tag{4.3}$$

where $F + D = 1.2573 \pm 0.0028$ and $F/D = 0.575 \pm 0.016$ [125, 126]. Once g_a and g_a^8 are known, the experiment is able to determine the singlet axial charge $\Delta\Sigma(x) = \delta u(x) + \delta\overline{u}(x) + \delta d(x) + \delta\overline{d}(x) + \delta s(x) + \delta\overline{s}(x)$. The EMC quoted the following result [20][1]:

$$\Delta\Sigma = 0.12 \pm 0.094 \pm 0.138. \tag{4.4}$$

This quantity was, and still largely is, interpreted as the fraction of the spin carried by the quarks.

The SU(6) nonrelativistic quark model predicts that $\Delta\Sigma = 1$ because there are only quarks in this sort of model. Relativistic models, like the bag, predict that $\Delta\Sigma \sim 0.65$ because the lower component of the Dirac spinor contributes with a negative sign in the calculation of $\Delta\Sigma$. The rest of the proton spin should be shared among gluons and orbital angular momentum. However, the small $\Delta\Sigma$ measured by the EMC did not seem to fit in any reasonable picture of the nucleon at the time. (A possible exception was the Skyrme model that indeed has a vanishing singlet axial coupling. Currently, it is established that the axial charge is no longer compatible with zero and there is, as yet, no consensus on mechanisms to render the Skyrme model with a nonzero axial charge [127].) In any case, the measurement of a vanishing proton axial charge became known as the "spin problem" or "spin crisis" [128, 129, 47].

Since then, many other polarized experiments have been performed and now there is a reasonable amount of data on the proton [20, 52, 64] neutron [54, 51, 49] and deuteron

[1]This result was obtained using values for F and D different from the ones listed after Eq. (4.3).

[53, 51, 49] spin structure functions [130].

4.1.1 Present Experimental Situation

All information on the first moment of the spin structure functions is summarized in tables 4.1, 4.2 and 4.3, where the results for the proton, neutron and deuteron are shown together with their respective axial charges.

Experiment	Γ_1^p	$\Delta\Sigma$	$Q^2\ (GeV^2)$
EMC [20]	$0.138 \pm 0.01 \pm 0.018$	0.27 ± 0.16	10.7
SMC [52]	$0.136 \pm 0.011 \pm 0.011$	$0.22 \pm 0.1 \pm 0.1$	10
E143 [64]	$0.127 \pm 0.04 \pm 0.01$	0.27 ± 0.1	3
SMC [52] + EMC [20] + E80/E130 [136]	$0.142 \pm 0.008 \pm 0.011$	$0.27 \pm 0.08 \pm 0.1$	10

Table 4.1: The first moment of the proton spin structure function. The EMC and SMC extraction of $\Delta\Sigma$ was made using $O(\alpha_s)$ QCD corrections [93] while the E143 used $O(\alpha_s^3)$ QCD corrections [131].

Some comments on these tables are in place. First, the shown value for Γ_1^p of the EMC is different from the one quoted previously, Eq. (4.1), because it was extracted using improved parametrizations for F_2 and R [130]. Second, the neutron structure function has to be extracted from the deuteron and proton data through the following relation:

$$g_1^n(x) = \frac{2g_1^d(x)}{(1 - 1.5\omega_d)} - g_1^p(x), \tag{4.5}$$

where $\omega_D = 0.05 \pm 0.01$ [51, 49] is the probability to find the deuteron in a D-state. (We point out that a recent study [132] on the extraction of the neutron structure function

Experiment	Γ_1^n	$\Delta\Sigma$	$Q^2\ (GeV^2)$
E142 [54]	$-0.022 \pm 0.007 \pm 0.009$	0.57 ± 0.11	2
E143 [51]	$-0.037 \pm 0.008 \pm 0.011$	-	3
SMC [49]	$-0.063 \pm 0.024 \pm 0.013$	-	10

Table 4.2: The first moment of the neutron spin structure function. The E142 extraction of $\Delta\Sigma$ was made using $O(\alpha_s)$ QCD corrections [93].

Experiment	Γ_1^d	$\Delta\Sigma$	$Q^2\ (GeV^2)$
E143 [51]	$0.042 \pm 0.003 \pm 0.004$	0.3 ± 0.06	3
SMC [49]	$0.034 \pm 0.009 \pm 0.006$	0.2 ± 0.11	10

Table 4.3: The first moment of the deuteron spin structure function.The E143 and SMC extraction of $\Delta\Sigma$ was made using $O(\alpha_s^3)$ QCD corrections [131].

from polarized deuterium which showed that the formula (4.5) is not good for large x.) The measurement of $g_1^d(x)$ by the E143 and SMC experiments in conjunction with their respective $g_1^p(x)$ then determine the $\Gamma_1^n(x)$ shown. The exception goes to the E142 experiment where $g_1^n(x)$ was measured directly from polarized ^3He [54]. Of course, measurements at a different x are at a different momentum transfer Q^2. In particular, Q^2 can vary from $\sim 1\ GeV^2$ at small x to $\sim 60\ GeV^2$ at large x. To calculate the integrals over x, it is usually assumed that the asymmetry, defined in Eq. (2.23) and used in the extraction of $g_1(x)$ through Eq. (4.1), is Q^2 independent. This approximation is used to bring all the data to a common Q^2 and hence determine the value of the integrals listed in the tables. However, the assumption of a

Q^2 independent asymmetry seems to be contradicted by recent studies of the QCD evolution of the spin structure functions at next-to-leading order [133, 134], at least for small values of Q^2. Recent measurements by the E143 collaboration [135] seem to confirm this conclusion.

That the first moment of the spin structure functions differ from theoretical expectations can be seen directly from the Ellis-Jaffe sum rule, Eq. (2.49), where the assumption of an unpolarized sea leads directly to the naive expectation $\Delta\Sigma \sim g_a^8$, a conclusion clearly not sustainable from the data. For instance, at 10 GeV^2, the Ellis-Jaffe prediction for the proton spin structure function is [52]:

$$\Gamma_1^{p,EJ} = 0.176 \pm 0.006, \tag{4.6}$$

where QCD corrections up to one loop [93] were included [2] and $\alpha_s(10\ GeV^2) = 0.23 \pm 0.02$.

To show the degree of disagreement between theory and experiment, we reproduce here Fig. (9) of [130] where the measured first moments are plotted against the theoretical predictions for a range of Q^2.

Finally, the measurement of the proton and neutron spin structure functions, allow us to test the Bjorken sum rule, Eq. (2.47). Table 4.4 shows the experimental results of the various experiments together with theoretical expectations where QCD corrections were included.

Both experimental results agree well with the theoretical predictions and a nice conclusion can be drawn from it. The Bjorken sum rule is pure nonsinglet in the sense that it involves only g_a which in turn reflects the difference in the axial charges carried by the u and d quarks. The Ellis-Jaffe sum rule involves both singlet and nonsinglet combinations, meaning that if everything is fine for nonsinglet combinations through the Bjorken sum rule, the problem

[2] These corrections will be studied in some detail in the next chapter when we study next-to-leading order corrections to the parton distributions.

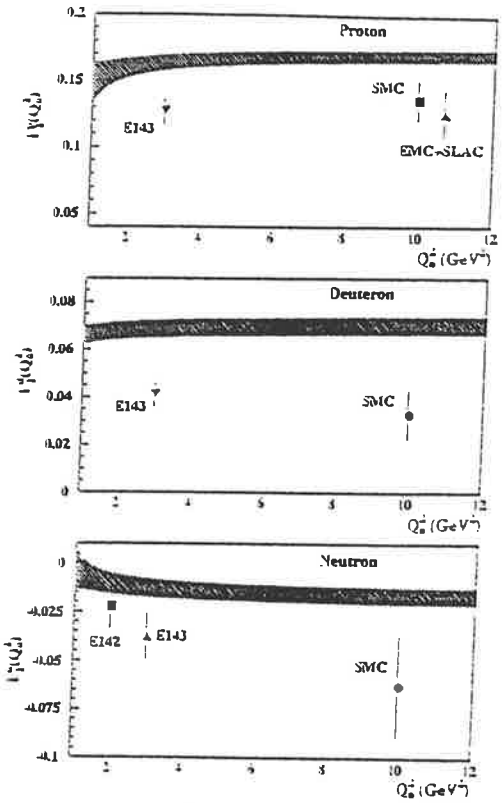

Figure 4.1: Figures from Voss

in the Ellis-Jaffe sum rule is restricted to its singlet part ($\Delta\Sigma$). Besides this, the Bjorken sum rule connects weak interactions, through g_a, to the strong forces holding the nucleon together, through the structure functions. Its verification is a landmark in the study of QCD.

For definiteness, throughout this chapter we will use the result for Γ_1^p obtained by the SMC [52] in conjunction with the EMC [20] and early SLAC data [136], listed in the last line of table 4.1.

Experiment	$\Gamma_1^p - \Gamma_1^n$	Theory	$Q^2\ (GeV^2)$
E143 [64] + [51]	$0.163 \pm 0.01 \pm 0.016$	0.171 ± 0.008	3
SMC [52] + [49]	0.199 ± 0.038	0.187 ± 0.003	10

Table 4.4: Tests of the Bjorken sum rule .The theoretical estimation of the Bjorken sum rule was made using $O(\alpha_s^3)$ QCD corrections [56].

4.1.2 The Small x Region

Of course, experimentally it is not possible to go to $x = 1$ or $x = 0$. In the case of SMC [52] the limits are $0.003 < x < 0.7$. For the new E143 SLAC data [51], the limits are $0.029 < x < 0.8$ and their integral of $g_1(x)$ agrees within errors with the SMC results as seen in table 4.1. Extrapolations have to be made to cover the whole x interval. The large x region is well behaved and perturbation theory predicts that $A_1 \to 1$ as $x \to 1$ [137]. For small x a Regge type behaviour [138], $g_1^p \propto x^\alpha$, $0 < \alpha < 0.5$ [139], has been assumed - with the errors in the quoted data reflecting the uncertainty in α. However, the SMC [52] data shows a tendency to increase for $x < 0.02$. In their analysis of the data, the SMC did not consider that the measured tendency of the data to rise at small x was enough to motivate the use of some other extrapolation of g_1^p in that region. Close and Roberts [140] considered a few other possibilities. They are:

a) $-Lnx$, derived using the fact that the Froissart bound [141] for the total unpolarized cross section, $\sigma \leq Log^2 s$ with s the square of the center of mass energy, is saturated. Then $g_1 \propto -Lnx$ follows if one calculates the behaviour of the spin asymmetry for a vector potential in which case $A \propto 1/sLogs$ and hence $g_1 \propto -Lnx$ as $x \to 0$.

b) $1/xLn^2x$. This is derived as in a) but in this case the potential transforms like an

axial vector.

c) $-(1+2Lnx)$. This was derived by Bass and Landshoff [142] using a model for the non-perturbative Pomeron exchange simulated through non-perturbative gluons. Their calculation affects only the singlet part of g_1.

According to the data shown by Close and Roberts, the $-Lnx$ and $-(1+2Lnx)$ forms tend to fit the data, though point at smallest x is missed, while the very singular behaviour $1/xLn^2x$ tends to fit the data over the whole small x region. On the other hand, the extrapolation used by the SMC appears to be somewhat below the trend of the data. Some comments on these results seem appropriate. First, in their analysis Close and Roberts extrapolated the individual data of each x to a common $Q^2 = 10\ GeV^2$, using the assumption of a Q^2 - independent asymmetry. As we commented before, this does not seen to be the case. In fact, if one considers the Q^2 dependence of the asymmetry calculated in Ref. [133], one may conclude that the data used by Close and Roberts is overestimated - at least for the last two x points. Second, the rise of g_1^p at small x should be reflected also in the singlet part of the deuteron spin structure function. However, recent deuteron data shows no signal of a rapid raise of g_1^d [49]. Thus a very singular g_1 can be ruled out but the question of its precise behaviour at small x is still open.

4.1.3 Modelling the Data

The discrepancy between the Ellis-Jaffe sum rule and the measured Γ_1^p and $\Delta\Sigma$ launched a huge amount of research aimed at understanding why the axial charge is much smaller than predicted [128, 129, 143, 47]. As we commented before, nonrelativistic quark models predicted that $\Delta\Sigma \sim 1$. This value is reduced to something near 0.65 if relativistic wave functions are used because:

$$\overline{\psi}\gamma^3\gamma_5\psi \propto \left(f^2 - \frac{g^2}{3}\right), \tag{4.7}$$

and the lower component of $\psi(g)$, acts as a p wave, diluting part of the spin into orbital angular momentum. Meson dressing tends to reduce the spin carried by quarks somewhat more [144, 147]. Here, because of mass effects, the dominant contribution will come from pions. As they are (pseudo-)scalars, they will take some spin from the quarks in the form of orbital angular momentum. In fact, specific calculations in the Cloudy Bag Model [144, 145] give Γ_1^p close to what is expected from the Ellis-Jaffe sum rule. For instance, a particular version of the CBM gives [145] $\Gamma_1^p = 0.161$ and $\Gamma_1^n = -0.048$ for $g_a = 1.254$. These numbers are corroborated by a recent calculation of meson dressed quark distributions where similar results are found [146]. Other calculations involving Chiral Bag Models [147, 109, 113, 148] also concluded that mesons are important in nucleon spin structure. However, we do not know of any consistent model calculation that can explain both the first moment of the spin structure functions and their x dependence. As a matter of fact, not many publications worry about this fact. From the few works where the first moment and the x dependence were calculated [149, 150, 151, 152, 146], it can be concluded that bag models with meson dressing and one gluon exchange, can provided a fair picture of the nucleon structure functions as seen by experiments [153, 146]. The study of the x dependence, suggests that the region of small x (< 0.1) is responsible for the low value of Γ_1^p. Details of these calculations will be provided in the next chapter.

Maybe the most important point derived from the EMC and related experiments involving the spin structure functions is the one related to the axial anomaly [92]. In the next sections we will study it in some detail but now it suffices to say that it is probably because of the axial anomaly that the models of the nucleon discussed before are close to the Ellis-Jaffe

sum rule but not to the experimental results. Moreover, as will be clear from the discussion of the next section, the problem with such models is that the matrix elements of their axial currents are related to spin while the measured $\Delta\Sigma$ *is not* the spin fraction carried by quarks [21, 129].

The axial anomaly as the source of the spin problem was originally advocated by Altarelli and Ross [154], Carlitz, Collins and Mueller [155] and Efremov, Soffer and Teryaev [156]. These authors have argued that the axial charges of each quark flavour should be replaced by:

$$\Delta q \to \Delta q - \frac{\alpha_s}{2\pi}\Delta g, \tag{4.8}$$

where Δg is the amount of spin carried by gluons in the nucleon and the new Δq would be the "intrinsic" spin carried by quarks. As $\Delta\Sigma = \sum_q \Delta q$, this means that the integral of $g_1(x)$ over x would be:

$$\int_0^1 g_1^p(x) \sim \frac{1}{9}\Delta\Sigma - \frac{1}{9}\frac{\alpha_s}{2\pi}N_f\Delta g, \tag{4.9}$$

where only the singlet contribution was written. However, according to the OPE, there is no gauge invariant, twist-2, gluon operator contributing to Γ_1^p [93]. From the OPE point of view, eq. (4.9) would be meaningless [128], because there is no gauge invariant gluon operator contributing to the first moment of $g_1(x)$. Following some major works on the subject [154, 155, 156, 157, 128, 158, 159, 21, 160, 129, 143] we will explain why the view of $g_1(x)$ according to Eq. (4.9), can actually make sense. Meanwhile, we point out that the anomalous gluon contribution, Eq. (4.9), was derived in the context of the Improved Parton Model (IPM) [82, 161] approach to QCD. In such a model, the Wilson coefficients are calculated with the help of the factorization [161, 162] of the DIS cross sections, which

is separated into a hard and a soft part according to the size of the transverse momentum (squared) of the quarks, relative to some arbitrary factorization scale μ^2. The part of the cross section with high transverse momentum ($k_T^2 > \mu^2$) is said to be hard and it is associated with a particular Wilson coefficient, while the part with low transverse momentum ($k_T^2 < \mu^2$) is said to be soft. The latter plays the role of the matrix elements of the quark and gluon operators between hadron states, as seen in the OPE. The soft part contain all the low momentum scale of the theory and, as such, is subject to infrared divergences (because gluons and some quark flavours are massless). In this way, the soft part is dependent on the infrared regularization of the cross section, a point that will be better explained later when we give some calculational details of the photon-gluon cross section.

Whithin the IPM, the nucleon spin structure function is given by the calculation of the full photon-nucleon cross section. For the case of polarized scattering this is just $g_1(x)$ and if we denote the hard parts of the cross section by C'^s, then:

$$\begin{aligned} g_1^p(x,Q^2) &= \int_x^1 \frac{dy}{y} C_q^{NS}(x/y, Q^2/\mu^2)\Delta q^{NS}(y,\mu^2) + \int_x^1 \frac{dy}{y} C_q^S(x/y, Q^2/\mu^2)\Delta q^s(y,\mu^2) \\ &+ \frac{1}{9}\int_x^1 \frac{dy}{y} C_g(x/y, Q^2/\mu^2)\Delta g(y,\mu^2), \end{aligned} \tag{4.10}$$

where $\Delta q^{NS} = \frac{1}{12}g_a + \frac{1}{36}g_a^8$, while the singlet charge is $\Delta q^S = \frac{1}{9}\Delta\Sigma$. These combinations contain all the infrared (and hence nonperturbative) information about the nucleon, while the hard coefficients, C, are well determined perturbatively.

Hence, the anomaly interpretation of the EMC results says that the measured Γ_1^p is small because of a cancellation from polarized gluons. In this sense, models that do not have the axial anomaly should not to be expected to reproduce the measured results. On the other hand one can modify existing models so that they obey decompositions like (4.8). For instance, if one introduces instanton interactions in the MIT model [163], a modification of

the quark axial current of the form of Eq. (4.8) can be obtained. This is possible because the instanton breakes chiral symmetry and is in fact the suggested [164] mechanism for the solution of the $U_A(1)$ problem. The same conclusion has been drawn [165] from models like the Nambu-Jona-Lasinio model [166] when point-like, quark-quark interactions, arising from instantons (as proposed by /t Hooft [164]) are built in.

Initially, the amount of polarized glue need to fit the data through the modified expression (4.9) was very large [167, 168] but recent calculations have brought these values to more acceptable standards [169, 170, 133]. Nevertheless, while the axial anomaly is a strong candidate to solve the spin problem there is, as yet, no consensus that it helps as much as it should in the x region of the present experiments [169].

Finally we note that there are a few parametrizations of the quark distributions that are able to fit the measured data without resorting to an anomalous contribution. For instance, in Ref. [137] a parametrization was constructed where there is a significant, polarized strange quark contribution to the singlet charge but no gluon term, although its contribution to the spin sum rule is not negligible. In an other approach, a modified SU(6) proton wave function is used [171]. The authors of this work conclude that the measured asymmetries can be fitted without the use of polarized strange quarks or an anomalous gluon term. We notice that both approaches may be misleading because they identify the measured axial charge with spin.

4.2 The Spin Sum Rule

We start this section studying the decomposition of the proton spin in its parts. As the proton is composed of quarks and gluons, the obvious spin decomposition is:

$$\frac{1}{2}\Delta\Sigma + \Delta g + L_q + L_g = \frac{1}{2}, \tag{4.11}$$

where $\Delta\Sigma$ is to be identified with the total spin carried by the quarks, Δg with the total spin carried by gluons and L_q and L_g with the orbital angular momentum of quarks and gluons. Notice that the above formula does not say anything about the sign of the quark or gluon contribution. Moreover, in contrast to the momentum sum rule, seen in Sect. 1.2.2, inclusive measurements of g_1 alone does not say anything about the amount of polarized glue, which means that Δg is not constrained by g_1 measurements[3]. This can be easily seen from the fact that the integral of g_1 is related only to $\Delta\Sigma$ and, if we do not know L_q and L_g, Eq. (4.11) does not tell us anything about Δg.

It is very instructive to see the origins of Eq. (4.11). As usual, it can be derived from the angular momentum tensor and here we follow the derivation of Jaffe and Manohar [128] and Ji et al. [172]. If the $M^{\lambda\mu\nu}$ is the QCD angular momentum tensor, then the conserved charges that are the generators of the Lorentz transformations are [128, 172]:

$$J^{\mu\nu} = \int d^3x M^{0\mu\nu}. \tag{4.12}$$

If the the nucleon is in a state $|P, 1/2>$ moving in the z direction, then:

$$\frac{1}{2} = \frac{< P, 1/2|J^{12}|P, 1/2 >}{< P, 1/2|P, 1/2 >} \tag{4.13}$$

because $J^{12}|P, 1/2 >= 1/2|P, 1/2 >$. The matrix elements of Eq. (4.13) can be readily calculated in classical QCD if one notices that from the Lagrangian $L_{QCD} = \overline{\psi}(i\gamma^\mu\partial_\mu - g\gamma^\mu A_\mu - m) - F^2/4$, the classical, unrenormalized, angular momentum tensor is [172]:

[3] As a matter of fact, interpretations of g_1 that include gluonic contributions through the axial anomaly, can be used to constrain the total gluon. This will be seen later in this chapter.

$$M^{\lambda\mu\nu} = i\overline{\psi}\gamma^{\lambda}(x^{\mu}\partial^{\nu} - x^{\nu}\partial^{\mu})\psi + \frac{i}{4}\overline{\psi}\gamma^{\lambda}[\gamma^{\mu},\gamma^{\nu}]\psi - F^{\lambda\rho}(x^{\mu}\partial^{\nu} - x^{\nu}\partial^{\mu})A_{\rho} - F^{\lambda\mu}A^{\nu} + F^{\lambda\nu}A^{\mu}, \quad (4.14)$$

from which immediately follows that:

$$\frac{1}{2}\Delta\Sigma + \Delta g + L_q + L_g = \frac{1}{2}, \quad (4.15)$$

where

$$\begin{aligned}
\Delta\Sigma &= \frac{< P,1/2| \int d^3x \overline{\psi}\gamma^3\gamma_5\psi |P,1/2 >}{< P,1/2|P,1/2 >} \\
\Delta g &= \frac{< P,1/2| \int d^3x (E^1A^2 - E^2A^1) |P,1/2 >}{< P,1/2|P,1/2 >} \\
L_q &= \frac{< P,1/2| \int d^3x i\overline{\psi}\gamma^0(x^1\partial^2 - x^2\partial^1)\psi |P,1/2 >}{< P,1/2|P,1/2 >} \\
L_g &= \frac{< P,1/2| \int d^3x E^i(x^2\partial^1 - x^1\partial^2)A^i |P,1/2 >}{< P,1/2|P,1/2 >}.
\end{aligned} \quad (4.16)$$

$\Delta\Sigma$ is obviously invariant under gauge transformations but a direct computation shows that Δg, L_q and L_g are not - though their sum is[4]. That L_q can be identified with the orbital angular momentum of quarks follows immediately from its form, $(\vec{x} \times \vec{\nabla})$. The same can be said for the gluon orbital angular momentum L_g. The identification of Δg with the spin carried by gluons is less obvious. One needs to go to an axial gauge, like the light-cone gauge in light-cone coordinates, in which case it can be shown [159, 174] that Δg is indeed the

[4]In a recent work [173], it is argued that it is possible to decompose the spin sum rule in two general gauge invariant parts. They are the total quark and gluon angular momentum: $J_q = \Delta\Sigma + L_q$ and $J_g = \Delta g + L_g$. However, the decomposition of the spin sum rule into four gauge invariant parts is still troublesome, and our discussion is completely unaltered. In any case, it would be extremely interesting to investigates the consequences from the approach of Ref. [173].

gluon spin content of the proton. It is worth noting that it is in the axial gauges that the parton distributions, including the polarized gluon distribution, are actually defined [175]. Finally, a direct inspection of $\Delta\Sigma$ in Eq. (4.16) shows that it is the expectation value of the Pauli spin matrix σ_3, the natural definition of spin. Moreover, as seen in the introductory discussion of deep inelastic scattering, the spin four vector has to be perpendicular to the momentum four vector. From the Dirac equation in momentum space, $(\not{p} - m)u(p,s) = 0$, one has:

$$\overline{u}(p,s)\not{p}\gamma_5 u(p,s) = -m\overline{u}(p,s)\gamma_5 u(p,s) \Rightarrow p_\mu \cdot [\overline{u}(p,s)\gamma^\mu\gamma_5 u(p,s)] = 0. \tag{4.17}$$

in the chiral limit. But the important feature in Eq. (4.17) is that it says that the classical, unrenormalized, axial current, has the basic property of the spin vector, $p_\mu s^\mu = 0$; it is often denoted by $\overline{u}\gamma^\mu\gamma_5 u = 2ms^\mu$. Eq. (4.17) is also an expression of the conservation of the classical axial current: $\partial_\mu\overline{\psi}(x)\gamma^\mu\gamma_5\psi(x) = 0$.

4.2.1 The Anomalous Gluon Contribution

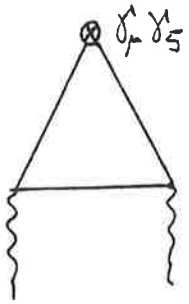

Figure 4.2: The triangle graph

When one goes to quantum field theory, the interpretation of the axial current in terms of spin, which we have just described, is not possible anymore because of the axial anomaly [92, 22]. The axial anomaly arises in the calculation of the triangle graph of Fig. 4.2, involving the axial vector and two bosons. It was first derived in the context of QED [92] but it appears in QCD as well [22, 93]. The triangle graph essentially forces the axial current to be extended by an extra term in order to ensure gauge invariance [92]. This happens because the triangle graph is superficially lineraly divergent and the Ward identity compatible with the classical axial current ceases to the respected when the triangle graph is present. The extra term in the current ensures that a correct Ward identity is used. In this case the divergence of the unrenormalized current, in the chiral limit, should be modified to [92, 22]:

$$\partial_\mu \overline{\psi}(x)\gamma^\mu\gamma_5\psi(x) = \frac{\alpha_s}{2\pi} TrG_{\mu\nu}\tilde{G^{\mu\nu}}, \tag{4.18}$$

which defines a new classical axial current. With this equation, the correct renormalized divergence equation of the axial current can then be obtained. As the axial current is a composite operator, it has a renormalization constant itself[5]: $J_5^{\mu R} = Z_A J_5^\mu$. Hence,

$$\partial_\mu J_5^{\mu R} = \frac{\alpha_s}{2\pi}[TrG_{\mu\nu}\tilde{G^{\mu\nu}}]^R, \tag{4.19}$$

where $\frac{\alpha_s}{2\pi}[TrG_{\mu\nu}\tilde{G^{\mu\nu}}]^R = \frac{\alpha_s}{2\pi}TrG_{\mu\nu}\tilde{G^{\mu\nu}} + (Z_A - 1)\partial_\mu J_5^\mu$. As emphasized by Bardeen [22], this renormalized, physical (gauge invariant) axial current, has nothing to do with the chiral transformations in the sense that the axial charge of the renormalized current is not conserved and thus cannot be the generator of chiral transformations. Bardeen also defines another axial current, $J_5^{\mu S}$, that is conserved and whose conserved charge generates the chiral

[5]This renormalization constant would be one if the unrenormalized current was not modified, that is, if it was conserved.

transformations:

$$J_5^{\mu S}(x) = J_5^{\mu}(x) - \frac{\alpha_s}{2\pi} K^{\mu}(x), \tag{4.20}$$

where $K_\mu = \epsilon_{\mu\nu\alpha\beta} Tr A^\nu (G^{\alpha\beta} - 2/3 A^\alpha A^\beta)$ and $\partial_\mu K^\mu = Tr G_{\mu\nu} \tilde{G^{\mu\nu}}$. Of course, the current $J_5^{\mu S}(x)$ is not gauge invariant as it misses exactly the term added to preserve gauge invariance when calculating the triangle graphs.

That the gauge invariant, renormalized, axial current does not have a spin interpretation should be clear by now but we give a very simple demonstration that this is indeed the case. We first notice that $p_\mu \cdot [\overline{u}(p,s)\gamma^\mu\gamma_5 u(p,s)]^S = 0$ from Eq. (4.17) because the renormalized, but gauge dependent axial current, $J_5^{\mu S}$, has the same divergence equation of its classical counterpart. Hence:

$$p_\mu \cdot [\overline{u}(p,s)\gamma^\mu\gamma_5 u(p,s)]^R \neq 0. \tag{4.21}$$

because, in general, $p_\mu < p|K^\mu|p > \neq 0$. We are then forced to conclude that the gauge invariant axial current is not related to spin. The same conclusions can easily be draw from the analysis of the algebra obeyed by the renormalized "spin" operators. Bass and Thomas [143] showed that these "spin" operators, constructed from the renormalized gauge invariant axial current, do not obey the required spin algebra.

How do these considerations on the interpretation of $\Delta\Sigma$ affect the spin structure function $g_1(x)$? From Eq. (4.10) we see that the integral of $g_1(x, Q^2)$, Γ_1^p, is given by:

$$\Gamma_1^p \sim \frac{1}{9}\Delta\Sigma(1 - \frac{\alpha_s(Q^2)}{3\pi} + ...) + \frac{1}{9}\Delta g(\mu^2) \int_0^1 C_g(x, Q^2/\mu^2) dx, \tag{4.22}$$

where the nonsinglet part was not explicitly written, the perturbative result up to order α_s for C_q^S [93] was shown and the integral over x of C_g was left undone. In the operator

product expansion for g_1, there is no gluon operator contribution to Γ_1^p [93], which means that $\int_0^1 C_g(x, Q^2/\mu^2)dx = 0$. In this case, measurements of g_1 would determine $\Delta\Sigma$. As we saw before in our discussion on the operator product expansion, only gauge invariant operators enter in the computation of the matrix elements, Eq. (2.75). Hence, from our discussion, it follows that the $\Delta\Sigma$ of the operator product expansion *is not* the spin fraction carried by quarks. We will call this quantity of $\Delta\Sigma^{OPE}$. On the other hand, Eq. (4.22) together with Eq. (4.20) says that in schemes where $\Delta\Sigma$ is the spin carried by quarks, $\int_0^1 C_g(x, Q^2/\mu^2)dx \neq 0$.

We can understand better why the renormalized operators do not have a spin interpretation if we notice that it is a property of renormalized operators having anomalous dimension different from zero that they will not always have the same symmetry properties as their classical counterparts. This is a well known fact of quantum field theory, where regularization can spoil some of the classical symmetries. The process of renormalization should restore such symmetries but in anomalous theories this is not what happens. Of course, the anomalous dimension beyond leading order is dependent on the renormalization scheme used, which means that one can always find a scheme where the anomalous dimension of the axial current is zero. In such a scheme, one would have again the identification of the axial current with spin. However, such schemes break gauge invariance, as seen in Eq. (4.20).

In view of this discussion, it is disturbing that many articles, including *all* the articles communicating experimental results, continually refer to the "measured quark spin content of the proton". Such a quantity has never been measured. What was measured was the spin asymmetry that is related to the $g_1(x)$ structure function which, in turn, is unambiguously related to $\Delta\Sigma^{ope}$ through Eq. (2.83). In this sense, there was never a problem with the spin of the proton. There was (is) a problem of using the language of the parton model, which is built upon conserved currents, to interpret a structure function, $g_1(x)$, built upon currents

that are not conserved because of the anomaly.

It is still possible to interpret g_1 in terms of the parton model [154, 155, 156] if the non-conserved, gauge invariant, axial current is separated into two gauge dependent parts, Eq. (4.20). This separation has been widely discussed and debated [154, 155, 156, 128, 158, 176, 177, 159, 178, 129, 143] exactly because of the lack of gauge invariance of such a separation . Although, at first sight, the use of a current that is conserved but gauge dependent is a high price to pay, we notice again that the decomposition of the spin into its parts in Eq. (2.3) *is not*[6] gauge invariant itself [172]. Moreover, the parton model is formulated in a specific gauge, the axial gauge, in which case the gluon distribution is given by the forward matrix element of the gluon operator in Eq. (4.20) [159, 174]. Hence one can, in principle, express Γ_1^p in terms of the quark and gluon spin. This is a very fragile interpretation, valid only in the axial gauge but, again, it is this gauge that is used to define parton distributions as well. If we change gauge we no longer have a clear quark and gluon helicity decomposition but neither do we have the parton model. Finally we note that up to large gauge transformations, like the ones that change the topological number, the forward matrix elements of the conserved axial current and gluon operator are gauge invariant [128, 178]. Thus, as long as we remain in perturbation theory, the separation of Γ_1^p is reliable and each term is separately gauge invariant - although their separate contributions are dependent on the renormalization scheme used [178, 31]. As a conclusion, it seems that if one wants to talk about spin carried by quarks, then one should use a renormalization scheme that allows such a thing, like the cut off scheme, and also a gauge where such interpretations through the parton model are allowed.

After renormalization, the matrix elements of the angular momentum tensor between

[6]See the footnote of page 88 for extended comments.

physical hadron states keep the same form as the classical one. Moreover, as the angular momentum tensor is an observable and conserved, it is invariant under the renormalization group equations in the sense that its anomalous dimension is zero and hence it has no Z to renormalize it. It also has to be independent of the renormalization point. The same is not true for all of the quantities appearing in its decomposition. And as QCD does not have a natural mass scale, renormalization cannot be made on-shell - hence they will depend on an arbitrary renormalization scale μ^2:

$$\frac{1}{2}\Delta\Sigma^{OPE}(\mu^2) + \Delta g(\mu^2) + L_q(\mu^2) + L_g(\mu^2) = \frac{1}{2}, \tag{4.23}$$

We would like to express the above sum rule directly in terms of the of the spin content of quarks, $\Delta\Sigma$. We then use [154, 155, 156]:

$$\Delta\Sigma^{OPE}(\mu^2) = \Delta\Sigma(\mu^2) - \frac{\alpha_s}{2\pi}N_f\Delta g(\mu^2). \tag{4.24}$$

Eq. (4.24), when used in the spin sum rule, will force the appearance of some other contribution to cancel the anomalous gluon. In other words, as $\Delta\Sigma^{OPE}$ is related to a nonconserved quantity, there should be a term in (4.23) that compensates this fact. This term is the quark orbital angular momentum [172]. To see how this works, consider the splitting of a gluon with helicity +1 into a massless quark antiquark pair, as shown in Fig. (4.3).

The gluon has chirality 0, which means that if chirality is to be conserved, the quark has to have its helicity opposite to the antiquark as in the massless limit chirality and helicity are the same. If the helicities are opposite, the spins of the quark and of the antiquark sum to zero, meaning that they have to have a relative orbital angular momentum +1 in order to conserve the total angular momentum. However, in the case of the currents used to construct $\Delta\Sigma^{OPE}$, chirality is not conserved, as discussed before. Hence, the quark and antiquark are

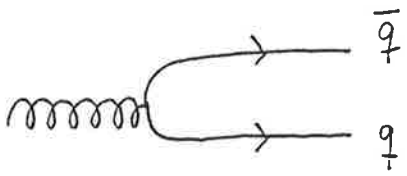

Figure 4.3: Gluon decay to a $q\bar{q}$ pair.

no longer restricted to have opposite helicities. Eq. (4.24) says that the chiral breaking term, the anomalous gluon, tends to force the appearance of negative helicities (-1/2) for the quark and for the antiquark. Thus, to conserve the total angular momentum, the relative orbital angular momentum of the quark antiquark pair has to be +2. In this way, the reshuffling of Eq. (4.23) using Eq. (4.24) implies a new value for the quark orbital angular momentum. The important feature is that in this picture, the total angular momentum *is not* sensitive to the anomalous gluon term.

We now proceed to make an explicit calculation of g_1 in a scheme that allows its separation into a quark and gluon contribution.

4.3 g_1^p in a Cut-off Scheme

The main assumption behind perturbative QCD is the factorization theorem [162]. It basically says that the cross sections are a product of two parts and that each part depends only on physics characteristic to one momentum scale. For instance, the formulas for the moments of the structure functions, Eqs. (2.82) and (2.83), are derived using factorization.

The OPE expresses the factorization automatically when separating the singular part of the product of currents, Eq. (2.72). The singular part is calculated in perturbation theory and it is what is meant by the hard part of the cross section. Its characteristic momentum scale is Q^2. The finite part is expressed in terms of the constants A_n, has μ^2 as its momentum scale and it reflects the large distance and nonperturbative nucleon wave function - as is clear from Eq. (2.75).

The OPE formulation is not the only recipe for perturbative QCD. One could go directly to the calculation of the relevant cross sections and separate them into soft and hard parts. Take the $g_1^p(x)$ spin structure function. In this case, the cross section involved is the one of a virtual photon on a proton. Applied to it, the factorization theorem says that:

$$g_1^p(x,Q^2) = \Delta\sigma_h^{\gamma^* q}(x,Q^2/\mu^2) \otimes \Delta f_{q/p}(x,\mu^2) + \Delta\sigma_h^{\gamma^* g}(x,Q^2/\mu^2) \otimes \Delta f_{g/p}(x,\mu^2), \qquad (4.25)$$

where $\Delta\sigma_h^{\gamma^* q}$ and $\Delta\sigma_h^{\gamma^* g}$ are the virtual photon-quark and virtual photon-gluon polarized hard cross sections and $\Delta f_{q(g)/p}$ is the polarized quark (gluon) spin distribution inside the nucleon. That this is the case can be intuitively seen from the analysis of the hadronic tensor. We know that it describes the virtual photon-nucleon cross section in the lepton-nucleon cross section, Eq. (2.1), and the factorization theorem applied to it says [162]:

$$W^{\mu\nu} = \sum_q \int_x^1 \frac{dy}{y} f_{q/N} H_q^{\mu\nu} \qquad (4.26)$$

where the sum is over all partons (quarks and gluons) and H is the hard part of the cross section. The structure functions are obtained by projecting $W^{\mu\nu}$ onto a particular structure function. Then, for instance, Eq. (4.25) follows.

The factorization theorem can also be used to define the parton distributions. We know from our studies of the simple parton model that $F_1(x) = \frac{1}{2}\sum_q e_q^2(q(x)+\overline{q}(x))$. Also, the hard

scattering cross section between the photon and the quark is just a delta function, $e_q^2\delta(1-x)/2$, in the parton model approximation as can be seen from Eq. (2.32). Then, following Jaffe [40], the commutator of currents in the hadronic tensor, Eq. (2.54), can be calculated in the Bjorken limit and in leading order in the strong coupling constant. Projecting the hadronic tensor to extract F_1 and comparing with the parton model expression, $F_1(x) = (q(x)+\overline{q}(x)) \otimes \sigma_h^{\gamma^* q}(x) = \frac{1}{2}\sum_q e_q^2(q(x)+\overline{q}(x))$, one gets [40]:

$$q(x)+\overline{q}(x) = \frac{1}{8\pi}\int dz^- e^{-ixMz^-/\sqrt{2}} < P|\overline{\psi}(z^-)\gamma^+\psi(0) - \overline{\psi}(0)\gamma^+\psi(z^-)|P > \qquad (4.27)$$

In the next chapter, when we study the x dependence of the parton distributions, we will see these objects in some detail. The important aspect now is that we can use the factorization hypothesis to calculate the momentum dependence of the structure functions. Once we know the coefficients f (in Eq. (4.26)), we just have to use perturbative QCD to calculate the hard cross section to any order. The calculation of these perturbative cross sections can also be done through the Wilson coefficients of the OPE. Both schemes are equivalent in the sense that the moments of the hard cross sections are just proportional to the Wilson coefficients:

$$\int_0^1 dx x^{n-1}\sigma_h(x) \propto C^n, \quad n = 1,3,5,... \qquad (4.28)$$

Conversely, the inverse transform of the Wilson coefficients are the hard cross sections. Also the anomalous dimensions have their interpretation in this parton model language. Their inverse transforms are know as splitting functions that measure the variation with scale of the probabilities to find a quark inside a quark, a quark and a gluon inside a quark, a quark-antiquark pair inside a gluon, etc. This formulation of perturbative QCD is known as the Improved Parton Model (IPM) [179, 82, 161].

There are a few subtle points in the relation between the OPE and the IPM. For example, the OPE involves strictly gauge invariant operators. This means that in the calculation of the Wilson coefficients, renormalization schemes that respect gauge invariance are used. In dealing with the IPM, one should also use such renormalization schemes in order to preserve gauge invariance. However, as we stated before, factorization has to be used in order to separate the cross sections into soft and hard parts. This separation is dependent on the renormalization scheme used when one goes to two loops and beyond in perturbative QCD - a well known fact [65]. In general, the cross sections will also have infrared singularities because the particles involved, quarks and gluons, are massless (at least for the u and d quarks). Depending on how these infrared singularities are treated, the parton distributions defined in one scheme or another, will be different. For instance, parton distributions are quite often defined in terms of a cut-off in the quark transverse momentum. This means that such distributions will have problems with gauge invariance. In this way, if one calculates these distributions in this cut-off scheme and use it to separate the hard part of the cross section, then one will get results different from the OPE. But this difference, as we already discussed at length, is obvious because these distributions are calculated in different schemes. They should not agree at all. Of course, g_1 as a physical object, is invariant under the choice of scheme.

To demonstrate this point clearly, we will calculate the gluon hard coefficient in a cut-off scheme and then compare with a scheme that respects gauge invariance. We also will show that $g_1(x)$ is scheme invariant. Finally, we will take the calculation of the gluon contribution very seriously and study the effects that the quark masses may have on the first moment and shape of $g_1(x)$.

4.3.1 Theoretical Construction

The hard gluon cross section is extracted from the full photon-gluon fusion cross section, $\Delta\sigma^{\gamma^* g}$ and is calculated through the box graphs which start at order α_s. The other contribution from which it must be separated is the quark distribution inside the gluon [180]. Mathematically, the factorization for the photon-gluon fussion cross section is expressed as:

$$\Delta\sigma^{\gamma^* g}(x,Q^2) = \Delta\sigma_h^{\gamma^* g}(x,Q^2/\mu^2) \otimes \Delta f_{g/g}(x,\mu^2) + \Delta\sigma_h^{\gamma^* q}(x,Q^2/\mu^2) \otimes \Delta f_{q/g}. \tag{4.29}$$

The full as well as the hard photon-gluon cross section are of order α_s, which means that $\Delta f_{g/g}$ should be just a delta function, as a zero order approximation in the parton model. On the other hand $\Delta f_{q/g}$ is the quark distribution inside the gluon, it has to be of order zero. Thus, the zero order approximation for $\Delta\sigma_h^{\gamma^* q}$ has to be used. With these considerations, Eq. (4.29) is rewritten as:

$$\Delta\sigma^{\gamma^* g}(x,Q^2) = \Delta\sigma_h^{\gamma^* g}(x,Q^2/\mu^2) + \Delta q^g(x,\mu^2), \tag{4.30}$$

where $\Delta q^g = \Delta f_{q/g}$.

The full photon-gluon cross section has been calculated to be [181, 182]:

$$\begin{aligned}
\Delta\sigma^{\gamma^* g}(x,Q^2) \quad = & -\frac{\alpha_s}{2\pi} N_f \frac{\sqrt{1-\frac{4m_q^2}{W^2}}}{1-\frac{4x^2P^2}{Q^2}} \left[(2x-1)(1-\frac{2xP^2}{Q^2}) \right. \\
& \left(1 - \frac{1}{\sqrt{1-\frac{4m_q^2}{W^2}}\sqrt{1-\frac{4x^2P^2}{Q^2}}} ln \left(\frac{1+\sqrt{1-\frac{4m_q^2}{W^2}}\sqrt{1-\frac{4x^2P^2}{Q^2}}}{1-\sqrt{1-\frac{4m_q^2}{W^2}}\sqrt{1-\frac{4x^2P^2}{Q^2}}} \right) \right) \\
& \left. + \left(x-1+\frac{xP^2}{Q^2} \right) \frac{2m_q^2(1-\frac{4x^2P^2}{Q^2}) - P^2x(2x-1)(1-\frac{2xP^2}{Q^2})}{m_q^2(1-\frac{4x^2P^2}{Q^2}) - P^2x(x-1+\frac{xP^2}{Q^2})} \right],
\end{aligned} \tag{4.31}$$

with $P^2 = -p^2$ the gluon virtuality, m_q the quark mass and $W^2 = \frac{Q^2(1-x)-P^2x}{x}$ the invariant mass squared of the photon-gluon system. For very large momentum transfer, $Q^2 >> m_q^2, P^2$, the full cross section reduces to:

$$\begin{aligned}\Delta\sigma^{\gamma^* g}(x,Q^2) &= \frac{\alpha_s}{2\pi}N_f\left[(2x-1)\left(ln\frac{Q^2}{m_q^2+P^2x(1-x)}+ln\frac{1-x}{x}-1\right)\right. \\ &\left.+(1-x)\frac{2m_q^2-P^2x(2x-1)}{m_q^2+P^2x(1-x)}\right]. \qquad (4.32)\end{aligned}$$

It remains to calculate Δq^g. This is given by computing the triangle diagram or, equivalently, the integral over the transverse momentum of the square of the norm of the light-cone $q\bar{q}$ wave function of the gluon [155, 180, 183]. As Δq^g is a soft contribution, the integral over the transverse momentum has to have a cut off, μ^2:

$$\begin{aligned}\Delta q^g(x,\mu^2) &= \frac{\alpha_s}{2\pi}N_f\int_0^{\mu^2}dk_\perp^2\frac{m_q^2+(2x-1)k_\perp^2}{[m_q^2+P^2x(1-x)+k_\perp^2]^2} \\ &= \frac{\alpha_s}{2\pi}N_f\left\{(2x-1)ln\left(\frac{\mu^2+P^2x(1-x)+m_q^2}{m_q^2+P^2x(1-x)}\right)\right. \\ &+ \left.(1-x)\frac{2m_q^2+P^2x(1-2x)}{m_q^2+P^2x(1-x)}\frac{\mu^2}{\mu^2+P^2x(1-x)+m_q^2}\right\}. \qquad (4.33)\end{aligned}$$

Equation (4.33) is a generalization of previous results [155, 180] including the dependence on the factorization scale for any values of the quark masses and gluon virtuality. Its first moment is zero for $\mu^2 << m_q^2, P^2$. If $\mu^2 >> m_q^2, P^2$ the first moment of $\Delta q^g(x,\mu^2)$ is 0 for $P^2 >> m_q^2$, while it is $\frac{\alpha_s}{2\pi}N_f$ for $m_q^2 >> P^2$. Using Eqs. (4.30), (4.32) and (4.33) we can calculate the hard gluon coefficient:

$$\Delta\sigma_h^{\gamma^v g}(x,Q^2,\mu^2) = \frac{\alpha_s}{2\pi}N_f\left\{(2x-1)\left[ln\left(\frac{Q^2}{\mu^2+P^2x(1-x)+m_q^2}\right)+ln\left(\frac{1-x}{x}\right)-1\right]\right.$$
$$\left. + (1-x)\frac{2m_q^2+P^2x(1-2x)}{\mu^2+m_q^2+P^2x(1-x)}\right\}. \quad (4.34)$$

Notice that the first moment of Eq. (4.34) does not depend on the ratio m_q^2/P^2 in the region $\mu^2 >> m_q^2, P^2$ - it is a legitimate hard contribution. Equation (4.34) is also a generalization of previous results and from its limit, $\mu^2 >> m_q^2, P^2$, it may be argued [154] that the gluons contribute to the first moment of $g_1(x,Q^2)$ because $\int_0^1 \Delta\sigma_h^{\gamma^v g}(x,Q^2)dx = -\frac{\alpha_s}{2\pi}N_f$.

On the other hand, if one calculates the quark distribution inside a gluon through the triangle graph, which we call Δq^g_{OPE}, using a regularization scheme that respects the axial anomaly but breakes chiral invariance, it is found that [7]:

$$\Delta q^g(x) - \Delta q^g_{OPE}(x) = \frac{\alpha_s}{2\pi}N_f\left[(2x-1)ln\left(\frac{\mu^2+P^2x(1-x)+m_q^2}{\mu^2}\right)\right.$$
$$\left. + \frac{2\mu^2(1-x)}{\mu^2+P^2x(1-x)+m_q^2}\right], \quad (4.35)$$

where the renormalization scale in the regularization of Δq^g_{OPE} (using $\overline{MS}$) has been taken to coincide with the factorization scale.

Equipped with Eq. (4.35) we can understand exactly why the hard gluon coefficient in the IPM (with the parton distribution defined with the help of a cut-off in the quark transverse momentum) has a first moment different from zero. The reason is that in the process of factorization the axial anomaly was shifted from the quark distribution inside the gluon to the hard coefficient. Equation (4.35) reflects the fact that the regularization of

[7] The triangle graph regularized with a cut off on the transverse momentum results in Eq. (4.33).

Δq^g_{OPE} respects the axial anomaly while the regularization of Δq^g does not. We also see that in the limit $m_q^2 >> \mu^2$, the discrepancy between the two calculations disappears (at least for the first moment - the x dependence depends on the regularization method). A similar phenomenon is found in unpolarized deep inelastic scattering where an analysis by Bass [184] has shown that the trace anomaly induces the same sort of shift when a cut off over the transverse squared momenta of the quarks is used to separate the soft and hard regions.

4.3.2 Scheme Independence of g_1

The spin structure function is a physical observable (it is just a cross section). As such, it has to be independent of the scheme used to define the Wilson coefficients (or the hard part of the cross sections) and the parton distributions. This can be show explicitly:

$$g_1(x) = \Delta\Sigma^{\overline{MS}} \otimes C_q^{\overline{MS}} + \Delta g^{\overline{MS}} \otimes C_g^{\overline{MS}} \equiv \Delta\Sigma \otimes C_q + \Delta g \otimes C_g, \tag{4.36}$$

where for convenience of notation $C_g \equiv \Delta\sigma_h^{\gamma^* g}$ and all quantities without labels refer to a scheme where the axial current is conserved. From Eqs. (4.33), (4.34) and (4.35) we get:

$$C_g^{\overline{MS}}(x) = C_g(x) + \frac{\alpha_s}{\pi} N_f (1-x), \tag{4.37}$$

in the limit of infinite momentum transfer. On the other hand, if one pays attention to Eq. (4.20), $\Delta\Sigma^{\overline{MS}}$ and $\Delta\Sigma$ are related by [22]:

$$\int_0^1 \Delta\Sigma^{\overline{MS}}(x)dx = \int_0^1 \Delta\Sigma(x)dx + \frac{\alpha_s}{2\pi}\langle p,s|K_+|p,s\rangle, \tag{4.38}$$

where the + refers to light cone coordinates. The matrix elements of K_+ are given by [159]:

$$\langle p,s|K_+|p,s\rangle = -\int_0^1 \Delta g(x)dx, \tag{4.39}$$

for each flavor, where $\Delta g(x)$ is the polarized gluon distribution of Eq. (4.36). Eq. (4.38) can be generalized for all higher moments [129] and the general decomposition for $\Delta\Sigma$ would be:

$$\Delta\Sigma^{\overline{MS}}(x) = \Delta\Sigma(x) - \frac{\alpha_s}{\pi}N_f(1-x)\otimes\Delta g(x). \tag{4.40}$$

We can use these definitions in the expression for g_1 and obtain:

$$\begin{aligned} g_1(x) &= (\Delta\Sigma^{\overline{MS}}(x) + \frac{\alpha_s}{\pi}N_f(1-x)\otimes\Delta g(x))\otimes C_q(x) + \Delta g(x)\otimes(C_g^{\overline{MS}}(x) - \frac{\alpha_s}{\pi}N_f(1-x)) \\ &= \Delta\Sigma^{\overline{MS}}(x)\otimes C_q(x) + \Delta g\otimes C_g^{\overline{MS}}(x), \end{aligned} \tag{4.41}$$

to order α_s. We can relate the polarized gluon distribution and the Wilson coefficients in the two schemes. As it is well known, the anomalous dimensions and Wilson coefficients are dependent on the renormalization scheme when one goes beyond leading order in perturbative QCD. As the parton distributions are determined once the perturbative objects are given, as discussed in the beginning of section 3.3, they will be scheme dependent as well. In this sense, we write

$$\Delta g(x) = \Delta g^{\overline{MS}}(x) + \delta g(x), \;\; C_q(x) = C_q^{\overline{MS}}(x) + \delta C_q(x), \tag{4.42}$$

where $\delta g(x)$ and $\delta C_q(x)$ are some functions relating the two schemes. Their particular form is of no interest right now but the existence of such functions. With these definitions, Eq. (4.41) is rewritten as:

$$\begin{aligned} g_1(x) &= \Delta\Sigma^{\overline{MS}}(x) \otimes C_q^{\overline{MS}}(x) + \Delta g^{\overline{MS}}(x) \otimes C_g^{\overline{MS}}(x) \\ &\quad -\Delta\Sigma^{\overline{MS}}(x) \otimes \delta C_q(x) - \delta g(x) \otimes C_g^{\overline{MS}}(x). \end{aligned} \tag{4.43}$$

Comparison with Eq. (4.36) results in a consistency relation:

$$\Delta\Sigma^{\overline{MS}}(x) \otimes \delta C_q(x) = -\delta g(x) \otimes C_g^{\overline{MS}}(x). \tag{4.44}$$

This equality must hold if g_1 is to be an observable. The first moment of Eq. (4.44) certainly respects the equality as $\int_0^1 dx C_g^{\overline{MS}}(x) = 0$ and $\int_0^1 dx \delta C_q(x) = 0$ because the quark singlet and nonsinglet Wilson coefficients are the same, at least to order α_s [93]. Then, if $C_{NS}(x) = C_{NS}^{\overline{MS}}(x) + \delta C_{NS}(x)$, it follows that $\delta C_{NS}(x) = \delta C_q(x)$. As the change of scheme of the Wilson coefficient is dictated by the change of scheme of the anomalous dimension, and the first moment of the nonsinglet anomalous dimension in next-to-leading order is zero due to current conservation, if follows that $\int_0^1 dx \delta C_{NS}(x) = 0$. Hence. $\int_0^1 dx \delta C_q(x) = 0$ as well. More of the relation between the Wilson coefficient and the anomalous dimensions beyond leading order will be seen in the next chapter. Eq. (4.44) could be used in a reversed argument: the scheme invariance of g_1 implies that the first moment of the quark Wilson coefficient is independent of scheme.

4.3.3 Quark Masses, Factorization Point and the First Moment of the Hard Gluon Coefficient

It is interesting to study the dependence on μ^2 of the first moment of $\Delta\sigma_h^{\gamma^* g}$. In an early study of this subject[8], Mankiewicz and Schäfer [185] determined the first moment of the box

[8]We thank S. Bass for pointing out to us this work.

graph as a function of the minimum transverse momentum carried by the quarks. Their results for $Q^2 \to \infty$ agree qualitatively with ours, as will soon be seen. But it was also found in Ref. [185] that for momentum transfers of the order of 10 to 100 GeV^2, the contribution from light quarks[9] ($m_q = 10\ MeV$) is deeply affected by the choice of the minimum value for the transverse quark momentum. In the method used here, such an ambiguity does not exist for the light quarks and its anomalous contribution for $Q^2 = 10$ or 100 GeV^2 is well defined and independent of $k_\perp$. We use this result to argue that the hard gluon coefficient calculated here is more stable from the point of view of infrared singularities.

Even with the known variations of the anomalous contribution with the factorization scale, it has been widely assumed in the literature [47] that for light quarks (u, d and s) the first moment of $\sigma_h^{\gamma^v g}$ is $-\alpha_s/2\pi$ and for heavy quarks (like c or b) it is zero (because, for $m_q^2 >> \mu^2$, $\Delta\sigma_h^{\gamma^v g}$ reduces to $C_g^{\overline{MS}}$). But it also happens that the gluonic contribution to $g_1(x, Q^2)$ is of the form $\Delta\sigma_h^{\gamma^v g}(x, Q^2/\mu^2) \otimes \Delta g(x, \mu^2)$. This means that the scale μ^2 at which the gluon distribution is calculated (or parametrized) is the same scale μ^2 that has to be used in the calculation of the hard gluon coefficient, and that it does not make sense to talk about the magnitude of the hard gluon coefficient without specifying the factorization scale. Thus, the heavy quark contribution is negligible only when the polarized gluon contribution is calculated at a very low scale compared with the quark mass.

In Fig. 4.4 we show the first moment of $\Delta\sigma_h^{\gamma^v g}$ as a function of the factorization scale for the u and d quarks ($m_q^2 \sim 25 \times 10^{-6}\ GeV^2$), for the s quark ($m_q^2 \sim 0.04\ GeV^2$) and for the c quark ($m_q^2 \sim 9/4\ GeV^2$). We see that, as is well known [155, 177, 180, 182, 47], the c quark does not contribute when $m_c^2 >> \mu^2$, as one can also verify directly from Eq. (4.34).

[9] We assume for the quark masses their current values. We do not take into account variation of the masses with the factorization point but note that our conclusions are not significantly altered by small changes in the quark mass.

However, for reasonable values of μ^2 there is a contribution large enough to be taken into account. Thus, the significance of the charm contribution to $g_1(x, Q^2)$ depends on where the polarized gluon distribution is calculated. For instance. calculations have been made in the literature using input polarized gluon distributions at a scale of typically 4 GeV^2. The authors of these calculations usually disregard the charm contribution. We note in passing that in the region of μ^2 where polarized charm can be disregarded, the polarized strange quarks yield only half of the contribution given by u and d quarks. As we see from Fig. 4.4, the c quark gives around 64% of the contribution of the light quarks for $\mu^2 \sim 4\ GeV^2$ and so it should not be disregarded if the gluon distribution is calculated at this scale. We also see from Fig. 4.4 that the u and d quarks give the same contribution, independent of the factorization scale. We further notice that, for practical purposes, the hard gluon coefficient is independent of the exact value of the gluon virtuality P^2.

The discussion of the preceding paragraph was based on the not so realistic assumption that the momentum transfer Q^2 is infinitely bigger than any other scales in the theory. It implies, for instance, that when integrating the hard cross section we allow x to go from zero to one. But from simple kinematic arguments we know that x has a maximum value of $x_{max} = Q^2/(Q^2 + P^2 + 4m_q^2)$ and so $x_{max} \to 1$ only when $Q^2 >> m_q^2, P^2$. For the finite Q^2 of the current experiments, x_{max} never reaches 1 and so the integral in x has a cut off. For instance if one calculates the first moment of $\sigma_h^{\gamma^* g}$ for the c quark ($m_q^2 = 9/4\ GeV^2$) at $\mu^2 = Q^2 = 4\ GeV^2$, using Eq. (4.34), one finds that its value changes from -0.64, when x is artificially allowed to reach 1, to ~ 0.015 when the physical cut off in x is applied. What happens is that expression (4.34) itself was obtained under the assumption of an infinitely large Q^2. To be more consistent when dealing with finite Q^2, one should derive the hard cross section from the full cross section without any approximation.

In the general case we then write:

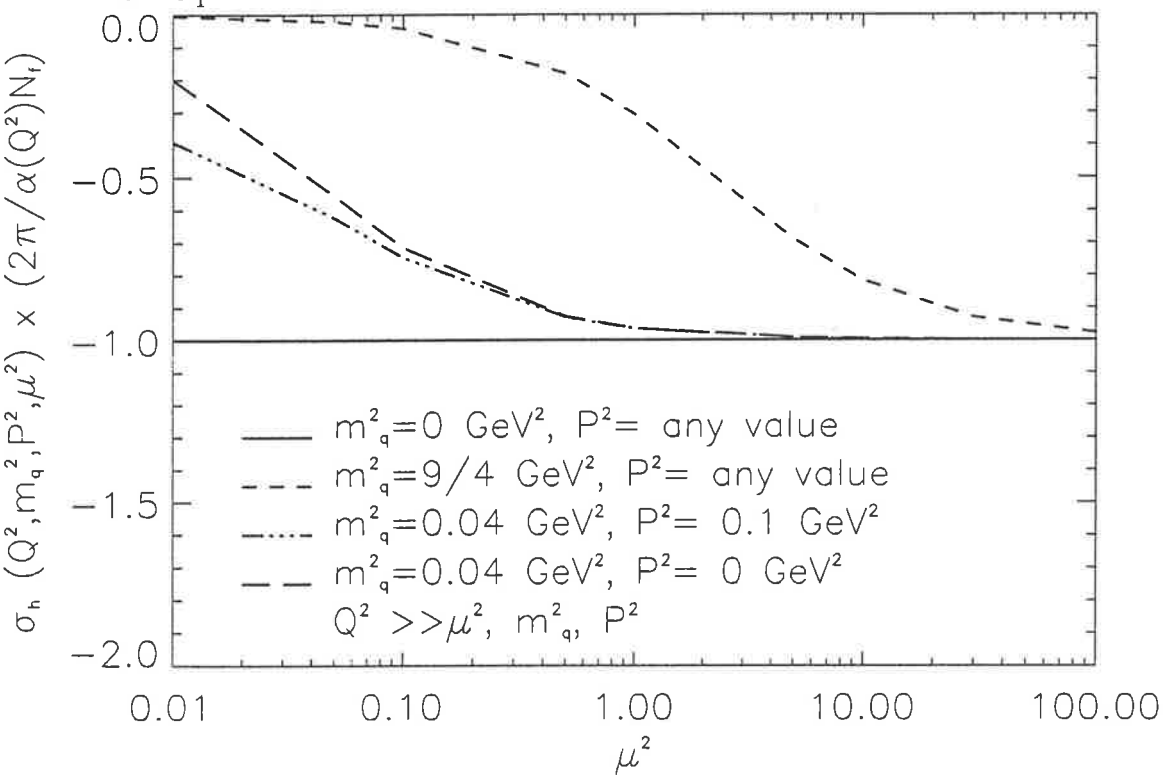

Figure 4.4: Hard gluon coefficient as given by Eq. (4.34), calculated with the assumption of infinite momentum transfer as a function of the factorization scale. For realistic scales ($\mu^2 > 1\ GeV^2$), the charm contribution is seen to be important.

$$C_g^{\overline{MS}} = \Delta\sigma^{\gamma_v g} - \Delta q^g_{OPE}, \tag{4.45}$$

$$\Delta\sigma_h^{\gamma^v g} = \Delta\sigma^{\gamma_v g} - \Delta q^g, \tag{4.46}$$

with $\Delta\sigma^{\gamma_v g}$ given by Eq. (4.31) and Δq^g and Δq^g_{OPE} given by Eqs. (4.33) and (4.35). We stress that these equations are the complete result at order α_s. In Figs. 4.5 and 4.6 we show the first moment of $\Delta\sigma_h^{\gamma^v g}$, defined in Eq. (4.46), as a function of the factorization scale μ^2 for $Q^2 = 10\ GeV^2$ and $Q^2 = 3\ GeV^2$, respectively. These values were chosen because

they are the average Q^2 of the EMC [20, 52] and SLAC [64] experiments. The resulting dependence is very interesting. It shows that in the region of interest ($\mu^2 \geq 1\ GeV^2$) there is no appreciable dependence on the gluon virtuality or on μ^2 (at least for $Q^2 = 10\ GeV^2$) but the mass dependence is strong. Remarkably, the contribution from the s quark is never the same as the contribution from the u and d quarks, contrary to what is usually claimed. The s contribution is $\sim 0.9\ \alpha_s(Q^2)/2\pi$ for the EMC data and $\sim 0.75\ \alpha_s(Q^2)/2\pi$ for the E143-SLAC data. We also find a nonnegligible contribution coming from the c quarks. For the EMC data, the c quark contributes $\sim 0.2\ \alpha_s(Q^2)/2\pi$ and for the E143-SLAC data $\sim 0.1\ \alpha_s(Q^2)/2\pi$. Figure 4.5 is unaltered [10] if we go from $m_q^2 = 0$ to $m_q^2 = 1 \times 10^{-4} GeV^2$. If we then compare our Fig. 4.5 with Fig. 2 of Ref. [185] we see clearly that the present approach does not have a convergence problem in Q^2 and yields a perfectly unambiguous contribution from the light quarks. Finally, we show in Fig. 4.7 the Q^2 dependence of the polarized charm contribution calculated with $\mu^2 = 3\ GeV^2$. This contribution, obviously, tends to the value calculated in Fig. 4.4 ($\sim -0.57\ \alpha_s(Q^2)/2\pi$).

4.3.4 Relevance in Analysing the Fraction of Nucleon Spin Carried by Gluons

In terms of the polarized quark and gluon distributions, $g_1^p(x, Q^2)$ for 4 flavors is written as:

$$\begin{aligned} g_1^p(x,Q^2) &= \frac{1}{12}\Delta q_3(x,Q^2) + \frac{1}{36}\Delta q_8(x,Q^2) - \frac{1}{36}\Delta q_{15}(x,Q^2) \\ &\quad + \frac{5}{36}\Delta\Sigma(x,Q^2) + \frac{5}{36}\Delta\sigma_h^{\gamma^* g}(x,Q^2,\mu^2) \otimes \Delta g(x,\mu^2), \end{aligned} \tag{4.47}$$

[10] In reality, there is a $\sim 1\%$ correction for $\mu^2 \sim 0.01\ GeV^2$. This result is in complete accord with the fact that the anomalous contribution for the u and d quarks goes to zero as μ^2 goes to zero.

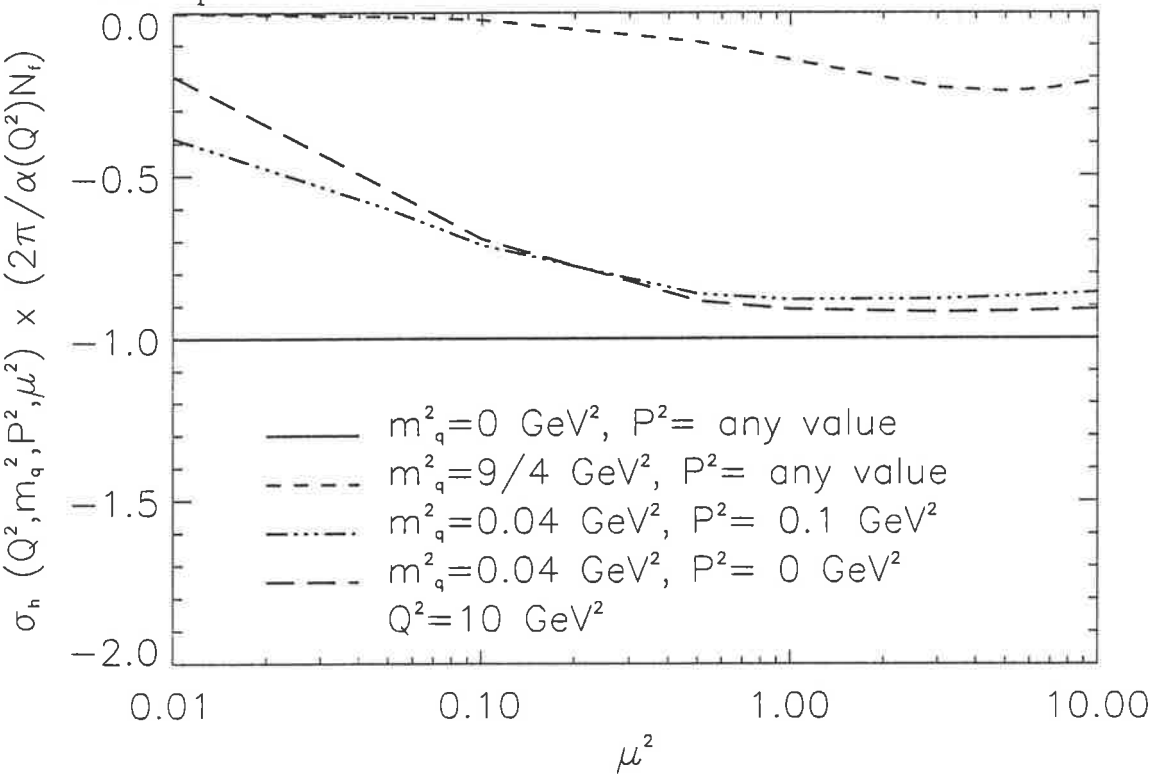

Figure 4.5: Hard gluon coefficient as given by Eqs. (4.31), (4.33) and (4.46). The momentum transfer is fixed at 10 GeV^2. It is seen that the strange quark contribution never equals that from the up and down quarks and the charm quark contribution is sizable for $\mu^2 > 1\ GeV^2$.

where Δq_3 and Δq_8 are defined after Eq. (4.2), $\Delta q_{15} = \Delta u + \Delta d + \Delta s - 3\Delta c$ and $\Delta\Sigma = \Delta u + \Delta d + \Delta s + \Delta c$. For 3 flavors the coefficient of the singlet part changes from 5/36 to 1/9 and Δq_{15} does not exist. To order $\alpha_s(Q^2)$ [93], the first moment of (4.47) is:

$$\begin{aligned}\Gamma_1^p(Q^2) &= I_3(Q^2) + I_8(Q^2) - I_{15}(Q^2) + I_0(Q^2) \\ &\quad -\frac{5}{36}\left(2\frac{\alpha_s(Q^2)}{2\pi} + s_1\frac{\alpha_s(Q^2)}{2\pi} + c_1\frac{\alpha_s(Q^2)}{2\pi}\right)\Delta g(Q^2). \qquad (4.48)\end{aligned}$$

The coefficients of $\alpha_s(Q^2)$ have the following meaning. The 2 indicates that the u and d quarks give the same contribution $\frac{\alpha_s(Q^2)}{2\pi}$, as discussed before. The s_1 and c_1 factors give the amount of strange and charm quark contributions, according to Eq. (4.46) and Figs. 4.14 - 4.16.

To extract the value of $\Delta g(Q^2)$ we will closely follow Refs. [186, 126]. For the sake of comparison, we begin with only 3 flavors and with the common assumption that the u, d and s quarks give the same anomalous contribution.

Under the assumption that the polarized sea originates exclusively from the anomalous gluon contribution we have, for 3 flavors, the following identities:

$$\begin{aligned} I_3 &= \frac{1}{12}(F+D)(1-\frac{\alpha_s}{\pi}) \\ I_8+I_0 &= \frac{1}{36}(3F-D)\left[(1-\frac{\alpha_s}{\pi})+4(1-\frac{\alpha_s}{3\pi})\right], \end{aligned} \tag{4.49}$$

where the the quark spin fractions were expressed in terms of the F and D couplings and corrections from the two loop expansion of the beta function and anomalous dimension were incorporated. In NLO, α_s is given as the solution of the following transcendental equation:

$$ln\frac{Q^2}{\Lambda^2} = \frac{4\pi}{\beta_0\alpha_s} - \frac{\beta_1}{\beta_0^2} ln\left[\frac{4\pi}{\beta_0\alpha_s}+\frac{\beta_1}{\beta_0^2}\right], \tag{4.50}$$

with $\beta_0 = 11-2N_f/3$ and $\beta_1 = 102-38N_f/3$. We use $\Lambda = \Lambda^{(3)} = 248\ MeV$, determined by fixing $\Lambda^{(4)} = 200\ MeV$ [187]. A remark is necessary here. The calculation of the hard gluon coefficient was performed through a cut off on the transverse momenta of the partons in order to regularize the integrals. This procedure is the definition of the parton model. On the other hand, α_s (or λ) is determined within a given sheme because λ is a scheme dependent object. In general, $\overline{MS}$ scheme is used [125]. The problem is not as bad as it looks because

a different scheme will result in a simple redefinition of the parameter Λ, maintaining α_s unaltered.

Using the experimental values of F and D as given in [126], we determine I_3 and $I_8 + I_0$ at $Q^2 = 10\ GeV^2$ (with $\alpha_s(Q^2 = 10\ GeV^2) \simeq 0.209$):

$$\begin{aligned} I_3 &= 0.0977 \pm 0.001 \\ I_8 + I_0 &= 0.0779 \pm 0.002 \end{aligned} \tag{4.51}$$

We now use Eq. (4.48) to determine $\Delta g(Q^2)$. On the left hand side, we use the experimental result from the SMC[52], displayed in the last line of table 4.1. On the right hand side we use the results (4.51), $s_1 = 1$, $c_1 = 0$ and remember that for 3 flavors the singlet coefficient is $1/9$ and $I_{15} = 0$. The result is:

$$\Delta g(Q^2 = 10 GeV^2) = 3.04 \pm 1.4. \tag{4.52}$$

For 4 flavors the analysis is similar. One just has to redefine the integral of $g_1^p(x, Q^2)$:

$$\begin{aligned} I_3 &= \frac{1}{12}(F + D)(1 - \frac{\alpha_s}{\pi}) \\ I_8 + I_0 - I_{15} &= \frac{5}{36}(3F - D)\left(1 - \frac{\alpha_s}{3\pi}\right). \end{aligned} \tag{4.53}$$

We then proceed as before and calculate Δg using the result for the gluon coefficient as displayed in Fig.4.5. We see that for $\mu^2 = Q^2 = 10\ GeV^2$, $s_1 \sim 0.9$, $c_1 \simeq 0.21$ and $\alpha_s(Q^2 = 10\ GeV^2) = 0.2142$, resulting in:

$$\begin{aligned} I_3 &= 0.0976 \pm 0.001 \\ I_8 + I_0 - I_{15} &= 0.0786 \pm 0.002 \\ \Delta g(Q^2 = 10\ GeV^2) &= 2.32 \pm 1.06 \end{aligned} \tag{4.54}$$

In passing we notice that if the usual assumption of infinite momentum transfer were used, then according to the results of Fig.4.4, at 10 GeV^2 $s_1 = 1$, $c_1 \simeq 0.81$ and hence $\Delta g \simeq 1.89$.

4.3.5 The x dependence

The exact x dependence of the anomalous contribution is a matter of convention because the freedom in the factorization scheme while calculating $\Delta\sigma_h^{\gamma_v g}$. Other choices of regularization would result in different functions of x. But, as shown by Glück et al. [168], the exact form of the x dependence seems not to be very important. Once we do not know the form of the polarized gluon distribution, the best we can do is constrain it by some general considerations. For instance, there is the positivity condition:

$$|\Delta g(x, Q^2)| \leq g(x, Q^2), \tag{4.55}$$

where $g(x, Q^2)$ is the unpolarized gluon distribution. A very simple form that satisfies the above condition is:

$$\Delta g(x) = x^\alpha g(x), \tag{4.56}$$

where α is determined through the normalization of Δg. For Δg of Eq. (4.54), $\alpha = 0.49$. The advantage of using this form to study the x dependence is its simplicity. The problem

with Eq. (4.56) is that it does not have the correct behavior as $x \to 0$. As proposed by Brodsky et al. [137],

$$\frac{\Delta g(x)}{g(x)} \to x, \tag{4.57}$$

as $x \to 0$. From the many ways to satisfy both conditions (4.55) and (4.57), we choose:

$$\Delta g(x, \mu^2 = 9\ GeV^2) = \alpha x g(x, \mu^2 = 9\ GeV^2)(1-x)^3, \tag{4.58}$$

where $\alpha = 6.92$ for $\Delta g = 2.32$. We made this choice guided only by the desire of simplicity and to produce a polarized gluon distribution that resembles an already existing one [186]. For the unpolarized gluon distribution, we use the one given by the NMC [188], determined from inelastic J/ψ production:

$$xg(x) = \frac{1}{2}(\eta+1)(1-x)^\eta. \tag{4.59}$$

This parametrization is valid for $\mu^2 = 9\ GeV^2$ and should not be trusted for $x \leq 0.01$. Again, this choice is based on simplicity and we note that a further parametrization by the NMC [189] group agrees with Eq. (4.59) for $x \geq 0.01$. The parameter η is $\eta = 5.1 \pm 0.9$. Given these choices, we show in Fig. 4.8 the forms (4.56) and (4.58) for the polarized gluon distributions plus the forms of Brodsky et al. [137] and Gehrmann and Stirling (GS) [186], calculated at 4 GeV^2. Our parametrization (4.58) is slightly higher than that of GS because of the normalization factor. If we use the same normalization as theirs[11], both curves would be essentially the same. Evolution from 4 to 9 GeV^2 for the GS distribution also has small effects. The parametrization of Brodsky et al. [137] is much smaller than the others because

[11] We note that in [186], the coupling constant is calculated in leading order rather than in NLO. This would lead to an increase of the total polarization carried by the gluons.

in their approach the polarized gluons are not responsible for the small experimental value of table (4.1).

Using the constructed gluon distributions, we can estimate where in x the anomalous contribution is located. In Fig. 4.9 we show the anomalous contribution, $\frac{5}{36}\Delta\sigma_h^{\gamma^* g}(x, Q^2, \mu^2) \otimes \Delta g(x, \mu^2)$, for $\Delta g(x) = \alpha x g(x)(1-x)^3$. We see that its contribution inside the experimental region is important. To better evaluate its importance, we calculated the amount of the total gluon that lies inside the region $0.01 \leq x \leq 1$. For 4 flavors, the contribution from $x \geq 0.01$ corresponds to about 66% of the total anomalous contribution. In the case of 3 flavors, this percentage is $\sim 69\%$. For $\Delta g(x) = x^\alpha g(x)$ this conclusion is not dramatically altered.

4.4 Final Remarks

It should be clear from our discussion that the quark spin content of the nuclen has never been measured. This conclusion follows from the fact that the measured axial current is not the source of the chiral transformations - a very well known fact in the context of anomalies in quantum field theory [22]. Nevertheless, it is possible to interpret the measured axial current in terms of quark spin if an anomalous gluon contribution is introduced in a particular gauge [154, 155, 156, 159, 174]. We discussed here the existence of this gluonic contribution to the proton spin when the IPM hard gluon coefficient is defined through Eq. (4.46) with Δq^g defined as the quark distribution inside the gluon with transverse squared momentum less than the factorization scale. As a consequence, this anomalous gluonic contribution in the IPM is free of infrared ambiguities. We showed that using the common assumption of an infinitely big momentum transfer, there is a c quark contribution to the spin in addition to the u, d and s quark contributions. The contribution from the massive quarks is dependent on the factorization scale at which the polarized gluon distribution is calculated. The c quark

contribution is small only in the region $\mu^2 < 1\ GeV^2$, in which case the s quark contribution is also strongly affected.

We also calculated what would be the possible anomalous corrections when the momentum transfer is in the region of the present experiments. To perform such a calculation we have to keep all terms in m_q^2/Q^2 and P^2/Q^2 in the full photon-gluon cross section when calculating the hard gluon coefficient. This means that we are including higher twist effects and, although we use the complete result at order $\alpha_s(Q^2)$, possible corrections coming from higher order terms in $\alpha_s(Q^2)$ could be important and so our calculation is incomplete. Even so, we think that our results are more consistent than simply using the approximate expression (4.34) for the hard gluon coefficient in the case of massive quarks and relatively low Q^2. The corrections due to finite Q^2 are not small and we think they should be taken into account when calculating the amount of spin carried by gluons. When studying the x dependence of the anomalous contribution, we conclude that both 3 and 4 flavors give approximately the same contribution inside the experimental region. But the amount of polarized glue needed to fit the data is much smaller when charm is included. Moreover, we showed that from the conceptual point of view, it would be wrong not to include a fourth flavor.

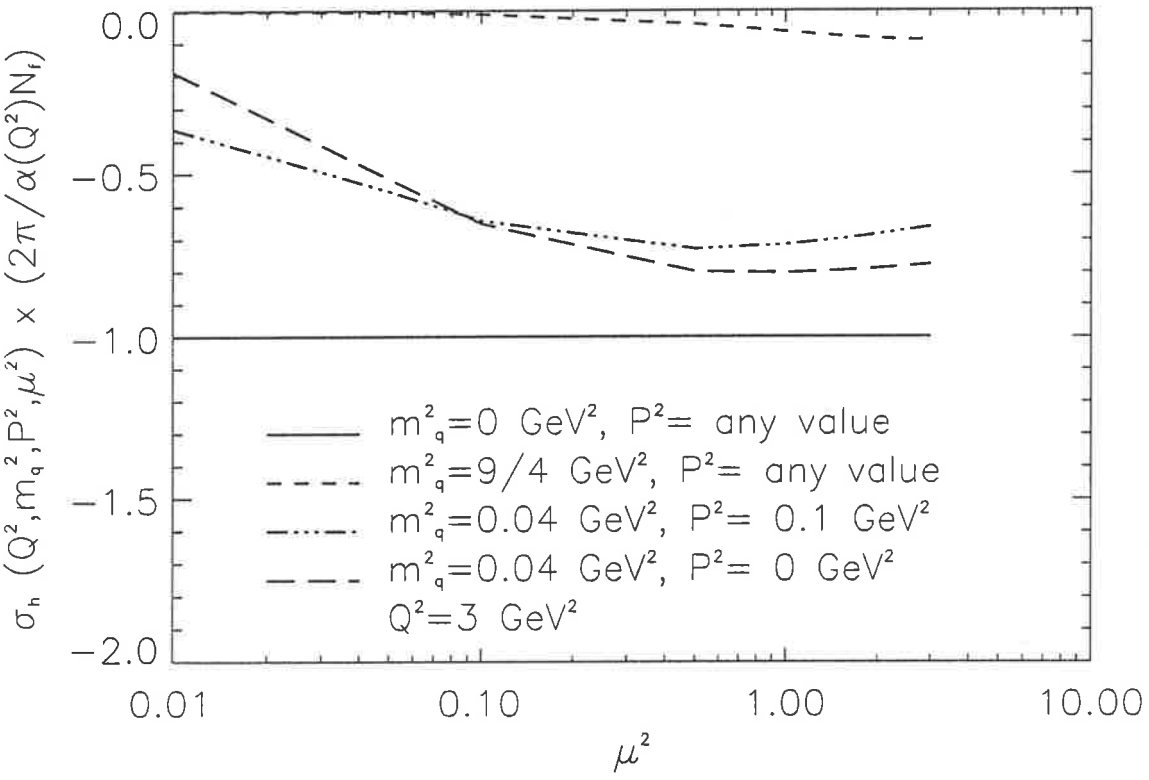

Figure 4.6: Hard gluon coefficient as given by Eqs. (4.31), (4.33) and (4.46). The momentum transfer is fixed at 3 GeV^2. It is seen that the strange quark gives approximately 75% of the contribution of the up and down quarks in the realistic region of $\mu^2 > 1\ GeV^2$. In the same region, the charm quark gives a 10% contribution.

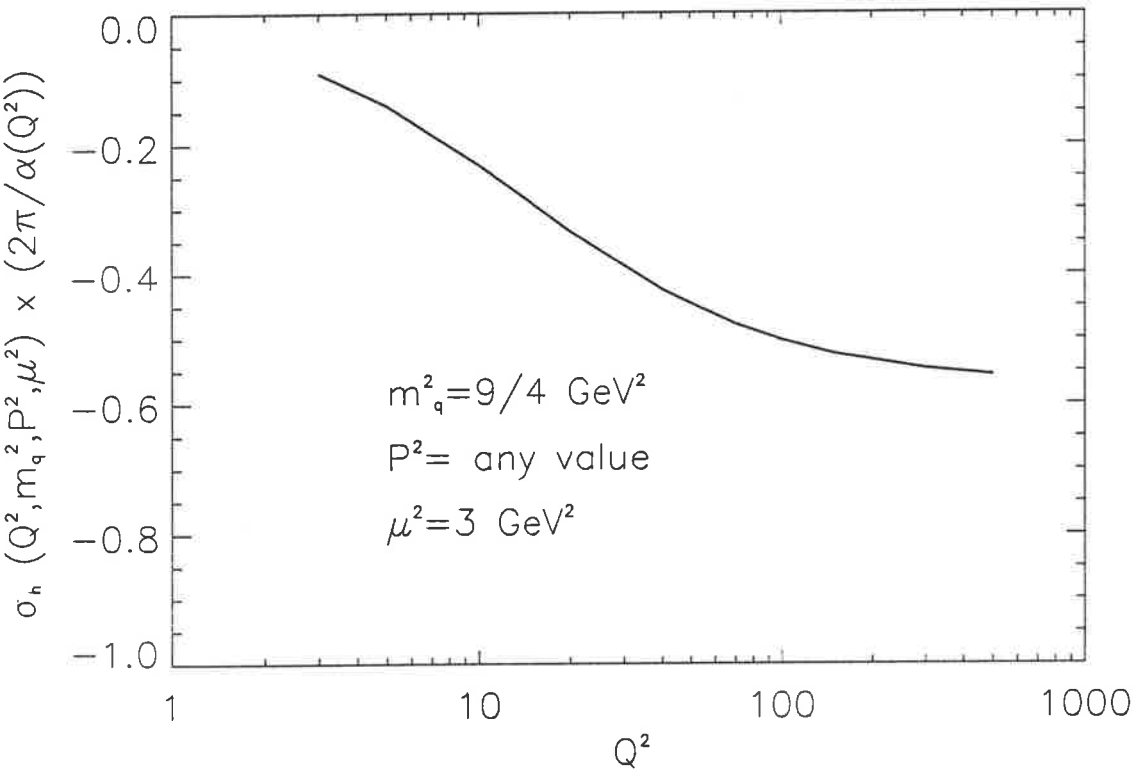

Figure 4.7: Hard gluon coefficient for the charm quark, calculated with Eqs. (4.31), (4.33) and (4.46). The factorization scale is fixed at 3 GeV^2 and the Q^2 dependence is studied.

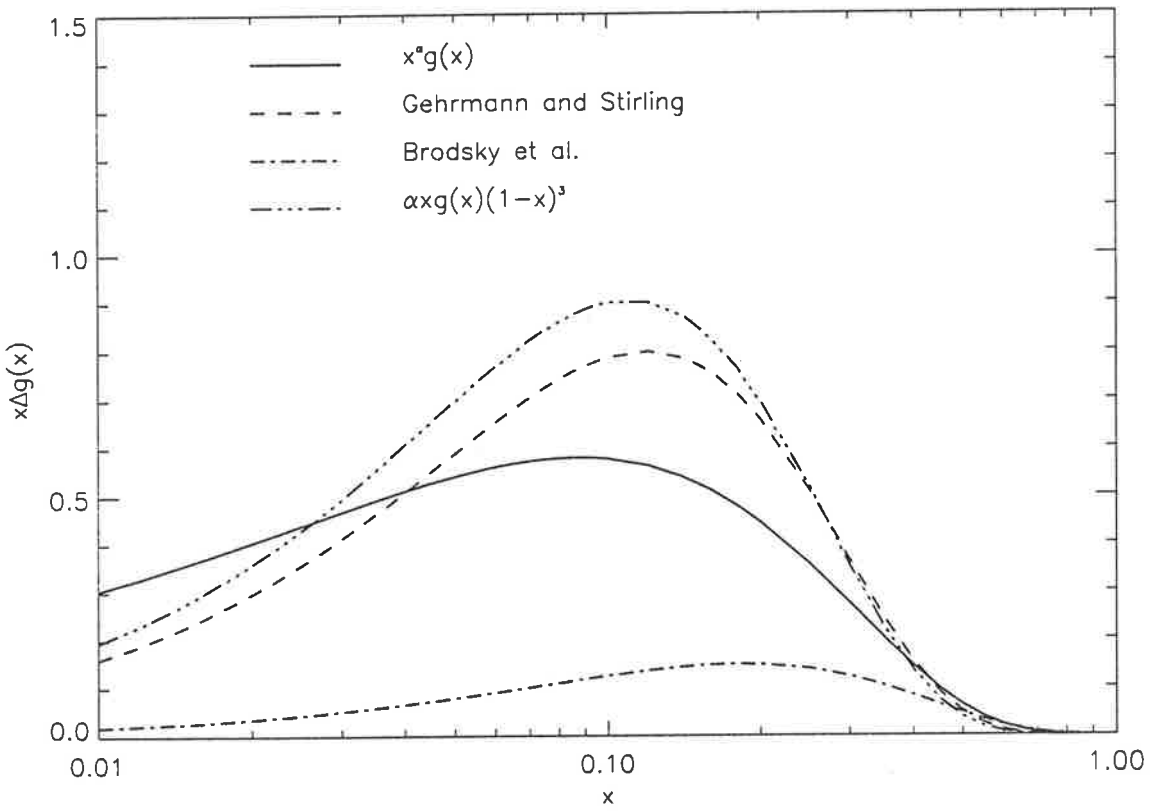

Figure 4.8: Comparison of various polarized gluon distributions considered in the text.

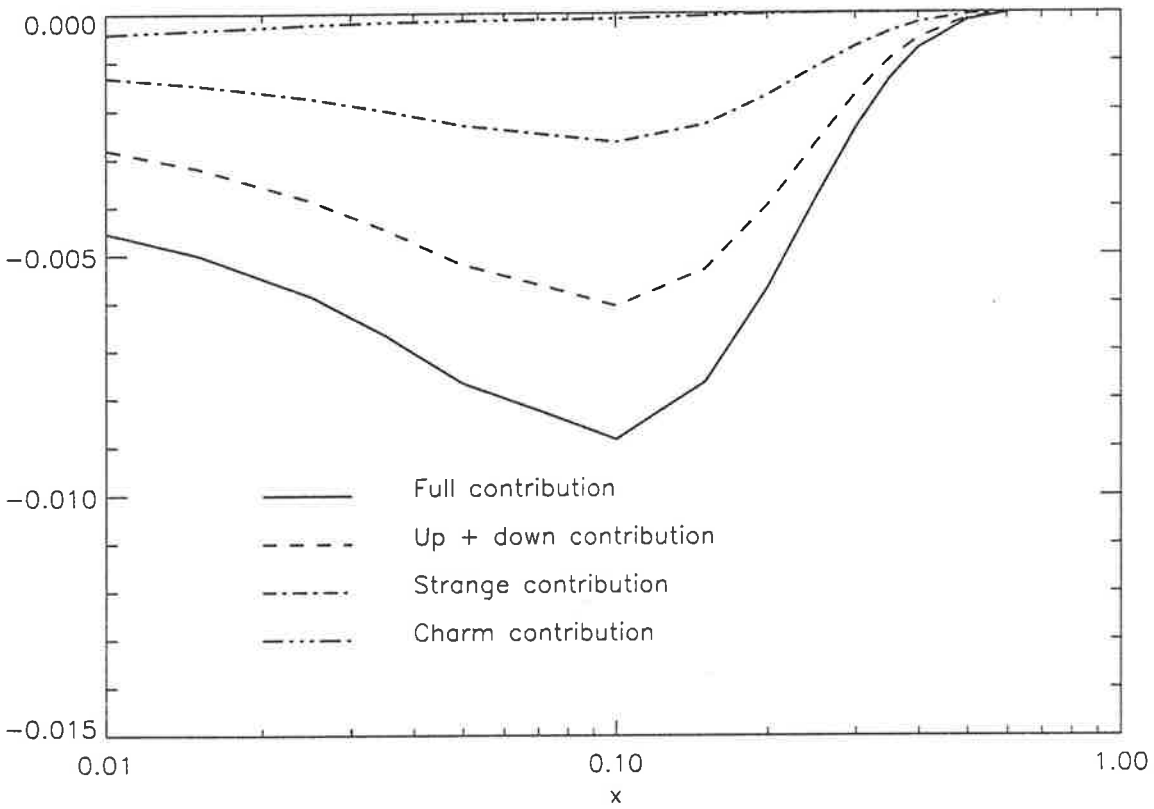

Figure 4.9: Comparison of the x-dependence of the non-strange, strange and charm quark distributions to $g_1(x)$. The anomalous contribution is given by $\frac{5}{36}\sigma_h^{\gamma^* g}(x, Q^2, \mu^2) \otimes \Delta g(x, \mu^2)$ and it is used the form $\Delta g(x, \mu^2 = 9\ GeV^2) = \alpha x g(x)(1-x)^3$ for the polarized gluon.

Chapter 5

The x Dependence of Quark Distributions

5.1 Introduction

The ultimate test of our understanding of the nucleon structure is to explain, when data is available, the x dependence of the relevant structure functions. In the unpolarized sector, there is an impressive amount of data from deep inelastic lepton-nucleon scattering with x ranging from 10^{-4} to 0.9 and momentum transfer squared from 0.1 to 5000 GeV^2 [190, 191, 192, 193]. Based on these data, parametrizations of the parton distributions and the structure functions abound in the literature [194, 195, 196, 197]. More recently, motivated by some early EMC data [20] on the polarized proton structure function, a considerable effort has also been made by experimentalist to map the proton, neutron and deuteron spin structure functions over a wide range of x and Q^2 [20, 53, 52, 32, 49, 54, 64, 135, 51]. Also in this case, there are a few parametrizations available in the literature [133, 198]. However, the

available polarized experimental data does not constrain the parametrizations as much as it does in the unpolarized case. Presently, most of the parametrizations for the polarized parton distributions that fit the measured structure functions differ among themselves. In particular, the polarized sea and the polarized glue are poorly constrained. Even the parametrizations for polarized valence quarks, whose distributions have been recently measured [199], have a higher degree of uncertainty. The situation should be improved in the near future when better data for the valence distributions will be available and also the polarized gluon distribution in the proton will be measured [200, 201]. On the other hand, although highly convenient and necessary, parametrizations of the data do not add very much to the picture of the nucleon. A better approach would be to find a solid calculational scheme which could provide the parton distributions.

When we reviewed the main points of the Renormalization Group Equations (RGE) relevant to our purposes, we saw that the parton distributions are related, by definition, to the matrix elements between proton (or neutron or any other hadron) states of some operators. For instance, in the case of spin, the operator would be the axial current. However, to calculate these matrix elements, one would need to know the proton wave function in QCD. In the absence of a QCD calculated wave function, the solution is to use a model to extract this quantity. This wave function, in its turn, is supposed to be valid only in a determined scale - the renormalization scale μ, in the spirit of the RGE. Convolution with the Wilson coefficients, as shown in Eqs. (2.82) and (2.83), is then used to calculate the structure functions at any scale (of course, this scale has to be above μ). In this chapter we will see in some detail how to perform evolution up to Next-to-Leading Order (NLO) in perturbative QCD.

Although there are a variety of possibilities for calculating the quark distributions at the starting scale, like non-relativistic [202, 203] and relativistic [204] quark models or vertex

functions [205], here we shall work with the MIT bag. This choice is based on its success in low energy physics, its simplicity and the insights it has already yielded in connecting low and high energy data [149, 150, 153, 151, 206]. The free parameters of the model are fixed by fitting the calculated total valence distribution of the proton to some parametrization of the data. Predictions can then be made for the various, polarized and unpolarized, structure functions - not only their integrated values but also theirs x dependence. We stress once again that any model candidate to explain, among others, the NMC result for the Gottfried sum rule, the NA51 experiment and the small value for the singlet axial constant should also explain the x dependence of the associated structure functions.

This chapter will be organized as follows. We first review some main properties of the calculations of quark distributions as developed in Adelaide [41, 42. 150]. In particular, we study the importance of correct support for the quark distributions. We will also make some general considerations on the behaviour of some classes of candidate nucleon wave functions as $x \to 1$. We then proceed to study parton distributions in general where we derive some simple relations for the quark and gluon evolution equations in NLO perturbative QCD. The effects of NLO evolution in the parameters of the model are considered and some updated bag model calculations are presented. Results for the spin distributions are shown. Finally, we study the impact of a meson cloud in the proton and in the neutron spin structure functions.

5.2 A Model for the Quark Distributions

In the OPE, the matrix elements of the operators between hadron states appearing in the expansion are proportional to some general coefficients (viz. Eq. (2.75)):

$$A_n p_{\mu_1} ... p_{\mu_n} = < p|\overline{\psi}(0)\gamma_{\mu_1} iD_{\mu_2} ... iD_{\mu_n}\psi(0)|p > . \tag{5.1}$$

Following Jaffe [175], one can define parton distributions associated to the coefficient A_n if one goes to the light cone coordinates and use the light cone gauge ($A_+ = 0$). In this case, one can set $\mu_1 = +, \ldots, \mu_n = +$. $D_{\mu=+}$ in the light cone gauge is reduced to ∂_+, and:

$$A_n(p_+)^n = < p|\overline{\psi}(0)\gamma_+(i\partial_+)^{(n-1)}\psi(0)|p > . \tag{5.2}$$

The twist-2 parton distribution is then defined as [175]:

$$H(x) = \frac{p_+}{2\pi}\int dz_- e^{-ixp_+z_-} < p|T\overline{\psi}(z_-)\gamma_+\psi(0)|p >_c, \tag{5.3}$$

where only connected diagrams contribute and T denotes temporal order. It then follows that:

$$A_n = \int_{-\infty}^{+\infty} dx x^{n-1} H(x). \tag{5.4}$$

Thus, the matrix elements of the twist-2 operators appearing in the OPE can be related to the parton distributions. We now show that the function $H(x)$ has indeed the properties of parton distributions (roughly, they should vanish outside the energy-momentum conservation domain, $0 < x < 1$, and all intermediate states have to be on-mass-shell).

As shown by Jaffe [175], the temporal order in Eq. (5.3) is illusory and one has:

$$\begin{aligned} H(x) &= \frac{p_+}{2\pi}\int dz_- e^{-ixp_+z_-} < p|\overline{\psi}(z_-)\gamma_+\psi(0)|p >_c \\ &= -\frac{p_+}{2\pi}\int dz_- e^{-ixp_+z_-} < p|\psi(0)\overline{\psi}(z_-)\gamma_+|p >_c . \end{aligned} \tag{5.5}$$

Using $\gamma_+ = (\gamma_0 + \gamma_3)/\sqrt{2}$ and $\psi_+ = P_+\psi = (1 + \gamma_0\gamma_3)\psi/2$, one finds that $\overline{\psi}(z_-)\gamma_+\psi(0) = \psi_+^\dagger(z_-)\psi_+$. Then, the first equality of Eq. (5.5) becomes:

$$H(x) = p_+ \sum_n \delta(p_+^n - p_+(1-x)) \mid< n|\psi_+(0)|p>\mid^2, \tag{5.6}$$

where we introduced a complete set of intermediate states, n, of momentum p^n, and we used $\psi_+^\dagger(z_-) = e^{i\hat{p}_+ z_-}\psi(0)e^{-i\hat{p}_+ z_-}$. Also, a factor $\sqrt{2}$ in the numerator was incorporated in the definition of p_+. Similarly, the second equality of Eq. (5.5) leads to:

$$H(x) = -p_+ \sum_n \delta(p_+^n - p_+(1+x)) \mid< n|\psi_+^\dagger(0)|p>\mid^2 . \tag{5.7}$$

Eqs. (5.6) and (5.7) have the simple interpretation of quark and antiquark distributions, respectively [175]. This can be seen as follows. $H(x)$ of Eq. (5.6) gives rise to four independent contributions. The one we want to retain in the parton model is the one denoted by (a) in Fig. 5.1, where one quark is annihilated in the target, taking a momentum fraction xp_+ from it and leaving a intermediate state of momentum $(1-x)p_+$. The quark is then recreated in the target to form a final state of momentum p_+. Clearly, $x \leq 1$ in order to keep the intermediate state with positive momentum. It is easy to see that the other contributions to $H(x)$ restrict x to negative values. Hence, the graph (a) of Fig. 5.1 is the only one contributing in the region $0 \leq x \leq 1$. We will call it $H_a(x)$. By its turn, the three remaining contributions from Eq. (5.6) are related to the analogous contribution of $H_a(x)$ of Fig. 5.1 coming from Eq. (5.7). In this case, there are again four contributions but the argument is reversed: as a quark is inserted in the target with momentum fraction xp_+ it forms an intermediate state with momentum $(1+x)p_+$ and is subsequently removed from the intermediate state to form the final state of momentum p_+. Clearly, this is the only contribution with $-1 \leq x \leq 0$. The sum of each of the two described contributions from Eqs. (5.6) and (5.7) is then the total contribution coming from the sum of all graphs of either $H(x)$ of Eq. (5.6) or (5.7). Hence, $H(x)$ does not have support for x from $-\infty$ to $+\infty$ but for $-1 \leq x \leq +1$. It is possible

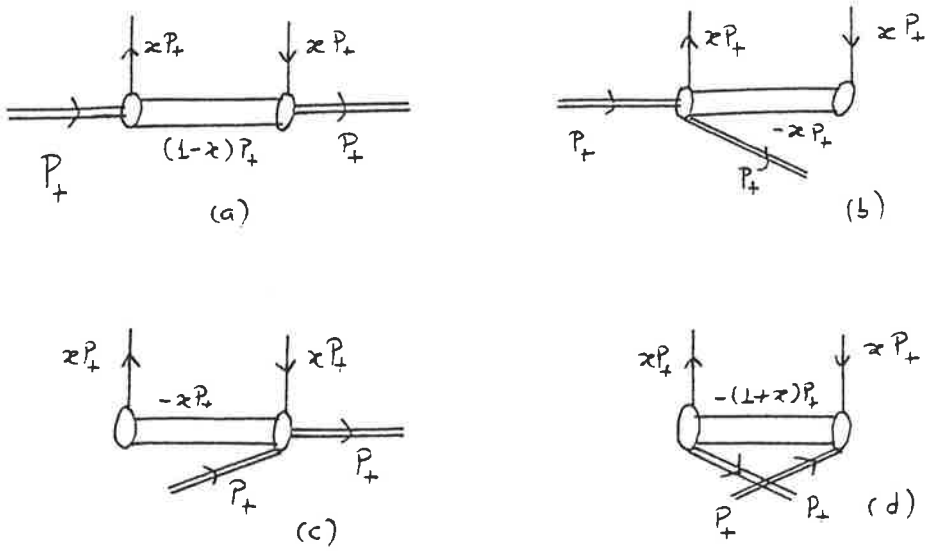

Figure 5.1: Graphical representation of the four contributions from Eq. (5.6).

to make a further simplification if one notices that $H_a(x)$ from Eq. (5.7) has support only for $0 \leq x \leq 1$ if $x \rightarrow -x$. Moreover, it is clear now the interpretation of this contribution as being associated with antiquarks as it would correspond to a quark being inserted in the target with a negative fraction of momentum or a antiquark being removed from the target with a positive fraction of momentum. Denoting this contribution as $\overline{H}_a(x) = -H_a(-x)$, the equation for H is then written as:

$$\int_{-\infty}^{+\infty} H(x)dx = \int_0^1 (H_a(x) + \overline{H}_a(x))dx. \tag{5.8}$$

Jaffe [207] and others [208, 209, 210, 211, 212, 213] were among the first to use model wave functions to calculate $H(x)$ as given by Eq. 5.3. However, these calculations have a serious problem because they use MIT bag model wave functions which are known to break

translational invariance. As a result, energy-momentum conservation is not guaranteed and the calculated quark distributions do not vanish beyond the physical limit $x = 1$. This problem was solved in a series of papers by Signal and Thomas [41, 42], where they started with Eq. (5.6) before making any approximation and thus ensuring energy-momentum through the use ot the delta function.

To minimize the problem of broken translational invariance of the MIT bag model wave functions, Signal and Thomas used the Peierls-Yoccoz projection [214] to obtain approximate momentum eigenstates:

$$\langle \vec{x}_1 \vec{x}_2 ... \vec{x}_l | \vec{p} \rangle = \frac{1}{\phi_l(\vec{p})} \int d\vec{R} e^{i\vec{p}\cdot\vec{R}} \psi(\vec{x}_1 - \vec{R}) \psi(\vec{x}_2 - \vec{R}) ... \psi(\vec{x}_l - \vec{R}), \tag{5.9}$$

where the normalization condition on the momentum eigenstates, $< \vec{p}|\vec{p}' >= (2\pi)^3 \delta(\vec{p} - \vec{p}')$, determines $\phi(\vec{p})$:

$$| \phi_l(\vec{p}) |^2 = \int d\vec{x} e^{-i\vec{p}\cdot\vec{x}} \left[\int d\vec{y} \psi^\dagger(\vec{y} - \vec{x}) \psi(\vec{y}) \right]^l . \tag{5.10}$$

We follow the previous works [41, 42, 150, 215] and work in the target rest frame, where according to the convention used here $p_+ = M$ (the proton mass) and $\vec{p} = 0$, as the quark distribution defined by (5.8) is frame independent. We will work in the coordinate representation and for the field operators ψ of Eq. (5.6). Denoting the quark distribution by $q(x)$, we have:

$$q(x) = M \sum_n \delta(M(1-x) - p_+) \left| \int d\vec{x}_1 d\vec{x}_2 d\vec{x}_3 d\vec{y}_1 d\vec{y}_2 d\vec{y}_3 \langle \vec{p}_n | \vec{x}_1 \vec{x}_2 \vec{x}_3 \rangle \langle \vec{x}_1 \vec{x}_2 \vec{x}_3 | \psi_+(0) | \vec{y}_1 \vec{y}_2 \vec{y}_3 \rangle \langle \vec{y}_1 \vec{y}_2 \vec{y}_3 | \vec{0} \rangle \right|^2 . \tag{5.11}$$

where two sets of states were included. Hence:

$$q(x) = M \sum_n \delta(M(1-x) - p^+) \left| \int d\vec{x}_1 d\vec{x}_2 \langle \vec{p}_n | \vec{x}_1 \vec{x}_2 \rangle \langle \vec{x}_1 \vec{x}_2 \vec{0} | \vec{0} \rangle \right|^2 . \tag{5.12}$$

The Peierls-Yoccoz projection, Eq. (5.9), then allow us to write down the modulus squared appearing in the expression for $q(x)$:

$$\left| \int d\vec{x}_1 d\vec{x}_2 \langle \vec{p}_n | \vec{x}_1 \vec{x}_2 \rangle \langle \vec{x}_1 \vec{x}_2 \vec{0} | \vec{0} \rangle \right|^2 = \frac{|\phi_2(\vec{p}_n)|^2}{|\phi_3(0)|^2} |\tilde{\psi}_+(\vec{p}_n)|^2, \tag{5.13}$$

where $\tilde{\psi}_+$ is the Fourier transform of ψ_+, $\tilde{\psi}_+(\vec{p}_n) = \int d\vec{x} e^{i\vec{p}_n \cdot \vec{x}} \psi(\vec{x})$. Insertion of Eq. (5.13) into the definition of the quark distribution, Eq. (5.12), yields:

$$q(x) = \frac{M}{(2\pi)^3} \int d\vec{p}_n \frac{\mid \phi_2(\vec{p}_n) \mid^2}{\mid \phi_3(0) \mid^2} \delta(M(1-x) - p_n^+) \mid \tilde{\psi}_+(\vec{p}_n) \mid^2 . \tag{5.14}$$

In equation (5.14) we changed the the sum to an integration over the momentum of the intermediate diquark states, which carries a normalization factor of $(2\pi)^3$. The integration over $\vec{p}_n$ can be made, for example, over the magnitude of $\vec{p}_n$ and the transverse momentum $\vec{p}_n^{\perp}$ variables. Carrying out the integration, we find:

$$q(x) = \frac{M}{(2\pi)^2} \int_{[M^2(1-x)^2 - M_n^2]/2M(1-x)}^{+\infty} \mid \vec{p}_n \mid d \mid \vec{p}_n \mid \frac{|\phi_2(\vec{p}_n)|^2}{|\phi_3(0)|^2} |\tilde{\psi}_+(\vec{p}_n)|^2. \tag{5.15}$$

A similar equation can be derived for the antiquark distribution. Also, a expression that makes the spin and flavour indexes explicit can be derived. Its form was calculated in Ref. [150] and we quote it here:

$$q_f^{\uparrow\downarrow}(x) = \frac{M}{(2\pi)^2} \sum_m < \mu | P_{f,m} | \mu > \int_{[M^2(1-x)^2 - M_n^2]/2M(1-x)}^{+\infty} \mid \vec{p}_n \mid d \mid \vec{p}_n \mid \frac{|\phi_2(\vec{p}_n)|^2}{|\phi_3(0)|^2} |\tilde{\psi}_+^{\uparrow\downarrow}(\vec{p}_n)|^2. \tag{5.16}$$

where $|\mu>$ is the spin-flavour wave function, f is a given flavour and m refers to the spin projections. There are a few important points implicit in Eqs. (5.15) and (5.16). One of the points is that besides the Peierls-Yoccoz projection, no other approximation was made to derive them. The only requirement is that the states are eigenfunctions of the momentum operator. The expressions are thus independent of the model and should be valid for any given wave function. A second point is that they were written having in mind only intermediate states with $n = 2$, as is clear from the weighting function ϕ_2 in Eq. (5.14). Of course, other intermediate states are allowed and the total quark distribution involves a sum over all possible n. In particular, the $n = 2$ contribution means that ψ annihilates one quark in the target. In addition to this, ψ can also create an antiquark in the target, forming a intermediate state with 3 quarks and one antiquark [150]. This can be visualized as a photon decaying into a $q\overline{q}$ pair. The antiquark then is inserted into the nucleon and forms the intermediate state. Eventually, it is annihilated and the photon-nucleon system reappears. For the antiquark distribution, the same analysis applies. However, in this case, if one considers that there are no antiquarks in the nucleon, the antiquark distribution receives only one contribution. Again the photon goes to a $q\overline{q}$ pair but now it is the quark that interacts with the nucleon in the intermediate state.

Some final remarks on the projection procedure are necessary. First, the projection is a nonrelativistic approximation with a wave function normalization that is momentum dependent. Second, if one calculates the number of valence quarks, the result will be dependent on the mass of the intermediate state [42, 150]. Hence, if the masses of the intermediate states are not consistently calculated within the model, problems with the number of quarks are expected to be found, as indeed they are [42, 150]. Third, the Peierls-Yoccoz projection for the intermediate states breaks down for large x [42] meaning that we may have problems in that region. Finally, there is the ambiguity related to which projection is the best to be

used [216] as others methods, like the Peierls-Thouless [217], are available.

5.2.1 A Simple Model

To illustrate the discussion on the calculation of quark distributions, we will employ a very simple form for the quark wave functions inside the nucleon:

$$\psi(\vec{x}) = \frac{e^{-r^2/2R^2}}{(\pi R^2)^{3/4}}, \tag{5.17}$$

with $r = |\vec{x}|$ and R the nucleon radius. The form (5.17) is typical of models based in nonrelativistic harmonic oscillators. If we write:

$$|\phi_l(\vec{p}_n)|^2 = \int d\vec{y} e^{i\vec{y}\cdot\vec{p}_n} I_l(\vec{y}), \tag{5.18}$$

then,

$$I_l(\vec{y}) = e^{-ly^2/4R^2}. \tag{5.19}$$

Thus it is easily seen that:

$$\frac{|\phi_2(\vec{p}_n)|^2}{|\phi_3(0)|^2} = \left(\frac{3}{2}\right)^{3/2} e^{-|\vec{p}_n|^2R^2/2}. \tag{5.20}$$

Similarly, the result for the squared modulus of $\tilde{\psi}(\vec{p}_n)$ is:

$$|\tilde{\psi}(\vec{p}_n)|^2 = 8R^3\pi^{3/2}e^{-|\vec{p}_n|^2R^2}. \tag{5.21}$$

Combining all the results in the expression for $q(x)$, Eq. (5.15), we get:

$$q(x) = \frac{4}{\beta}\sqrt{\frac{6}{\pi}}e^{-\frac{3}{2\beta^2}\left[(1-x)-\frac{M_n^2/M^2}{1-x}\right]^2}\Theta(1-x). \tag{5.22}$$

with $\beta = 2/MR$.

This distribution is roughly Gaussian type with a peak at $x_p = 1 - M_n/M$, but it dies away rapidly as $x \to 1$. Expression (5.22) is valid only at the momentum scale at which the model is applicable and the evolution to energies where it can be compared with data is done by means of QCD evolution.

It is interesting to explore the behaviour of the quark distributions when $x \to 1$ in order to select the appropriate wave function. It is well known since the work of Brodsky and Ferrar [218] and subsequent extensions [219] that for large x, the quark distribution in the nucleon behaves as:

$$q(x) \sim (1-x)^{2n-1}, \tag{5.23}$$

where n is the number of spectators. So, as a basic property, every model for the nucleon should at least reproduce the above behaviour. In particular, wave functions that do not fall off with inverse powers of momentum cannot satisfy equ. (5.23).

Models based on nonrelativistic oscillators, will have a wave function of the form (5.17) and in this case we can see from the quark distribution, Eq. (5.22), that:

$$q(x) \propto \frac{n}{n+1} e^{-\frac{n+1}{n(1-x)^2}}, \tag{5.24}$$

as $x \to 1$. Thus, the quark distribution has the wrong behaviour in the large x region for any number of spectator quarks. On the other hand, we could have used bag model wave functions. Their behaviour with momentum is

$$\tilde{\psi}(\vec{p}) \propto \frac{sin(|\vec{p}|R)}{|\vec{p}|^2}, \tag{5.25}$$

and

$$\tilde{I}_n(\vec{p}) = |\phi_n(\vec{p})|^2 \propto |\vec{p}|^{n-3}. \tag{5.26}$$

In this case, the quark distribution behaves as

$$q(x) \propto c_1(1-x)^{5-n} + c_2(1-x)^{7-n} \tag{5.27}$$

when $x \to 1$ and c_1 and c_2 are some constants. Hence, the bag model has the correct behaviour as $x \to 1$ for $n = 2$ (which is the dominant contribution) because the $(1-x)^3$ term dominates over $(1-x)^5$. For any other number of spectators, the model has a wrong behaviour in the large x region.

5.2.2 Importance of the Correct Support

There are in the recent literature some calculations of quark distributions in nonrelativistic quark models [202] or bag models [151] that do not ensure energy-momentum conservation and hence have quarks in a region physically forbidden. In particular, in Ref. [151], it is argued that to circumvent eventual problems with normalization, one should allow for some breaking of the energy-momentum relations.

In this section, we make a simple comparison of our quark distributions for models based in harmonic oscillators with an other approach in the literature that do not vanish beyond the physical limits $0 \leq x \leq 1$. We then are able to show how important it is to insist in the correct support for the quark distributions.

Some time ago it was proposed to calculate quark distributions in constituent quark models through the use of the matrix density formalism [202]. Given a wave function for the three quark system representing the hadron, one can calculate the momentum distribution $n(\vec{p})$:

$$n(\vec{p}) = \frac{1}{(2\pi)^3} \int d\vec{r} d\vec{r'} \rho(\vec{r}, \vec{r'}) e^{i\vec{p}\cdot(\vec{r}-\vec{r'})}, \tag{5.28}$$

with $\rho(\vec{r}, \vec{r'})$ the density matrix. The result for the harmonic oscillator case is:

$$n(p) = \frac{2}{\alpha^3 \pi^{3/2}} \left(\frac{3}{2}\right)^{3/2} e^{-3p^2/2\alpha^2}, \tag{5.29}$$

where $\alpha = 1.35 fm^{-2}$ is the harmonic oscillator constant fixed by the r.m.s. radius of the proton. Expression (5.29) is normalized to two for later convenience. The extension of this calculation for the Isgur-Karl model is straightforward and is shown explicitly in Ref. [202].

In this formalism, the quark distribution is given by:

$$xq(x, \mu^2) = \pi m_q \int_{k_m^2(x)}^{+\infty} d|\vec{k}^2| n_q(|\vec{k}|), \tag{5.30}$$

where $\vec{k}$ is the momentum of the struck quark and k_m is given by:

$$k_m = \frac{M}{2}\left[x - \frac{m_q^2/M^2}{x}\right]. \tag{5.31}$$

Therefore the u quark distribution is written as:

$$xu_v(x, \mu^2) = \left(\frac{3}{2}\right)^{3/2} \frac{m_u}{\alpha\sqrt{\pi}} \frac{4}{3} e^{-\frac{3}{2\alpha^2}k_m^2}. \tag{5.32}$$

Note that this does not vanish beyond $x = 1$.

In calculating the quark distributions we used the input parameters given in Ref. [202] so that the two methods could be directly compared. The mass scale was chosen so that the second moment of the nucleon structure function, F_2^N, agreed with the EMC data. This furnished $\mu = 244.67$ MeV for the scale parameter with the QCD scale parameter $\Lambda = 200$ MeV. We still have to choose the mass of the intermediate state. Agreement with Ref. [202]

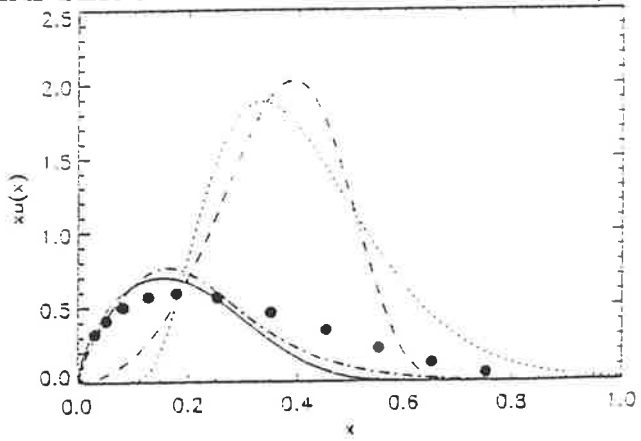

Figure 5.2: Quark distribution for u_v quarks for both $\mu = 244.67$ MeV and after evolution until $Q^2 = 15$ GeV^2, with $M_n = 2M/3$ and $R = 0.86fm$. The notation is as follows: dotted and dotted-dashed lines correspondent to equ. (24), before and after evolution respectively. Our results, corresponding to equ. (16), are the dashed and continuous lines. The EMC data is from [220].

requires that $M_n = 2M/3$. Just for the sake of comparison, we also will work with a mass of the intermediate state given by $M_n = 3M/4$, which corresponds in quark model terms to the case when the virial theorem is applicable and the bag boundary carries the same energy as each of the quarks confined in the bag. We use $R = 0.86fm$ which corresponds to the experimental r.m.s. proton radius.

In Fig. 5.2 we show the quark distribution, xu_v, corresponding to expressions (5.22) and (5.32) both for the mass scale μ and after evolution to $Q^2 = 15$ GeV^2. There is clearly a very significant difference between the two methods of calculation. Most notably, the distribution calculated using Eq. (5.22) vanishes rapidly beyond $x = 0.6$ (before evolution). It also has the correct support in the range $0 \leq x \leq 1$. In contrast the plot of the quark distribution (5.32) is sizeable in the large x region and also shows an unphysical contribution in the region $x > 1$. The EMC data [220] is also shown and one can clearly see the disagreement between

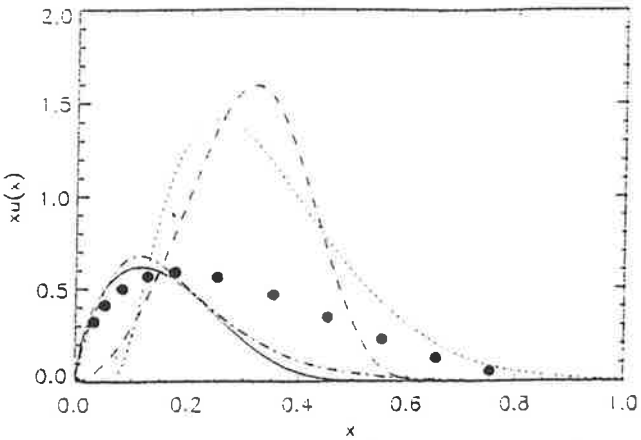

Figure 5.3: Quark distribution for u_v quarks for both $\mu = 244.67$ MeV and after evolution until $Q^2 = 15$ GeV^2, with $M_n = 3M/4$ and $R = 0.86fm$. The notation is as follows: dotted and dotted-dashed lines for the method of Ref. [202] before and after evolution respectively. Our prefered results are the dashed and continuous lines. The EMC data is from [220].

it and the theoretically calculated distributions.

Figure 5.3 shows the quark distribution for $M_n = 3M/4$. As expected the curves are moved to the left because the peak of the distribution depends on the mass of the intermediate state, as stated before. In Fig. 5.4 we show the total valence quark distributions. For $x \leq 0.1$ the two methods give similar answers, showing a reasonable agreement with data, while for $0.1 \leq x \leq 0.3$ our results are slightly favoured. However for $x \geq 0.3$ there is a significant discrepancy between the data and the theoretical calculations - as one would expect from our earlier discussions of the behaviour as $x \rightarrow 1$.

Finally in Fig. 5.5 we show the ratio of the up valence quark distribution calculated with incorrect support to that calculated with our prefered method. Of course the ratio is infinite at $x = 1$, but is important to emphasize how large the differences are just beyond $x = 0.5$. These differences would be even more important if one were to investigate nuclear structure functions in the region beyond $x = 1$, which is forbidden for a free nucleon.

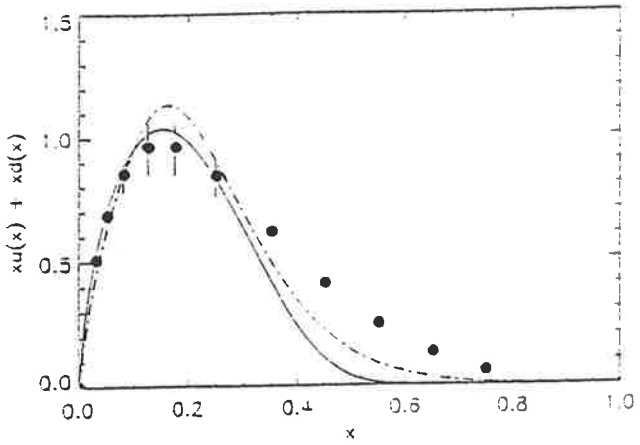

Figure 5.4: The total valence quark distribution, $u_v + d_v$, with $Q^2 = 15$ GeV^2, $M_n = 2M/3$ and $R = 0.86fm$. The notation is as follows: dotted-dashed lines for the method of Ref. [202] and continuous lines for our prefered procedure. The EMC data is from [220].

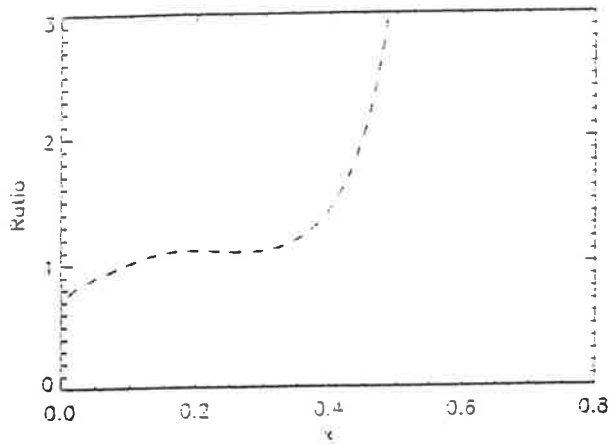

Figure 5.5: Ratio of the up valence quark distribution calculated with Eq. (5.32) to that calculated with Eq. (5.22). The inputs are the same as those for Fig. 5.4.

Once we have a reliable scheme to calculate quark distributions, through Eqs. (5.15) and (5.16), we can proceed to calculate the various polarized and unpolarized structure functions. In general, as already discussed, we only know how these structure functions and quark distributions evolve with the scale, Eqs. (2.82) and (2.83), but the initial scale where the constants A_n (and hence the quark distributions) are valid is not know a priori. In general, this scale is chosen to fit a given quantity. In the simple case studied here, the mass scale was chosen so that the second moment of the calculated F_2, $n = 2$ in Eq. (2.82), agreed with the data. This produced $\mu^2 \simeq 0.06 GeV^2$, which is a extremely low scale. Such μ^2 produces a very large coupling constant, as can be seen from Eq. (2.95), throwing doubt on the whole procedure of QCD evolution.

In this case, we included only α_s corrections to the quark distributions and given the problems with the size of these corrections, we are led to include higher order corrections in the evolution in order to make the application of the RGE analysis more reliable. This is what is done in the next section.

5.3 Next-to-Leading Order QCD Corrections

The moments of the structure functions are given by (Eqs. (5.15) and (5.16)):

$$M_n(Q^2) = \sum_i C_n^i(Q^2/\mu^2, g) A_n^i(\mu^2). \tag{5.33}$$

The sum runs over all spin-n, twist-2 operators and $M_n = \int_0^1 dx x^{n-1} F(x)$, with $F(x)$ a given structure function.

As we saw before, Eq. (5.33) is a direct result of the operator product expansion applied to the forward scattering of the photon from the hadronic state through the e.m. current, J_μ.

Page 138 missing in print and digital.

appendix A. Finally, we point out that the anomalous dimensions and the beta function are universal in the sense that they are not attached to a particular structure function but the same is not true for the Wilson coefficients.

We start by considering the leading order (LO) case (up to order g^2). From Eqs. (5.34), (5.35) and (5.36) we get:

$$\begin{aligned} C_n(Q^2,\mu^2,g^2) &= C_n(1,\overline{g}^2)exp\left[-\int_{\overline{g}(\mu^2)}^{\overline{g}(Q^2)} dg' \frac{\gamma^{(0)n}g'^2}{-\beta_0 g'^3}\right] \\ &= C_n(1,\overline{g}^2)\left(\frac{\alpha_s(Q^2)}{\alpha_s(\mu^2)}\right)^{\gamma^{(0)n}/2\beta_0}, \end{aligned} \tag{5.38}$$

where $\alpha_s = \overline{g}^2/4\pi$. Hence:

$$M_n(Q^2) = \sum_i A_n^i(\mu^2)\left(\frac{\alpha_s(Q^2)}{\alpha_s(\mu^2)}\right)^{\gamma^{(0)n}/2\beta_0}. \tag{5.39}$$

Here the sum runs only over the nonsinglet operators as we are dealing only with this case. Note that in LO, $C_n(1,g) = 1$ and the moments of the quark distributions A_n are just the moments of the structure functions M_n as $M_n(Q^2) = A_n(Q^2)$. It is this equality that allows one to write down the simple expressions for the structure functions in the parton model in terms of a sum of parton distributions. In next-to-leading order (NLO), such simple relations no longer exist because in this case, $C_n(1,g) = 1 + F_n g^2/16\pi^2$ and thus $M_n(Q^2) \neq A_n(Q^2)$. Moreover, as will become clear, parton distributions in higher orders are scheme dependent objects. This conclusion is natural in the sense that partons in QCD (quarks and gluons) are not observable.

The singlet case is more complicated and, as we are going to study the NLO evolution, we treat the singlet case only there, keeping in mind that the LO expression will be just a special case.

In NLO, the nonsinglet moments are slightly more complicated. In this case,

$$C_n(Q^2,\mu^2,g^2) = C_n(1,\overline{g}^2)exp\left[-\int_{\overline{g}(\mu^2)}^{\overline{g}(Q^2)} dg' \frac{\gamma^{(0)n}+\gamma^{(1)n}\frac{g'^2}{16\pi^2}}{-\beta_0 g' - \beta_1 \frac{g'^3}{16\pi^2}}\right] \tag{5.40}$$

If $\beta_1\alpha_s(Q^2)/(4\pi\beta_0)$ and $\beta_1(\alpha_s(\mu^2)-\alpha_s(Q^2))/(4\pi\beta_0)$ are small numbers, then after some algebra:

$$C_n(Q^2,\mu^2,g^2) = C_n(1,\overline{g}^2)\left(\frac{\alpha_s(Q^2)}{\alpha_s(\mu^2)}\right)^{\gamma^{(0)n}/2\beta_0}\left(1+\frac{\alpha_s(Q^2)-\alpha_s(\mu^2)}{4\pi}\left(\frac{\gamma^{(1)n}}{2\beta_0}-\beta_1\frac{\gamma^{(0)n}}{2\beta_0^2}\right)\right), \tag{5.41}$$

and the moments of the structure functions, $M_n(Q^2)$, are:

$$\begin{aligned} M_n(Q^2) &= \left(1+F_n\frac{\alpha_s(Q^2)}{4\pi}+\frac{\alpha_s(Q^2)-\alpha_s(\mu^2)}{4\pi}\left(\frac{\gamma^{(1)n}}{2\beta_0}-\beta_1\frac{\gamma^{(0)n}}{2\beta_0^2}\right)\right)\left(\frac{\alpha_s(Q^2)}{\alpha_s(\mu^2)}\right)^{\gamma^{(0)n}/2\beta_0} A_n(\mu^2) \\ &= (1+F_n\frac{\alpha_s(Q^2)}{4\pi})A_n(Q^2). \end{aligned} \tag{5.42}$$

In writing this equation, we have also defined the evolution of the NLO quark distributions:

$$A_n(Q^2) = \left(1+\frac{\alpha_s(Q^2)-\alpha_s(\mu^2)}{4\pi}\left(\frac{\gamma^{(1)n}}{2\beta_0}-\beta_1\frac{\gamma^{(0)n}}{2\beta_0^2}\right)\right)\left(\frac{\alpha_s(Q^2)}{\alpha_s(\mu^2)}\right)^{\gamma^{(0)n}/2\beta_0} A_n(\mu^2). \tag{5.43}$$

Of course, this definition is arbitrary. One could as well define the whole right hand side of Eq. (5.42) as the quark distribution so that the LO relation between the moments of the structure functions and of quark distributions is still valid ($M_n(Q^2) = A_n(Q^2)$). However, as the Wilson coefficients are different for different structure functions, one would have to define distinct quark distributions for each structure function. This would mean that one looses the very basic property of the distributions, that is their universality. To circumvent

this, one could define the quark distribution for a certain structure function and use the same distribution for all other structure functions. In general, F_2 is chosen to be valid as $F_2(x) = \sum_q e_q^2 q(x)$ to all orders in perturbation theory and these distributions are often called DIS parton distributions [227]. On the other hand, to calculate any other structure function, one would have to use a expression like the one after the second equality of (5.42), resulting in an asymmetric treatment of the different structure functions.

It is well known that F^n and $\gamma^{(1)}$ are scheme dependent objects [221, 224, 225, 93]. Hence, the DIS scheme would correspond to the one where the quark Wilson coefficient for F_2 is zero. But in general, $\overline{MS}$ schemes are used in renormalizing QCD meaning that one should find a transformation that takes the calculated quantities from one scheme to the other. In our opinion, nothing is gained with such a redefinition and the use of Eq. (5.43) for all structure functions is simpler, more direct and symmetric. Also, at first glance it would seem that Eq. (5.42) is scheme dependent as F^n and $\gamma^{(1)}$ enter with different coefficients. However, this is not the whole story because the moments of the quark distributions, $A_n(\mu^2)$, are scheme dependent themselves. In fact, if the derivative in lnQ^2 of Eq. (5.42) is taken, then [228]:

$$\frac{dM(Q^2)}{dlnQ^2} = -\frac{1}{2}\left[\frac{\alpha_s(Q^2)}{4\pi}\gamma^{(0)} + 2\beta_0\left(\frac{\alpha_s(Q^2)}{4\pi}\right)^2\left[F + \frac{\gamma^{(1)}}{2\beta_0}\right]\right] M(Q^2), \tag{5.44}$$

where the index n was omitted for notational convenience. Eq. (5.44) is scheme independent because M is a physical quantity and thus $F + \frac{\gamma^{(1)}}{2\beta_0}$ *must* be independent of scheme. Thus, Eq. (5.42) is a correct expression for the calculation of the moments of structure functions in NLO.

Many authors like to express Eq. (5.42) in the form [229]:

$$M_n(Q^2) = \left(1 + \frac{\alpha_s(Q^2) - \alpha_s(\mu^2)}{4\pi}\left(F_n + \frac{\gamma^{(1)n}}{2\beta_0} - \beta_1\frac{\gamma^{(0)n}}{2\beta_0^2}\right)\right)\left(\frac{\alpha_s(Q^2)}{\alpha_s(\mu^2)}\right)^{\gamma^{(0)n}/2\beta_0} M_n(\mu^2). \tag{5.45}$$

We are now going to argue that Eq. (5.45) is not suitable for practical calculations. First, when we deal with models, we always calculate quark distributions meaning that one should transform the initial quark distributions into an initial structure function through the relation $M_n(\mu^2) = (1 + F_n\alpha_s(\mu^2))A_n(\mu^2)$. This does not look as a strong constraint to the use of Eq. (5.45) but one should realize that this equation is formally derived using a cut in α_s because $M_n(\mu^2)$ has already built in itself a factor in α_s. This can be seen if one attempts to derive Eq. (5.42) from Eq. (5.45). In this case, a term proportional to $\alpha_s(\mu)(\alpha_s(Q^2) - \alpha_s(\mu^2))$ will appear that is implicit in Eq. (5.45) but has to be disregarded to obtain Eq. (5.42). This is not a question of scheme used as both Eqs. (5.42) and (5.45) obey Eq. (5.44) and are scheme invariant. The problem is that to write down Eq. (5.45) one implicitly assumes that it is formally valid only to order α_s. This point has been overlooked in the literature and as a conclusion, we point out that for practical purposes Eq. (5.42) should be used to calculate the moments of structure functions. Of course, the calculation of the parton distributions, through Eq. (5.43), is insensitive to this discussion.

In LO QCD, the moments of singlet combinations will have the form:

$$M_n(Q^2) = \Sigma_n^{LO}(Q^2), \tag{5.46}$$

where $\Sigma_n^{LO}(Q^2)$ are the moments of the singlet quark distributions. Following the preceding discussion, in NLO the quark distributions have to be multiplied by their respective Wilson coefficients in order to obtain the structure functions. Moreover, a gluon distribution has to be included in the expression for the structure function because in two loops it contributes to the calculation of the Wilson coefficients via the box graphs. If $\Sigma_n(Q^2)$ and $G_n(Q^2)$ are the distributions in NLO, then:

$$M_n^q(Q^2) = (1 + \frac{\alpha_s(Q^2)}{4\pi} F_n^{qq})\Sigma_n(Q^2) + \frac{\alpha_s(Q^2)}{4\pi} F_n^{qg} G_n(Q^2) \tag{5.47}$$

where F_n^{qq} and F_n^{qg} are the quark and gluon Wilson coefficients and the index q in M_n^q denotes the fact that there is no symmetry under the replacement $q \leftrightarrow g$ because the gluon has no flavour. But to make discussions easier, we introduce the analogue of Eq. (5.47), following Ref. [228], just for computational convenience, noticing that the contributions from this extra expression are naturally dropped in the end. Its form is:

$$M_n^g(Q^2) = (1 + \frac{\alpha_s(Q^2)}{4\pi} F_n^{gg})G_n(Q^2) + \frac{\alpha_s(Q^2)}{4\pi} F_n^{gq} \Sigma_n(Q^2). \tag{5.48}$$

Introducing the notation:

$$\vec{q} = \begin{bmatrix} \Sigma_n \\ G_n \end{bmatrix}, \hat{F} = \begin{bmatrix} F_n^{qq} & F_n^{qg} \\ F_n^{gq} & F_n^{gg} \end{bmatrix}, \vec{M} = \begin{bmatrix} M_n^q \\ M_n^g \end{bmatrix}, \hat{\gamma}^{tot} = \begin{bmatrix} \gamma_{qq}^{tot} & \gamma_{qg}^{tot} \\ \gamma_{gq}^{tot} & \gamma_{gg}^{tot} \end{bmatrix}, \tag{5.49}$$

where $\hat{\gamma}^{tot} = \hat{\gamma}^{(1)}/2\beta_0 - \beta_1\hat{\gamma}^{(0)}/2\beta_0^2$ and the index n was again omitted for convenience. The equation for the vector of the structure functions is then written as:

$$\vec{M}(Q^2) = (1 + \frac{\alpha_s(Q^2)}{4\pi}\vec{F})\vec{q}(Q^2) \tag{5.50}$$

where:

$$\vec{q}(Q^2) = \left(1 + \frac{\alpha_s(Q^2) - \alpha_s(\mu^2)}{4\pi}\hat{\gamma}^{tot}\right)\left(\frac{\alpha_s(Q^2)}{\alpha_s(\mu^2)}\right)^{\hat{\gamma}^{(0)}/2\beta_0}\vec{q}(\mu^2). \tag{5.51}$$

There is a diagonalization technique due to Gross and Wilzeck [230] for the terms containing a power of $\hat{\gamma}^{(0)}$:

$$\left(\frac{\alpha_s(Q^2)}{\alpha_s(\mu^2)}\right)^{\hat{\gamma}^{(0)}/2\beta_0} = \frac{\hat{\gamma}^{(0)}-\gamma_+ I}{\gamma_- - \gamma_+}\left(\frac{\alpha_s(Q^2)}{\alpha_s(\mu^2)}\right)^{\gamma_-/2\beta_0} - \frac{\hat{\gamma}^{(0)}-\gamma_- I}{\gamma_- - \gamma_+}\left(\frac{\alpha_s(Q^2)}{\alpha_s(\mu^2)}\right)^{\gamma_+/2\beta_0}, \quad (5.52)$$

where:

$$\gamma_\pm = \frac{1}{2}[\gamma_{qq}^{(0)} + \gamma_{gg}^{(0)} \pm \sqrt{(\gamma_{qq}^{(0)} + \gamma_{gg}^{(0)})^2 - 4(\gamma_{qq}^{(0)}\gamma_{gg}^{(0)} - \gamma_{qg}^{(0)}\gamma_{gq}^{(0)})}]. \quad (5.53)$$

Using expressions (5.49) and (5.52) in Eq. (5.51), one derives, after some algebra, the quark singlet and gluon distributions in NLO:

$$\begin{aligned}\Sigma(Q^2) &= \left(1 + \frac{\alpha_s(Q^2)-\alpha_s(\mu^2)}{4\pi}\left(\frac{\gamma_{qq}^{(1)}}{2\beta_0} - \beta_1\frac{\gamma_{qq}^{(0)}}{2\beta_0^2}\right)\right)\Sigma^{LO}(Q^2) \\ &\quad + \frac{\alpha_s(Q^2)-\alpha_s(\mu^2)}{4\pi}\left(\frac{\gamma_{qg}^{(1)}}{2\beta_0} - \beta_1\frac{\gamma_{qg}^{(0)}}{2\beta_0^2}\right)G^{LO}(Q^2), \quad (5.54)\end{aligned}$$

$$\begin{aligned}G(Q^2) &= \left(1 + \frac{\alpha_s(Q^2)-\alpha_s(\mu^2)}{4\pi}\left(\frac{\gamma_{gg}^{(1)}}{2\beta_0} - \beta_1\frac{\gamma_{g}^{(0)}}{2\beta_0^2}\right)\right)G^{LO}(Q^2) \\ &\quad + \frac{\alpha_s(Q^2)-\alpha_s(\mu^2)}{4\pi}\left(\frac{\gamma_{gq}^{(1)}}{2\beta_0} - \beta_1\frac{\gamma_{gq}^{(0)}}{2\beta_0^2}\right)\Sigma^{LO}(Q^2), \quad (5.55)\end{aligned}$$

The LO distributions were defined so that the singlet distributions in NLO agree with an early definition, Eq. (5.43), for the evolution of the nonsinglet distributions. They are given by:

$$\begin{aligned}\Sigma^{LO}(Q^2) &= \left(\frac{\gamma_{qq}^{(0)}-\gamma_+}{\gamma_- - \gamma_+}\Sigma(\mu^2) + \frac{\gamma_{qg}^{(0)}}{\gamma_- - \gamma_+}G(\mu^2)\right)\left(\frac{\alpha_s(Q^2)}{\alpha_s(\mu^2)}\right)^{\gamma_-/2\beta_0} \\ &\quad - \left(\frac{\gamma_{qq}^{(0)}-\gamma_-}{\gamma_- - \gamma_+}\Sigma(\mu^2) + \frac{\gamma_{qg}^{(0)}}{\gamma_- - \gamma_+}G(\mu^2)\right)\left(\frac{\alpha_s(Q^2)}{\alpha_s(\mu^2)}\right)^{\gamma_+/2\beta_0}, \quad (5.56)\end{aligned}$$

and

$$G^{LO}(Q^2) = \left(\frac{\gamma_{gg}^{(0)}-\gamma_+}{\gamma_- - \gamma_+}G(\mu^2) + \frac{\gamma_{gq}^{(0)}}{\gamma_- - \gamma_+}\Sigma(\mu^2)\right)\left(\frac{\alpha_s(Q^2)}{\alpha_s(\mu^2)}\right)^{\gamma_-/2\beta_0} - \left(\frac{\gamma_{gg}^{(0)}-\gamma_-}{\gamma_- - \gamma_+}G(\mu^2) + \frac{\gamma_{gq}^{(0)}}{\gamma_- - \gamma_+}\Sigma(\mu^2)\right)\left(\frac{\alpha_s(Q^2)}{\alpha_s(\mu^2)}\right)^{\gamma_+/2\beta_0} . \quad (5.57)$$

The expressions (5.54) and (5.55) for the quark and gluon distributions in NLO are not the ones commonly used in the literature (see, for instance, Refs. [231] or [134] for the standard forms). However, we think that the forms derived here are simpler to handle and they are, of course, equivalent to the standard forms[1].

Finally, we notice that in two loops, the running coupling constant is determined by solving the transcendental equation [229] introduced in Eq. (4.50) and reproduced here:

$$ln\frac{Q^2}{\Lambda^2} = \frac{16\pi^2}{\beta_0\overline{g}^2} - \frac{\beta_1}{\beta_0^2}ln\left[\frac{16\pi^2}{\beta_0\overline{g}^2} + \frac{\beta_1}{\beta_0^2}\right]. \quad (5.58)$$

The QCD scale parameter, Λ, defined after Eq. (2.95), is determined by comparing the theoretical calculations with the experimental data. As in our calculations of Δg of last chapter, we will use $\Lambda = 200\ MeV$.

5.3.1 Quark Distributions Beyond Leading Order

To calculate the quark distribution at the initial scale, we are going to use the MIT bag model wave functions, Eq. (3.22), in the expression for $q(x)$, Eq. (5.16). The full calculation, for the case with two quarks in the intermediate state, was presented before by Schreiber, Signal and Thomas [150].

[1] I thank S. Braendl for checking the equivalence of the two forms numerically.

Once we have a model to calculate the quark distributions, and hence the matrix elements A_n, we can proceed to evaluate the moments of the structure functions. Before doing so, a few remarks need to be made. The first deals with the spin of the intermediate states. In the case of a two-quark spectator system, the sum of the spins may be zero (a scalar diquark with a lower mass M_s), or one (a vector diquark with a higher mass M_v). The mass difference between these states is found to be around $200MeV$ in most quark models, and this is crucial to understanding the spin and flavour dependence of the distributions [232]. Taking this into account, one can calculate the contributions to the quark distribution due to the scalar and vector diquark systems, by using the $SU(6)$ wave function for $|\mu\rangle$ in Eq. (5.16).

Another point of concern are the four quark (or 3 quarks plus one antiquark) contributions. As we commented before, $q(x)$ has, besides the case where one quark is annihilated in the target, a contribution where an antiquark is inserted in the target. Similarly, $\overline{q}(x)$ has contributions from a quark being inserted and an antiquark being annihilated in the target. As in the present model, there is no antiquark in the initial scale (a basic assumption of the simple MIT bag), only the quark insertion contributes to $\overline{q}(x)$. Hence, there are two extra terms to consider along with the case of a two-quark spectator system. It is also well known that the two-quark system has problems with the normalization of the number of quarks. But as we discussed before when the model was presented, the normalization depends on the bag radius and the masses of the intermediate states [42, 150]. A coherent and consistent calculation of the model, where the masses of the intermediate states are self-consistently determined, should saturate the normalization condition, as one can indeed find values for the masses that do so. Instead, we will play with the two extra contributions involving more than two quarks in the intermediate states, to fulfill the condition on the number of quarks. There is no real problem with that because we are including all possible terms in

the calculation of the total quark distribution and instead of fixing the masses of the intermediate states through the normalization condition, we will keep than free and play with the normalization of the two extra contributions. We will choose for the four quark terms a form like $(1-x)^7$ and fix its normalization so that the sum of this term plus the calculated two-quark piece gives the total number of valence quarks. Moreover, $(1-x)^7$ resembles the actual form of the two extra contributions [150]. To the suspicious mind, we emphasize that all that was done was to choose a convenient set of free parameters in the model. We finally point out that there is an alternative study [151] of distributions in the bag model that adds contributions outside the limits allowed by energy-momentum conservation to saturate the normalization condition. As we discussed earlier in this chapter, this procedure can give a misleading interpretation of the calculated parton distributions while in the approach taken here, the only consequence is to finish up with different values for the free parameters of the model.

The free parameters of the model are its radius, the masses of the intermediate states and the initial scale at which the model is supposed to be valid. They are determined by evolving the total unpolarized valence distribution, in LO and NLO, and comparing it with some parametrization of the data at a higher scale. In this case, the parametrization for the data used is the MRS [233] and the scale is $Q^2 = 10\ GeV^2$. In reality, the masses of the intermediate states are not completely free because if one uses the virial theorem in the bag, where the bag itself carries the same energy as each of the three quarks confined in it, one roughly expects $M_s \simeq 750\ MeV - 150\ MeV$ and $M_v \simeq 750\ MeV + 50\ MeV$. But this is, of course, only an approximation and we have some freedom around these values.

Using the set of parameters determined in this way, we can then calculate the predictions of the model for other quantities. When this work was developed [215], only the nonsinglet anomalous dimension for polarized scattering were known in NLO. As we were primarily

interested on the effects of two-loop evolution in the polarized distributions, we did not make a extensive study of NLO in all the unpolarized structure functions but only in the total valence distributions. Thus, we will restrict ourselves here to only the nonsinglet part of the distributions. However, since then the complete matrix of the anomalous dimension in NLO has been calculated [226]. At the present we are performing a complete study of polarized and unpolarized structure functions for the bag model in NLO [234].

In LO it is found that for $R = 0.8\ fm$, $M_s = 0.55\ GeV$, $M_v = 0.75\ GeV$ and $\mu^2 = 0.0676\ GeV^2$, the unpolarized valence distribution of the proton in the bag model fits the MRS parametrization of the data. The result is displayed in Fig. 5.6 together with the bag model distribution at scale μ^2. The agreement is excellent, with no significant discrepancy. However, at such a low scale the coupling constant is $\alpha(Q^2 = \mu^2) = 2.66$. This is a rather large value (as found in ref. [150]), and raises doubts about the whole procedure.

In NLO the parameters used to fit the unpolarized valence distribution have the following values: $R = 0.8\ fm$, $M_s = 0.7\ GeV$, $M_v = 0.9\ GeV$ and $\mu^2 = 0.115\ GeV^2$. We notice that the radius for LO and NLO is the same but not the masses, being slightly bigger in the latter case. This is because in NLO one need not evolve as far, the scale μ^2 is larger and so the masses of the intermediate states need to be larger (the parton distributions peak at a larger x for smaller intermediate state masses). In Fig. 5.7 the NLO results are shown and again we see a very good agreement between the calculated valence distribution and the MRS parametrization of the data. What is remarkable now is the fact that the strong coupling constant drops to 0.77 at $\mu^2 = 0.115$ in NLO. Although this value is still large, it is much smaller than the LO case, making the evolution more reliable. Both LO and NLO moments are evolved to $Q^2 = 10\ GeV^2$.

Once we have determined the parameters of the model, we are in the position to calculate other quantities. In Fig. 5.8 we plot the polarized u valence distribution for the bag model

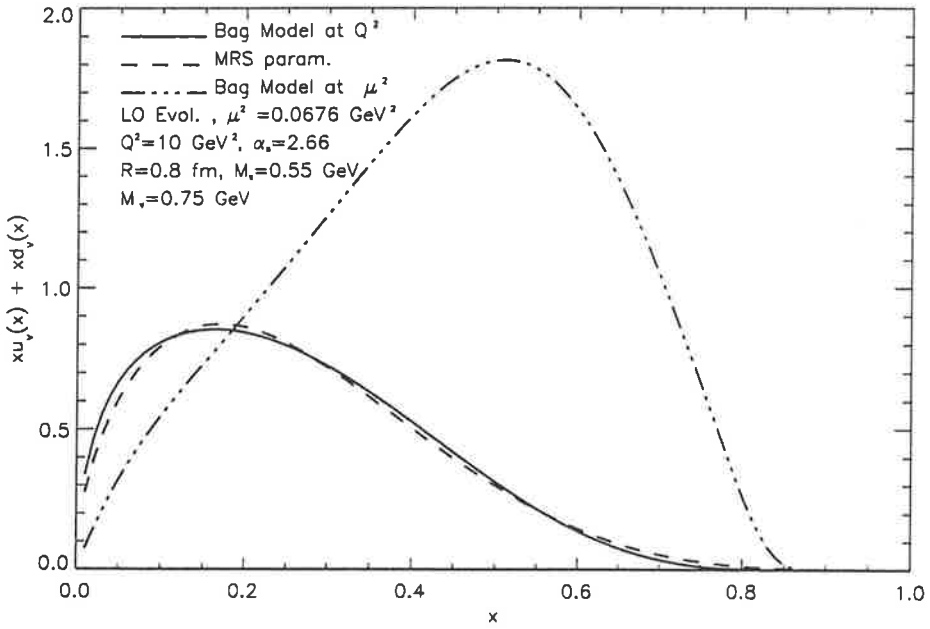

Figure 5.6: Total valence distribution in the bag compared with the MRS [233] parametrization of the data in the $\overline{MS}$ scheme. The quark distributions are evolved in LO QCD.

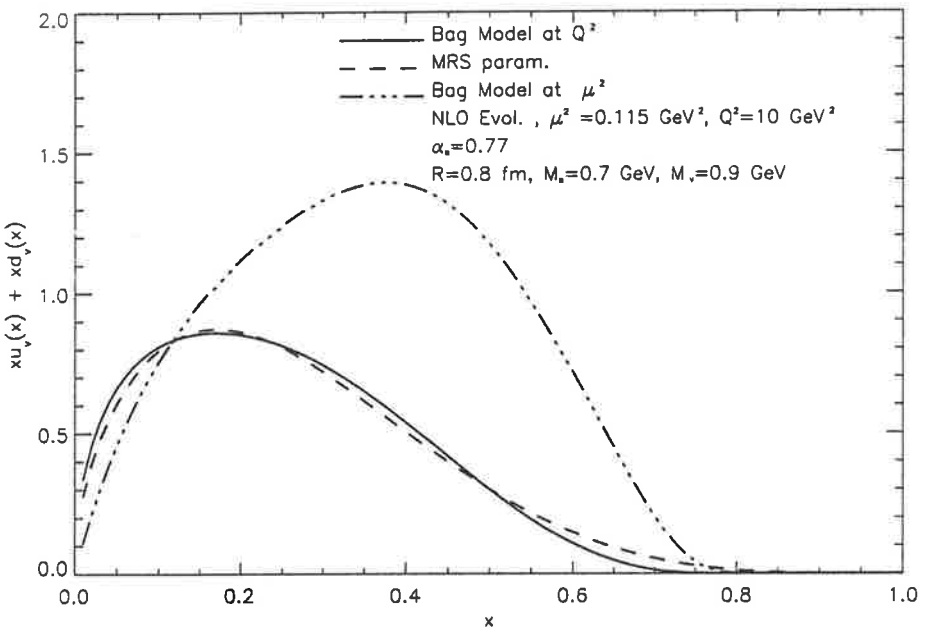

Figure 5.7: Total valence distribution in the bag compared with the MRS [233] parametrization of the data in the $\overline{MS}$ scheme. The quark distributions are evolved in NLO QCD.

in LO and NLO against some very recent experimental data [199]. There is no real difference between the LO and NLO curves (besides, of course, the parameters the parameters that generates each of them), hence we put both under the same line. Due to the large errors in the data it is impossible to conclude anything for the region $x \leq 0.1$. But for $x \geq 0.1$ the theoretical curves certainly have the correct behaviour. Moreover, the polarized valence distributions are pure nonsinglet and we might expect that the bag model would give, in this case, a description of the data as good as in the unpolarized case. This is because, as we discussed at length in the last chapter, the polarized distributions have a problem of interpretation in the parton/quark model language only for the singlet sector. The same considerations can be drawn from Fig. 5.9, where the polarized d valence distributions in LO and NLO are shown together with the data at $Q^2 = 10\ GeV^2$.

It is clear from the close agreement of the various quark distributions calculated in LO and NLO that the excellent results obtained in earlier studies [149, 150, 153] based on the bag model were reliable. That the di-quark masses required (700 and 900 MeV) were so close to the values expected in the model (600 and 800 MeV) is very reassuring. Furthermore, the strong coupling constant in NLO is small enough that one can be quite confident in the convergence of the calculation.

Of course we do not expect that the bag model alone contains all the physics we need because we know that mesons should play a role as well. For instance, we know [122] that chiral symmetry in the bag is restored through a meson cloud. Moreover, the meson cloud is already known to give important corrections to some sum rules [144, 105, 107, 112, 114]. Thus, it is imperative to perform a global analysis of the effects of the meson cloud in the polarized and unpolarized quark distributions.

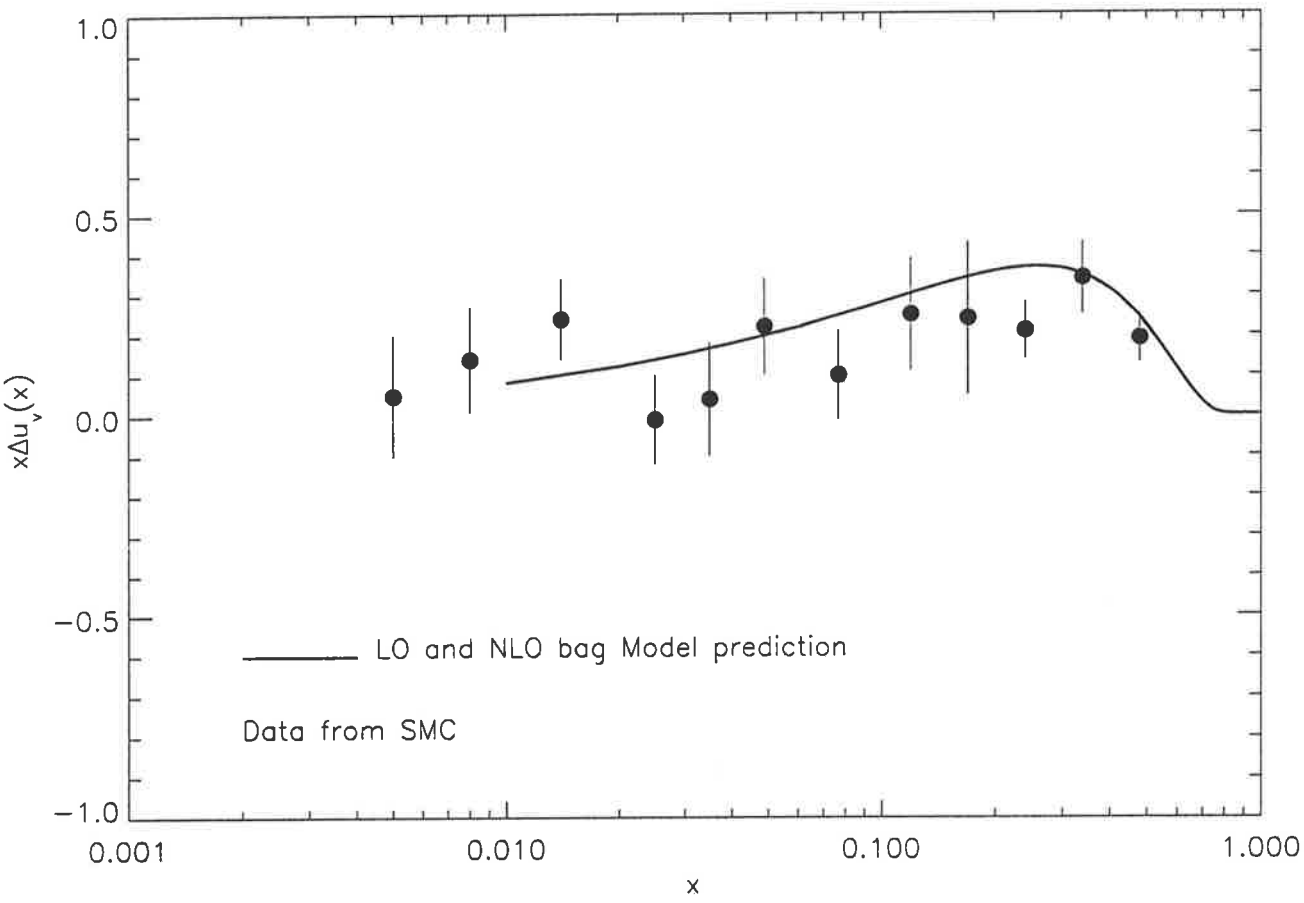

Figure 5.8: The polarized valence Δu_v quark distribution is evolved using LO and NLO QCD evolution.

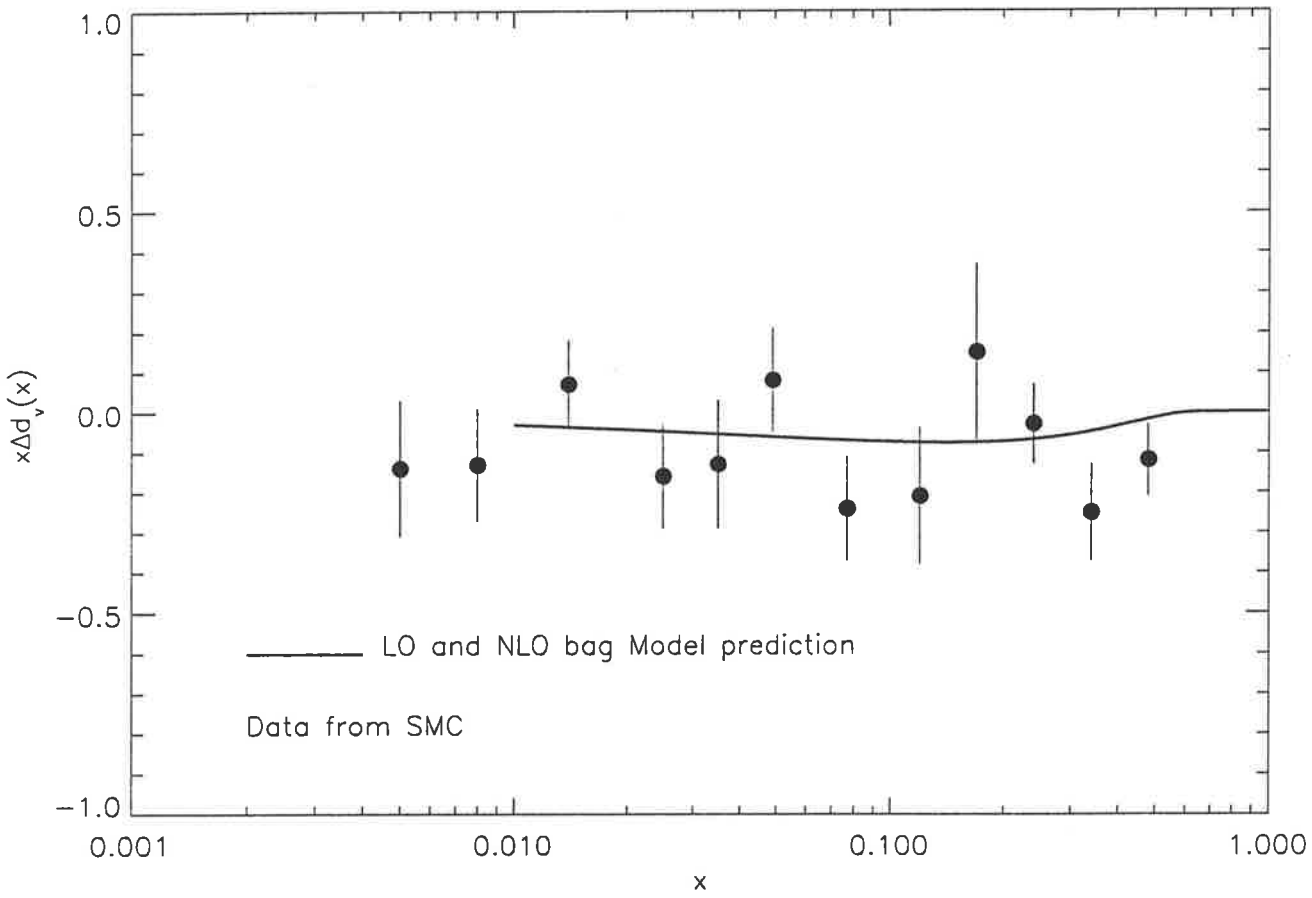

Figure 5.9: The polarized valence Δd_v quark distribution is evolved using LO and NLO QCD evolution.

5.4 Mesonic Corrections to the Shape of Quark Distributions

As important as it is to correct the integrated quark distributions, the study of the effect of the meson cloud on the x dependence of the quark distributions themselves is at least as important [153, 107, 106]. In this section we calculate the x dependence of the polarized and unpolarized quark distributions in the proton in a bag model dressed by mesons. We perform the calculations in NLO QCD for the nonsinglet part of the structure functions and in leading order for the singlet part for the same reasons explained in the last section. Moreover, we present for the first time[146] the x dependence of the combined effect of the N - Δ interference term [153] and one gluon exchange [232]. The interference term is important because, as noticed before [149, 150], in the Ellis-Jaffe sum rule it cancels part of the reduction coming from pions. As we shall see, the interference terms have a determinant role in the shape of the polarized quark distribution of the neutron.

We introduce mesons in the model through the Sullivan process [99], simply noting that there are unresolved questions about the model, particularly the validity of the impulse approximation [40]. The modern study of the mesonic contribution via convolution started with Thomas [98] and was later extended to the study of structure functions by the Adelaide group [105, 106, 112]. A problem remaining in these calculations is the freedom for the value of the cut-off in the form factor. To avoid this problem, we shall follow the approach of the Jülich group [235], where the cut-off is fixed through the use of high energy pp data.

The basic hypothesis in this sort of model is that the physical nucleon wave function (in the infinite momentum frame) can be written as a superposition of a few Fock states:

$$|N\rangle_{phys} = Z^{1/2}\left[|N\rangle_{bare} + \sum_{BM}\int_0^1 dx \int d^2k_\perp \phi_{BM}(x,k_\perp)|B(x,k_\perp), M(1-x,-k_\perp)\rangle\right]. \quad (5.59)$$

The wave function renormalization factor

$$Z = \left[1 + \sum_{BM}\int_0^1 dx \int d^2k_\perp |\phi_{BM}(x,k_\perp)|^2\right]^{-1}, \quad (5.60)$$

measures the probability that the physical nucleon contains a bare nucleon. The Fock states used in our calculation involve the low mass particles which are important to describe nucleon properties, namely the nucleon $SU(3)$ octet (N, Λ, Σ) and decuplet (Δ, Σ^*) and the first pseudoscalar and vector meson octet (π, K, ρ, ω, K^*). We have included the hyperon-kaon contributions for completeness, but their actual size is very small ($\sim 2\%$) [236, 112]

The Fock state expansion Eq.(5.59) has consequences for the structure function of the nucleon. Due to the presence of baryon-meson Fock states, the virtual photon can scatter either on the nucleon core or on the meson-baryon system. Formally, the quark distribution $q(x)$ of the nucleon is given by:

$$q(x) = Z\left[q^N_{bare}(x) + \sum_{BM}\left(\delta^M q(x) + \delta^B q(x)\right)\right]. \quad (5.61)$$

The contributions from the virtual meson and baryon can be written as the convolution of the meson (baryon) structure function with its longitudinal momentum distribution in the nucleon:

$$\delta^M q(x) = \int_x^1 f_{MB}(y) q^M\left(\frac{x}{y}\right)\frac{dy}{y} \qquad \text{and} \qquad \delta^B q(x) = \int_x^1 f_{BM}(y) q^B\left(\frac{x}{y}\right)\frac{dy}{y}, \quad (5.62)$$

where f_{MB} and f_{BM} are given by:

$$f_{MB}(x) = \int d^2k_\perp |\phi_{BM}(1-x,-k_\perp)|^2, \qquad \text{and} \qquad f_{BM}(x) = \int d^2k_\perp |\phi_{BM}(x,k_\perp)|^2. \quad (5.63)$$

In order to conserve charge and momentum, we have the following relation:

$$f_{BM}(1-y) = f_{MB}(y). \quad (5.64)$$

The functions $f_{BM}(y)$ and $f_{MB}(y)$ can be calculated using time ordered perturbation theory in the infinite momentum frame [112, 235, 110]. The analytic forms for $f_{BM}(y)$ and $f_{MB}(y)$, can be found in Refs. [112, 235].

In practical calculations we need more information, namely the various coupling constants and the vertex form factors G_{BM}. The coupling constants can be extracted from scattering experiments and are rather well known [237]. For the vertex form factor we use an exponential parametrization:

$$G_{BM} = exp\left[\frac{1}{2\Lambda_{BM}^2}(m_N^2 - M_{BM}^2(y,k_\perp^2))\right], \quad (5.65)$$

with

$$M_{MB}^2(y,k_\perp^2) = \frac{m_B^2 + k_\perp^2}{y} + \frac{m_M^2 + k_\perp^2}{1-y}. \quad (5.66)$$

The cut-off parameters Λ_{BM} can be estimated, using one boson exchange models, from n, Λ and Δ^{++} production in high energy pp scattering (for details see Ref. ([235])). They were found to be $\Lambda_{N\pi} = \Lambda_{N\rho} = 1.08\ GeV$ and $\Lambda_{\Delta\pi} = \Lambda_{\Delta\rho} = 0.98\ GeV$. The procedure used to obtain the cut-off parameters may be questioned because the assumption of single meson exchange being responsible for the process is fairly simple. However, it certainly gives an upper bound for the values of the various $\Lambda's$.

At this point we are still left without the input distributions in equations (5.61) and (5.62). For the quark distribution in the pion we use a recent parameterization by Sutton et al. [238]. By using $SU(3)$ symmetry, the quark distributions of all the mesons can then be obtained. For the bare quark distribution of the baryons we use the bag model calculation, discussed in the last section.

As before, we also use the MRS parametrization [233] of the unpolarized structure functions to fix the parameters of the model; e.g., the radius of the bag, the average masses M_s M_v of the intermediate state and the low scale, μ^2, at which the model is supposed to be valid. In Fig. 5.10 we show the total valence distribution computed in NLO in the $\overline{MS}$ scheme for the bag dressed with mesons. Very good agreement with the MRS parametrization is found for $\mu^2 = 0.165\ GeV^2$, $R = 0.8\ fm$, $M_s = 0.65\ GeV$ and $M_v = 0.85\ GeV$. Notice that this set of parameters, with the exception of the initial scale μ^2 is practically identical to the ones found in the last section, when only the bare bag was studied. The results for LO, showed in 5.11, have a set of parameters even more identical with the case of last section, with only the initial scale being higher when mesons are present. In this case, the coupling constant $\alpha_s(\mu^2)$ decreases from ~ 2.66 for the fitting for the bare bag to ~ 1.52 for the case where mesons are incorporated. For comparison, we also show in both figures 5.10 and 5.11 the bare bag calculated with the same set of parameters use to fit the bag dressed with mesons. It is also worth to call attention that there is a bonus from the use of a NLO fit, as it provides a decrease of α_s at μ^2 from ~ 1.52 in a LO fit to ~ 0.6 in NLO. This is also a decrease in comparison with the value $\alpha_s \sim 0.77$ found in a NLO fit without mesons, as obtained in the last section [206].

After we have fixed all parameters in the unpolarized deep inelastic scattering sector, we can explore the consequences for the polarized sector. The calculation of effects due to the presence of higher BM Fock states for the $g_1(x)$ structure function is similar to those for

$q(x)$ given in (5.61). The contribution from the scattering on the recoil baryon is:

$$\delta^B \Delta q(x) = \sum_M \int_x^1 d_{BM}(y) \Delta q^B \left(\frac{x}{y}\right) \frac{dy}{y}, \tag{5.67}$$

where $d_B(y)$ is the polarized, longitudinal momentum distribution. It can be calculated using the same techniques as for the unpolarized case (for details see [235]). The mesonic contribution vanishes because of the pseudoscalar character of the pion. The main difference from the unpolarized structure function is the presence of the N-Δ interference term [153], which can also be written as a convolution [235]:

$$\delta^{int} \Delta q(x) = \int_x^1 d_{int}(y) \Delta q^{N\Delta} \left(\frac{x}{y}\right) \frac{dy}{y}. \tag{5.68}$$

The necessary polarized splitting functions d_{BM} and d_{int} are:

$$d_{N\pi}(y) = \frac{g_{NN\pi}^2}{16\pi^2} \int_0^\infty dk_\perp^2 \frac{|G_{N\pi}(y,k_\perp^2|^2}{y^2(1-y)} \frac{m_N^2(1-y)^2 - k_\perp^2}{[m_N^2 - M_{N\pi}^2(y,k_\perp^2)]^2}, \tag{5.69}$$

$$\begin{aligned} d_{\Delta\pi}(y) &= \frac{g_{N\Delta\pi}^2}{96\pi^2} \int_0^\infty dk_\perp^2 \frac{|G_{\Delta\pi}(y,k_\perp^2)|^2}{y^4(1-y)m_\Delta^2} \\ &\times \frac{[(ym_N + m_\Delta)^2 + k_\perp^2][(y^2m_N^2 - m_\Delta^2)^2 + 8ym_Nm_\Delta k_\perp^2 - k_\perp^4]}{[m_N^2 - M_{\Delta\pi}^2(y,k_\perp^2)]^2}. \end{aligned} \tag{5.70}$$

and

$$\begin{aligned} d_{int}(y) &= \frac{g_{N\Delta\pi}g_{NN\pi}}{16\sqrt{6}\pi^2} \int_0^\infty dk_\perp^2 \frac{G_{\Delta\pi}(y,k_\perp^2)G_{N\pi}(y,k_\perp^2)}{y^3(1-y)m_\Delta} \\ &\times \left\{ \frac{-m_N(1-y)(ym_N + m_\Delta)^2(ym_N - m_\Delta)}{[m_N^2 - M_{\Delta\pi}^2(y,k_\perp^2)][m_N^2 - M_{N\pi}^2(y,k_\perp^2)]} \right. \\ &\left. + \frac{(2m_\Delta^2 + (3y-2)m_Nm_\Delta - ym_N^2)k_\perp^2 - k_\perp^4}{[m_N^2 - M_{\Delta\pi}^2(y,k_\perp^2)][m_N^2 - M_{N\pi}^2(y,k_\perp^2)]} \right\}. \end{aligned} \tag{5.71}$$

Combining all these contributions, g_1 for the nucleon is given by:

$$g_1^{phys} = Z\left[g_1^{bare} + \sum_{BM}\left(\delta^B g_1^B + \delta g_1^{int}\right)\right]. \tag{5.72}$$

We now apply Eqs. (5.67) - (5.72) to calculate $g_1(x)$. In the meson sector only the pseudoscalars are included. The vector mesons are omitted because we are not aware of any model to extract their polarized quark distribution functions. Once again we need a model for the bare quark distributions in the nucleon and, as before, we use the MIT bag model. For the polarized case we need to specify the spin-flavor part of the wave function. We shall use the usual $SU(6)$ wave function in which case, for the interference terms, we have:

$$\langle p^\uparrow, n^\uparrow | u^{\uparrow\uparrow} u^\uparrow | \Delta^{+,\uparrow}, \Delta^{0,\uparrow}\rangle = \langle p^\uparrow, n^\uparrow | d^{\uparrow\downarrow} d^\downarrow | \Delta^{+,\uparrow}, \Delta^{0,\uparrow}\rangle = \frac{\sqrt{2}}{3}, \tag{5.73}$$

$$\langle p^\uparrow, n^\uparrow | u^{\uparrow\downarrow} u^\downarrow | \Delta^{+,\uparrow}, \Delta^{0,\uparrow}\rangle = \langle p^\uparrow, n^\uparrow | d^{\uparrow\uparrow} d^\uparrow | \Delta^{+,\uparrow}, \Delta^{0,\uparrow}\rangle = -\frac{\sqrt{2}}{3}. \tag{5.74}$$

We notice that in the matrix elements (5.73) and (5.74) only mixed symmetric terms contribute and, as a consequence, the intermediate state always forms a spin vector.

The first moment of the polarized structure function for the proton, $g_1^p(x)$, is expressed in NLO as:

$$\int_0^1 g_1^p(x,Q^2)dx = \left(\frac{g_a}{12} + \frac{g_8}{36}\right)\left(1 - \frac{\alpha_s(Q^2)}{\pi}\right) + \frac{\Delta\Sigma}{9}\left(1 - \frac{\alpha_s(Q^2)}{3\pi}\right), \tag{5.75}$$

with g_a and g_8 nonsinglet distributions and $\Delta\Sigma$ a singlet distribution, as seen before, Eq. (4.2). However, the full singlet anomalous dimensions (for any moment) for polarized scattering in NLO was not known at the time of this work [146] and, because of that, it was not possible to calculate the x dependence of $\Delta\Sigma$ in NLO. Faced with this problem, we decided to take the following two approaches to the evolution of g_1:

• In the first approach, **case (a)**, we evolved g_a and g_8 as nonsinglet in NLO and $\Delta\Sigma$ as a singlet in LO so that g_0 did not pick up the $(1-\frac{\alpha_s(Q^2)}{3\pi})$ correction and the whole structure function was overestimated.

• In the second approach, **case (b)**, we treated g_a, g_8 and $\Delta\Sigma$ as nonsinglet combinations and evolved them in NLO. In this case, $\Delta\Sigma$ picked up a correction of the form $(1-\frac{\alpha_s(Q^2)}{\pi})$ such that the corrections due to the NLO evolution were over estimated and the structure function were underestimated. The actual curve must be somewhere between the two approaches.

In Fig. 5.12 we show the EMC and earlier SLAC data for $xg_1^p(x)$ together with the bare bag, the bag plus mesons but without the N-Δ mixing terms and the bag plus mesons plus mixing terms. We stress that the parameters for the bare bag differ significantly from those used in earlier calculations [150]. The meson cloud lowers the bag model prediction over the entire range of x, in accordance with earlier estimates for the Ellis-Jaffe sum rule in the bag [144]. This is because some of the spin of the nucleon is carried as angular momentum by the mesons. The actual value of the calculated Ellis-Jaffe sum rule at 10 GeV^2drops from 0.209 in the bare bag to ~ 0.173 in the bag plus mesons for case (a) and to ~ 0.169 for case (b). The actual value of the sum rule in the bag model plus mesons, calculated using Eq. (5.75) as it stands, is ~ 0.171, supporting our claim that the full NLO prediction for the x dependence of $g_{1p}(x)$ in the present model is somewhere between the results for case (a) and (b) of Fig. 5.12. The inclusion of vector mesons is expected to reduce the value of the sum rule somewhat more. We further show in Fig. (5.13) the predictions of this model for $g_1^p(x)$ for the LO evolution. The results are of high quality, comparable with the NLO case.

The x dependence for the model, compared with the SLAC E143 data [64] for $g_1^p(x)$, is shown in Fig. 5.14, and is quite impressive. This data was taken at an average 3 GeV^2 and has smaller error bars than earlier experiments. Comparison with this set is also a good test of our model once we have to move to a different Q^2. The resulting agreement between

theoretical and experimental values for $g_1(x)$ is inspiring and provides some confidence in the model. At this value of Q^2 the calculated value for the Ellis-Jaffe sum rule is ~ 0.171 for case(a) and ~ 0.166 for case (b). We also show in Fig. (5.15) the results for the LO evolution.

These results shed light on how the spin in the physical proton is shared, suggesting strongly that mesons are responsible for part of the dilution of the spin. In general, we can say that the agreement between the data and the theoretical calculation is very impressive and that further corrections might well bring the entire curve within experimental errors. For instance, we show in Fig. 5.16 the bag model prediction of Fig. 5.12 against some experimental data and the anomalous gluon contribution for the case of 3 and 4 flavors from section 4.3.5. We notice that the integral over x of the valence contribution calculated here (~ 0.169) is in complete agreement with the estimates calculated previously in the last chapter. The two curves below the origin, are the anomalous contributions that should be added to the solid curve for N_f =3 or 4. As we fixed the normalization of the total polarized glue for either 3 or 4 flavors, there is no noticeable difference between the two cases. We see that the anomalous contribution is potentially important to correct the x dependence of the polarized valence distribution inside the proton. Of course the procedure is not completely consistent because the model calculation and the anomalous gluon were made in different schemes, although the situation is not as bad as it looks if one follows the discussion after Eq. (4.50) of last chapter. A proper procedure would be to calculate the quark distribution, the anomalous dimensions and the Wilson coefficients in the same scheme. The transformation that takes these quantities from the $\overline{MS}$ where they were calculated [226] to a scheme where the gluon does contribute (like the one of last chapter) is underway and the complete results for a consistent bag model calculation will be presented elsewhere.

We would also like to call attention to the role of the N-Δ mixing term. As said before,

it tends to increase the Ellis-Jaffe sum rule. In fact, if the mixing terms were absent, the new value of the sum rule at $Q^2 = 10\ GeV^2$ would be ~ 0.159 for case (a) and ~ 0.155 for case (b). For the Q^2 compatible with the SLAC E143 data, these values would be reduced to ~ 0.158 for case (a) and to ~ 0.152 for case(b). Figures 5.12 and 5.14 tell us that the rise of $g_1^p(x)$ due to the mixing terms is confined to the region $x \leq 0.3$. This is because for the mixing term, the mass of the intermediate state is always M_v, and then the contribution is isolated at smaller x when compared with the other contributions (similar to the down quark distribution in the bag [150]).

The most interesting effect associated with the mixing terms can be observed in Fig. 5.17, where $g_1^n(x)$ is shown. Although in $g_1^p(x)$ the effect of the mixing terms in the x distribution is not too dramatic because one is adding a small number to a large number, in $g_1^n(x)$ the effect is relatively large because one is subtracting from numbers near to zero. In fact, for $g_1^n(x)$ the mixing terms are essential to give to the theoretical curve the shape of the experimental data as measured by the SLAC E142 [54] experiment. The first moment of the calculated polarized distribution of the neutron turns out to be ~ 0.004 for case (a) and ~ -0.003 for case (b). In Fig. (5.18), the results for $g_1^n(x)$ in LO are shown and in this case, again because the numbers involved are so small, it is possible to see some small advantage in the use of NLO evolution over LO. It is also worth noticing that there is a consistency between the calculation of $g_{1p}(x)$ and $g_{1n}(x)$ - the same calculation that fits the unpolarized data also makes a good prediction for both $g_{1p}(x)$ and $g_{1n}(x)$.

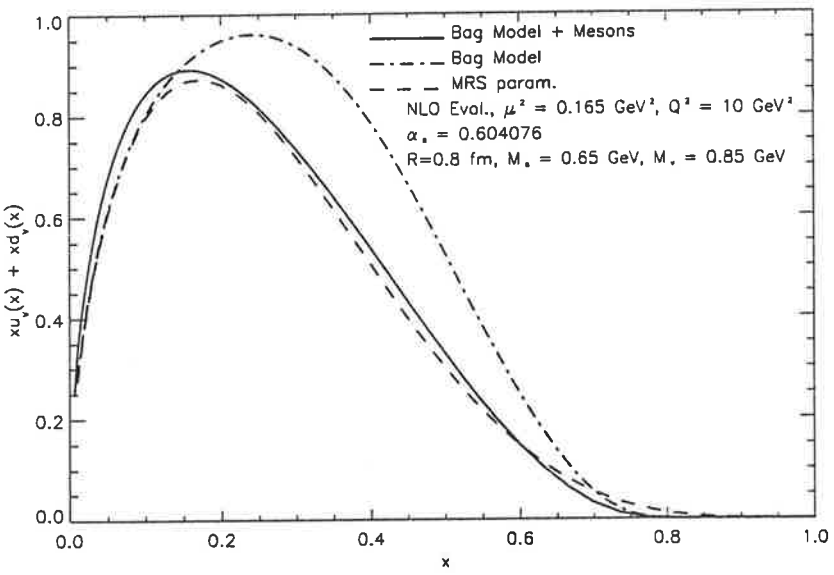

Figure 5.10: Total valence distribution in the bag and in the bag dressed with mesons compared with the MRS [233] parametrization of the data in the $\overline{MS}$ scheme. The quark distributions are evolved in NLO QCD.

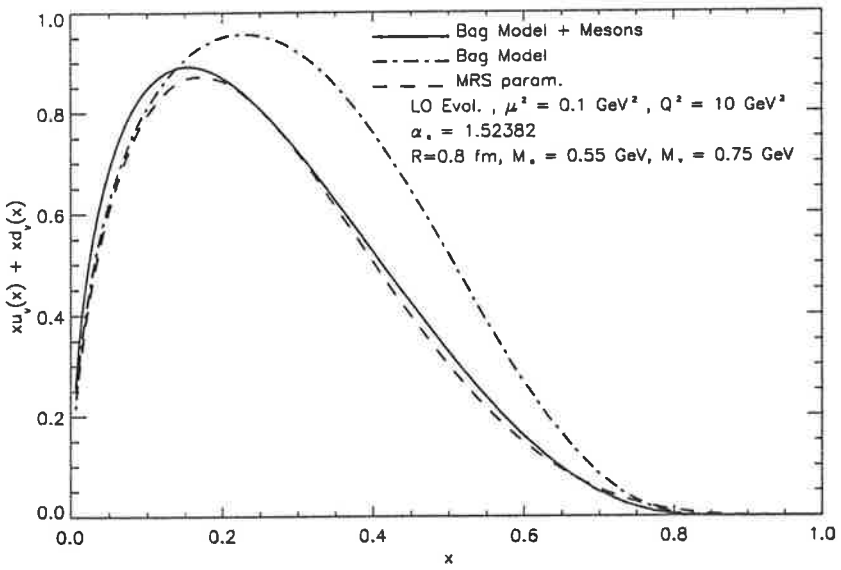

Figure 5.11: Total valence distribution in the bag and in the bag dressed with mesons compared with the MRS [233] parametrization of the data. The quark distributions are evolved in LO QCD.

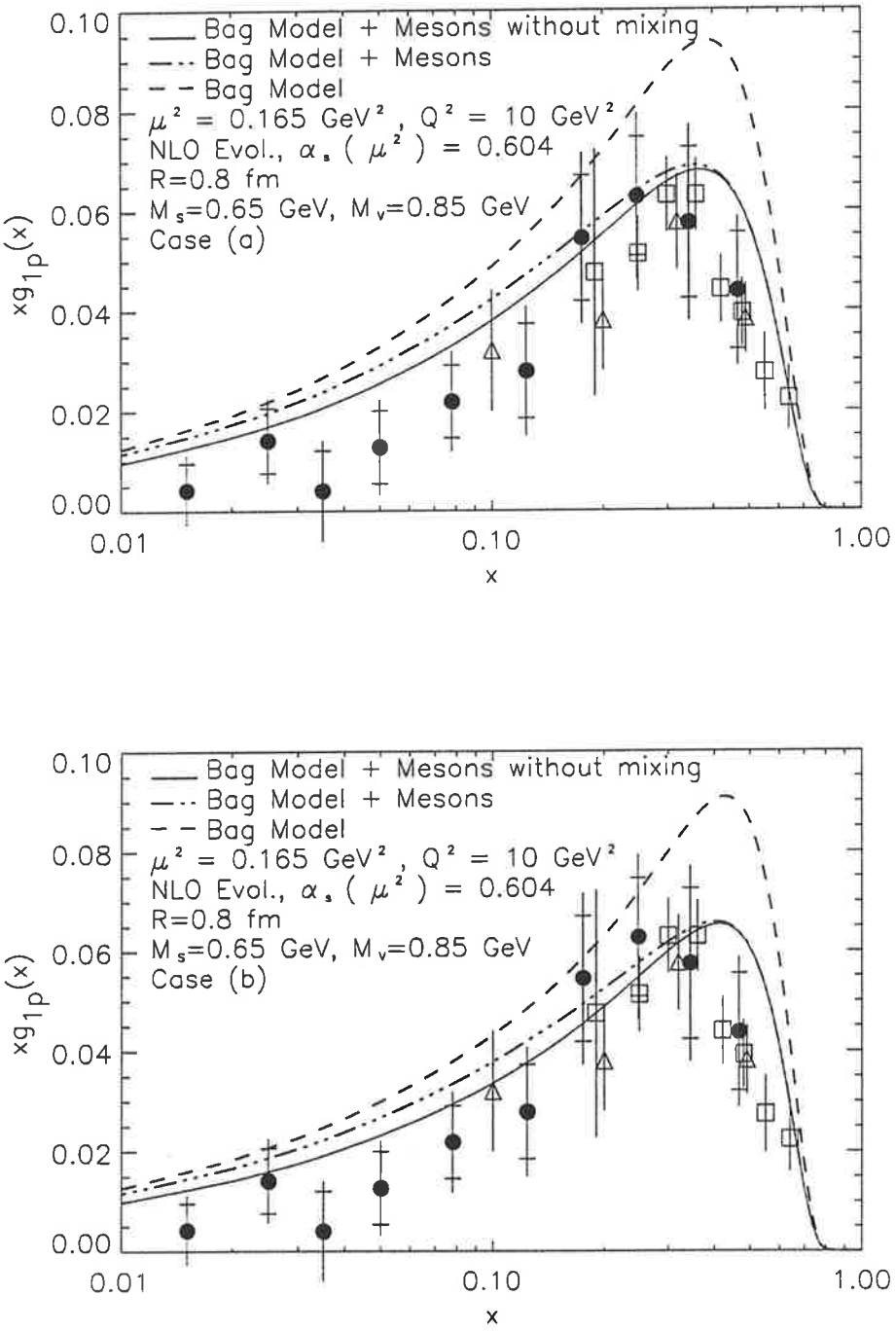

Figure 5.12: Polarized quark distribution of the proton as measured by the EMC collaboration [20] against NLO theoretical predictions for a bare bag, a bag with mesons without mixing terms and a bag with mesons and mixing terms.

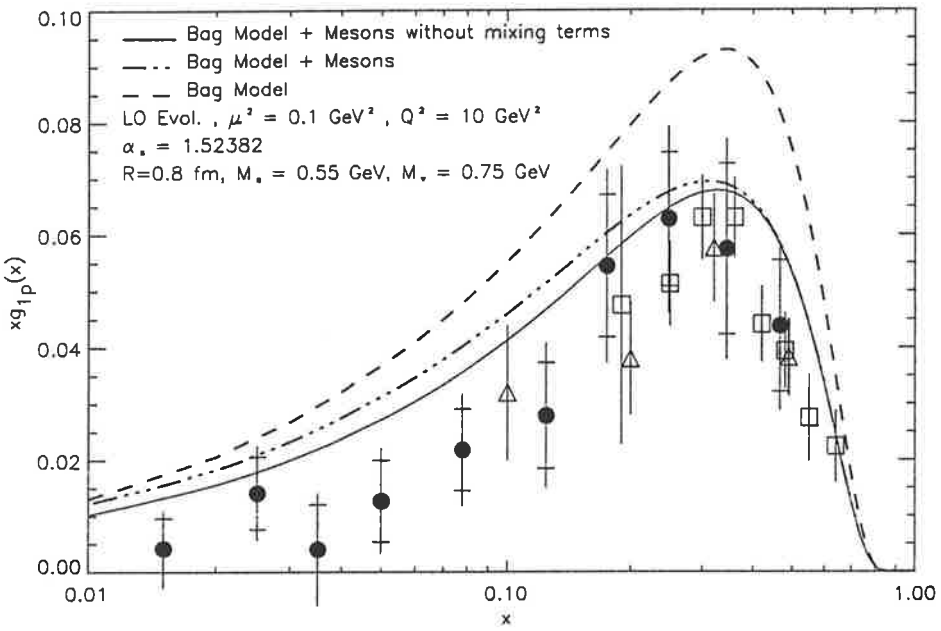

Figure 5.13: Polarized quark distribution of the proton as measured by the EMC collaboration [20] against LO theoretical predictions for a bare bag, a bag with mesons without mixing terms and a bag with mesons and mixing terms.

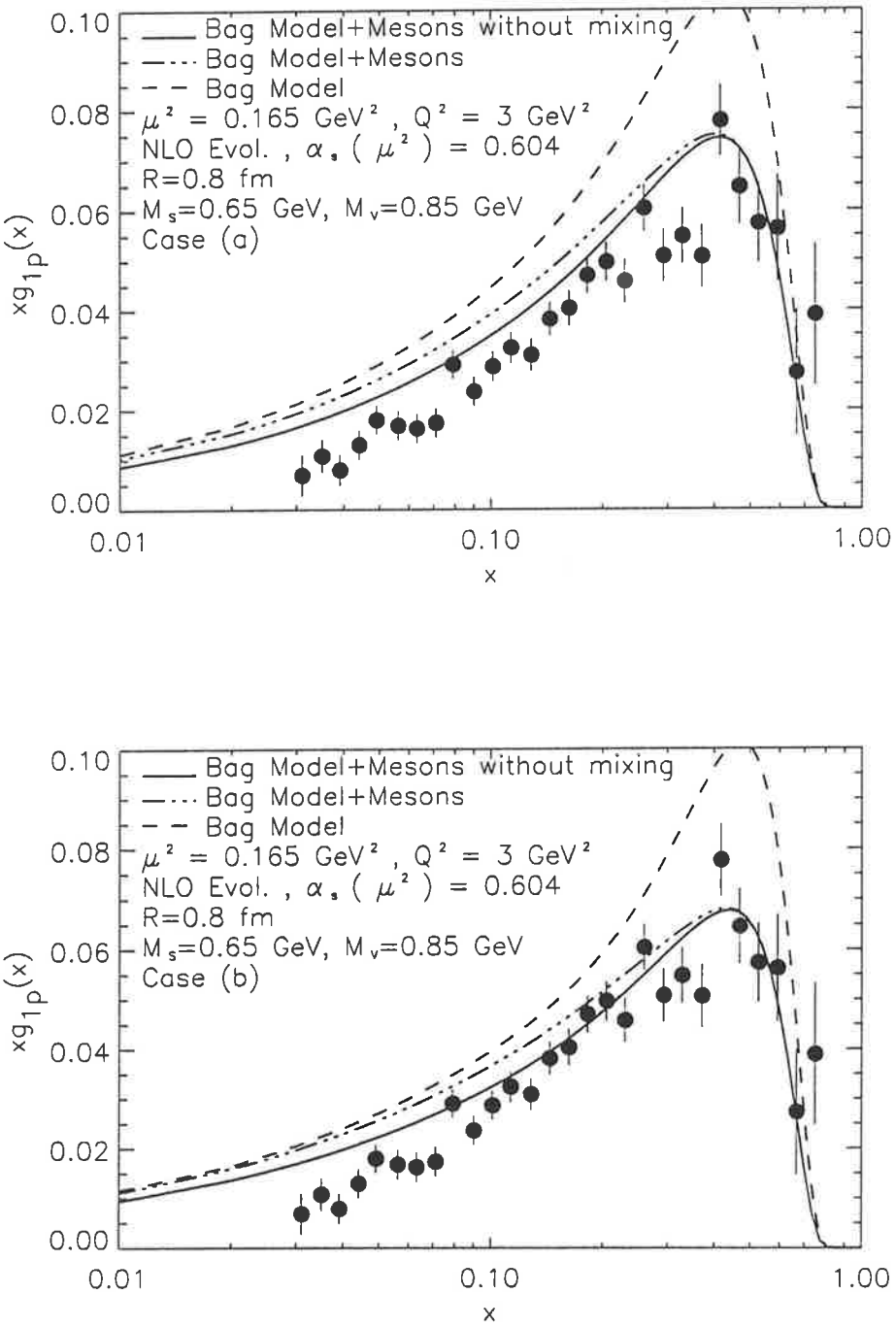

Figure 5.14: Polarized quark distribution of the proton as measured by the SLAC-E143 experiment [64] against NLO theoretical predictions for a bare bag, a bag with mesons without mixing terms and a bag with mesons and mixing terms.

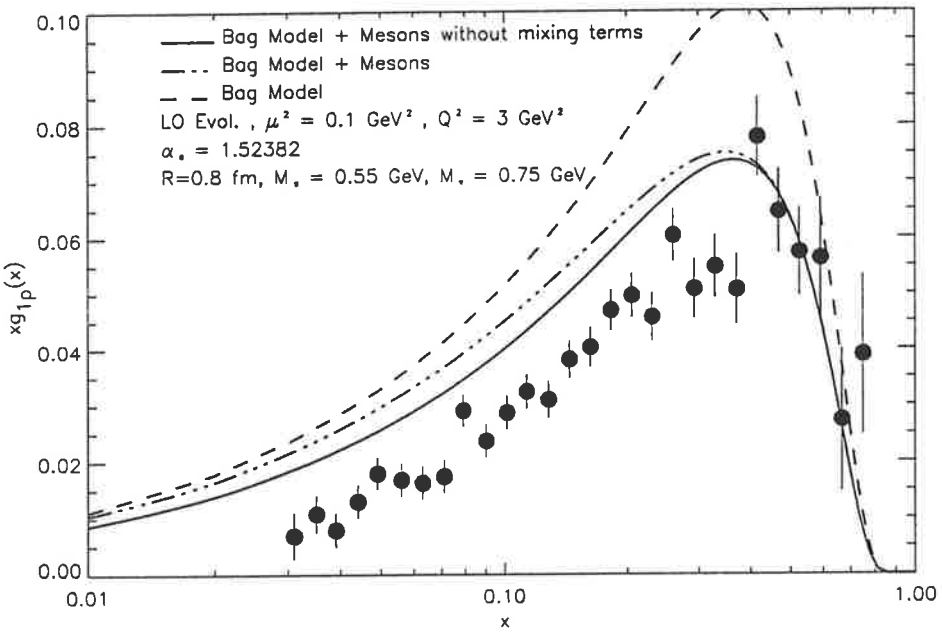

Figure 5.15: Polarized quark distribution of the proton as measured by the SLAC-E143 experiment [64] against LO theoretical predictions for a bare bag, a bag with mesons without mixing terms and a bag with mesons and mixing terms.

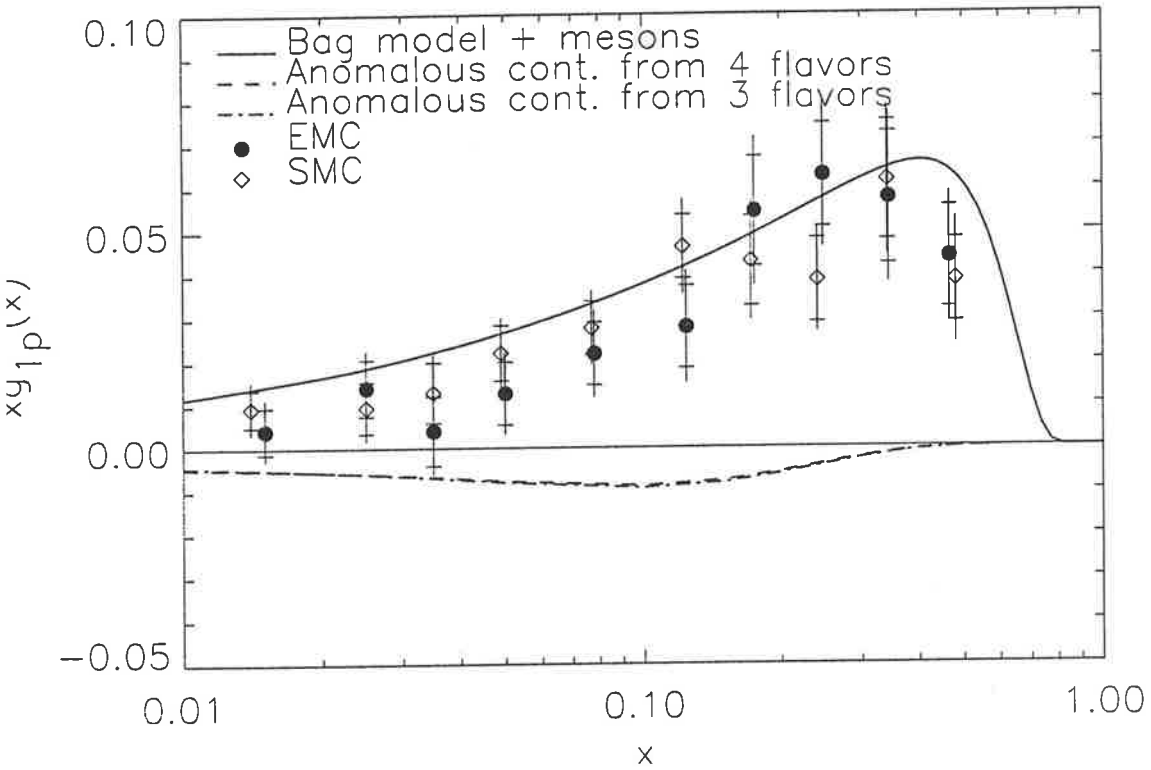

Figure 5.16: EMC [20] and SMC [52] data for $g_{1p}(x)$ at 10 GeV^2. The theoretical curve for the polarized valence distribution is calculated in NLO. The anomalous contribution is to be subtracted from the theoretical curve.

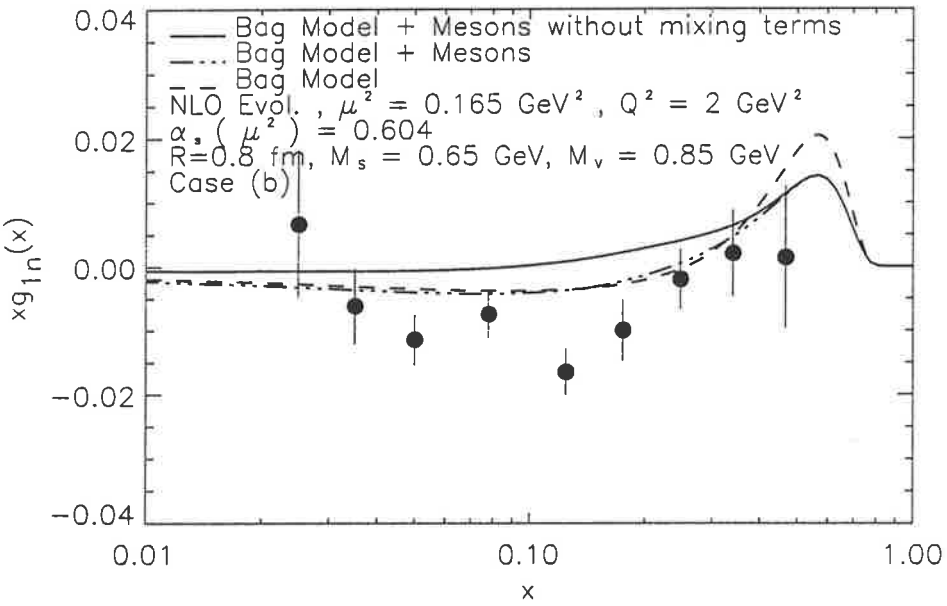

Figure 5.17: Polarized quark distribution of the neutron as measured by the SLAC-E142 experiment [54] against NLO theoretical predictions for a bare bag, a bag with mesons without mixing terms and a bag with mesons and mixing terms.

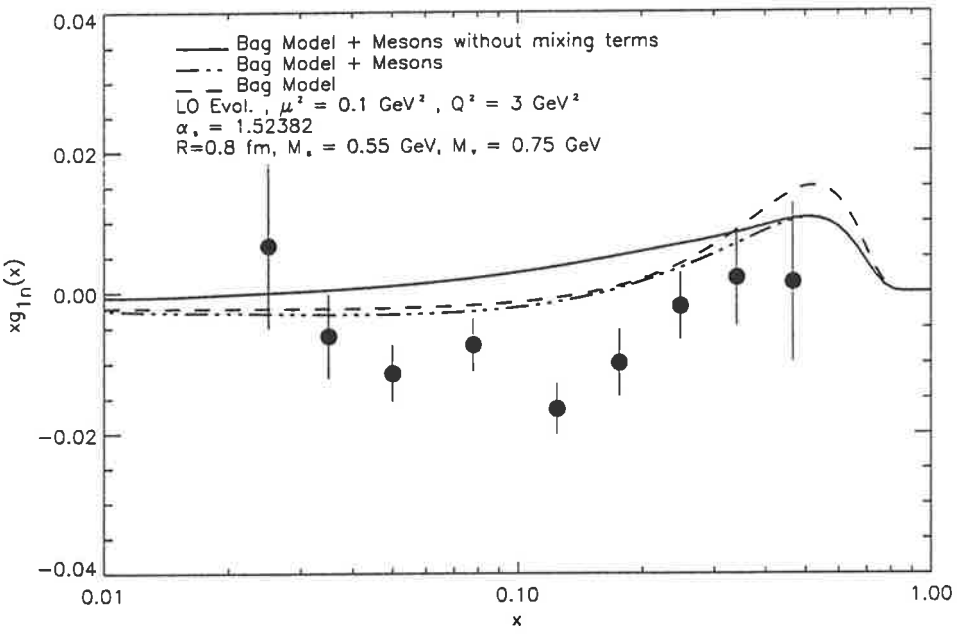

Figure 5.18: Polarized quark distribution of the neutron as measured by the SLAC-E142 experiment [54] against LO theoretical predictions for a bare bag, a bag with mesons without mixing terms and a bag with mesons and mixing terms.

Chapter 6

Summary and Outlook

We have studied a few different aspects of the nucleon structure, but our main concern was to study how the quarks are distributed inside the proton. In particular, we paid attention to the flavour of the sea, the spin content carried by quarks and gluons and how these, polarized and unpolarized quarks, are classified according to the momentum fraction of the proton that they carry.

In the flavour structure of the sea chapter, we analyzed two of the main experiments in the area, the NMC and NA51 experiments. It has been generally assumed that the NMC result implies in an asymmetry in the sea ($\overline{d} > \overline{u}$). This conclusion comes from two main observations: the Pauli principle allows more antiquarks of the type $\overline{d}$ than of the type $\overline{u}$ be created [96] and pion emission leds naturally to an excess of π^+ over any other pion thus providing more $\overline{d}$ than $\overline{u}$ [98]. However, at the moment there is not a complete explanation for the NMC result because pions alone, and even with Pauli blocking effects included [106], are not able to provide results that match the value of the measured Gottfried sum rule, its x dependence and what is known from other sources about the sea

quarks and gluon distributions [114]. A consistent picture for the sea is then still an open question and should be attacked. In any case, the second experiment, the NA51, was carried out to clearer a possible theoretical possibility [103] which says that in the region that the NMC made its measurement, the sea is symmetric ($\overline{d} = \overline{u}$) and that the deficiency in the value of the Gotfried sum rule has its origins in a very small, unmeasured, x region. The NA51 collaboration measured a $p - n$ Drell-Yan asymmetry and from it concluded that the sea is strongly asymmetric, in favour of $\overline{d}$, at $x = 0.18$. In our study on the subject, we concluded that, as a matter of fact, if one includes charge symmetry breaking effects, there are important corrections to the value of the ratio $\overline{d}/\overline{u}$. In practice, we estimated that this ratio could be corrected by as much as 20% if charge symmetry breaking of order of 10% were present at a particular x, even if the integrated value (in x) of this breaking is zero. However, our results are not entirely consistent because to derive our results, we had to use quark parametrizations that do not included charge symmetry breaking. Thus, it would be extremally interesting, although difficult, to construct parametrizations that include the above mentioned breaking. On the other hand, our analyses indicate that it is a urgent matter to find a theoretical (and experimentally feasible) way to separate charge symmetry breaking between the proton and the neutron from isospin breaking in the proton sea [239]. Until this question is solved, it looks impossible to be sure of any conclusions regarding the flavour of the sea.

We mentioned before that the Pauli principle and pion effects are the candidate mechanisms to explain the NMC and NA51 experiments. However, our study of chapter 3 showed that one should be cautious about them, mainly if one tries to use the Pauli principle in the $q\overline{q}$ pair production in the sea. Naively, as suggested by Field and Feynman, it would be easy for the gluon decay into a $d\overline{d}$ pair than into a $u\overline{u}$ in the proton. We concluded that this is indeed the case if graphs containing interference between sea and valence quarks are

excluded. As they should be included, it seems that the Pauli principle naive expectation is not supported when dealing with gluons. We proceeded and studied this antisymmetrization effects in the case of pion emission. Fortunately, it appears that the terms where they contribute can be safely neglected, although a more general and systematic study of this effect is called for.

The discussion on the proton spin has been hot and full of controversies along the last few years. There are a few myths about it that has been perpetuated in the literature. One of the myths, is that the spin carried by quarks was measured and it was (is) small. We tryed over chapter 4, based on some few earlier works [21, 129] and our own developments, to establish once more that the spin fraction carried by quarks is still not experimentally known. What is known, and by now rather well, is the value of the singlet axial charge of the proton. To extract from it the fraction of spin carried by quarks, we also should know the amount of polarized gluon inside the proton. What brings us to a second myth, or quasi-myth, which says that the gluon polarization enter in a equation with the same multiplicative factor for the three light quarks and that it does not contribute for charm of other heavier quarks. We showed that this approach can be misleading and one should be careful to not excluded charm corrections in the present energy scales. This conclusion can be reached if the Wilson coefficient for the gluon is calculated in a scheme where chiral symmetry is not broken and the quark mass terms are fully kept. We then showed that in the usual infinite momentum transfer assumption, the gluon term fails to give to the three light quarks the same contribution, and the charm quark (as well as the b quark, although not shown explicitly in our discussion) gives a very significant contribution for many reasonable renormalization scales used. If the infinite momentum transfer assumption is dropped, as it should be, and we perform the calculations suitable to the scales of the present experiments, we still have a reasonable charm contribution as well as a strange quark contribution different

from both the u and d quarks. Then, we estimated the amount of polarized gluon necessary to fit the measured singlet axial charge to naive expectations for the spin fraction carried by quarks. We saw that a proper treatment of the gluon term can change Δg by 50% ! This is extremely important because Δg will be soon measured [200, 201], and if a proper calculation for the gluon term is not used, one could get a wrong value for the spin fraction of the proton carried by quarks. Thus, the future measurement of Δg is one of the most important facts in hadron physics in the next few years. Even its sign is not know and much of the evidence, as presented by us in this thesis, suggests that it is positive. However, in a recent calculation Jaffe [241] concluded that Δg in various nucleon models is negative. Moreover, he concludes that the sign of the polarized gluon is directly related to the $N - \Delta$ splitting: a negative Δg results from the fact that the Δ is heavier than the nucleon. If Δg were positive, the Δ would be lighter than the nucleon. His conclusions are supposed to be valid at the scale of the model. If QCD evolution or (in his calculations) the omission of gluon self interactions do not change the sign of Δg, one would be forced to accept a negative Δg, in which case the we would have a huge problem with the proton spin. On the other hand, even the connection between the sign of Δg and the baryon spin splitting used by Jaffe, has been challenged by another recent calculation. In a study of lattice QCD, K. F. Liu [242] calculated some hadron properties in a valence approximation, where one gluon exchange is not switched off. He found that the nucleon and the Δ were degenerate, in contradiction with the many nucleon model calculations where one gluon exchange is used to justify the baryon spin splitting. Thus, this is a completely open subject which may still present many useful insights both in the perturbative structure of proton as well as in the models for it.

Late in chapter 4, we showed that a large fraction of the gluonic corrections are inside of the x range currently being measured. However, to perform this calculation, we had to

keep higher order twist effects as terms of the form m_q^2/Q^2 could be important. On the other hand we kept the full result only to order α_s. Terms of higher order in α_s could be important and we do not know of any obvious way to estimate them at the present. But supposing that the coupling constant is small enough, the corrections omited are likely to be small. In any case, this study showns how important mass effects can be in the energy region of the present experiments. A complete study of mass effects, where the proton and quark masses are included, in the polarized structure functions is necessary and is one more possible extension of this work.

To add to the discussion of whether or not the gluons contribute to the first moment of the spin structure function, g_1, we completed chapter 4 with a section where it was shown that this discussion is, ultimately, a discussion on the choice of a renormalization scheme. One just should be careful to not identify terms with the same apparent form with the same physical significance. In this sense, the defined quark distribution in the renormalization scheme that can be identified with spin is different from a defined quark distribution in a renormalization scheme that breaks chiral symmetry and thus cannot be identified with spin in accord with the discussion of last paragraph and the whole chapter 4.

Finally, the study of the x dependence of the quark distributions and structure functions rendered precious results. First, it reconfirmed a simple model like the MIT bag as a good guide to the study of quark distributions. Of course, the model has its limitations as already reasoned in chapter 5. Maybe the two main points against it, are the large coupling constant necessary to fit the data and its known bad predictions for the unpolarized gluon distributions. The first of them, we attacked in this thesis where it was shown that the inclusion of NLO corrections alone are enough to bring the coupling constant to more acceptable standards. This is a very important result when we remind the reader that previous calculations used $\alpha_s(\mu^2) \sim 2.66$ and here we brought this value down to $\alpha_s(\mu^2) \sim 0.77$. As

a immediate result, it can be said that the evolution procedure now is more trustworthy. The second problem, the one related to the gluon deficiency in the model, being presently accessed where NLO corrections for the singlet evolution of the quark distributions are being incorporated in the evolution program [234]. This is the first time that a complete NLO evolution study is being done for a model for the nucleon. Although these corrections will probably improve the results for the gluon sector, it should be kept in mind that they are not likely to improve totally the situation as the LO evolution results in a gluon distribution around 50% below what is expected experimentally. There should be some gluon at the initial scale. The same conclusion is reached if one tries to build a parametrization for the parton distributions which is valid at a low scale [187, 231]. This would be an interesting extension of the model where a gluon term is to be incorporated perturbatively in the bare quark wave function of the nucleon, similar to the case where the pion was incorporated in a perturbative fashion to the bare nucleon in chapter 3. The new distributions should be more realistic but the calculation of the gluon distribution itself would be troublesome. In any case, we used the results from the MIT bag as they stand now and calculated, besides the already mentioned NLO corrections for the nonsinglet sector, what would be the effect of meson dressing of the proton (and neutron) on the quark distributions. The result is rewarding and, once more, it shows the important role of mesons taking some of the spin in the form of the orbital angular momentum. The effect on the proton and neutron spin structure function is very positive, with a very good agreement between data data and model for $x > 0.1$, where it was expected to be valid. We remind the reader again that these are *predictions* of the present calculations. Moreover, the meson dressing when spin is involved allows for extra terms coming from mixing between nucleon and delta states. These extra terms are essential to give the neutron spin structure functions the correct shape.

Many important subjects were left out in our study. Notably, we only mentioned some

general proposals for the behaviour of the polarized distributions in the region of small x. More attention should be devoted to this area in the future as it may give important clues on the nonperturbative structure of the Pomeron and, hence, the proton itself. We also did not discuss the semi-inclusive experiments which are extremely important to get information on the polarized valence quarks, sea quarks and gluons, separately. The list goes on. Nevertheless, we think that this shows how broad this subject is and how exciting it has proven itself in the last few years. Five years ago, the sea was generally thought flavour symmetric. Today, we have many ideas to explain why it should not be. The spin of the proton carried by quarks was thought to be zero and the neutron and deuteron spin structure functions were only speculations. Today, we are clearer that we do not know the amount of spin carried by quarks and the speculation now is about the polarized gluon and sea distributions as well as the small x region of the structure functions. The large numbers of experiments being carried now or planned for the near future show the vitality of the subject [200, 201, 243, 244]. As stated in the introduction, the study of hadron structure is the last one in a long tradition to unveil the structure of matter. Its achievement, the understanding of how the proton (and hadrons in general) is built, how it shares its properties among its constituents, is a reward not only for particle and nuclear physicists, but for the whole physics community.

Appendix A

Anomalous Dimensions and Wilson coefficients

The coefficients appearing in the expansion of the beta function were calculated in Refs. [12, 13, 14, 221] and up to two loops they are independent of the scheme. They are common to both polarized and unpolarized scattering and their form are:

$$\beta_0 = \frac{11C_A - 4T_R N_f}{3}, \tag{A.1}$$

$$\beta_1 = \frac{34}{3}C_A^2 - 4\left(\frac{5}{3}C_A + C_F\right)T_R N_f. \tag{A.2}$$

For the case of $SU(3)_c$, $C_F = \frac{4}{3}$, $C_A = 3$ and $T_R = \frac{1}{2}$. We now list the anomalous dimensions calculated in one and two loops in perturbative QCD.

A.1 Unpolarized Scattering

A.1.1 Leading Order case

The nonsinglet anomalous dimension is [12, 13, 14]:

$$\gamma_{NS}^{(o)n} = 2C_F \left[4S_1(n) - 3 - \frac{2}{n(n-1)} \right]. \tag{A.3}$$

The matrix elements of the singlet anomalous dimension are [12, 13, 14]:

$$\gamma_{qq}^{(0)n} = \gamma_{NS}^{(0)n}, \tag{A.4}$$

$$\gamma_{qg}^{(0)n} = -8T_R \frac{n^2+n+2}{n(n+1)(n+2)}, \tag{A.5}$$

$$\gamma_{gq}^{(0)n} = -4C_F \frac{n^2+n+2}{n(n+1)(n-1)}, \tag{A.6}$$

and

$$\gamma_{gg}^{(0)n} = 2C_A \left[4S_1(n) - \frac{11}{3} - \frac{4}{n(n-1)} - \frac{4}{(n+1)(n+2)} \right] + \frac{8}{3} T_R. \tag{A.7}$$

The function $S_1(n)$ can be obtained from the general function $S_i(n)$:

$$S_i(n) = \sum_{j=1}^{n} \frac{1}{j^i}, \tag{A.8}$$

A.1.2 Next to Leading Order Case

The nonsinglet anomalous dimension in the $\overline{MS}$ scheme is [221]:

$$\begin{aligned}
\gamma_{NS}^{(1)n} &= (C_F^2 - \frac{1}{2}C_F C_A)\left\{16S_1(n)\frac{2n+1}{n^2(n+1)^2} + 16\left[2S_1(n) - \frac{1}{n(n+1)}\right][S_2(n) - S_2'\left(\frac{n}{2}\right)]\right. \\
&\left. +64\tilde{S}(n) + 24S_2(n) - 3 - 8S_3'\left(\frac{n}{2}\right) - 8\frac{3n^3+n^2-1}{n^3(n+1)^3} - 16\eta\frac{2n^2+2n+1}{n^3(n+1)^3}\right\} \\
&+C_F C_A\left\{S_1(n)\left[\frac{536}{9} + 8\frac{2n+1}{n^2(n+1)^2}\right] - 16S_1(n)S_2(n)\right. \\
&\left. +S_2(n)\left[-\frac{52}{3} + \frac{8}{n(n+1)}\right] - \frac{43}{6} - 4\frac{151n^4+263n^3+97n^2+3n+9}{9n^3(n+1)^3}\right\} \\
&+\frac{C_F N_f}{2}\left\{-\frac{160}{9}S_1(n) + \frac{32}{3}S_2(n) + \frac{4}{3} + 16\frac{11n^2+5n+-3}{9n^2(n+1)^2}\right\}. \qquad \text{(A.9)}
\end{aligned}$$

The functions S_i' and $\tilde{S}$ are given by:

$$S_i'\left(\frac{n}{2}\right) = \frac{1+\eta}{2}S_i\left(\frac{n}{2}\right) + \frac{1-\eta}{2}S_i\left(\frac{n-1}{2}\right), \qquad \text{(A.10)}$$

$$\tilde{S}(n) = \sum_{j=1} n\frac{(-1)^j}{j^2}S_1(j). \qquad \text{(A.11)}$$

The parameter $\eta = (-1)^n$ is 1 or -1, depending on which combination of parton distributions is going to be evolved. This is so because the moments are defined only for n even or odd, according to the OPE. Thus, it is necessary to extend the validity of the equations for the whole interval of n. This is done through analytic continuation in which case the values of the anomalous dimensions starting from even or odd n coincide. A detailed account on how to do the analytic continuation of the various S functions can be found in the work of Glück et al. [231] or in the recent work of Melnitchouk and Weigl [134]. The parameter η is -1 for the combinations $u-\overline{u}$ and $d-\overline{d}$ [231] and +1 for the others nonsinglet combinations. For the singlet combinations, η is always +1. For polarized scattering, it is just the opposite. These conclusions can be reached from considerations on the properties under crossing symmetry of the various structure functions involved.

The matrix elements of the singlet anomalous dimension in the $\overline{MS}$ scheme are [221]:

$$\gamma_{qq}^{(1)n} = \gamma_{NS}^{(1)n} - 16C_F T_R \frac{5n^5+32n^4+49n^3+38n^2+28n+8}{(n-1)n^3(n+1)^3(n+2)^2}, \tag{A.12}$$

$$\begin{aligned}
\gamma_{qg}^{(1)n} &= -8C_A T_R \left[(-2S_1^2(n)+2S_2(n)-2S_2'(n/2)) \frac{n^2+n+2}{n(n+1)(n+2)} \right. \\
&\left. + \frac{8S_1(n)(2n+3)}{(n+1)^2(n+2)^2} + 2\frac{n^9+6n^8+15n^7+25n^6+36n^5+85n^4+128n^3+104n^2+64n+16}{(n-1)n^3(n+1)^3(n+2)^3} \right] \\
&-8C_F T_R \left[(2S_1^2(n)-2S_2(n)+5)\frac{n^2+n+2}{n(n+1)(n+2)} - \frac{4S_1(n)}{n^2} + \frac{11n^4+26n^3+15n^2+8n+4}{n^3(n+1)^3(n+2)} \right],
\end{aligned} \tag{A.13}$$

$$\begin{aligned}
\gamma_{gq}^{(1)n} &= -4C_F^2 \left[(-2S_1^2(n)+10S_1(n)-2S_2(n)) \frac{n^2+n+2}{(n-1)n(n+1)} - \frac{4S_1(n)}{(n+1)^2} \right. \\
&\left. - \frac{12n^6+30n^5+43n^4+28n^3-n^2-12n-4}{(n-1)n^3(n+1)^3} \right] \\
&-8C_F C_A \left[(S_1^2(n)+S_2(n)-S_2'(n/2)) \frac{n^2+n+2}{(n-1)n(n+1)} - S_1(n)\frac{17n^4+41n^2-22n-12}{3(n-1)^2n^2(n+1)} \right. \\
&\left. + \frac{109n^9+621n^8+1400n^7+1678n^6+695n^5-1031n^4-1304n^3-152n^2+432n+144}{9(n-1)^2n^3(n+1)^3(n+2)^2} \right] \\
&-\frac{32}{3}C_F T_R \left[(S_1(n)-\frac{8}{3})\frac{n^2+n+2}{(n-1)n(n+1)} + \frac{1}{(n+1)^2} \right],
\end{aligned} \tag{A.14}$$

and

$$\begin{aligned}
\gamma_{gg}^{(1)n} &= C_A T_R \left[-\frac{160}{9} S_1(n) + \frac{32}{3} + \frac{16}{9} \frac{38n^4 + 76n^3 + 94n^2 + 56n + 12}{(n-1)n^2(n+1)^2(n+2)} \right] \\
& C_F T_R \left[8 + 16 \frac{2n^6 + 4n^5 + n^4 - 10n^3 - 5n^2 - 4n - 4}{(n-1)n^3(n+1)^3(n+2)} \right] \\
& + C_A^2 \left[\frac{536}{9} S_1(n) + 64 S_1(n) \frac{2n^5 + 5n^4 + 8n^3 + 7n^2 - 2n - 2}{(n-1)^2 n^2 (n+1)^2 (n+2)^2} - \frac{64}{3} \right. \\
& + 32 S_2'(n/2) \frac{n^2 + n + 1}{(n-1)n(n+1)(n+2)} - 16 S_1(n) S_2'(n/2) + 32 \check{S}(n) - 4 S_3'(n/2) \\
& - \frac{4}{9} \left(\frac{457n^9 + 2742n^8 + 6040n^7 + 6098n^6 + 1567n^5 - 2344n^4 - 1632n^3}{(n-1)^2 n^3 (n+1)^3 (n+2)^3} \right. \\
& \left. \left. + \frac{560n^2 + 1488n + 576}{(n-1)^2 n^3 (n+1)^3 (n+2)^3} \right) \right] . \qquad \text{(A.15)}
\end{aligned}$$

A.2 Polarized Scattering

A.2.1 Leading Order Case

The nonsinglet anomalous dimension is [222, 223, 95]:

$$\gamma_{NS}^{(0)n} = 4 C_F \left[2 S_1(n) - \frac{1}{n(n+1)} - \frac{3}{2} \right] . \qquad \text{(A.16)}$$

The matrix elements of the singlet anomalous dimension are [222, 223, 95]:

$$\gamma_{qq}^{(0)n} = \gamma_{NS}^{(0)n} , \qquad \text{(A.17)}$$

$$\gamma_{qg}^{(0)n} = -8 T_R \frac{n-1}{n(n+1)} , \qquad \text{(A.18)}$$

$$\gamma_{gq}^{(0)n} = -4C_F \frac{n+2}{n(n+1)}, \tag{A.19}$$

and

$$\gamma_{gg}^{(0)n} = 4C_A \left[2S_1(n) - \frac{4}{n(n+1)} - \frac{11}{6} \right] + \frac{8}{3} T_R. \tag{A.20}$$

A.2.2 Next to Leading Order Case

The polarized nonsinglet anomalous dimension at two loops is the same as the unpolarized one [224]. The singlet anomalous dimensions in the $\overline{MS}$ scheme are [226]:

$$\gamma_{qq}^{(1)n} = \gamma_{NS}^{(1)n} + 16 C_F T_R \frac{n^4 + 2n^3 + 2n^2 + 5n + 2}{n^3(n+1)^3}, \tag{A.21}$$

$$\begin{aligned}
\gamma_{qg}^{(1)n} &= 8 C_F T_R \left[2 \frac{n-1}{n(n+1)} (S_2(n) - S_1^2(n)) + 4 \frac{n-1}{n^2(n+1)} S_1(n) \right. \\
&\left. - \frac{5n^5 + 5n^4 - 10n^3 - n^2 + 3n - 2}{n^3(n+1)^3} \right] \\
&+ 16 C_A T_R \left[\frac{n-1}{n(n+1)} (-S_2(n) + S_2'(n/2) + S_1^2(n)) - \frac{4}{n(n+1)^2} S_1(n) \right. \\
&\left. - \frac{n^5 + n^4 - 4n^3 + 3n^2 - 7n - 2}{n^3(n+1)^3} \right],
\end{aligned} \tag{A.22}$$

$$\begin{aligned}\gamma_{gq}^{(1)n} &= 32C_FT_R\left[-\frac{n+2}{3n(n+1)}S_1(n)+\frac{5n^2+12n+4}{9n(n+1)^2}\right]\\ &+C_F^2\left[2\frac{n+2}{n(n+1)}(S_2(n)+S_1^2(n))-2\frac{3n^2+7n+2}{n(n+1)^2}S_1(n)\right.\\ &\left.+\frac{9n^5+30n^4+24n^3-7n^2-16n-4}{n^3(n+1)^3}\right]\\ &+8C_AC_F\left[\frac{n+2}{n(n+1)}(-S_2(n)+S_2'(n/2)-S_1^2(n))+\frac{11n^2+22n+12}{3n^2(n+1)}S_1(n)\right.\\ &\left.-\frac{76n^5+271n^4+254n^3+41n^2+72n+36}{9n^3(n+1)^3}\right],\end{aligned} \tag{A.23}$$

and

$$\begin{aligned}\gamma_{gg}^{(1)n} &= 8C_FT_R\frac{n^6+3n^5+5n^4+n^3-8n^2+2n+4}{n^3(n+1)^3}\\ &+32C_FT_R\left[-\frac{5}{9}S_1(n)+\frac{3n^4+6n^3+16n^2+13n-3}{9n^2(n+1)^2}\right]\\ &+4C_A^2\left[-S_3'(n/2)-4S_1(n)S_2'(n/2)+8\tilde{S}(n)+\frac{8}{n(n+1)}S_2'(n/2)\right.\\ &2\frac{67n^4+134n^3+67n^2+144n+72}{9n^2(n+1)^2}S_1(n)\\ &\left.-\frac{48n^6+144n^5+469n^4+698n^3+7n^2+258n+144}{9n^3(n+1)^3}\right].\end{aligned} \tag{A.24}$$

A.2.3 The Wilson Coefficients

The quark Wilson coefficient for g_1 was originally calculated by Kodaira et al. [225] in the $\overline{MS}$ scheme and their result corroborated by a recent calculation [226]. It is given by:

$$F_n^{qq} = C_F\left(-9+\frac{1}{n}+\frac{2}{n+1}+\frac{2}{n^2}+3S_1(n)-4S_2(n)-\frac{2}{n(n+1)}S_1(n) +2(S_1^2(n)+S_2(n))\right). \tag{A.25}$$

And the Wilson gluon coefficient, according to our discussion of chapter 4, is [158, 226, 240]:

$$C_{g,n}^{\overline{MS}} = F_n^{qg} = T_R\left[\frac{4(n-1)(1-n-S_1(n))}{n^2(n+1)}\right]. \tag{A.26}$$

Notice that it vanishes for $n = 1$ meaning that the gluons do not contribute to g_1 in the $\overline{MS}$ scheme, as discussed at length in chapter 4.

Bibliography

[1] L. D. Fadeev and V. N. Popov, Phys. Lett. 25B (1967) 29.

[2] G. 't Hooft, Nucl. Phys. B 33 (1971) 173.

[3] H. Fritzsch, M. Gell-Mann and H. Leutwyler, Phys. Lett. 47B (1973) 365.

[4] T. Muta, *Foundations of Quantum Chromodynamics*, World Scientific. 1987.

[5] M. Gell-Mann, Phys. Lett. 8 (1964) 214.

[6] G. Zweig, CERN preprint 8419/TH 412 (1964).

[7] E. D. Bloom et al., Phys. Rev Lett. 23 (1969) 930; M. Breidenbach et al., Phys. Rev. Lett. 23 (1969) 935.

[8] R. P. Feynman, Phys. Rev. Lett. 23 (1969) 1415.

[9] R. P. Feynman *Photon-Hadron Interactions*, Benjamin, New York, 1972.

[10] J. D. Bjorken and E. A. Paschos, Phys. Rev. 185 (1969) 1975.

[11] M. Y. Han and Y. Nambu, Phys. Rev. 139 (1965) B1006.

[12] D. J. Gross and F. Wilczek, Phys. Rev. Lett. 30 (1973) 1343; Phys. Rev. D8 (1973) 3633.

[13] H. D. Politzer, Phys. Rev. Lett. 30 (1973) 1346.

[14] H. Georgi and H. D. Politzer, Phys. Rev. D9 (1974) 416.

[15] K. G. Wilson, Phys. Rev. 179 (1969) 1499.

[16] R. A. Brandt and G. Preparata, Nucl. Phys. B27 (1971) 541.

[17] W. Zimmermann, in *Lectures on Elementary Particles abd Quantum Field Theory*, Proc. 1970 Brandeis Summer Institute in Theoretical Physics, eds. S. Deser et al., MIT press, 1971.

[18] NMC, P. Amaudruz et al., Phys. Rev. Lett. 66 (1991) 2712; NMC, M. Arneodo et al., Phys. Rev. D50 (1994) R1.

[19] NA51 collaboration, A. Baldit, Phys. Lett. 332B (1994) 244.

[20] EMC, J. Ashman et al., Phys. Lett. 206B (1988) 364; Nucl. Phys. B328 (1989) 1.

[21] G. Veneziano, Mod. Phys. Lett. A4 (1989) 1615; G. M. Shore and G. Veneziano, Phys. Lett. 244B (1990) 75; Nucl. Phys. B381 (1992) 23.

[22] W. Bardeen, Nucl. Phys. B 75 (1974) 246.

[23] J. D. Bjorken and S. D. Drell, *Relativistic Quantum Mechanics*, McGraw-Hill, 1964.

[24] F. E. Close, *An Introduction to Quarks and Partons*, Academic Press, 1979.

[25] N. Dombey, Rev. Mod. Phys. 41 (1969) 236.

[26] E. Leader and E. Predazzi, *An Introduction to Gauge Theories and the New Physics*, Cambridge University Press, 1982.

[27] I. J. R. Aitchison and A. J. Hey, *Gauge Theories in Particle Physics*, Adam Hilger, 1989 second edition.

[28] C. Itzykson abd J. Zuber, *Quantum Field Theory*, McGraw-Hill, 1985.

[29] L. N. Hand, Phys. Rev. 129 (1963) 1834.

[30] W. Greiner and A. Schäfer, *Quantum Chromodynamics*, Springer, 1994.

[31] J. Kodaira, Prog. of Theor. Phys. Suppl. 120 (1995) 37.

[32] SMC, D. Adams et al., Phys. Lett. 336B (1994) 125.

[33] M. G. Doncel and E. de Rafael, Nuovo Cimento 4A (1971) 363.

[34] L. W. Whitlow et al., Phys. Lett. 250B (1990) 193.

[35] R. Voss, in *XVI International Symposium on Lepton-Photon-Interactions*, Proceedings pp. 144, Ithaca, NY, 1993, CERN preprint PPE/93-211.

[36] J. D. Bjorken, Phys. Rev. 179 (1969) 1547.

[37] C. G. Callan and D. Gross, Phys. Rev. Lett. 22 (1969) 156.

[38] R. L. Jaffe and Xiangdong Ji, Phys. Rev. D43 (1991) 724.

[39] G. Altarelli, B. Lampe, P. Nason and G. Ridolfi, Phys. Lett. 334B (1994) 187.

[40] R. L. Jaffe, in: *Relativistic Dynamics and Quark-Nuclear Physics*, Proceedings of the Workshop, Los Alamos, New Mexico, 1985, edited by M. B. Johnson and A. Pickleseimer (New York, Wiley) p.537.

[41] A. I. Signal and A. W. Thomas, Phys. Lett. 221B (1988) 481.

[42] A. I. Signal and A. W. Thomas, Phys. Rev. D40 (1989) 2832.

[43] P. V. Landshoff and J. C. Polkinghorne, Phys. Rep. 5C (1972) 1.

[44] J. D. Jackson, G. G. Ross and R. G. Roberts, Phys. Lett. 226B (1989) 159.

[45] S. Wandura and F. Wilczec. Phys. Lett. B72

[46] R. L. Jaffe, Comm. Nucl. Part. Phys. 19 (1990) 239.

[47] M. Anselmino, A. Efremov and E. Leader, Phys. Rep. 261 (1995) 1.

[48] J. D. Bjorken, Phys. Rev. 148 (1966) 1467.

[49] SMC, D. Adams et al., Phys. Lett. 357B (1995) 248.

[50] G. Baum on behalf of the SMC, Proceedings of the Seventh Conference on Perspectives in Nuclear Physics at Intermediate Energies, ICTP Triste (1995), hep-ex/9509007.

[51] The E143 Collaboration, K. Abe et al., Slac preprint SLAC-PUB-95-6734.

[52] SMC, D. Adams et al., Phys. Lett. 329B (1994) 399; Erratum, Phys. Lett. 339B (1994) 332.

[53] SMC, B. Adeva et al., Phys. Lett. 302B (1993) 533.

[54] SLAC E142, P. L. Anthony et al., Phys. Rev. Lett 71 (1993) 959;

[55] S. G. Gorishny and S. A. Larin, Phys. Lett. 172B (1986) 109.

[56] S. A. Larin and J. A. M. Vermaseren, Phys. Lett. 259B (1991) 345.

[57] E. B. Zijlstra and W. van Neerven, Phys. Lett. 297B (1992) 377.

[58] J. Ellis, E. Gardi, M. Karliner and M. A. Samuel, CERN preprint CERN-TH-95-155 (1995), hep-ph/9509312.

[59] E. Stein, P. Gornicki, L. Mankiewicz and A. Schäfer, Phys. Lett. 353B (1995) 107.

[60] H. Kawamura and T. Uematsu, Phys. Lett. 343B (1995) 346.

[61] O. V. Teryaev, Int. Symp. Dubna Deuteron 95, Dubna, Russia July 1995, hep-ph/9508374.

[62] K. Gotfried, Phys. Rev. Lett. 18 (1967) 1174.

[63] J. Ellis and R. L. Jaffe, Phys. Rev. D9 (1974) 1444; Erratum, Phys. Rev. D10 (1974) 1669.

[64] The E143 Collaboration, K. Abe et al., Phys. Rev. Lett. 74 (1995) 346.

[65] A. J. Buras, Rev. of Mod. Phys. 52 (1980) 199.

[66] D. J. Gross and C. H. Llewellyn Smith, Nucl. Phys. B14 (1969) 337.

[67] CDHS Collab., J. G. H. de Groot et al., Phys. Lett. 82B (1979) 292.

[68] CHARM Collab., F. Bergsma et al., Phys. Lett. 123B (1983) 269.

[69] CCFRR Collab., D. B. MacFarlane et al., Z. Phys. C26 (1984) 1.

[70] WA 25 Collab., D. Allasia et al., Phys. Lett. 135B (1984) 231; Z. Phys. C28 (1985) 321.

[71] E. Oltman et al., Z. Phys. C53 (1992) 51.

[72] CCFR Collab., W. C. Leung et al., Phys. Lett. 317B (1993) 655.

[73] M. J. Lighthill, *Introduction to Fourier Analysis and Generalised Functions*, Cambridge University Press, 1958.

[74] F. J. Ynduráin, *The Theory of Quarks and Gluon Interactions*, Springer-Verlag, 1993 second edition.

[75] N. N. Bogoliubov and D. V. Shirkov, *Introduction to the Theory of Quantized Fields*, John Wiley, 1980 third edition.

[76] N. Christ, B. Hasslacher and A. H. Mueller, Phys. Rev. D6 (1972) 3543.

[77] W. Zimmermann, Ann. Phys. 77 (1973) 570.

[78] A. J. Hey and J. E. Mandula, Phys. Rev. D5 (1972) 2610.

[79] M. A. Ahmed and G. G. Ross, Nucl. Phys. B111 (1976) 441.

[80] H. Burkhardt and W. N. Cottingham, Ann. Phys. 56 (1970) 453.

[81] The E143 Collaboration, K. Abe et al., Phys. Rev. Lett. 76 (1996) 587.

[82] G. Altarelli and G. Parisi, Nucl. Phys. 126B (1977) 298.

[83] J. Kodaira et al., Phys. Lett. 345B (1995) 527.

[84] R. G. Roberts and G. G. Ross, preprint RAL-95-TR-057, hep-ph/9601235.

[85] E. C. G. Stueckelberg and A. Petermann, Helv. Phys. Acta 26 (1953)499.

[86] M. Gell-Mann and F. E. Low, Phys. Rev. 95 (1954) 1300.

[87] K. Symanzik, Comm. Math. Phys. 18 (1970) 227.

[88] C. G. Callan, Phys. Rev. D2 (1970) 1541.

[89] W. Pauli and F. Villars, Rev. of Mod. Phys. 21 (1949) 434.

[90] G. 't Hooft and M. Veltman, Nucl. Phys. B44 (1972) 189; C. G. Bollini and J. J. Giambiagi, Phys. Lett. 40B (1972) 566.

[91] Ta-Pei Cheng and Ling-Fong Li, *Gauge Theory of Elementary PArticle Physics*, Clarendon Press - Oxford, 1984.

[92] S. L. Adler, Phys. Rev. 177 (1969) 129; J. S. Bell and R. J. Jackiw, Nuovo Cimento 51 A (1969) 47.

[93] J. Kodaira, Nucl. Phys. B 165 (1980) 129.

[94] E. de Rafael and J. L. Rosner, Ann. Phys. 82 (1974) 369.

[95] H. Ito, Prog. Theor. Phys. 54 (1975) 555.

[96] R. D. Field and R. P. Feynman, Phys. Rev. D15 (1977) 2590.

[97] A. S. Ito et al., Phys. Rev. D23 (1981) 604.

[98] A. W. Thomas, Phys. Lett. 126B (1983) 97.

[99] J. D. Sullivan, Phys. Rev. D5 (1972) 1732.

[100] M. Ericson and A. W. Thomas, Phys. Lett. 148B (1984) 191.

[101] A. D. Martin, W, J. Stirling and R. G. Roberts, Phys. Rev. D47 (1993) 867.

[102] A. D. Martin, W, J. Stirling and R. G. Roberts, Phys. Lett. 252B (1990) 653.

[103] S. D. Ellis and W. J. Stirling, Phys. Lett. 256B (1991) 258.

[104] E. M. Henley and G. A. Miller, Phys. Lett. 251B (1990) 453.

[105] A. I. Signal, A. W. Schreiber and A. W. Thomas, Mod. Phys. Lett. A6 (1991) 271.

[106] W. Melnitchouk, A. W. Thomas and A. I. Signal, Z. Phys. A340 (1991) 85.

[107] S. Kumano and J. T. Londergan, Phys. Rev. D44 (1991) 717.

[108] W-Y. P. Hwang, J. Speth and G. E. Brown, Z. Phys. A339 (1991) 383.

[109] E. J. Eichten, I. Hinchliffe and C. Quigg, Phys. Rev. D45 (1992) 2269.

[110] V. R. Zoller, Z. Phys. C54 (1992) 425.

[111] A. Szczurek and J. Speth, Nucl. Phys. A555 (1993) 249.

[112] A. W. Thomas and W. Melnitchouk, in: New Frontiers in Nuclear Physics, eds. S. Homma, Y. Akaishi and M. Wada (World Scientific, Singapore, 1993), pp. 41 - 106.

[113] T. P. Cheng and Ling-Fong Li, Phys. Rev. Lett. 74 (1995) 2872.

[114] W. Koepf, L. L. Frankfurt and M. Strikman, Tel Aviv University preprint TAUP-2273-95, hep-ph 9507218.

[115] D. A. Ross and C. T. Sachrajda, NUcl. Phys. B149 (1979) 497.

[116] Bo-Qiang Ma, Phys. Lett. 274B (1992) 111.

[117] NMC, P. Amaudruz et al., Phys. Lett. 295B (1992) 159.

[118] E. N. Rodionov, A. W. Thomas and J. T. Londergan, Mod. Phys. Lett. A 9 (1994) 1799; E. Sather, Phys. Lett. B 274 (1992) 433.

[119] A. Szczurek, M. Ericson, H. Holtmann and J. Speth, Nucl. Phys. A 596 (1996) 397.

[120] J. F. Donoghue and E. Golowich, Phys. Rev. D15 (1977) 3421.

[121] S. Théberge, A. W. Thomas and G. A. Miller, Phys. Rev. D22 (1980) 2838; D23 (1981) 2106 (E).

[122] A. W. Thomas, Adv. in Nucl. Phys. 13 (1984) 1.

[123] S. Théberge, G. A. Miller and A. W. Thomas, Can. J. Phys. 60 (1981) 59.

[124] H. J. Lipkin, Phys. Lett. 337B (1994) 157.

[125] Particle Data Group, L. Montanet et al., Phys. Rev. D50 (1994) 1173.

[126] F. E. Close and R. G. Roberts, Phys. Lett. 316B (1993) 165.

[127] A. Schäfer, in the proceedings of the "Workshop on the Prospects of Spin Physics at Hera", Zeuthen - Germany, August 1995, edited by Johannes Blümlein and Wolf-Dieter Nowak, page 318.

[128] R. L. Jaffe and A. Manohar, Nucl. Phys. B337 (1990) 509.

[129] S. D. Bass and A. W. Thomas, J. Phys. G 19 (1993) 925.

[130] R. Voss, Cern preprint CERN-PPE/95-131, august 1995, invited Talk at the Workshop on Deep Inelastic Scattering and QCD, Paris, April 1995.

[131] S. A. Larin, Phys. Lett. 334B (1994) 192.

[132] W. Melnitchouk, G. Piller and A. W. Thomas, Phys. Lett. 346B (1995) 165.

[133] M. Glück et al., Dortmund preprint DO-TH 95/13, hep-ph/9508347; T. Gehrmann and W. J. Stirling, Durham preprint DTP/95/82, hep-ph/9512406.

[134] T. Weigl and W. Melnitchouk, Munich Tech. Uni. preprint TUM-T39-95-9, sept. 95, to appear in Nucl. Phys. B; hep-ph/9601294.

[135] The E143 Collab.. Phys. Lett. 364B (1995) 61.

[136] SLAC E80, M. J. Alguard et al., Phys. Rev. Lett. 37 (1976) 1261; ibid. 41 (1978) 70; SLAC E130 G. Baum et al., Phys. Rev. Lett. 51 (1983) 1135.

[137] S. J. Brodsky, M. Burkardt and I. Schmidt, Nucl. Phys. B441 (1995) 197.

[138] R. L. Heimann, Nucl. Phys. B64 (1973) 429.

[139] J. Ellis and M. Karliner, Phys. Lett. 213B (1988) 73.

[140] F. E. Close and R. G. Roberts, Phys. Lett. 336B (1994) 257.

[141] M. Froissart, Phys. Rev. 123 (1961) 1053.

[142] S. D. Bass and P. V. Landshoff, Phys. Lett. 336B (1994) 537.

[143] S. D. Bass and A. W. Thomas, Prog. Part. Nucl.

[144] A. W. Schreiber and A. W. Thomas, Phys. Lett. 215B (1988) 141.

[145] K. Kubodera, Y. Kohyama, K. Tsushima and T. Yamaguchi, proceedings of the XXII Yamada Conference in Nuclear Weak Process and Nuclear Structure, pg. 408 , June 1988, Osaka - Japan.

[146] F. M. Steffens, H. Holtmann and A. W. Thomas, Phys. Lett. 358B (1995) 139.

[147] H. Høgaasen and F. Myhrer, Phys. Lett. 214B (1988) 123.

[148] H. Høgaasen and F. Myhrer, Z. Phys. C 68 (1995) 625.

[149] A. W. Schreiber, A. W. Thomas and J. T. Londergan, Phys. Rev. D 42 (1990) 2226.

[150] A. W. Schreiber, A. I. Signal and A. W. Thomas, Phys. Rev. D 44 (1991) 2653.

[151] M. Stratman, Z. Phys. C 60 (1993) 763.

[152] X. Song and J. S. McCarthy, Phys. Rev. D 49 (1994) 3169; Erratum D 50 (11994) 4718.

[153] A. W. Schreiber, P. J. Mulders, A. I. Signal and A. W. Thomas, Phys. Rev. D 45 (1992) 3069.

[154] G. Altarelli and G. G. Ross, Phys. Lett. 212B (1988) 391.

[155] R. D. Carlitz, J. C. Collins and A. H. Mueller, Phys. Lett. B214 (1988) 299.

[156] A. V. Efremov, J. Soffer and O. V. Teryaev, Nucl. Phys. B246 (1990) 97.

[157] G. Altarelli and B. Lampe, Z. Phys. C 47 (1990) 315.

[158] G. T. Bodwin and J. Qui, Phys. Rev. D 41 (1990) 2755.

[159] A. V. Manohar, Phys. Rev. Lett. 65 (1990) 2511.

[160] S. D. Bass, Z. Phys. C55 (1992) 653. Phys. 33 (1994) 449.

[161] G. Altarelli, Phys. Rep. 81 (1982) 1.

[162] J. C. Collins, D. E. Soper and G. Sterman, in: Perturbative Quantum Chromodynamics, pg. 1, ed. by A. H. Mueller, World Scientific, 1989.

[163] A. E. Dorokhov, N. I. Kochelev and YU. A. Zubov, Int. J. Mod. Phys. A8 (1993) 603; A. E. Dorokhov and N. I. Kochelev, Mod. Phys. Lett. A5 (1990) 55.

[164] G. 't Hooft, Phys. Rev. D14 (1976) 3432.

[165] M. Takizawa and W. Weise, Phys. Lett. 268B (1991) 323; K. Steininger and W. Weise, Phys. Rev. D 48 (1993) 1433.

[166] Y. Nambu and G. Jona-Lasinio, Phys. Rev. 122 (1961) 345; 124 (1961) 246.

[167] G. Altarelli and W. J. Stirling, Particle World 1 (1990) 40.

[168] M. Gück, E. Reya and W. Vogelsang, Phys. Rev. D 45 (1992) 2552.

[169] F. M. Steffens and A. W. Thomas, Phys. Rev. D53 (1996) 1191.

[170] R. D. Ball, S. Forte and G. Ridolfi, CERN - TH/95-266, Edinburgh 95/556, GeF-TH-9/95, hep-ph/9510449.

[171] B. Ehrnsperger and A. Schäfer, Phys. Rev. D52 (1995) 2709.

[172] X. Ji, J. Tang and P. Hoodbhoy, Phys. Rev. Lett. 76 (1996) 740.

[173] X. Ji, MIT preprint MIT-CPT-2517, hep-ph/9603249.

[174] I. I. Balitsky and V. M. Braun, Phys. Lett. 267B (1991) 405.

[175] R. L. Jaffe, Nucl. Phys. B229 (1983) 205.

[176] S. Forte, Nucl. Phys. B 331 (1990) 1.

[177] S. D. Bass, B. L. Ioffe, N. N. Nikolaev and A. W. Thomas, J. Moscow Phys. Soc. 1 (1991) 317.

[178] A. Efremov, J. Soffer and N. A. Törnqvist, Phys. Rev. D 44 (1991) 1369.

[179] J. Kogut and L. Susskind, Phys. Rev. D9 (1974) 3391.

[180] L. Mankiewicz, Phys. Rev. D43 (1991) 64.

[181] S. D. Bass, N. N. Nikolaev and A. W. Thomas, University of Adelaide Report No. ADP-133-T-80, 1990 (unpublished).

[182] W. Vogelsang, Z. Phys. C50 (1991) 275.

[183] G. P. Lepage and S. J. Brodsky, Phys. Rev. D22 (1980) 2157.

[184] S. D. Bass, Phys. Lett. 342B (1995) 233.

[185] L. Mankiewicz and A. Schäfer, Phys. Lett. 242B (1990) 455.

[186] T. Gehrmann and W. J. Stirling, Z. Phys. C 65 (1995) 461.

[187] M. Glück, E. Reya and A. Vogt, Z. Phys. C 53 (1992) 53.

[188] NMC, D. Allasia et al., Phys. Lett. 258B (1991) 493.

[189] NMC, M. Arneodo et al., Phys. Lett. 309B (1993) 222.

[190] ZEUS Collaboration, M. Derrick et al., Z. Phys. C65 (1995) 379.

[191] NMC, M. Arneodo et al., Cern preprint CERN-PPE/95-138, hep-ph/9509406.

[192] ZEUS Collaboration, M. Derrick et al., Desy preprint DESY 95-193, hep-ex/9510009.

[193] E665 Collaboration, M. R. Adamn et al., Fermilab preprint FERMILAB-PUB-95-396-E.

[194] A. Donnachie and P. V. Landshoff, Z. Phys. C61 (1994) 139.

[195] M. Glück, E. Reya and A. Vogt, Z. Phys. C 67 (1995) 433.

[196] A. D. Martin, W, J. Stirling and R. G. Roberts, Phys. Lett. 354B (1995) 155.

[197] CTEQ, H. L. Lai et al., Phys. Rev. D51 (1995) 4763.

[198] G. A. Ladinsky, in the proceedings of the "Workshop on the Prospects of Spin Physics at Hera", Zeuthen - Germany, August 1995, edited by Johannes Blümlein and Wolf-Dieter Nowak, page 285, hep-ph/9601287.

[199] SMC, B. Adeva et al., Phys. Lett. 369B (1996) 93.

[200] E. Nappi et al., Letter of intent for the experiment, Cern preprint CERN/SPSLC 95-27; G. Mallot, in the proceedings of the "Workshop on the Prospects of Spin Physics at Hera", Zeuthen - Germany, August 1995, edited by Johannes Blümlein and Wolf-Dieter Nowak, page 273.

[201] R. W. Robinett, Argonne preprint ANL-HEP-CP-95-28, hep-ph/9506230.

[202] M. Traini, L. Conci and U. Moschella, Nucl. Phys. **A554** (1992), 731; L.Conci and M. Traini, Few-Body Systems 8 (1990) 123.

[203] C. J. Benesh, T. Goldman and G. J. Stephenson, Jr., Phys. Rev. **C48** (1993), 1379; H. J. Weber, U. Virginia preprint (1994).

[204] S. A. Kulagin, W. Melnitchouk, T. Weigl and W. Weise, Nucl. Phys. A 597 (1996) 515.

[205] H. Meyer and P. J. Mulders, Nucl. Phys. A 528 (1991) 589; P. J. Mulders, A. W. Schreiber and H. Meyer, Nucl. Phys. A 549 (1992) 498; W. Melnitchouk, A. W. Schreiber and A. W. Thomas, Phys. Rev. D 49 (1994) 127; W. Melnitchouk and W. Weise, Phys. Lett. B 334 (1994) 275.

[206] F. M. Steffens and A. W. Thomas, Prog. of Theor. Phys. Suppl. 120 (1995) 145.

[207] R. L. Jaffe, Phys. Rev. D 11 (1975) 1953.

[208] A. Le Yaouanc et al., Phys. Rev. D11 (1975) 2636.

[209] R. J. Hughes, Phys. Rev. D 16 (1977) 622.

[210] J. S. Bell and A. J. G. Hey, Phys. Lett. 74B (1978) 77; *ibid* 78B (1978) 67.

[211] J. A. Bartelski, Phys. Rev. D 20 (1979) 1229.

[212] L. S. Celenza and C. M. Shakin, Phys. Rev. C 27 (1983) 1561 ; (E) C 39 (1989) 2477.

[213] C. J. Benesh and G. A. Miller Phys. Rev. D 36 (1987) 1344; Phys. Lett. 215B (1988) 381; Phys. Rev. D 38 (1988) 48; Phys. Lett. 222B (1989) 476.

[214] R. E. Peierls and J. Yoccoz, Proc. Phys. Soc. London A70 (1957) 381.

[215] F. M. Steffens and A. W. Thomas, Nucl. Phys. A568 (1994) 798.

[216] A. Ardekani and A. I. Signal, Phys. Lett. 311B (1993) 281.

[217] R. E. Peierls and D. J. Thouless, Nucl. Phys. 38 (1962) 154.

[218] S. J. Brodsky and G. Farrar, Phys. Rev. Lett. 31 (1973) 2157; Phys. Rev. D 11 (1975) 1309.

[219] See for example, D. Silvers, Ann. Rev. Part. Sci. 32 (1982) 149.

[220] EMC, J. J. Aubert et al., Nucl. Phys. B 293 (1987) 74.

[221] D. R. T. Jones, Nucl. Phys. B 75 (1974) 531; E. G. Floratos, D. A. Ross and C. T. Sachrajda, Nucl. Phys. B 129 (1977) 66; and Erratum B139 (1978) 545; B152 (1979) 493; A. González-Arroyo, C. López and F. J. Ynduráin, Nucl. Phys. B 153 (1979) 161; C. López and F. J. Ynduráin, Nucl. Phys. B 183 (1981) 157.

[222] M. A. Ahmed and G. G. Ross, Phys. Lett 56 B (1975) 385.

[223] K. Sasaki, Prog. Theor. Phys. (1975) 54.

[224] J. Kodaira, S. Matsuda, K. Sasaki and T. Uematsu, Nucl. Phys. B 159 (1979) 99.

[225] J. Kodaira, S. Matsuda, T. Muta, T. Uematsu and K. Sasaki; Phys. Rev. D 20 (1979) 627.

[226] R. Mertig and W. L. van Neerven, preprint number INLO-PUB-6/95 and NIKHEF-H/95-031, hep-ph/9506451; for erratum, see M. Gück et al. in Ref. [133].

[227] G. Altarelli, R. K. Ellis and G. Martinelli, Nucl. Phys. B 143 (1978) 521; (E) B 146 (1978) 544; B 157 (1979) 461.

[228] M. Glück and E. Reya, Phys. Rev. D 25 (1982) 1211.

[229] R. G. Roberts, *The Structure of the Proton*, Cambridge Monographs of Mathematical Physics, Cambridge University Press, 1990.

[230] D. J. Gross and F. Wilczek, Phys. Rev. D 9 (1974) 980.

[231] M. Glück, E. Reya and A. Vogt, Z. Phys. C 48 (1990) 471.

[232] F. E. Close and A. W. Thomas, Phys. Lett. 212B (1988) 227.

[233] A. D. Martin, W. J. Stirling and R. G. Roberts, Phys. Lett. 306B (1993) 145.

[234] Work in progress.

[235] H. Holtmann, A. Szczurek and J. Speth, Nucl. Phys. A 596 (1996) 631.

[236] A. I. Signal and A. W. Thomas, Phys. Lett. 191B (1987) 3.

[237] R. Machleidt, K. Holinde and Ch. Elster, Phys. Rep. 149 (1987) 1.

[238] P. J. Sutton, A. D. Martin, R. G. Roberts and W. Stirling, Phys. Rev. D 45 (1992) 2349.

[239] In a private communication, J. T. Londergan showed us some results in advance where it is claimed that certain combinations of the F_3 structure function give a clear separation bewteen charge symmetry and isospin breaking.

[240] E. B. Zijlstra and W. L. van Neerven, Nucl. Phys. B 417 (1994) 61; erratum B 426 (1994) 245.

[241] R. L. Jaffe, Phys. Lett. 365B (1996) 359.

[242] K-F. Liu and S-J. Dong, in Glascow 94, Proceedings, High energy physics, vol.2 page 717 and hep-lat/9411067.

[243] S. Rock, in the proceedings of the "Workshop on the Prospects of Spin Physics at Hera", Zeuthen - Germany, August 1995, edited by Johannes Blümlein and Wolf-Dieter Nowak, page 259, plus the whole section on future experiments.

[244] CLAS Collaboration, S. E. Kuhn et al., CEBAF-PROPOSAL-93-009, Apr. 1993.

Steffens, F.M., and Thomas, A.W., (1994) A study of quark-parton distributions in a simple quark model.
Nuclear Physics A, v. 568 (4), pp. 798-808.

Steffens, F.M., and Thomas, A.W., (1995) A study of structure functions for the bag beyond leading order.
Progress of Theoretical Physics, v. 120, pp. 145-156.

Reprinted from

PHYSICS LETTERS B

Physics Letters B 358 (1995) 139–145

Mesonic corrections to the shape of quark distributions

F.M. Steffens [a], H. Holtmann [a,b], A.W. Thomas [a]

[a] *Department of Physics and Mathematical Physics, University of Adelaide, Adelaide, SA 5005, Australia*
[b] *Institut für Kernphysik, Forschungszentrum Jülich GmbH., 52425 Jülich, Germany*

Received 12 March 1995
Editor: H. Georgi

ELSEVIER

PHYSICS LETTERS B

Aims and Scope
Physics Letters B ensures the rapid publication of letter-type communications in the fields of Nuclear Physics/Intermediate Energy Physics, High Energy Physics and Field Theory.

Abstracted/indexed in:
Current Contents: Physical, Chemical & Earth Sciences; INSPEC; Physics Briefs.

Subscription Information 1995
PHYSICS LETTERS A (ISSN 0375-9601) and PHYSICS LETTERS B (ISSN 0370-2693) will each be published weekly. For 1995 13 volumes, volumes 198–210 (78 issues altogether) of Physics Letters A have been announced. For 1995 24 volumes, volumes 341–364 (96 issues altogether) of Physics Letters B have been announced. The subscription prices for these volumes are available upon request from the Publisher. PHYSICS REPORTS (ISSN 0370-1573) will be published approximately weekly. For 1995 12 volumes, volumes 252–263 (72 issues altogether) of Physics Reports have been announced.
The subscription price for these volumes is available upon request from the Publisher.
A combined subscription to the 1995 issues of Physics Letters A, Physics Letters B and Physics Reports is available at a reduced rate.
Subscriptions are accepted on a prepaid basis only and are entered on a calendar year basis. Issues are sent by SAL (Surface Air Lifted) mail wherever this service is available. Airmail rates are available upon request. Please address all enquiries regarding orders and subscriptions to:

Elsevier Science B.V.
Order Fulfilment Department
P.O. Box 211, 1000 AE Amsterdam
The Netherlands
Tel.: +31 20 4853642, Fax: +31 20 4853598

Claims for issues not received should be made within six months of our publication (mailing) date.

U.S mailing notice - Physics Letters B (ISSN 0370-2693) is published weekly by Elsevier Science B.V., P.O. Box 211, 1000 AE Amsterdam, The Netherlands. Annual subscription price in the USA is US$ 4863.00 (valid in North, Central and South America only), including air speed delivery. Second class postage paid at Jamaica, NY 11431.
USA POSTMASTERS: Send address changes to Physics Letters B, Publications Expediting, Inc., 200 Meacham Avenue, Elmont, NY 11003.
AIRFREIGHT AND MAILING in the USA by Publications Expediting, Inc., 200 Meacham Avenue, Elmont, NY 11003.

♾ The paper used in this publication meets the requirements of ANSI/NISO 239.48-1992 (Permanence of Paper).

Printed in The Netherlands

North-Holland, an imprint of Elsevier Science

21 September 1995

PHYSICS LETTERS B

ELSEVIER

Physics Letters B 358 (1995) 139–145

Mesonic corrections to the shape of quark distributions

F.M. Steffens [a], H. Holtmann [a,b], A.W. Thomas [a]

[a] *Department of Physics and Mathematical Physics, University of Adelaide, Adelaide, SA 5005, Australia*

[b] *Institut für Kernphysik, Forschungszentrum Jülich GmbH., 52425 Jülich, Germany*

Received 12 March 1995

Editor: H. Georgi

Abstract

We compute the full x dependence of the proton and neutron spin structure functions in the MIT bag model, including the effect of gluon exchange and the meson cloud. Impressive agreement is found for x larger than 0.1, where polarised gluons are not expected to play a significant role.

At the present moment there is an impressive collection of high energy data on nucleon structure functions that defy a complete understanding. To quote a few, we mention the NMC [1] measurement of the Gottfried sum rule, the NA51 [2] measurement of the sea asymmetry and the (already classical) problem with the polarized structure functions as measured by EMC/SLAC [3–6]. In the particular case of the polarized structure functions, it now seems that one has reached the end of the "spin crisis" and the beginning of the spin problem [6,7]. As it is unlikely that perturbative QCD corrections alone are enough to solve the problem, we should examine the possibility that at least some of the discrepancy arises in the non-perturbative regime. A common approach has been to calculate the desired quantities at some low scale and then evolve them, using the QCD renormalization group equations, to the experimental scale. Unless the model has been specifically derived from QCD, the starting scale at which it best approximates the structure of the nucleon is unknown. It is usually adjusted to fit the experimental parton distributions as well as possible. Of course, one might expect that some models would give a better description of the data than others and there is considerable interest in using DIS to help choose amongst models [8].

Although there are a variety of possibilities to calculate quark distributions at the starting scale, like non-relativistic quark models [9] or vertex functions [10], here we shall work with the MIT bag. This choice is based on its success in low energy physics, its simplicity and the insights it has already yielded in connecting low and high energy data [11,12]. Of course we do not expect that the bag model alone contains all the physics we need because we know that mesons should play a role as well. For instance, we know [13] that chiral symmetry in the bag is restored through a meson cloud. Moreover, the meson cloud is already known to give important corrections to some sum rules [14–19]

As important as it is to correct the integrated quark distributions, the study of the effect of the meson cloud on the x dependence of the quark distributions themselves is at least as important [21–24]. In this letter we calculate the x dependence of the polarized and unpolarized quark distributions in the proton in a

0370-2693/95/$09.50
SSDI 0370-2693(95)00923-X

bag model dressed by mesons. We perform the calculations in next-to-leading order (NLO) QCD. Moreover, we present for the first time the x dependence of the combined effect of the N–Δ interference term [21] and one gluon exchange [22]. The interference term is important because, as noticed before [14], in the Ellis-Jaffe sum rule it cancels part of the reduction coming from pions. As we shall see, the interference terms have a determinant role in the shape of the polarized quark distribution of the neutron.

We introduce mesons in the model through the Sullivan process [25], simply noting that there are unresolved questions about the model, particularly the validity of the impulse approximation [26]. The modern study of the mesonic contribution via convolution started with Thomas [27] and was later extended to the study of structure functions by the Adelaide group [16,24,28]. A problem remaining in these calculations is the freedom for the value of the cut-off in the form factor. To avoid this problem, we shall follow the approach of the Jülich group [19,29], where the cut-off is fixed through the use of high energy pp data.

The basic hypothesis in this sort of model is that the physical nucleon wave function (in the infinite momentum frame) can be written as a superposition of a few Fock states:

$$|N\rangle_{\text{phys}} = Z^{1/2}\Big[|N\rangle_{\text{bare}} + \sum_{BM}\int_0^1 dx \int d^2k_\perp \phi_{BM}(x,k_\perp) \times |B(x,k_\perp), M(1-x,-k_\perp)\rangle\Big]. \quad (1)$$

The wave function renormalization factor

$$Z = \Big[1 + \sum_{BM}\int_0^1 dx \int d^2k_\perp |\phi_{BM}(x,k_\perp)|^2\Big]^{-1} \quad (2)$$

measures the probability that the physical nucleon contains a bare nucleon. The Fock states used in our calculation involve the low mass particles which are important to describe nucleon properties, namely the nucleon $SU(3)$ octet (N, Λ, Σ) and decuplet (Δ, Σ^*) and the first pseudoscalar and vector meson octet (π, K, ρ, ω, K^*). We have included the hyperon-kaon contributions for completeness, but their actual size is very small ($\sim 2\%$) [19,20,28].

The Fock state expansion Eq. (1) has consequences for the structure function of the nucleon. Due to the presence of baryon-meson Fock states, the virtual photon can scatter either on the nucleon core or on the meson-baryon system. Formally, the quark distribution $q(x)$ of the nucleon is given by:

$$q(x) = Z\left[q^N_{\text{bare}}(x) + \sum_{BM}\left(\delta^M q(x) + \delta^B q(x)\right)\right]. \quad (3)$$

The contributions from the virtual meson and baryon can be written as the convolution of the meson (baryon) structure function with its longitudinal momentum distribution in the nucleon:

$$\delta^M q(x) = \int_x^1 f_{MB}(y) q^M\left(\frac{x}{y}\right)\frac{dy}{y},$$

$$\delta^B q(x) = \int_x^1 f_{BM}(y) q^B\left(\frac{x}{y}\right)\frac{dy}{y}, \quad (4)$$

where f_{MB} and f_{BM} are given by:

$$f_{MB}(x) = \int d^2k_\perp |\phi_{BM}(1-x,-k_\perp)|^2,$$

$$f_{BM}(x) = \int d^2k_\perp |\phi_{BM}(x,k_\perp)|^2. \quad (5)$$

In order to conserve charge and momentum, we have the following relation:

$$f_{BM}(1-y) = f_{MB}(y). \quad (6)$$

The functions $f_{BM}(y)$ and $f_{MB}(y)$ can be calculated using time ordered perturbation theory in the infinite momentum frame [28,29,31]. The analytic forms for $f_{BM}(y)$ and $f_{MB}(y)$ can be found in Refs. [28,29].

In practical calculations we need more information, namely the various coupling constants and the vertex form factors G_{BM}. The coupling constants can be extracted from scattering experiments and are rather well known [30]. For the vertex form factor we use an exponential parametrization:

$$G_{BM} = \exp\left[\frac{1}{2\Lambda^2_{BM}}(m_N^2 - M^2_{BM}(y,k_\perp^2))\right], \quad (7)$$

with

$$M^2_{MB}(y,k^2_\perp) = \frac{m^2_B + k^2_\perp}{y} + \frac{m^2_M + k^2_\perp}{1-y}.$$

The cut-off parameters Λ_{BM} can be estimated, using one boson exchange models, from n, Λ and Δ^{++} production in high energy pp scattering (for details see Ref. [19]). They were found to be $\Lambda_{N\pi} = \Lambda_{N\rho} = 1.08$ GeV and $\Lambda_{\Delta\pi} = \Lambda_{\Delta\rho} = 0.98$ GeV. The procedure used to obtain the cut-off parameters may be questioned because the assumption of single meson exchange being responsible for the process is fairly simple. However, it certainly gives an upper bound for the values of the various Λ's.

At this point we are still left without the input distributions in Eqs. (3) and (4). For the quark distribution in the pion we use a recent parameterization by Sutton et al. [32]. By using $SU(3)$ symmetry, the quark distributions of all the mesons can then be obtained. For the bare quark distribution of the baryons we use the bag model calculation of the Adelaide group [11,33]. The main advantage of this method is that it ensures energy-momentum conservation and hence the correct support of the quark distributions. It has also been successful in describing data at high momentum transfer, Q^2, both in leading order [11] and in next-to-leading order [12]. Mesonic corrections lead to further improvement in the predictions of the model and will, among other things, reduce the amount of evolution needed [34]. The form of the quark distribution is given by [11]:

$$q^{\uparrow\downarrow}_f(x) = \frac{M}{(2\pi)^2}\sum_m \langle\mu|P_{f,m}|\mu\rangle \times \int_{[M^2(1-x)^2 - M^2_n]/2M(1-x)}^{+\infty} |\,\boldsymbol{p}_n\,|\,d\,|\,\boldsymbol{p}_n\,| \times \frac{|\phi_2(\boldsymbol{p}_n)|^2}{|\phi_3(0)|^2}|\tilde{\psi}^{\uparrow\downarrow}_m(\boldsymbol{p}_n)|^2. \quad (8)$$

Here $|\mu\rangle$ is the spin-flavor part of the wave function of the initial state (at rest), $P_{f,m}$ makes the projection onto flavor f and spin projection m, M_n is the mass of the intermediate state and $\tilde{\psi}$ the Fourier transform of the quark wavefunction. Eq. (8) gives the two quark contribution to the total quark distribution which dominates at intermediate and large x. We should also account for the contributions coming from four quarks in the intermediate state, but for simplicity we shall mimic this contribution by a term of the form $(1-x)^7$, properly normalized (further discussion on this subject can be found in Ref. [11]).

We use the MRS parametrization [35] of the unpolarized structure functions to fix the parameters of the model; e.g., the radius of the bag, the average mass of the spin scalar (M_s) and spin vector (M_v) diquark in the intermediate state and the low scale, μ^2, at which the model is supposed to be valid. In Fig. 1 we show the total valence distribution computed in NLO [1] in the $\overline{\rm MS}$ scheme for the bag dressed with mesons. Very good agreement with the MRS parametrization is found for $\mu^2 = 0.165$ GeV^2, $R = 0.8$ fm, $M_s = 0.65$ GeV and $M_v = 0.85$ GeV. For comparison, we also show the bare bag calculated with the same set of parameters. The bonus of the NLO fit is that it provides a decrease of α_s at μ^2 from ~ 1.52 in a LO fit to ~ 0.6 in NLO. This is also a drop in comparison with the value $\alpha_s \sim 0.77$ found in a NLO fit without mesons [12]. For completeness, we note that these values of the coupling constant were found using $\Lambda_{\rm QCD} = 0.2$ GeV and three active flavors.

After we have fixed all parameters in the unpolarized deep inelastic scattering sector, we can explore the consequences for the polarized sector. The calculation of effects due to the presence of higher BM Fock states for the $g_1(x)$ structure function is similar to those for $q(x)$ given in Eq. (3). The contribution from the scattering on the recoil baryon is

$$\delta^B\Delta q(x) = \sum_M \int_x^1 d_{BM}(y)\Delta q^B\left(\frac{x}{y}\right)\frac{dy}{y}, \quad (9)$$

where $d_B(y)$ is the polarized, longitudinal momentum distribution. It can be calculated using the same techniques as for the unpolarized case (for details see [19]). The mesonic contribution vanishes because of the pseudoscalar character of the pion. The main difference from the unpolarized structure function is the presence of the N–Δ interference term [21], which can also be written as a convolution [29]:

[1] Details for the NLO calculation in the bag can be found in [12].

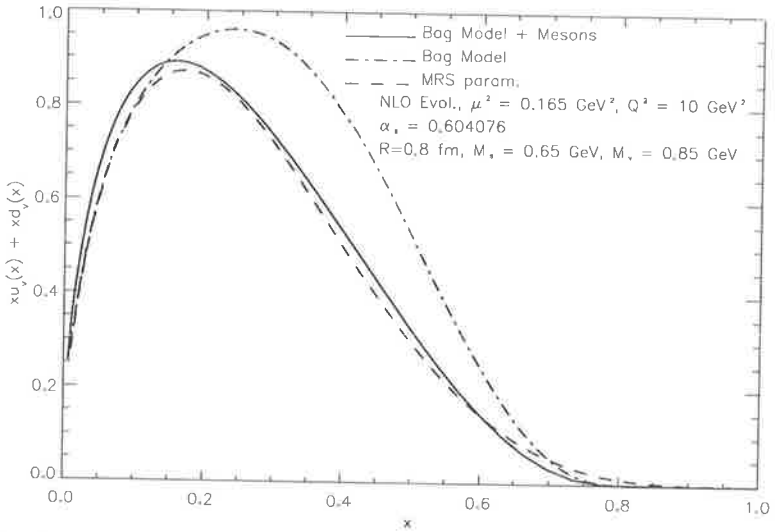

Fig. 1. Total valence distribution in the bag and in the bag dressed with mesons compared with the MRS [35] parametrization of the data in the $\overline{\text{MS}}$ scheme. The quark distributions are evolved in next-to-leading-order QCD.

$$\delta^{\text{int}}\Delta q(x) = \int_x^1 d_{\text{int}}(y)\Delta q^{N\Delta}\left(\frac{x}{y}\right)\frac{dy}{y}. \tag{10}$$

The necessary polarized splitting functions d_{BM} and d_{int} can be found in the Appendix.

Combining all these contributions, g_1 for the nucleon is given by:

$$g_1^{\text{phys}} = Z\left[g_1^{\text{bare}} + \sum_{BM}\left(\delta^B g_1^B + \delta g_1^{\text{int}}\right)\right]. \tag{11}$$

We now apply Eqs. (9)–(11) to calculate $g_1(x)$. In the meson sector only the pseudoscalars are included. The vector mesons are omitted because we are not aware of any model to extract their polarized quark distribution functions. Once again we need a model for the bare quark distributions in the nucleon and, as before, we use the MIT bag model. For the polarized case we need to specify the spin-flavor part of the wave function. We shall use the usual $SU(6)$ wave function in which case, for the interference terms, we have:

$$\langle p^\uparrow, n^\uparrow|u^\uparrow|\Delta^{+,\uparrow}, \Delta^{0,\uparrow}\rangle = \langle p^\uparrow, n^\uparrow|d^\downarrow|\Delta^{+,\uparrow}, \Delta^{0,\uparrow}\rangle = \frac{\sqrt{2}}{3}, \tag{12}$$

$$\langle p^\uparrow, n^\uparrow|u^\downarrow|\Delta^{+,\uparrow}, \Delta^{0,\uparrow}\rangle = \langle p^\uparrow, n^\uparrow|d^\uparrow|\Delta^{+,\uparrow}, \Delta^{0,\uparrow}\rangle = -\frac{\sqrt{2}}{3}. \tag{13}$$

We notice that in the matrix elements (12) and (13) only mixed symmetric terms contribute and, as a consequence, the intermediate state always forms a spin vector.

The first moment of the polarized structure function for the proton, $g_1^p(x)$, is expressed in NLO as:

$$\int_0^1 g_1^p(x,Q^2)dx = \left(\frac{g_a}{12} + \frac{g_8}{36}\right)\left(1 - \frac{\alpha_s(Q^2)}{\pi}\right) + \frac{g_0}{9}\left(1 - \frac{\alpha_s(Q^2)}{3\pi}\right), \tag{14}$$

with g_a and g_8 nonsinglet distributions and g_0 a singlet distribution. However, the full singlet anomalous dimensions (for any moment) for polarized scattering in NLO are still not known and, because of that, it is not possible to calculate the x dependence of g_0 in NLO. Faced with this problem, we decided to take the following two approaches to the evolution of g_1:

– In the first approach, *case (a)*, we evolve g_a and g_8 as nonsinglet in NLO and evolve g_0 as a singlet in LO so that g_0 does not pick up the $(1 - \frac{\alpha_s(Q^2)}{3\pi})$ correction and the whole structure function is overestimated.

– In the second approach, *case (b)*, we treat g_a, g_8 and g_0 as nonsinglet combinations and evolve them in NLO. In this case, g_0 picks up a correction of the form $(1 - \frac{\alpha_s(Q^2)}{\pi})$ such that the corrections due to the NLO evolution are overestimated and the structure function is underestimated. The actual curve must be somewhere between the two approaches.

In Fig. 2 we show the EMC and earlier SLAC data for $xg_1^p(x)$ together with the bare bag, the bag plus mesons but without the N–Δ mixing terms and the bag plus mesons plus mixing terms. We stress that the parameters for the bare bag differ significantly from those used in earlier calculations [11]. The meson cloud lowers the bag model prediction over the entire range of x, in accordance with earlier estimates for the Ellis-Jaffe sum rule in the bag [14]. This is because some of the spin of the nucleon is carried as angular momentum by the mesons. The actual value of the calculated Ellis-Jaffe sum rule at 10 GeV^2 drops from 0.209 in the bare bag to ~ 0.173 in the bag plus mesons for case (a) and to ~ 0.169 for case (b). The actual value of the sum rule in the bag model plus mesons, calculated using Eq. (14) as it stands, is ~ 0.171, supporting our claim that the full NLO prediction for the x dependence of $g_{1p}(x)$ in the present model is somewhere between the results for case (a) and (b) of Fig. 2. The inclusion of vector mesons is expected to reduce the value of the sum rule somewhat more.

The x dependence for the model, compared with the SLAC E143 data [6] for $g_1^p(x)$, is shown in Fig. 3, and is quite impressive. These data were taken at an average 3 GeV^2 and have smaller error bars than earlier experiments. Comparison with this set is also a good test of our model once we have to move to a different Q^2. The resulting agreement between theoretical and experimental values for $g_1(x)$ is inspiring and provides some confidence in the model. At this value of Q^2 the calculated value for the Ellis-Jaffe sum rule is ~ 0.171 for case (a) and ~ 0.166 for case (b).

These results shed light on how the spin in the physical proton is shared, suggesting strongly that mesons are responsible for part of the dilution of the spin. In general, we can say that the agreement between the data and the theoretical calculation is very impressive and that further corrections might well bring the entire curve within experimental errors. For instance, we

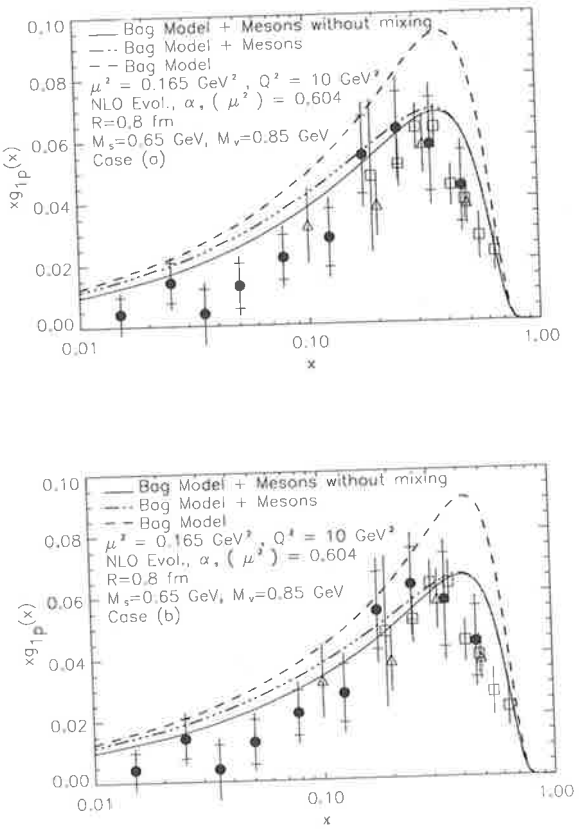

Fig. 2. Polarized quark distribution of the proton as measured by the EMC collaboration [3] against theoretical predictions for a bare bag, a bag with mesons without mixing terms and a bag with mesons and mixing terms.

know that in the axial gauge the axial anomaly is related to the polarized gluon distribution [36]. In this context, we think that a reasonable polarized gluon distribution [37] could bring the curve down in the region $x < 0.4$.

We would also like to call attention to the role of the N–Δ mixing term. As said before, it tends to increase the Ellis-Jaffe sum rule. In fact, if the mixing terms were absent, the new value of the sum rule at $Q^2 = 10$ GeV^2 would be ~ 0.159 for case (a) and ~ 0.155 for case (b). For the Q^2 compatible with the SLAC E143 data, these values would be reduced to ~ 0.158 for case (a) and to ~ 0.152 for case(b). Figs. 2 and 3 tell us that the rise of $g_1^p(x)$ due to the mixing terms is confined to the region $x \leq 0.3$. This is because for the mixing term, the mass of the intermediate state is always M_v, and then the contribution

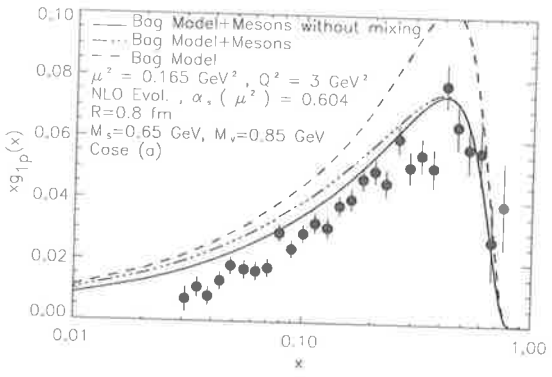

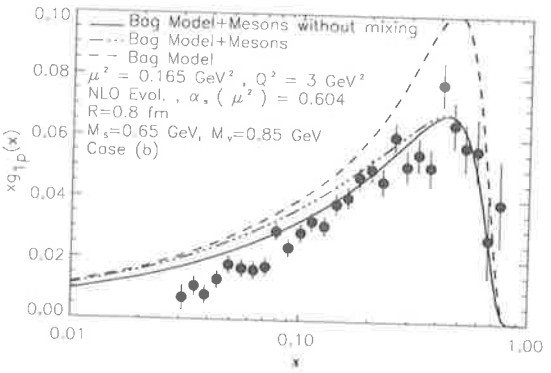

Fig. 3. Polarized quark distribution of the proton as measured by the SLAC E143 experiment [6] against theoretical predictions for a bare bag, a bag with mesons without mixing terms and a bag with mesons and mixing terms.

is isolated at smaller x when compared with the other contributions (similar to the down quark distribution in the bag [11]).

The most interesting effect associated with the mixing terms can be observed in Fig. 4, where $g_1^n(x)$ is shown. Although in $g_1^p(x)$ the effect of the mixing terms in the x distribution is not too dramatic because one is adding a small number to a large number, in $g_1^n(x)$ the effect is relatively large because one is subtracting from numbers near to zero. In fact, for $g_1^n(x)$ the mixing terms are essential to give to the theoretical curve the shape of the experimental data as measured by the SLAC E142 [5] experiment. The first moment of the calculated polarized distribution of the neutron turns out to be ~ 0.004 for case (a) and ~ -0.003 for case (b). It is also worth noticing that there is a consistency between the calculation of

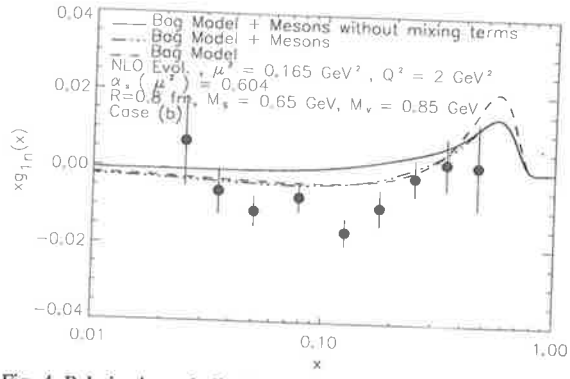

Fig. 4. Polarized quark distribution of the neutron as measured by the SLAC E142 experiment [5] against theoretical predictions for a bare bag, a bag with mesons without mixing terms and a bag with mesons and mixing terms.

$g_{1p}(x)$ and $g_{1n}(x)$ – the same calculation that fits the unpolarized data also makes a good prediction for both $g_{1p}(x)$ and $g_{1n}(x)$.

We would like to thank S. Bass, W. Melnitchouk, G. Piller, A.W. Schreiber and J. Speth for valuable discussions during the development of this work. One of the authors (H.H.) would like to thank the German Academic Exchange Service (DAAD) for financial support for his visit to Adelaide. This work was supported by the Australian Research Council, by the DAAD and by CAPES (Brazil).

Appendix A

$$d_{N\pi}(y) = \frac{g_{NN\pi}^2}{16\pi^2}\int_0^\infty dk_\perp^2 \frac{|G_{N\pi}(y,k_\perp^2|^2}{y^2(1-y)} \times \frac{m_N^2(1-y)^2 - k_\perp^2}{[m_N^2 - M_{N\pi}^2(y,k_\perp^2)]^2}, \tag{A.1}$$

$$d_{\Delta\pi}(y) = \frac{g_{N\Delta\pi}^2}{96\pi^2}\int_0^\infty dk_\perp^2 \frac{|G_{\Delta\pi}(y,k_\perp^2)|^2}{y^4(1-y)m_\Delta^2} \times [(ym_N + m_\Delta)^2 + k_\perp^2] \times \frac{[(y^2m_N^2 - m_\Delta^2)^2 + 8ym_Nm_\Delta k_\perp^2 - k_\perp^4]}{[m_N^2 - M_{\Delta\pi}^2(y,k_\perp^2)]^2}. \tag{A.2}$$

and

$$d_{\rm int}(y) = \frac{g_{N\Delta\pi} g_{NN\pi}}{16\sqrt{6}\pi^2} \int_0^\infty dk_\perp^2 \frac{G_{\Delta\pi}(y,k_\perp^2) G_{N\pi}(y,k_\perp^2)}{y^3(1-y)m_\Delta}$$
$$\times \left\{ \frac{-m_N(1-y)(ym_N+m_\Delta)^2(ym_N-m_\Delta)}{[m_N^2 - M_{\Delta\pi}^2(y,k_\perp^2)][m_N^2 - M_{N\pi}^2(y,k_\perp^2)]} \right.$$
$$\left. + \frac{(2m_\Delta^2 + (3y-2)m_N m_\Delta - ym_N^2)k_\perp^2 - k_\perp^4}{[m_N^2 - M_{\Delta\pi}^2(y,k_\perp^2)][m_N^2 - M_{N\pi}^2(y,k_\perp^2)]} \right\}. \quad \text{(A.3)}$$

References

[1] NMC, P. Amaudruz et al., Phys. Rev. Lett. 66 (1991) 2712.
[2] NA51, A. Baldit et al., Phys. Lett. B 332 (1994) 244.
[3] EMC, J. Ashman et al., Nucl. Phys. B 328 (1989) 1.
[4] SMC, B. Adeva et al., Phys. Lett. B 302 (1993) 533.
[5] SLAC E142, P.L. Anthony et al., Phys. Rev. Lett 71 (1993) 959.
[6] SLAC E143, K. Abe et al., preprint SLAC-PUB-6508.
[7] A.W. Thomas, Invited paper at SPIN '94, Bloomington, September 1994, hep-ph/9410335.
[8] A.W. Thomas, Prog. Part. Nucl. Phys. 20 (1988) 21.
[9] M. Traini, L. Conci and U. Moschella, Nucl. Phys. A 554 (1992) 731;
C.J. Benesh, T. Goldman and G.J. Stephenson, Jr., Phys. Rev. C 48 (1993) 1379;
H.J. Weber, U. Virginia preprint (1994).
[10] H. Meyer and P.J. Mulders, Nucl. Phys. A 528 (1991) 589;
P.J. Mulders, A.W. Schreiber and H. Meyer, Nucl. Phys. A 549 (1992) 498;
W. Melnitchouk, A.W. Schreiber and A.W. Thomas, Phys. Rev. D 49 (1994) 127;
W. Melnitchouk and W. Weise, Phys. Lett. B 334 (1994) 275.
[11] A.W. Schreiber, A.W. Thomas and J.T. Londergan, Phys. Rev. D 42 (1990) 2226;
A.W. Schreiber, A.I. Signal and A.W. Thomas, Phys. Rev. D 44 (1991) 2653.
[12] F.M. Steffens and A.W. Thomas, Adelaide preprint ADP-94-27/T166.
[13] A.W. Thomas, Adv. Nucl. Phys. 13 (1984) 1.
[14] A.W. Schreiber and A.W. Thomas, Phys. Lett. B 215 (1988) 141.
[15] H. Høgassen and F. Myhrer, hep-ph 9501414; Z. Phys. C 48 (1990) 295.
[16] A.I. Signal, A.W. Schreiber and A.W. Thomas, Mod. Phys. Lett. A 6 (1991) 271.
[17] W. Koepf, E.M. Henley and M. Alberg, University of Washington preprint DOE/ER/40427-08-N94.
[18] A. Szczurek, J. Speth and G.T. Garvey, Nucl. Phys. A 555 (1993) 249.
[19] H. Holtmann, A. Szczurek and J. Speth, Jülich preprint KFA-IKP(TH)-1993-33.
[20] A.I. Signal and A.W. Thomas, Phys. Lett. B 191 (1987) 3.
[21] A.W. Schreiber, P.J. Mulders, A.I. Signal and A.W. Thomas, Phys. Rev. D 45 (1992) 3069.
[22] F.E. Close and A.W. Thomas, Phys. Lett. B 212 (1988) 227.
[23] S. Kumano and J.T. Londergan, Phys. Rev. D 44 (1991) 717.
[24] W. Melnitchouk, A.W. Thomas and A.I. Signal, Z. Phys. A 340 (1991) 85.
[25] J.D. Sullivan, Phys. Rev. D 5 (1972) 1732.
[26] R.L. Jaffe, in: Relativistic Dynamics and Quark - Nuclear Physics, eds. M.B. Johnson and A. Pickleseimer (New York, Wiley, 1985) p. 537.
[27] A.W. Thomas, Phys. Lett. B 126 (1983) 97.
[28] A.W. Thomas and W. Melnitchouk, in: New Frontiers in Nuclear Physics, eds. S. Homma, Y. Akaishi and M. Wada (World Scientific, Singapore, 1993) pp. 41–106.
[29] H. Holtmann, A. Szczurek and J. Speth, Jülich preprint KFA-IKP(TH)-1994-25.
[30] R. Machleidt, K. Holinde and Ch. Elster, Phys. Rep. 149 (1987) 1.
[31] V.R. Zoller, Z. Phys. C 54 (1992) 425;
W. Melnitchouk and A.W. Thomas, Phys. Rev. D 47 (1993) 3794.
[32] P.J. Sutton, A.D. Martin, R.G. Roberts and W. Stirling, Phys. Rev. D 45 (1992) 2349.
[33] A.I. Signal and A.W. Thomas, Phys. Lett. B 211 (1988) 481; Phys. Rev. D 40 (1989) 2832.
[34] A.W. Thomas, Nucl. Phys. A 518 (1990) 186.
[35] A.D. Martin, W.J. Stirling and R.G. Roberts, Phys. Lett. B 306 (1993) 145.
[36] G. Altarelli and G.G. Ross, Phys. Lett. B 212 (1988) 391;
R.D. Carlitz, J.C. Collins and A.H. Mueller, Phys. Lett. B 214 (1988) 299;
A.V. Efremov, J. Soffer and O.V. Teryaev, Nucl. Phys. B 246 (1990) 97;
S.D. Bass, B.L. Ioffe, N.N. Nikolaev and A.W. Thomas, J. Moscow Phys. Soc. 1 (1991) 317;
S.D. Bass, Z. Phys. C 60 (1993) 343;
S.D. Bass and A.W. Thomas, Prog. Part. Nucl. Phys. 33 (1994) 449.
[37] T. Gehrmann and W.J. Stirling, Durham preprint DTP/94/38 (1994), hep-ph-9406212.

PHYSICS LETTERS B

Instructions to Authors (short version)

(A more detailed version of these instructions is published in the preliminary pages to each volume.)

Submission of papers

Manuscripts (one original + two copies), accompanied by a covering letter, should be sent to one of the Editors indicated on page 2 of the cover.

Original material. By submitting a paper for publication in Physics Letters B the authors imply that the material has not been published previously nor has been submitted for publication elsewhere and that the authors have obtained the necessary authority for publication.

Refereeing. Submitted papers will be refereed and, if necessary, authors may be invited to revise their manuscript. If a submitted paper relies heavily on unpublished material, it would be helpful to have a copy of that material for the use of the referee.

Types of contributions

Letters. The total length of the paper should preferably not exceed four journal pages, equivalent to seven typewritten pages with double spacing, including the list of authors, abstract, references, figure captions and three figures. In the case that more figures are required, the text should be shortened accordingly. As proofs will *not* be sent, authors should check their papers carefully before submission.

Manuscript preparation

All manuscripts should be written in good English. The paper copies of the text should be prepared with double line spacing and wide margins, on numbered sheets. See notes opposite on electronic version of manuscripts.

Structure. Please adhere to the following order of presentation: Article title, Author(s), Affiliation(s), Abstract, PACS codes and keywords, Main text, Acknowledgements, Appendices, References, Figure captions, Tables.

Corresponding author. The name, complete postal address, telephone and fax numbers and the e-mail address of the corresponding author should be given on the first page of the manuscript.

PACS codes/keywords. Please supply one or more relevant PACS-1995 classification codes and 6–8 keywords of your own choice for indexing purposes.

References. References to other work should be consecutively numbered in the text using square brackets and listed by number in the Reference list. Please refer to the more detailed instructions for examples.

Illustrations

Illustrations should also be submitted in triplicate: one master set and two sets of copies. The *line drawings* in the master set should be original laser printer or plotter output or drawn in black india ink, with careful lettering, large enough (3–5 mm) to remain legible after reduction for printing. The *photographs* should be originals, with somewhat more contrast than is required in the printed version. They should be unmounted unless part of a composite figure. Any scale markers should be inserted on the photograph, not drawn below it.

Colour plates. Figures may be published in colour, if this is judged essential by the Editor. The Publisher and the author will each bear part of the extra costs involved. Further information is available from the Publisher.

After acceptance

Notification. You will be notified by the Editor of the journal of the acceptance of your article and invited to supply an electronic version of the accepted text, if this is not already available.

Copyright transfer. You will be asked to transfer the copyright of the article to the Publisher. This transfer will ensure the widest possible dissemination of information.

No proofs. In order to speed up publication, all proofreading will be done by the Publisher and proofs are *not* sent to the author(s).

Electronic manuscripts

The Publisher welcomes the receipt of an electronic version of your accepted manuscript (preferably encoded in LaTeX). If there is not already a copy of this (on diskette) with the journal Editor at the time the manuscript is being refereed, you will be asked to send a file with the text of the accepted manuscript directly to the Publisher by e-mail or on diskette (allowed formats 3.5" or 5.25" MS-DOS, or 3.5" Macintosh) to the address given below. Please note that no deviations from the version accepted by the Editor of the journal are permissible without the prior and explicit approval by the Editor. Such changes should be clearly indicated on an accompanying printout of the file.

Author benefits

No page charges. Publishing in Physics Letters B is free.

Free offprints. The corresponding author will receive 50 offprints free of charge. An offprint order form will be supplied by the Publisher for ordering any additional paid offprints.

Discount. Contributors to Elsevier Science journals are entitled to a 30% discount on all Elsevier Science books.

Contents Alert. Physics Letters B is included in Elsevier's pre-publication service Contents Alert.

Further information (after acceptance)

Elsevier Science B.V., Physics Letters B
Desk Editorial Department
P.O. Box 103, 1000 AC Amsterdam
The Netherlands
Tel.: + 31 20 4852634
Fax: + 31 20 4852319
E-mail: NHPDESKED@ELSEVIER.NL

North-Holland, an imprint of Elsevier Science

PHYSICAL REVIEW D VOLUME 53, NUMBER 3 1 FEBRUARY 1996

Role of strange and charm quarks in the nucleon spin structure function

F. M. Steffens and A. W. Thomas
Department of Physics and Mathematical Physics, University of Adelaide, Adelaide, S.A. 5005, Australia
(Received 1 September 1995)

We perform an analysis of the relation between the factorization scale and the masses of the quarks in the calculation of the hard gluon coefficient in polarized deep inelastic scattering. Particular attention is paid to the role of strange and charm quarks at finite momentum transfer. It is found that for the momentum transfer of the present experiments the contribution from the charm quark is significant.

PACS number(s): 13.60.Hb, 12.38.Bx, 13.88.+e

I. INTRODUCTION

In the usual analysis of the proton spin structure function, based upon QCD and the operator product expansion (OPE), the moments of the singlet part of $g_1(x,Q^2)$ are written as

$$\int_0^1 g_1^{(s)}(x,Q^2)x^{n-1}dx = \Delta\Sigma_n(\mu^2)C_n^q(Q^2/\mu^2) + \Delta g_n(\mu^2)C_n^g(Q^2/\mu^2), \quad (1)$$

with $C_n^q(Q^2/\mu^2) = 1 + O(\alpha_s)$ the Wilson coefficients for the quark operators and $C_n^g(Q^2/\mu^2) = O(\alpha_s)$ the Wilson coefficients for the gluon operators. The matrix elements $\Delta\Sigma_n(\mu^2)$ and $\Delta g_n(\mu^2)$ are not determined by perturbative QCD and should be either fixed by experimental constraints or calculated using nonperturbative techniques. Equation (1) can be inverted, using the inverse Mellin transformation, and the result is

$$g_1^{(s)}(x,Q^2) = \Delta\Sigma(x,\mu^2)\otimes C^q(x,Q^2/\mu^2) + \Delta g(x,\mu^2)\otimes C^g(x,Q^2/\mu^2), \quad (2)$$

where $\otimes$ denotes a convolution of the two functions.

Much of the debate on the proton spin in the last few years has been centered on whether or not the spin of the proton receives a contribution from the gluons [1–6]. On the basis of the OPE the picture is clear: there is no twist-2 gluon operator contributing to the first moment of g_1, and hence $\int_0^1 C^g(x,Q^2/\mu^2)dx = 0$. This result implies that the first moment of g_1 is given solely by the first moment of $\Delta\Sigma$. If $\Delta\Sigma$ were identified with the spin in the proton carried by the quarks then the gluons would give no contribution. In this scenario, following the parton model language, $\Delta\Sigma_n(\mu^2) = N\sum_f \Delta f_n(\mu^2)$, with $\Delta f = \Delta f_1$ the amount of spin carried by the f quark and $N = 1/9$ for three flavors, $5/36$ for four flavors, etc. It happens that $\Delta\Sigma$ cannot be identified with spin because of the axial anomaly. Indeed, the axial anomaly is at the heart of the disagreement between the OPE and the improved parton model (IPM) results for the role of gluons in the first moment of $g_1(x,Q^2)$. In this contribution, we are not going to make a complete analysis of the equivalence (or otherwise) of these approaches but will limit ourselves to the analysis of the gluon contribution in the light of the IPM only.

In the IPM the situation is more complicated. One calculates the full, polarized photon-proton cross section and uses the factorization theorem to separate the hard and soft parts:

$$\sigma^{\gamma^v N}(x,Q^2) = \sigma_h^{\gamma^v q}(x,Q^2/\mu^2)\otimes\Delta f_{q/N}(x,\mu^2) + \sigma_h^{\gamma^v g}(x,Q^2/\mu^2)\otimes\Delta f_{g/N}(x,\mu^2), \quad (3)$$

where μ^2 is the factorization scale, $\Delta f_{q(g)/N}$ is the polarized quark (gluon) spin distribution inside the nucleon, and σ_h is the polarized, hard photon-quark or hard photon-gluon cross section. One then could relate g_1 calculated in the IPM, Eq. (3), to g_1 calculated in the OPE, Eq. (2), by identifying the hard, perturbatively calculated, Wilson coefficients with the hard photon-quark and hard photon-gluon cross sections and identifying the matrix element $\Delta\Sigma(x,\mu^2)$ $[\Delta g(x,\mu^2)]$ with the factorized quark [gluon] distribution $\Delta f_{q(g)/N}$. However, as already mentioned, $\Delta\Sigma(x,\mu^2)$ cannot be identified with the quark spin distribution. The relation between them is beyond the scope of the present work. Instead, we will concentrate on the relation between the Wilson gluon coefficient and the hard gluon cross section of the IPM. Although there are excellent treatments of this subject in the literature [2, 6–8], we think that the present contribution adds significantly to the understanding of the behavior of $g_1(x,Q^2)$ at finite Q^2.

In Sec. II we will develop the basis for the calculation of the hard gluon coefficient in the IPM. The resulting expression interpolates the known limits of $-\frac{\alpha_s}{2\pi}N_f$ for $m_q^2 \ll \mu^2$ and 0 for $m_q^2 \gg \mu^2$ and overcomes convergence problems found in an early work [9]. The effects of this generalized, hard gluon coefficient are discussed in Sec. III. In particular, its effect on the contribution to $g_1^p(x,Q^2)$ from up, down, strange, and charm quarks is studied. Our results indicate that these corrections are sizable and must therefore be taken into account when extracting the polarized gluon distribution from the proton. We also point out in this section how this anomalous contribution is affected by finite Q^2. In Sec. IV we calculate the amount of polarized gluon in the proton necessary to explain the available data. We compare our

result with other estimates made using simply the limiting cases for the hard gluon coefficients. Section V is used to study the region in x where this contribution is located. In Sec. VI we summarize the results obtained in this article.

II. THEORETICAL CONSTRUCTION

The hard gluon cross section is extracted from the full photon-gluon fusion cross section $\sigma^{\gamma^* g}$ and is calculated through the box graphs which start at order α_s. The other contribution from which it must be separated is the quark distribution inside the gluon [7]. Mathematically this is expressed as

$$\sigma^{\gamma^* g}(x,Q^2) = \sigma_h^{\gamma^* g}(x,Q^2/\mu^2) + \Delta q^g(x,\mu^2), \tag{4}$$

where Δq^g is the polarized quark distribution inside a gluon and $\sigma_h^{\gamma^* g}$ is the hard photon-gluon cross section defined, in the IPM, as the contribution coming from quarks in the box graph with transverse momenta greater than the factorization scale.

The full photon-gluon cross section has been calculated to be [10, 11]

$$\begin{aligned}\sigma^{\gamma^* g}(x,Q^2) = -\frac{\alpha_s}{2\pi}N_f \frac{\sqrt{1-\frac{4m_q^2}{W^2}}}{1-\frac{4x^2P^2}{Q^2}}\Bigg\{&(2x-1)\left(1-\frac{2xP^2}{Q^2}\right)\\ &\times\left[1-\frac{1}{\sqrt{1-\frac{4m_q^2}{W^2}}\sqrt{1-\frac{4x^2P^2}{Q^2}}}\ln\left(\frac{1+\sqrt{1-\frac{4m_q^2}{W^2}}\sqrt{1-\frac{4x^2P^2}{Q^2}}}{1-\sqrt{1-\frac{4m_q^2}{W^2}}\sqrt{1-\frac{4x^2P^2}{Q^2}}}\right)\right]\\ &+\left(x-1+\frac{xP^2}{Q^2}\right)\frac{2m_q^2(1-\frac{4x^2P^2}{Q^2})-P^2x(2x-1)(1-\frac{2xP^2}{Q^2})}{m_q^2(1-\frac{4x^2P^2}{Q^2})-P^2x(x-1+\frac{xP^2}{Q^2})}\Bigg\},\end{aligned} \tag{5}$$

with $P^2 = -p^2$ the gluon virtuality, m_q the quark mass, and $W^2 = \frac{Q^2(1-x)-P^2x}{x}$ the invariant mass squared of the photon-gluon system. For very large momentum transfer, $Q^2 \gg m_q^2, P^2$, the full cross section reduces to

$$\sigma^{\gamma^* g}(x,Q^2/\mu^2) = \frac{\alpha_s}{2\pi}N_f\left[(2x-1)\left(\ln\frac{Q^2}{m_q^2+P^2x(1-x)}+\ln\frac{1-x}{x}-1\right)+(1-x)\frac{2m_q^2-P^2x(2x-1)}{m_q^2+P^2x(1-x)}\right]. \tag{6}$$

It remains to calculate Δq^g. This is given by computing the triangle diagram or, equivalently, the integral over the transverse momentum of the square of the norm of the light-cone $q\bar{q}$ wave function of the gluon [2, 7, 12]. As Δq^g is a soft contribution, the integral over the transverse momentum has to have a cutoff:

$$\begin{aligned}\Delta q^g(x,\mu^2) &= \frac{\alpha_s}{2\pi}N_f\int_0^{\mu^2} dk_\perp^2 \frac{m_q^2+(2x-1)k_\perp^2}{[m_q^2+P^2x(1-x)+k_\perp^2]^2}\\ &= \frac{\alpha_s}{2\pi}N_f\left\{(2x-1)\ln\left(\frac{\mu^2+P^2x(1-x)+m_q^2}{m_q^2+P^2x(1-x)}\right)+(1-x)\frac{2m_q^2+P^2x(1-2x)}{m_q^2+P^2x(1-x)}\frac{\mu^2}{\mu^2+P^2x(1-x)+m_q^2}\right\}.\end{aligned} \tag{7}$$

Equation (7) is a generalization of previous results [2, 7] including the dependence on the factorization scale for any values of the quark masses and gluon virtuality. Its first moment is zero for $\mu^2 \ll m_q^2, P^2$. If $\mu^2 \gg m_q^2, P^2$ the first moment of $\Delta q^g(x,\mu^2)$ is 0 for $P^2 \gg m_q^2$, while it is $\frac{\alpha_s}{2\pi}N_f$ for $m_q^2 \gg P^2$. Using Eqs. (4), (6), and (7) we can calculate the hard gluon coefficient:

$$\begin{aligned}\sigma_h^{\gamma^* g}(x,Q^2,\mu^2) = \frac{\alpha_s}{2\pi}N_f\Bigg\{&(2x-1)\left[\ln\left(\frac{Q^2}{\mu^2+P^2x(1-x)+m_q^2}\right)+\ln\left(\frac{1-x}{x}\right)-1\right]\\ &+(1-x)\frac{2m_q^2+P^2x(1-2x)}{\mu^2+m_q^2+P^2x(1-x)}\Bigg\}.\end{aligned} \tag{8}$$

Notice that the first moment of Eq. (8) does not depend on the ratio m_q^2/P^2 in the region $\mu^2 \gg m_q^2, P^2$—it is a legitimate hard contribution. Equation (8) is also a generalization of previous results and from its limit, $\mu^2 \gg m_q^2, P^2$, it may be argued [1] that the gluons contribute to the first moment of $g_1(x,Q^2)$ because $\int_0^1 \sigma_h^{\gamma^* g}(x,Q^2)dx = -\frac{\alpha_s}{2\pi}N_f$.

On the other hand, if one calculates the quark distribution inside a gluon through the triangle graph, which we call $\Delta q^g_{\rm OPE}$, using a regularization scheme that respects the axial anomaly, it is found that[1]

$$\Delta q^g(x) - \Delta q^g_{\rm OPE}(x) = \frac{\alpha_s}{2\pi}N_f\left[(2x-1)\ln\left(\frac{\mu^2+P^2x(1-x)+m_q^2}{\mu^2}\right) + \frac{2\mu^2(1-x)}{\mu^2+P^2x(1-x)+m_q^2}\right], \quad (9)$$

where the renormalization scale in the regularization of $\Delta q^g_{\rm OPE}$ [using the modified minimal subtraction scheme ($\overline{\rm MS}$)] has been taken to coincide with the factorization scale in the IPM.

Equipped with Eq. (9) we can understand exactly why the hard gluon coefficient in the IPM has a first moment different from zero. The reason is that in the process of factorization the axial anomaly was shifted from the quark distribution inside the gluon to the hard coefficient. Equation (9) reflects the fact that the regularization of $\Delta q^g_{\rm OPE}$ respects the axial anomaly while the regularization of Δq^g does not. We also see that in the limit $m_q^2 \gg \mu^2$ the discrepancy between the two calculations disappears (at least for the first moment, the x dependence depends on the regularization method). A similar phenomenon is found in unpolarized deep inelastic scattering where an analysis by Bass [13] has shown that the trace anomaly induces the same sort of shift when a cutoff over the transverse squared momenta of the quarks is used to separate the soft and hard regions.

As a consistency check of our equations, we calculate the OPE hard coefficient C^g. It is defined in the same way as $\sigma_h^{\gamma^* g}$ in Eq. (4) and calculated with the help of expressions (6) and (9):

$$C^g(x,Q^2/\mu^2) = \frac{\alpha_s}{2\pi}N_f\left\{(2x-1)\left[\ln\frac{Q^2}{\mu^2} + \ln\left(\frac{1-x}{x}\right) - 1\right] + 2(1-x)\right\}. \quad (10)$$

This result is independent of mass and its first moment is always zero, in accordance with the results of Kodaira [14] and Bodwin and Qiu [5].

[1]The triangle graph regularized with a cutoff on the transverse momentum results in Eq. (7).

III. CONSEQUENCES FOR THE FIRST MOMENT OF THE HARD GLUON COEFFICIENT

It is interesting to study the dependence on μ^2 of the first moment of $\sigma_h^{\gamma^* g}$. In an early study on this subject,[2] Mankiewicz and Schäfer [9] determined the first moment of the box graph as a function of the minimum transverse momentum carried by the quarks. Their results for $Q^2 \to \infty$ agree qualitatively with ours, as will soon be seen. But it was also found in Ref. [9] that for momentum transfers of the order of 10 to 100 GeV^2, the contribution from light quarks[3] ($m_q = 10$ MeV) is deeply affected by the choice of the minimum value for the transverse quark momentum. In the method used here, such an ambiguity does not exist for the light quarks and its anomalous contribution for $Q^2 = 10$ or 100 GeV^2 is well defined and independent of $k_\perp$. We use this result to argue that the hard gluon coefficient calculated here is more stable from the point of view of infrared singularities.

Even with the known variations of the anomalous contribution with the factorization scale, it has been widely assumed in the literature [8] that for light quarks (u, d, and s) the first moment of $\sigma_h^{\gamma^* g}$ is $-\alpha_s/2\pi$ and for heavy quarks (like c or b) it is zero (because, for $m_q^2 \gg \mu^2$, $\sigma_h^{\gamma^* g}$ reduces to C^g). But it also happens that the gluonic contribution to $g_1(x,Q^2)$ is of the form $\sigma_h^{\gamma^* g}(x,Q^2/\mu^2) \otimes \Delta g(x,\mu^2)$. This means that the scale μ^2 at which the gluon distribution is calculated (or parametrized) is the same scale μ^2 that has to be used in the calculation of the hard gluon coefficient, and that it does not make sense to talk about the magnitude of the hard gluon coefficient without specifying the factorization scale. Thus the heavy quark contribution is negligible only when the polarized gluon contribution is calculated at a very low scale compared with the quark mass.

In Fig. 1 we show the first moment of $\sigma_h^{\gamma^* g}$ as a function of the factorization scale for the u and d quarks ($m_q^2 \sim 25 \times 10^{-6}$ GeV^2), for the s quark ($m_q^2 \sim 0.04$ GeV^2), and for the c quark ($m_q^2 \sim 9/4$ GeV^2). We see that, as is well known [2, 6–8], the c quark does not contribute when $m_c^2 \gg \mu^2$, as one can also verify directly from Eq. (8). However, for reasonable values of μ^2 there is a contribution large enough to be taken into account. Thus the significance of the charm contribution to $g_1(x,Q^2)$ depends on where the polarized gluon distribution is calculated. For instance, calculations have been made in the literature using input polarized gluon distributions at a scale of typically 4 GeV^2. The authors of these calculations usually disregard the charm contribution. We note in passing that in the region of μ^2 where polarized charm can be disregarded the polarized strange quarks yield only half of the contribution given by u and d quarks. As we see from Fig. 1, the c quark

[2]We thank S. Bass for pointing out to us this work.

[3]We assume for the quark masses their current values. We do not take into account variation of the masses with the factorization scale but note that our conclusions are not significantly altered by small changes in the quark mass.

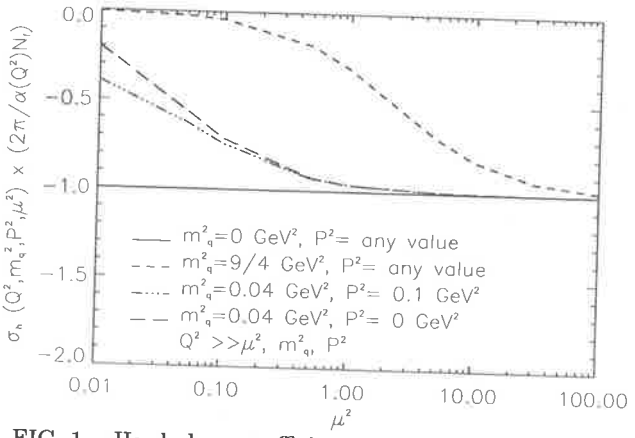

FIG. 1. Hard gluon coefficient as given by Eq. (8), calculated with the assumption of infinite momentum transfer as a function of the factorization scale. For realistic scales ($\mu^2 > 1$ GeV^2), the charm contribution is seen to be important.

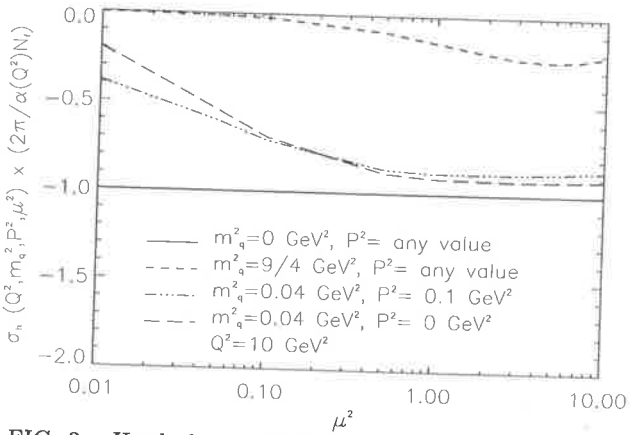

FIG. 2. Hard gluon coefficient as given by Eqs. (5), (7), and (12). The momentum transfer is fixed at 10 GeV^2. It is seen that the strange quark contribution never equals that from the up and down quarks and the charm quark contribution is sizable for $\mu^2 > 1$ GeV^2.

gives around 64% of the contribution of the light quarks for $\mu^2 \sim 4$ GeV^2 and so it should not be disregarded if the gluon distribution is calculated at this scale. We also see from Fig. 1 that the u and d quarks give the same contribution, independent of the factorization scale. We further notice that, for practical purposes, the hard gluon coefficient is independent of the exact value of the gluon virtuality P^2.

The discussion of the preceding paragraph was based on the not so realistic assumption that the momentum transfer Q^2 is infinitely bigger than any other scales in the theory. It implies, for instance, that when integrating the hard cross section we allow x to go from zero to 1. But from simple kinematic arguments we know that x has a maximum value of $x_{\max} = Q^2/(Q^2 + P^2 + 4m_q^2)$ and so $x_{\max} \to 1$ only when $Q^2 \gg m_q^2, P^2$. For the finite Q^2 of the current experiments, $x_{\max}$ never reaches 1 and so the integral in x has a cutoff. For instance, if one calculates the first moment of $\sigma_h^{\gamma^v g}$ for the c quark ($m_q^2 = 9/4$ GeV^2) at $\mu^2 = Q^2 = 4$ GeV^2, using Eq. (8), one finds that its value changes from -0.64, when x is artificially allowed to reach 1, to ~ 0.015 when the physical cutoff in x is applied. What happens is that expression (8) itself was obtained under the assumption of an infinitely large Q^2. To be more consistent when dealing with finite Q^2, one should derive the hard cross section from the full cross section without any approximation.

In the general case we then write

$$C^g = \sigma^{\gamma_v g} - \Delta q^g_{\rm OPE}, \tag{11}$$

$$\sigma_h^{\gamma^v g} = \sigma^{\gamma_v g} - \Delta q^g, \tag{12}$$

with $\sigma^{\gamma_v g}$ given by Eq. (5) and Δq^g and $\Delta q^g_{\rm OPE}$ given by Eqs. (7) and (9). We stress that these equations are the complete result at order α_s. In Figs. 2 and 3 we show the first moment of $\sigma_h^{\gamma^v g}$, defined in Eq. (12), as a function of the factorization scale μ^2 for $Q^2 = 10$ GeV^2 and $Q^2 = 3$ GeV^2, respectively. These values were chosen because they are the average Q^2 of the European Muon Collaboration (EMC) [15, 16] and SLAC [17] experiments. The resulting dependence is very interesting. It shows that in the region of interest ($\mu^2 \geq 1$ GeV^2) there is no appreciable dependence on the gluon virtuality or on μ^2 (at least for $Q^2 = 10$ GeV^2) but the mass dependence is strong. Remarkably, the contribution from the s quark is never the same as the contribution from the u and d quarks, contrary to what is usually claimed. The s contribution is $\sim 0.9\alpha_s(Q^2)/2\pi$ for the EMC data and $\sim 0.75\alpha_s(Q^2)/2\pi$ for the E143-SLAC data. We also find a non-negligible contribution coming from the c quarks. For the EMC data, the c quark contributes with $\sim 0.2\alpha_s(Q^2)/2\pi$ and for the E143-SLAC data with $\sim 0.1\alpha_s(Q^2)/2\pi$. Figure 2 is unaltered[4] if we go from $m_q^2 = 0$ to $m_q^2 = 1 \times 10^{-4}$ GeV^2. If we then compare our Fig. 2 with Fig. 2 of Ref.

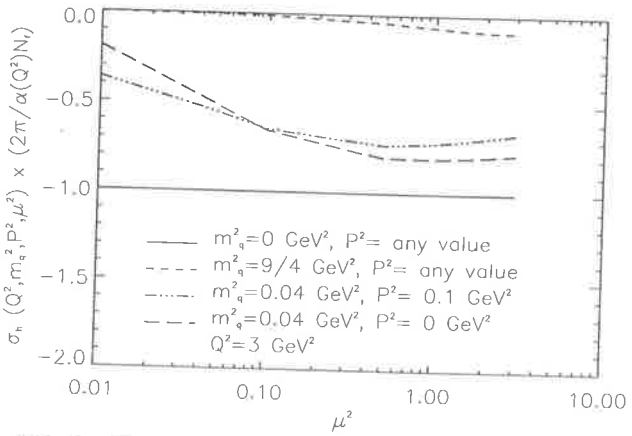

FIG. 3. Hard gluon coefficient as given by Eqs. (5), (7), and (12). The momentum transfer is fixed at 3 GeV^2. It is seen that the strange quark contributes with approximately 75% of the up and down quarks in the realistic region of $\mu^2 > 1$ GeV^2. In the same region, the charm quark gives a 10% contribution.

[4]In reality, there is a $\sim 1\%$ correction for $\mu^2 \sim 0.01$ GeV^2. This result is in complete accord with the fact that the anomalous contribution for the u and d quarks goes to zero as μ^2 goes to zero.

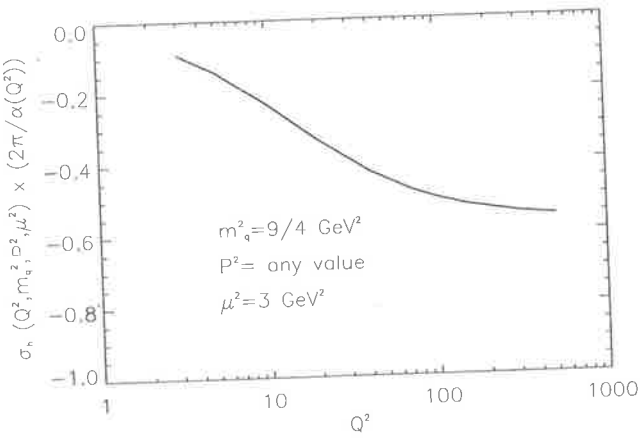

FIG. 4. Hard gluon coefficient for the charm quark, calculated with Eqs. (5), (7), and (12). The factorization scale is fixed at 3 GeV^2 and the Q^2 dependence is studied.

[9] we see clearly that the present approach does not have a convergence problem in Q^2 and yelds a perfectly unambiguous contribution from the light quarks. Finally, we show in Fig. 4 the Q^2 dependence of the polarized charm contribution calculated with $\mu^2 = 3$ GeV^2. This contribution, obviously, tends to the value calculated in Fig. 1 [$\sim -0.57\alpha_s(Q^2)/2\pi$].

IV. RELEVANCE IN ANALYZING THE FRACTION OF NUCLEON SPIN CARRIED BY GLUONS

In terms of the polarized quark and gluon distributions, $g_1^p(x,Q^2)$ for four flavors is written as

$$g_1^p(x,Q^2) = \frac{1}{12}\Delta q_3(x,Q^2) + \frac{1}{36}\Delta q_8(x,Q^2) - \frac{1}{36}\Delta q_{15}(x,Q^2) + \frac{5}{36}\Delta\Sigma(x,Q^2) + \frac{5}{36}\sigma_h^{\gamma^v g}(x,Q^2,\mu^2)\otimes\Delta g(x,\mu^2), \quad (13)$$

where $\Delta q_3 = \Delta u - \Delta d$, $\Delta q_8 = \Delta u + \Delta d - 2\Delta s$, $\Delta q_{15} = \Delta u + \Delta d + \Delta s - 3\Delta c$, and $\Delta\Sigma = \Delta u + \Delta d + \Delta s + \Delta c$. For three flavors the coefficient of the singlet part changes from 5/36 to 1/9 and Δq_{15} does not exist. To order $\alpha_s(Q^2)$ [14], the first moment of (13) is

$$\Gamma_1^p(Q^2) = I_3(Q^2) + I_8(Q^2) - I_{15}(Q^2) + I_0(Q^2) - \frac{5}{36}\left(2\frac{\alpha_s(Q^2)}{2\pi} + s_1\frac{\alpha_s(Q^2)}{2\pi} + c_1\frac{\alpha_s(Q^2)}{2\pi}\right)\Delta g(Q^2). \quad (14)$$

The coefficients of $\alpha_s(Q^2)$ have the following meaning. The 2 indicates that the u and d quarks give the same contribution $\frac{\alpha_s(Q^2)}{2\pi}$, as discussed before. The s_1 and c_1 factors give the amount of strange and charm quark contributions, according to Eq. (12) and Figs. 1–3.

To extract the value of $\Delta g(Q^2)$ we will closely follow Refs. [18, 19]. For the sake of comparison, we begin with only three flavors and with the common assumption that the u, d, and s quarks give the same anomalous contribution.

Under the assumption that the polarized sea originates exclusively from the anomalous gluon contribution we have, for three flavors, the identities

$$I_3 = \frac{1}{12}(F+D)\left(1-\frac{\alpha_s}{\pi}\right),$$
$$I_8 + I_0 = \frac{1}{36}(3F-D)\left[\left(1-\frac{\alpha_s}{\pi}\right) + 4\left(1-\frac{\alpha_s}{3\pi}\right)\right], \quad (15)$$

where the quark spin fractions were expressed in terms of the F and D couplings and corrections from the two-loop expansion of the beta function and anomalous dimension were incorporated. In nonleading order (NLO), α_s is given as the solution of the transcendental equation

$$\ln\frac{Q^2}{\Lambda^2} = \frac{4\pi}{\beta_0\alpha_s} - \frac{\beta_1}{\beta_0^2}\ln\left[\frac{4\pi}{\beta_0\alpha_s} + \frac{\beta_1}{\beta_0^2}\right], \quad (16)$$

with $\beta_0 = 11 - 2N_f/3$ and $\beta_1 = 102 - 38N_f/3$. We use $\Lambda = \Lambda^{(3)} = 248$ MeV, determined by fixing $\Lambda^{(4)} = 200$ MeV [20]. Using the experimental values of F and D as given in [19], we determine I_3 and $I_8 + I_0$ at $Q^2 = 10$ GeV^2 [with $\alpha_s(Q^2 = 10\ \text{GeV}^2) \simeq 0.209$]:

$$I_3 = 0.0977 \pm 0.001,$$
$$I_8 + I_0 = 0.0779 \pm 0.002. \quad (17)$$

We now use Eq. (14) to determine $\Delta g(Q^2)$. On the left hand side, we use the experimental result [16]

$$\Gamma_1^p(Q^2 = 10\ \text{GeV}^2) = 0.142 \pm 0.008 \pm 0.011. \quad (18)$$

On the right hand side we use the results (17), $s_1 = 1$, and $c_1 = 0$ and remember that for three flavors the singlet coefficient is 1/9 and $I_{15} = 0$. The result is

$$\Delta g(Q^2 = 10\ \text{GeV}^2) = 3.04 \pm 1.4. \quad (19)$$

For four flavors the analysis is similar. One just has to redefine the integral of $g_1^p(x,Q^2)$:

$$I_3 = \frac{1}{12}(F+D)\left(1-\frac{\alpha_s}{\pi}\right),$$
$$I_8 + I_0 - I_{15} = \frac{5}{36}(3F-D)\left(1-\frac{\alpha_s}{3\pi}\right). \quad (20)$$

We then proceed as before and calculate Δg using the result for the gluon coefficient as displayed in Fig. 2. We see that for $\mu^2 = Q^2 = 10$ GeV^2, $s_1 \sim 0.9$, $c_1 \simeq 0.21$, and $\alpha_s(Q^2 = 10\ \text{GeV}^2) = 0.2142$, resulting in

$$I_3 = 0.0976 \pm 0.001,$$
$$I_8 + I_0 - I_{15} = 0.0786 \pm 0.002,$$
$$\Delta g(Q^2 = 10\ \text{GeV}^2) = 2.32 \pm 1.06. \quad (21)$$

In passing we notice that if the usual assumption of infinite momentum transfer were used then according to the results of Fig. 1, at 10 GeV^2 $s_1 = 1$, $c_1 \simeq 0.81$, and hence $\Delta g \simeq 1.89$.

V. THE x DEPENDENCE

The exact x dependence of the anomalous contribution is a matter of convention because the freedom in the factorization scheme while calculating $\sigma_h^{\gamma_v g}$. Other choices of regularization would result in different functions of x. But, as shown by Glück *et al.* [21], the exact form of the x dependence seems not to be very important. Once we do not know the form of the polarized gluon distribution, the best we can do is constrain it by some general considerations. For instance, there is the positivity condition

$$|\Delta g(x,Q^2)| \leq g(x,Q^2), \tag{22}$$

where $g(x,Q^2)$ is the unpolarized gluon distribution. A very simple form that satisfies the above condition is

$$\Delta g(x) = x^\alpha g(x), \tag{23}$$

where α is determined through the normalization of Δg. For Δg of Eq. (21), $\alpha = 0.49$. The advantage of using this form to study the x dependence is its simplicity. The problem with Eq. (23) is that it does not have the correct behavior as $x \to 0$. As proposed by Brodsky *et al.* [22],

$$\frac{\Delta g(x)}{g(x)} \to x, \tag{24}$$

as $x \to 0$. From the many ways to satisfy both conditions (22) and (24), we choose

$$\Delta g(x,\mu^2 = 9 \ \text{GeV}^2) = \alpha x g(x,\mu^2 = 9 \ \text{GeV}^2)(1-x)^3, \tag{25}$$

where $\alpha = 6.92$ for $\Delta g = 2.32$. We made this choice guided only by the desire of simplicity and to produce a polarized gluon distribution that resembles an already existing one [18]. For the unpolarized gluon distribution, we use the one given by the New Muon Collaboration (NMC) [23], determined from inelastic J/ψ production:

$$xg(x) = \frac{1}{2}(\eta+1)(1-x)^\eta. \tag{26}$$

This parametrization is valid for $\mu^2 = 9$ GeV^2 and should not be trusted for $x \leq 0.01$. Again, this choice is based on simplicity and we note that a further parametrization by the NMC [24] group agrees with Eq. (26) for $x \geq 0.01$. The parameter η is $\eta = 5.1 \pm 0.9$. Given these choices, we show in Fig. 5 the forms (23) and (25) for the polarized gluon distributions plus the forms of Brodsky *et al.* [22] and Gehrmann and Stirling (GS) [18], calculated at 4 GeV^2. Our parametrization (25) is slightly higher than that of GS because of the normalization factor. If we use the same normalization as theirs,[5] both curves would be essentially the same.

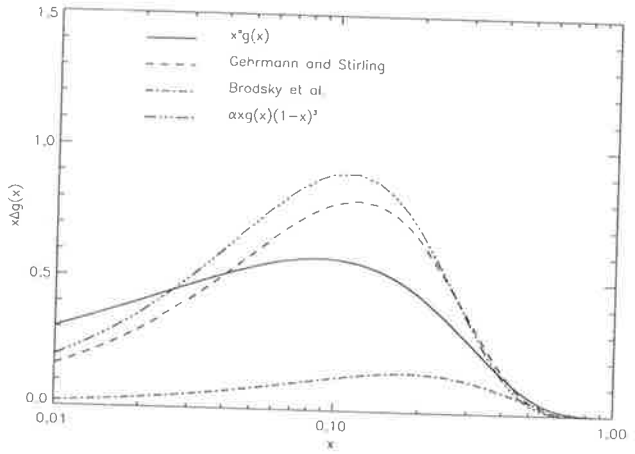

FIG. 5. Comparison of various polarized gluon distributions considered in the text.

Evolution from 4 to 9 GeV^2 for the GS distribution also has small effects. The parametrization of Brodsky *et al.* [22] is much smaller than the others because in their approach the polarized gluons are not responsible for the small experimental value of Eq. (18).

Using the constructed gluon distributions, we can estimate where in x the anomalous contribution is located. In Fig. 6 we show the anomalous contribution, $\frac{5}{36}\sigma_h^{\gamma_v g}(x,Q^2,\mu^2) \otimes \Delta g(x,\mu^2)$, for $\Delta g(x) = \alpha x g(x)(1-x)^3$. We see that its contribution inside the experimental region is important. To better evaluate its importance, we calculated the amount of the total gluon that lies inside the region $0.01 \leq x \leq 1$. For four flavors, the contribution from $x \geq 0.01$ corresponds to about 66% of the total anomalous contribution. In the case of three flavors, this percentage is $\sim 69\%$. For $\Delta g(x) = x^\alpha g(x)$ this conclusion is not dramatically altered.

It is also interesting to compare the anomalous gluon contribution directly with the experimental data. To this

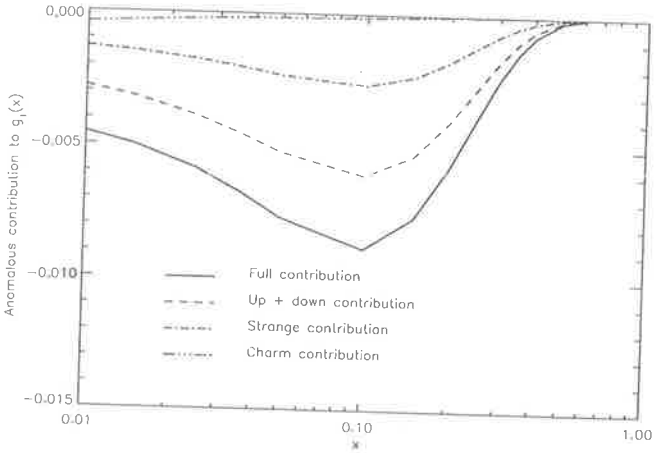

FIG. 6. Comparison of the x dependence of the nonstrange, strange, and charm quark distributions to $g_1(x)$. The anomalous contribution is given by $\frac{5}{36}\sigma_h^{\gamma_v g}(x,Q^2,\mu^2) \otimes \Delta g(x,\mu^2)$ and it is used in the form $\Delta g(x,\mu^2 = 9 \ \text{GeV}^2) = \alpha x g(x)(1-x)^3$ for the polarized gluon.

[5]We note that in [18] the coupling constant is calculated in leading order rather than in NLO. This would lead to an increase of the total polarization carried by the gluons.

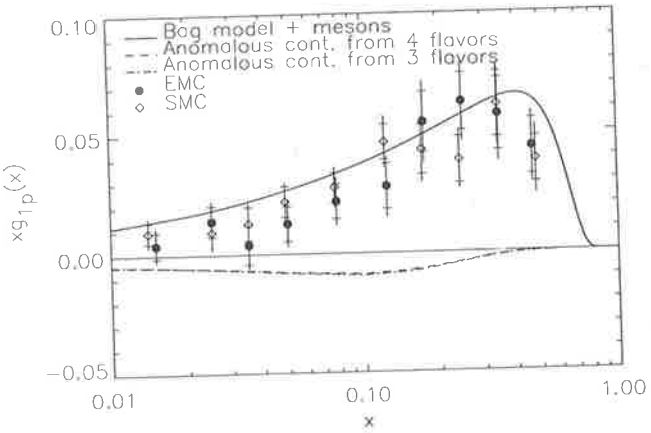

FIG. 7. EMC [15] and Spin Muon Collaboration (SMC) [16] data for $g_{1p}(x)$ at 10 GeV^2. The theoretical curve for the polarized valence distribution is calculated in NLO and taken from Ref. [25]. The anomalous contribution should be subtracted from the theoretical curve.

end, we plot in Fig. 7 the experimental data [15, 16] for $g_1^p(x)$ together with an early next-to-leading order estimate [25] for the valence quark distribution and the anomalous gluon contribution for the case of three and four flavors. A remark is necessary here. The calculation of the hard gluon coefficient was performed through a cutoff on the transverse momenta of the partons in order to regularize the integrals. This procedure is the definition of the parton model. On the other hand, we calculated the strong coupling constant, and also the evolution of g_1^p in Ref. [25], using the $\overline{\rm MS}$ scheme. In principle, showing the x dependence of two quantities in different schemes is not a consistent procedure. However, the problem is not as bad as it looks. First, if we change schemes we can mantain α_s unaltered by a simple redefinition of the parameter Λ in expression (16). Second, the theoretical curve for $g_1^p(x, Q^2)$ is to be interpreted as a guide of what a parametrization for the valence part of the polarized structure function would give, the regions in which it differs from the data and where it should be corrected. A proper procedure would be to calculate the quark distribution, the anomalous dimensions and the Wilson coefficients in the same scheme. That said we proceed noticing that the integral over x of the valence contribution calculated in [25] (~ 0.169) is in complete agreement with the estimates calculated previously in Sec. IV. The two curves below the origin are the anomalous contributions that should be added to the solid curve for $N_f = 3$ or 4. As we fixed the normalization of the total polarized glue for either three or four flavors, there is no noticeable difference between the two cases. We see that the anomalous contribution is potentially important to correct the x dependence of the polarized valence distribution inside the proton.

VI. DISCUSSION

In summary, there is a gluonic contribution to the proton spin when the IPM hard gluon coefficient is defined through Eq. (12) with Δq^g defined as the quark distribution inside the gluon with transverse squared momentum less than the factorization scale. As a consequence, this anomalous gluonic contribution in the IPM is free of infrared ambiguities. We showed that if we accept the commonly used assumption of an infinitely big momentum transfer there is a c quark contribution to the spin in addition to the u, d, and s quark contributions. The contribution from the massive quarks is dependent on the factorization scale at which the polarized gluon distribution is calculated. The c quark contribution is small only in the region $\mu^2 < 1$ GeV^2, in which case the s quark contribution is also strongly affected.

We also calculated what would be the possible anomalous corrections when the momentum transfer is in the region of the present experiments. To perform such a calculation we have to keep all terms in m_q^2/Q^2 and P^2/Q^2 in the full photon-gluon cross section when calculating the hard gluon coefficient. This means that we are including higher twist effects and, although we use the complete result at order $\alpha_s(Q^2)$, possible corrections coming from higher order terms in $\alpha_s(Q^2)$ could be important and so our calculation is incomplete. Even so, we think that our results are more consistent than simply using the approximate expression (8) for the hard gluon coefficient in the case of massive quarks and relatively low Q^2. The corrections due to finite Q^2 are not small and we think they should be taken into account when calculating the amount of spin carried by gluons. When studying the x dependence of the anomalous contribution, we conclude that both three and four flavors give approximately the same contribution inside the experimental region. But the amount of polarized glue needed to fit the data is much smaller when charm is included. Moreover, we showed that from the conceptual point of view, it would be wrong not to include a fourth flavor.

ACKNOWLEDGMENTS

We would like to thank to S. Bass, S. J. Brodsky, W. Melnitchouk, and G. Piller for helpful discussions. This work was supported by the Australian Research Council and by CAPES (Brazil).

[1] G. Altarelli and G. G. Ross, Phys. Lett. B **212**, 391 (1988).
[2] R. D. Carlitz, J. C. Collins, and A. H. Mueller, Phys. Lett. B **214**, 299 (1988).
[3] A. V. Efremov, J. Soffer, and O. V. Teryaev, Nucl. Phys. **B246**, 97 (1990).
[4] R. L. Jaffe and A. Manohar, Nucl. Phys. **B337**, 509 (1990).
[5] G. T. Bodwin and J. Qiu, Phys. Rev. D **41**, 2755 (1990).
[6] S. D. Bass, B. L. Ioffe, N. N. Nikolaev, and A. W.

Thomas, J. Moscow Phys. Soc. **1**, 317 (1991); S. D. Bass and A. W. Thomas, J. Phys. G **19**, 639 (1993); B. L. Ioffe, Report No. ITP-61, 1994 (unpublished).
[7] L. Mankiewicz, Phys. Rev. D **43**, 64 (1991).
[8] See M. Anselmino, A. Efremov, and E. Leader, Phys. Rep. **261**, 1 (1995), and references therein.
[9] L. Mankiewicz and A. Schäfer, Phys. Lett. B **242**, 455 (1990).
[10] S. D. Bass, N. N. Nikolaev, and A. W. Thomas, University of Adelaide Report No. ADP-133-T-80, 1990 (unpublished).
[11] W. Vogelsang, Z. Phys. C **50**, 275 (1991).
[12] G. P. Lepage and S. J. Brodsky, Phys. Rev. D **22**, 2157 (1980).
[13] S. D. Bass, Phys. Lett. B **342**, 233 (1995).
[14] J. Kodaira, Nucl. Phys. **B165**, 129 (1980).
[15] EMC Collaboration, J. Ashman *et al.*, Nucl. Phys. **B328**, 1 (1989); SMC Collaboration, B. Adeva *et al.*, Phys. Lett. B **302**, 533 (1993).
[16] SMC Collaboration, D. Adams *et al.*, Phys. Lett. B **329**, 399 (1994).
[17] SLAC E142 Collaboration, P. L. Anthony *et al.*, Phys. Rev. Lett **71**, 959 (1993); SLAC E143 Collaboration, K. Abe *et al.*, *ibid.* **74**, 346 (1995).
[18] T. Gehrmann and W. J. Stirling, Z. Phys. C **65**, 461 (1995).
[19] F. E. Close and R. G. Roberts, Phys. Lett. B **316**, 165 (1993).
[20] M. Glück, E. Reya, and A. Vogt, Z. Phys. C **53**, 53 (1992).
[21] M. Glück, E. Reya, and W. Vogelsang, Phys. Rev. D **45**, 2552 (1992).
[22] S. J. Brodsky, M. Burkardt, and I. Schmidt, Nucl. Phys. **B441**, 197 (1995).
[23] NMC Collaboration, D. Allasia *et al.*, Phys. Lett. B **258**, 493 (1991).
[24] NMC Collaboration, M. Arneodo *et al.*, Phys. Lett. B **309**, 222 (1993).
[25] F. M. Steffens, H. Holtmann, and A. W. Thomas, Phys. Lett. B **358**, 139 (1995).

ADP-96-03/T208 February 1996

Polarized Deep Inelastic Scattering

F.M. Steffens and A.W. Thomas

Department of Physics and Mathematical Physics
University of Adelaide
Adelaide, S.A. 5005, Australia

Abstract

We give an overview of present calculations involving the proton spin structure function.

1 Introduction

Experiments involving inclusive deep inelastic scattering have provided important information on nucleon structure. The experiments are able to tell us many things from the confirmation of the assumption of the quark model that the nucleon is made of 3 valence quarks to the spin fraction carried by quarks. Of course, there are still many questions to be answered and the answers to some of these have become extremely active research topics in the last few years. The search for a complete picture of hadron structure is in this sense the goal being sought.

Much of the interest in the area was revived several years ago by the EMC experiment where the proton spin structure function was measured in a region of small x previously unexplored. From this experiment it was concluded that the spin of the proton carried by quarks was very small, being compatible with zero. This became known as the spin problem. Since then, many other polarized experiments have been performed and now there are a reasonable amount of data on the proton, neutron and deuterium spin structure functions [1]. Many other experiments are also planned or being carried right now which will give further details on the spin structure of the proton. Nevertheless, a full understanding of the current experimental results

has not been achieved and, among others, the following questions remain to be answered:

- The combined experiments on the proton spin structure function seem to indicate that the quark singlet axial charge is about half of what was expected from the quark model. What is the mechanism behind such a reduction that can explain both the first moment and the x dependence of the structure function?
- Are the gluons important for the first moment of $g_1(x, Q^2)$? What is their actual contribution to the spin sum rule? Almost nothing is known about the polarization of the gluons, even its sign is not known, and its study is one of the major questions in hadron structure.
- What is the valence and sea decomposition of the polarized quark distributions? Is the polarized sea, like its unpolarized counterpart, asymmetric? Present experiments are unable to give a definite answer to these questions and only recently has data on the valence distribution become available from semi-inclusive data [2].
- The small x behaviour of polarized parton distributions is a complete unknown. A recent experiment suggests a rapid rise of g_1^p in that region. If this rise were steep enough, it could cause the saturation of the first moment of g_1 at its quark model value. Firm conclusions are not yet possible because of the large error bars.
- The role of higher twist terms, mainly in some small x data where Q^2 is small, is still to be evaluated; not only their contribution to the sum rules, which seems to be small [3], but also possible effects on the x dependence [4].

There are other topics to be addressed and those quoted above are only examples which show that there is much work to be done. We will briefly review these and some related topics in an attempt to summarise the present status of the subject. The number of subjects covered is by no means complete and follows the authors' interests.

2 The Problem

The proton spin structure function is given by:

$$g_1^p(x,Q^2) = \int_x^1 \frac{dy}{y} C_q^{NS}(x/y, Q^2/\mu^2)\Delta q^{NS}(y,\mu^2) + \int_x^1 \frac{dy}{y} C_q^S(x/y, Q^2/\mu^2)\Delta q^S(y,\mu^2) + \int_x^1 \frac{dy}{y} C_g(x/y, Q^2/\mu^2)\Delta g(y,\mu^2), \quad (1)$$

where the C denotes the gluon and quark Wilson coefficients for singlet and nonsinglet operators and μ^2 is the renormalization scale. For 3 flavours, the nonsinglet charge is $\Delta q^{NS} = \frac{1}{12}(\Delta u + \Delta\overline{u} - \Delta d - \Delta\overline{d}) + \frac{1}{36}(\Delta u + \Delta\overline{u} + \Delta d + \Delta\overline{d} - 2\Delta s - 2\Delta\overline{s}) = \frac{1}{12}g_a + \frac{1}{36}g_a^8$, while the singlet charge is $\Delta q^S = \frac{1}{9}(\Delta u + \Delta\overline{u} + \Delta d + \Delta\overline{d} + \Delta s + \Delta\overline{s}) = \frac{1}{9}\Delta\Sigma$.

The proton spin structure function measured by the EMC, SMC and E143 experiments are at a different average Q^2. Even so, their results tend to agree if the whole data set is evolved to a common Q^2. To perform the evolution, it is usually assumed that the measured asymmetries are Q^2 independent - an assumption on which we will comment later. Meanwhile, to fix ourselves to a definite number, we will use the SMC results [5] in conjunction with earlier EMC and SLAC data:

$$\int_0^1 dx g_1^p(x,Q^2) = \int_0^1 dx \frac{A_1^p(x,Q^2)F_2^p(x,Q^2)}{2x[1+R(x,Q^2)]} = 0.142 \pm 0.008 \pm 0.011, \quad (2)$$

calculated at an average of 10 GeV^2. The asymmetry A_1 is what is measured and the unpolarized structure functions F_2 and R are taken from previous experiments. Eq. (2) then predicts that $\Delta\Sigma = 0.27 \pm 0.008 \pm 0.011$. On the other hand, the Ellis-Jaffe prediction for the integral of g_1^p at 10 GeV^2 is $\int_0^1 dx g_1^p(x,Q^2) = 0.176 \pm 0.006$, where $O(\alpha_s)$ corrections were included. We remind the reader that the Ellis-Jaffe result is based on the assumption that the sea is not polarized and $\Delta\Sigma \sim g_a^8$ is expected to be of order 0.6. This discrepancy between theory and experiment is what is known as "the spin problem" [6, 7, 8]. In the following we discuss the various approximations made to get the quoted numbers, as well as a few possible solutions to the problem.

3 The Small x Region

Of course, experimentally it is not possible to go to $x = 1$ or $x = 0$. In the case of SMC the limits are $0.003 < x < 0.7$. For the new E143 SLAC data [9], the limits are $0.029 < x < 0.8$ and their integral of g_1 agrees within errors with the SMC results. Extrapolations have to be made to cover the whole x interval. The large x region is well behaved and perturbation theory predicts that $A_1 \to 1$ as $x \to 1$ [10]. For small x a Regge type behaviour [11], $g_1^p \propto x^\alpha$, $0 < \alpha < 0.5$ [12], has been assumed - with the errors in the quoted data expressing the uncertainty in α. However, the SMC data shows a tendency to increase for $x < 0.02$. In their analysis of the data, the SMC did not consider that the measured tendency of the data to rise at small x was enough to motivate the use of some other extrapolation of g_1^p in that region. Close and Roberts [13] considered a few other possibilities. They are:

a) $-Lnx$, derived using the fact that the Froissart bound [14] for the total unpolarized cross section, $\sigma \leq Log^2 s$ with s the square of the center of mass energy, is saturated. Then $g_1 \propto -Lnx$ follows if one calculates the behaviour of the spin asymmetry for a vector potential in which case $A \propto 1/sLogs$ and hence $g_1 \propto -Lnx$ as $x \to 0$.

b) $1/xLn^2x$. This is derived as in a) but in this case the potential transforms like an axial vector.

c) $-(1 + 2Lnx)$. This was derived by Bass and Landshoff [15] using a model for the non-perturbative Pomeron exchange simulated through non-perturbative gluons. Their calculation affects only the singlet part of g_1.

According to the data shown by Close and Roberts, the $-Lnx$ and $-(1 + 2Lnx)$ forms tend to fit the data, though the last point is missed, while the very singular behaviour $1/xLn^2x$ tends to fit the data over the whole small x region. On the other hand, the extrapolation used by the SMC appears to be somewhat below the trend of the data. Some comments on these results seem appropriate. First, in their analysis Close and Roberts extrapolated the individual data of each x to a common $Q^2 = 10\ GeV^2$, using the assumption of a Q^2 - independent asymmetry. This seems to be contradicted by recent studies of the QCD evolution of the spin structure functions at next-to-leading order [16, 17]. In fact, if one looks to the resulting Q^2 dependence of the asymmetry as calculated by [16], one may conclude that the data used by Close and Roberts may be overestimated - at least for the last two x

points. The tendency for the asymmetry to be Q^2 dependent in the region of $Q^2 \sim 1\ GeV^2$ has been recently corroborated by the first experimental test on the Q^2 dependence of A_1 made by the E143 experiment [18]. Second, the rise of g_1^p at small x should be reflected also in the singlet part of the deuteron spin structure function. However, recent deuteron data shows no signal of a rapid raise of g_1^d [19]. Thus a very singular g_1 can be ruled out but the question of its precise behaviour at small x is still open.

4 The Gluon Contribution

It is a fact that the spin sum rule should be satisfied:

$$\frac{1}{2} = \frac{1}{2}\Delta\Sigma + \Delta g + L_q + L_g, \tag{3}$$

where Δg is the total gluon spin and L denotes the z-component of the orbital angular momentum of the quarks and gluons. Notice that, contrary to unpolarized deep inelastic scattering where measurements of F_2 alone determine the momentum carried by gluons via the momentum sum rule, measurements of g_1 alone are not able to determine Δg[1].

According to Eq. (1), the integral of $g_1(x,Q^2)$, Γ_1^p, is given by:

$$\Gamma_1^p \sim \frac{1}{9}\Delta\Sigma(1 - \frac{\alpha_s(Q^2)}{3\pi} + ...) + \frac{1}{9}\Delta g(\mu^2)\int_0^1 C_g(x,Q^2/\mu^2)dx, \tag{4}$$

where the nonsinglet part was not explicitly written, the perturbative result up to order α_s for C_q^S [20] was shown and the integral over x of C_g was left undone.

In the operator product expansion for g_1, there is no gluon operator contribution to Γ_1^p [20], which means that $\int_0^1 C_g(x,Q^2/\mu^2)dx = 0$. In this case, measurements of g_1 would determine $\Delta\Sigma$ and hence the spin carried by quarks. However, the operator, $\overline{\psi}\gamma_\mu\gamma_5\psi$, giving rise to $\Delta\Sigma$ in the OPE is gauge invariant but not conserved even in the chiral limit due to the axial anomaly [21]:

[1] As a matter of fact, interpretations of g_1 that include gluonic contributions through the axial anomaly, can be used to constrain the total gluon spin. This will be discussed soon.

$$\partial_\mu J_{5R}^\mu = \frac{\alpha_s}{2\pi} Tr G_{\mu\nu}\tilde{G}^{\mu\nu}, \tag{5}$$

where $G_{\mu\nu}$ is the gluon tensor and $\tilde{G}^{\mu\nu}$ is its dual. As a first consequence, the matrix elements of $\overline{\psi}\gamma_\mu\gamma_5\psi$ *are not* the quark helicity of the naive parton model.

It is a property of renormalized operators having anomalous dimension different from zero that they will not always have the same symmetry properties as their classical counterparts. This is a well known fact of quantum field theory where regularization can spoil some of the classical symmetries. The process of renormalization should restore such symmetries but in anomalous theories this is not what happens. Of course, the anomalous dimension beyond leading order is dependent on the renormalization scheme used, which means that one can always find a scheme where the anomalous dimension is zero and hence one would have again the identification of the axial current with spin. However, such schemes break gauge invariance. So, as the operators appearing in the operator product expansion are, by definition, gauge invariant, the matrix elements of the axial current are not related to the spin carried by quarks and the first moment of the gluon Wilson coefficient is zero.

With respect to the x-dependence, this would mean that when calculating the cross sections related to such quantities, one should use renormalization schemes where gauge invariance is preserved, like $\overline{MS}$, in which case it also happens that chiral symmetry is broken. For the case of the hard gluon coefficient, an extensive study was done by Bodwin and Qiu [22] where they indeed found that in schemes where gauge invariance is preserved, $\int_0^1 C_g(x,Q^2/\mu^2)dx = 0$. If one uses a scheme involving a cut-off in tranverse momentum, where the parton model is often formulated, one finds that $\int_0^1 C_g(x,Q^2/\mu^2)dx \neq 0$, in which case gauge invariance is broken but the axial current is free from the anomaly. It is then possible to construct, inspired by Eq. (5), a new axial current that is conserved in the chiral limit with the price that it is gauge dependent [23].

Although, at first sight, this is a high price to pay, we notice that the decomposition of the spin into its parts in Eq. (3) *is not* gauge invariant itself [24]. Moreover, the parton model is formulated in a specific gauge, the axial gauge, in which case the gluon distribution is given by the forward matrix elements of the gluon operator in Eq. (5). Hence one can, in principle, express

Γ_1^p in terms of the quark and gluon spin. This is a very fragile interpretation, valid only in the axial gauge but, again, it is this gauge that is used to define parton distributions as well. If we change gauge we no longer have a clear quark and gluon helicity decomposition but neither do we have the parton model. Finally we note that up to large gauge transformations, like the ones that change the topological number, the forward matrix elements of the conserved axial current and gluon operator are gauge invariant [6]. As a conclusion, it seems that if one wants to talk about spin carried by quarks, then one should use a renormalization scheme that allows such a thing, like the cut off scheme, and also a gauge where such interpretations through the parton model are allowed.

In the parton model formulation where the gluons contribute to Γ_1^p, the sum rule has usually been written as [8]:

$$\Gamma_1^p = (\frac{1}{12}g_a + \frac{1}{36}g_a^8)(1 - \frac{\alpha_s}{\pi}) + \frac{1}{9}\Delta\Sigma(1 - \frac{\alpha_s}{3\pi}) + \frac{1}{3}\frac{\alpha_s}{2\pi}\Delta g, \qquad (6)$$

where $\Delta\Sigma$ is the spin content of the proton and 3 active flavours are considered. However, a recent study where the quark masses are treated consistently has shown that for the momentum transfer of the present experiments, Eq. (6) overestimates the strange quark contribution [25]. Moreover, it was also shown that there is a sizable charm contribution that should be taken into account. In practical terms it means that if we blame the discrepancy between experiment, Eq. (2) and the Ellis-Jaffe sum rule entirely on the gluon term in Eq. (6), Δg is reduced from 3.04 ± 1.4 to 2.32 ± 1.06 at 10 GeV^2 if the quark masses are treated correctly and charm is included.

The discussion of the polarised glue is far from settled. For instance, Jaffe [26] recently calculated Δg in various nucleon models. His results suggest that Δg is negative in any model for the nucleon, independent of its particular structure. Moreover, he concludes that the sign of the polarized gluon is directly related to the $N - \Delta$ splitting: a negative Δg results from the fact that the Δ heavier than the nucleon. If Δg were positive, the Δ would be lighter than the nucleon. His conclusions are supposed to be valid at the scale of the model. If QCD evolution or (in his calculations) the omission of gluon self interactions do not change the sign of Δg, one would be forced to accept a negative Δg, in which case the proton spin problem would worsen. However, even the connection between the sign of Δg and the baryon spin splitting used by Jaffe has been challenged by another recent calculation. In

a study of lattice QCD, K. F. Liu [27] calculated some hadron properties in a valence approximation, where one gluon exchange is not switched off. He found that the nucleon and the Δ were degenerate, in contradiction with the many nucleon model calculations where one gluon exchange is used to justify the baryon spin splitting.

To help resolve these question, there are a few planned experiments in the near future aimed to measure Δg through charm production [28] or gluon fusion in pp or Drell-Yan processes at RHIC [29]. The measurement of Δg would be one of the landmarks in the study of hadron structure.

5 Results from Lattice QCD

Motivated by the experimental results, a few groups [30] have engaged in the calculation of g_a, g_a^8 and $\Delta\Sigma$ in lattice QCD. So far, all the results have been obtained in quenched QCD but they are separated into connected and disconnected insertions, with the latter being identified with the sea quarks and the former containing both valence and cloud[2] contributions. In general, only gauge invariant operators are used which means that the $\Delta\Sigma$ calculated is directly related to the measured and previously quoted $\Delta\Sigma$ but it is not related to the quark spin content of the proton. We now quote a few results with some comments. The Kentucky group [32] calculated $\Delta\Sigma = 0.25 \pm 0.12$, $g_a = 1.2 \pm 0.1$ and $g_a^8 = 0.61 \pm 0.13$, where both connected and disconnected contributions are included. Interesting enough, in the connected approximation, they also found $\Delta\Sigma/g_a < 3/5$, the value expected from SU(6). However, if the valence approximation was taken (the cloud quarks in the connected graphs are disregarded), they indeed got the 3/5 from SU(6), in a remarkable result.

Other works, like the calculations by Fukugita et al. [31], also found similar results, with the exception of g_a: $\Delta\Sigma = 0.18 \pm 0.1$, $g_a = 0.985 \pm 0.025$ and $g_a^8 = 0.509 \pm 0.12$. Remarkably, g_a is around 20% smaller than the experimental value. Moreover this result seems not to depend on the quenched approximation [30]. On the other hand, the result for g_a from the Kentucky group tends to agree with the data, contrary to the world average of g_a in lattice calculations [30]. The large value of g_a obtained in [32] may be related to the small number of gauge configurations used there [33]. In any

[2]Cloud means that the connected quark lines form a connected loop.

case, it seems that the origin of the problems with g_a in the lattice is open, a disappointing observation in view of the fact they tend to get a reasonable value for $\Delta\Sigma$.

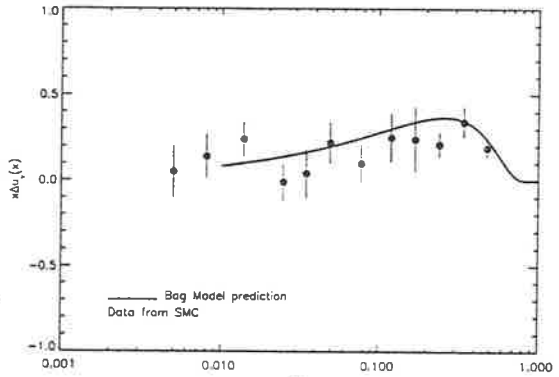

Figure 1: Polarized valence up quark data from SMC against bag model predictions.

6 The x Dependence

Although much attention has been paid to the first moment of g_1, not many calculations have been made for its x dependence. That is to say, besides the many parametrizations for the polarized parton distributions [16], there are very few predictions based on a genuine model of the nucleon structure. We will show some results from the Adelaide group [34, 35] noticing that there are others around. These calculations involved the use of bag model wave functions as an approximation for the proton wave function. The corresponding leading twist parton distributions were then evolved [35] in leading and next-to-leading order QCD evolution to the scale of the experiments. The resulting agreement between theory and experiment is very rewarding especially because of the simplicity of the model and the fact that all the free parameters were fixed in the unpolarized total valence distribution. Then all

the curves for the polarized distributions shown in Ref. [35] are predictions of the model. In Fig. 1 we show one of the predictions of the model against the very recent data from the SMC [2] for the polarized valence distributions. We note also that the calculated value of the Ellis-Jaffe sum rule agrees with usual expectations with its value being ~ 0.17. In these calculations, the anomaly is not present. If we then follow the work of ref. [25] where the x dependence of the anomalous gluon contribution was calculated, we see that it can affect the x dependence of g_1^p calculated in [35] exactly where it overestimates the data.

We would like to thank T. Hatsuda for discussions on the lattice calculations of the spin structure functions. This work was supported by the Australian Research Council and by CAPES (Brazil).

References

[1] R. Voss, Cern preprint CERN-PPE/95-131, august 1995. invited Talk at the Workshop on Deep Inelastic Scattering and QCD, Paris, April 1995.

[2] SMC, B. Adeva et al., Cern preprint CERN-PPE/95-187.

[3] L. Mankiewicz, E. Stein and A. Schäfer, hep-ph/9510418.

[4] A. I. Signal, this conference proceedings.

[5] SMC, D. Adams et al., Phys. Lett. 329B (1994) 399; Erratum, Phys. Lett. 339B (1994) 332.

[6] R. L. Jaffe and A. Manohar, Nucl. Phys. **B337**, 509 (1990).

[7] S. D. Bass and A. W. Thomas, J. Phys. G19, 639 (1993).

[8] M. Anselmino, A. Efremov and E. Leader, Phys. Rep. 261 (1995) 1.

[9] The E143 Collab., K. Abe et al., Phys. Rev. Lett. 74 (1995) 346.

[10] S. J. Brodsky, M. Burkardt and I. Schmidt, Nucl. Phys. **B441**, 197 (1995).

[11] R. L. Heimann, Nucl. Phys. B64 (1973) 429.

[12] J. Ellis and M. Karliner, Phys. Lett. 213B (1988) 73.

[13] F. E. Close and R. G. Roberts, Phys. Lett. 336B (1994) 257.

[14] M. Froissart, Phys. Rev. 123 (1961) 1053.

[15] S. D. Bass and P. V. Landshoff, Phys. Lett. 336B (1994) 537.

[16] M. Glück et al., Dortmund preprint DO-TH 95/13, hep-ph/9508347; T. Gehrmann and W. J. Stirling, Durham preprint DTP/95/82, hep-ph/9512406.

[17] T. Weigl and W. Melnitchouk, Munich Tech. Uni. preprint TUM-T39-95-9, sept. 95, to appear in Nucl. Phys. B; hep-ph/9601294.

[18] The E143 Collab., Phys. Lett. 364B (1995) 61.

[19] SMC, D. Adams et al., Phys. Lett. 357B (1995) 248.

[20] J. Kodaira, Nucl. Phys. **B165**, 129 (1980).

[21] S. L. Adler, Phys. Rev. 177 (1969) 129; J. S. Bell and R. J. Jackiw, Nuovo Cimento 51 A (1969) 47.

[22] G. T. Bodwin and J. Qiu, Phys. Rev. D 41 (1990) 2755.

[23] W. Bardeen, Nucl. Phys. B 75 (1974) 246.

[24] X. Ji, J. Tang and P. Hoodbhoy, MIT preprint MIT-CPT-2476, hep-ph/9510304.

[25] F. M. Steffens and A. W. Thomas, Phys. Rev. D53 (1996) 1191.

[26] R. L. Jaffe, MIT preprint MIT-CTP-2466, hep-ph/9509279.

[27] K-F. Liu and S-J. Dong, in Glacow 94, Proceedings, High energy physics, vol.2 page 717 and hep-lat/9411067.

[28] E. Nappi et al., Letter of intent for the experiment, Cern preprint CERN/SPSLC 95-27.

[29] R. W. Robinett, Argonne preprint ANL-HEP-CP-95-28, hep-ph/9506230.

[30] M. Okawa, KEK preprint KEK-CP-37, July 1995. hep-lat/9510047.

[31] M. Fukugita et al., Phys. Lett. 75 (1995) 2092.

[32] S. J. Dong, J-F. Lagaë and K. F. Liu, Phys. Lett 75 (1995) 2096.

[33] T. Hatsuda, private communication.

[34] A. W. Schreiber, A. I. Signal and A. W. Thomas, Phys. Rev. D44 (1991) 2653.

[35] F. M. Steffens and A. W. Thomas, Prog. Theor. Phys. Suppl. 120 (1995) 145; Phys. Lett. 358B (1995) 139.

ADP-96-12/T215 February 1996

On the Interpretation of the NA51 Experiment

F.M. Steffens and A.W. Thomas

Department of Physics and Mathematical Physics
University of Adelaide
Adelaide, S.A. 5005, Australia

Abstract

We study the $p-n$ Drell-Yan asymmetry, recently measured by the NA51 collaboration, and conclude that the value quoted by their experiment only sets a lower limit on the asymmetry of the proton sea. In particular, we notice that charge symmetry breaking between the proton and the neutron may produce corrections which should be taken into account.

The confirmation by the New Muon Collaboration (NMC) [1] of an earlier hint in SLAC data [2] of a sizeable violation of the Gottfried sum-rule [3] has stimulated enormous interest in the flavour structure of the parton distributions [4]. Early theoretical work by Feynman and Field [5] had suggested that the Pauli Exclusion Principle may lead to $\overline{d} > \overline{u}$, a result supported by calculations using the MIT bag model [6]. However, most of the work aimed at interpreting the NMC results has been based on the role the pion cloud of the nucleon, which as first noted in 1983, predicts $\overline{d} > \overline{u}$ [7].

Of course, the interpretation of the NMC results in terms of a violation of flavour symmetry in the sea is not unambiguous. One must correct for shadowing and meson cloud contributions in the deuteron in order to extract the neutron structure function. Nevertheless, there seems to be a consensus that these corrections enhance the violation of the GSR a little [8]. It has also been suggested that the violation may be merely apparent, because the expected Regge behaviour at small-x may set in less rapidly than is usually

assumed [9]. In any case, it is very important to look for other means to test whether in fact $\overline{d} > \overline{u}$.

Some time ago, the NA51 group [10] released a measurement of the $p-n$ cross section asymmetry defined as

$$A_{DY}(x) = \frac{\sigma^{pp}(x) - \sigma^{pn}(x)}{\sigma^{pp}(x) + \sigma^{pn}(x)}. \tag{1}$$

This experiment followed a suggestion by Ellis and Stirling [11] where it was argued that the sign and the size of A_{DY} can tell whether the sea is symmetric in flavour or not. This would be possible because $\sigma^{pN}(x) \propto \sum_i e_i^2 (q_i^p(x)\overline{q}_i^N(x) + \overline{q}_i^p(x) q_i^N(x))$ and then A_{DY} can be expressed as:

$$\begin{aligned} A_{DY}(x) \;=\; & \{(4\lambda_v(x)-1)(\lambda_s(x)-1) + (\lambda_v(x)-1)(4\lambda_s(x)-1) \\ & +2\overline{d}(x)(4\lambda_s(x)-1)(\lambda_s(x)-1)/d_v(x)\Big\} / \\ & \{(4\lambda_v(x)+1)(\lambda_s(x)+1) + (\lambda_v(x)+1)(4\lambda_s(x)+1) \\ & +2\overline{d}(x)(4\lambda_s(x)+1)(\lambda_s(x)+1)/d_v(x)\Big\}, \end{aligned} \tag{2}$$

with $\lambda_v(x) = u_v(x)/d_v(x)$ and $\lambda_s(x) = \overline{u}(x)/\overline{d}(x)$. For completeness, we have included sea-sea corrections in Eq. (2). It is then clear that for a sea which is SU(2) flavour symmetric, i.e. $\lambda_s = 1$, the asymmetry is always positive if λ_v is larger than unity. On the other hand the asymmetry can change sign for $\lambda_s \neq 1$. In particular, if $\lambda_v = 2$ the asymmetry is negative for $\lambda_s < 0.72$ - where, for simplicity, the last term (the sea-sea term) was neglected. However, the important feature of the $p-n$ cross section asymmetry is that, given a value for λ_v, the measured asymmetry determines whether or not there is any sort of isospin breaking. In this letter we will explore the idea that the measurement of A_{DY} is not enough to precisely determine λ_s and thus the degree of asymmetry in the quark sea, as has been claimed [10, 11]. This point will be clear from expression (7), where possible corrections from charge symmetry breaking between the neutron and the proton at a given x are included.

The NA51 collaboration quoted the following result [10]:

$$A_{DY}(x = 0.18) = -0.09 \pm 0.02(stat) \pm 0.025(syst) \tag{3}$$

from which they derived

$$\lambda_s(x=0.18) = 0.51 \pm 0.04(stat) \pm 0.05(syst), \qquad (4)$$

where sea-sea corrections were included but nuclear effects were left out. In this interpretation, the experiment indicates that there is a strongly asymmetric sea at $x = 0.18$. We are now going to show that, in fact, the λ_s quoted in Eq. (4) is only a limiting value set within the framework of Eq. (2) which was based on the assumption of charge symmetry (e.g. $\overline{u}^p(x) = \overline{d}^n(x)$ and $\overline{d}^p(x) = \overline{u}^n(x)$). We could as well have set the sea to be flavour symmetric and derived the following expression for the Drell-Yan asymmetry:

$$\begin{aligned} A_{DY}(x) \;=\; & \Big\{3(\lambda_v(x)-1) - (1+4\lambda_v(x))\overline{\delta}(x)/\overline{q}(x) + 3\delta(x)/d_v(x) \\ & -10\overline{\delta}(x)/d_v(x)\Big\}\,/ \\ & \Big\{13\lambda_v(x) + 7 + (4\lambda_v(x)+1)\overline{\delta}(x)/\overline{q}(x) - 3\delta(x)/d_v(x) + \\ & 10\overline{\delta}(x)/d_v(x) + 20\overline{q}(x)/d_v(x)\Big\}. \end{aligned} \qquad (5)$$

Here, we used $\overline{u}(x) = \overline{u}^p(x) = \overline{d}^n(x) - \overline{\delta}(x)$, $\overline{d}(x) = \overline{d}^p(x) = \overline{u}^n - \overline{\delta}(x)$, $u_v(x) = u_v^p(x) = d_v^n(x) - \delta(x)$ and $d_v(x) = d_v^p(x) = u_v^n(x) + \delta(x)$. The function $\delta(x)$ does not need to be the same for u_v and d_v but we use the same function to simplify the expressions as we illustrate the main idea. Also notice that different signs are used for the corrections in d_v^n and u_v^n as this seems to be suggested by theoretical evidence [12]. We have also considered the case where both signs coincide and the conclusions presented here are insensitive to such a choice. Of course, $\int_0^1 dx\delta(x) = 0$ to preserve the number of valence quarks. Using the experimental result for $A_{DY}(x)$, we can estimate the amount of charge symmetry breaking.

For that purpose, we will work with the MRS parametrization, S_0', for $\overline{q}(x)$, $u_v(x)$ and $d_v(x)$. In this parametrization the sea is symmetric and, for $x = 0.18$, $Q^2 = (5.22\ GeV)^2 = x^2 s$ for $s = (29\ GeV)^2$ the square of the center of mass energy of the NA51 experiment, it gives $\overline{q}(x=0.18) = 0.348$, $u_v(x=0.18) = 3.13$ and $d_v(x=0.18) = 1.486$. From the experimental result quoted in Eq. (3) we then obtain:

$$\overline{\delta}(x=0.18) = 0.2088 - 0.0933\delta(x=0.18). \qquad (6)$$

In calculating Eq. (6) we disregarded the sea-sea correction term $(20\overline{q}(x)/d_v(x))$ and took only the central value of the measured asymmetry. This is a good approximation as, using the same procedure when recalculating result (4), we get $\lambda_s(x=0.18) \simeq 0.53$. Eq. (6) tells us that the interpretation of the Drell-Yan asymmetry purely in terms of charge symmetry violation is very unlikely because of the size of the breaking necessary to fit the data. Of course, the procedure is not entirely consistent because the S_0' parametrization was constructed with the assumption $\overline{\delta}(x) = \delta(x) = 0$. Thus, Eq. (6) should be seen only as a guide.

If we take for instance $\delta(x) = \overline{\delta}(x)$, we have $\overline{\delta}(x=0.18) \simeq 0.19$, which means that the factor giving the breaking is about 55% of the antiquark distribution itself - clearly too large value. On the other hand, there is no reason at all to interpret the NA51 result solely in terms of isospin breaking between the proton and the neutron. In the general case, the Drell-Yan asymmetry would be:

$$\begin{aligned} A_{DY}(x) \;=\; & \{(4\lambda_v(x)-1)(\lambda_s(x)-1) + (4\lambda_s(x)-1)(\lambda_v(x)-1) \\ & -(4\lambda_v(x)+1)\overline{\delta}(x)/\overline{d}(x) - (1-4\lambda_s(x))\delta(x)/d_v(x) \\ & -2(4\lambda_s(x)+1) - 2(4\lambda_s(x)-1)(\lambda_s(x)-1)\overline{d}(x)/d_v(x)\Big\}\,/ \\ & \{(4\lambda_v(x)+1)(\lambda_s(x)+1) + (4\lambda_s(x)+1)(\lambda_v(x)+1) \\ & +(4\lambda_v(x)+1)\overline{\delta}(x)/\overline{d}(x) + (1-4\lambda_s(x))\delta(x)/d_v(x) \\ & +2(4\lambda_s(x)+1) + 2(4\lambda_s(x)+1)(\lambda_s(x)+1)\overline{d}(x)/d_v(x)\Big\}. \end{aligned} \qquad (7)$$

To write Eq. (7) we made the simplification that, even for broken sea flavour symmetry, the correction $\overline{\delta}(x)$ from charge symmetry breaking in the sea has the same form for the $\overline{u}$ and for the $\overline{d}$ quarks. Of course, this does not necessarily need to be the case.

Again, to extract any number from Eq. (7) we need to know the value of the sea and valence quark distributions at a given x. As we include isospin breaking terms, we have the problem that there is no standard quark distribution including these corrections. Moreover, the term involving $\overline{\delta}(x)$ is potentially important as it is multiplied by a large factor and divided by a small number (viz. $\overline{d}$). This is true whether the integral over x of $\overline{\delta}(x)$ (and $\delta(x)$) is zero or not. This means that to extract $\lambda_s(x)$ using the measured Drell-Yan asymmetry is at best ambiguous. To estimate the order

of magnitude of $\delta(x)$ and of $\overline{\delta}(x)$, we will assume that the quark and antiquark distributions are described by the D'_0 and D'_- parametrizations. For the D'_0 set, the Gottfried sum rule is 0.26 and for the D'_- this value is 0.24, which means that for both sets, $\int_0^1 \overline{\delta}(x)dx \simeq 0$, but this does not mean that $\overline{\delta}(x) = 0$ at $x = 0.18$. Using the measured asymmetry and disregarding sea-sea corrections, one gets:

$$\begin{aligned} \overline{\delta}(x=0.18) &= 0.169 - 0.053\delta(x=0.18), \ \lambda_s \sim 0.88, \ D'_0 \\ \overline{\delta}(x=0.18) &= 0.125 - 0.045\delta(x=0.18). \ \lambda_s \sim 0.78, \ D'_- \end{aligned} \quad (8)$$

In fig. 1 we show the behaviour of $\overline{\delta}(x)$ as a function of $\delta(x)$ for the various parametrizations discussed. A few comments are in place. First, we see that $\overline{\delta}$ is not strongly dependent on δ and this dependence becomes weaker as λ_s decreases. Moreover, we see that for $\lambda_s = 0.78$, the charge symmetry breaking is of the order $30\% \sim 40\%$ of the antiquark distribution. Although this value is high, it is at a specific value of x and we remember that $\lambda_s = 0.78$ is a correction of about 50% to the central value of $\lambda_s = 0.51$ quoted by the NA51 group. We could be less drastic and propose corrections of the order of 20%, bringing the measured central value to $\lambda_s = 0.6$, which is itself a huge correction, providing a sensitive test for any model trying to describe the flavour of the nucleon sea. As a consequence, if we make a linear extrapolation of $\overline{\delta}(x)$ with λ_s as suggested by Fig. 1, this correction of 20% would correspond to a value of $\overline{\delta}$ around 10% of the antiquark distribution itself. This could well be possible and, from this point of view, the λ_s quoted as being experimentally measured only sets a lower limit corresponding to $\overline{\delta}(x) = \delta(x) = 0$.

We can summarise this letter by saying that, in principle, the discrepancy between theory and experiment found by the NMC [1] could come from flavour symmetry violation in the nucleon sea and charge symmetry breaking in either the the nucleon sea or valence distributions. However, because of the enormous value for $\overline{\delta}$ needed to fit the experiment with charge symmetry breaking alone, it is more likely that the NMC result implies some strong flavour symmetry breaking in the nucleon sea with a small $\overline{\delta}$ admixture.

Of course, there are many successful calculations based on pion physics [4, 13, 14, 15] that give a clear indication of an excess of $\overline{d}$ over $\overline{u}$ in the nucleon. On the other hand, the interpretation of the NMC experiment as

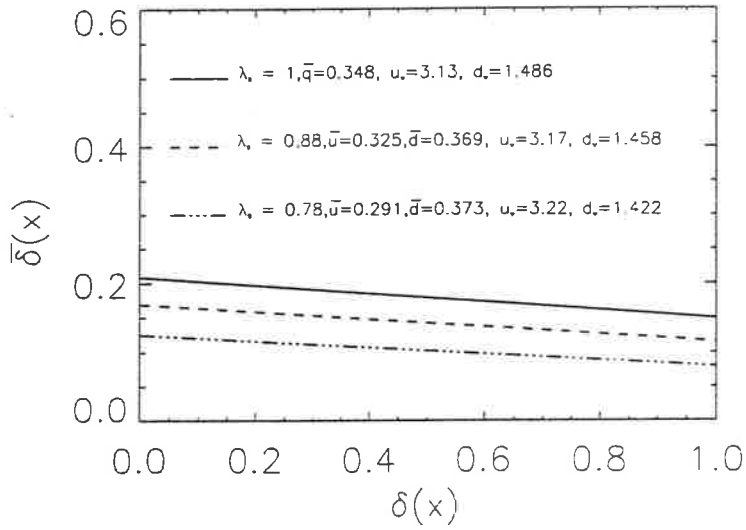

Figure 1: $\overline{\delta}(x)$ as a function of $\delta(x)$ for the various parametrizations discussed in the text.

a confirmation of broken sea symmetry, does not rule out the possibility that, at a particular x, charge symmetry breaking between the neutron and the proton may be at the same level as that of flavour symmetry breaking. Our analysis indicates that it is possible to have $\lambda_s(x)$ larger than the value quoted by the NA51 group at the cost of some charge symmetry breaking between the proton and the neutron at a particular x, even if the integrated value of this correction is zero or nearly zero. It is clearly an urgent matter to find experimental ways to separate these two contributions. For now, the important feature to note is that the NA51 result should be seen as a lower limit for $\lambda_s(x)$ and not as an absolute value.

This work was supported by the Australian Research Council and by CAPES (Brazil).

References

[1] NMC, P. Amaudruz et al., Phys. Rev. Lett. 66 (1991) 2712; NMC, M. Arneodo et al., Phys. Rev. D 50 (1994) R1.

[2] A. Bodek et al., Phys. Rev. Lett. 30 (1973) 1087.

[3] K. Gottfried, Phys. Rev. Lett. 18 (1967) 1174.

[4] E. M. Henley and G. A. Miller, Phys. Lett. B 251 (1990) 453; A. I. Signal, A. W. Schreiber and A. W. Thomas, Mod. Phys. Lett. A 6 (1991) 271; S. Kumano and J. T. Londergan, Phys. Rev. D 44 (1991) 717; W. Melnitchouk, A. W. Thomas and A. I. Signal, Z. Phys. A 340 (1991) 85; E. J. Eichten, I. Hinchliffe and C. Quigg, Phys. Rev. D 45 (1992) 2269; A. Szczurek and J. Speth, Nucl. Phys. A 555 (1993) 249.

[5] R. D. Field and R. P. Feynman, Phys. Rev. D 15 (1977) 2590.

[6] A. I. Signal and A. W. Thomas, Phys. Rev. D 40 (1989) 2832.

[7] A. W. Thomas, Phys. Lett. B 126 (1983) 97.

[8] W. Melnitchouk and A. W. Thomas, Phys. Rev. D 47 (1993) 3783; B. Badelek and J. Kwieciński, Phys. Rev. D 50 (1994) R4; G. Piller, W. Ratzka and W. Weise, ADP-95-10/T173, hep-ph/9504407.

[9] A. D. Martin, W, J. Stirling and R. G. Roberts, Phys. Lett. B 252 (1990) 653.

[10] NA51 collaboration, A. Baldit et al., Phys. Lett. B 332 (1994) 244.

[11] S. D. Ellis and W. J. Stirling, Phys. Lett. B 256 (1991) 258.

[12] E. N. Rodionov, A. W. Thomas and J. T. Londergan, Mod. Phys. Lett. A 9 (1994) 1799; E. Sather, Phys. Lett. B 274 (1992) 433.

[13] A. W. Thomas and W. Melnitchouk, in: New Frontiers in Nuclear Physics, eds. S. Homma, Y. Akaishi and M. Wada (World Scientific, Singapore, 1993), pp. 41 - 106.

[14] W. Koepf, L. L. Frankfurt and M. Strikman, Tel Aviv University preprint TAUP-2273-95, hep-ph/9507218.

[15] A. Szczurek, M. Ericson, H. Holtmann and J. Speth, Nucl. Phys. A 596 (1996) 397.